UNIVERSITY OF LONDON THESIS

Degree PhD Year 2007 Name of Author DENNIS, Paul Gareth

HOW DO RHIZOSPHERE BACTERIA INTERACT WITH THEIR ENVIRONMENT AT THE MICROHABITAT SCALE?

Paul Gareth Dennis

Presented for the degree of Doctor of Philosophy in the Faculty of Science, University of London

May 2007

Dept. of Geography, University College London, Gower Street, London WC1E 6BT, UK

Rothamsted Research, Harpenden, Hertfordshire AL5 2JQ, UK

The Natural History Museum, Cromwell Road, London SW7 5BD, UK

ProQuest LLC
789 East Eisenhower Parkway
P.O. Box 1346
Ann Arbor, MI 48106-1346

Declaration of authenticity

I, Paul Gareth Dennis, confirm that the work presented in this thesis is my own. Where information has been derived from other sources, I confirm that this has been indicated in the thesis.

ABSTRACT

The rhizosphere supports greater bacterial densities than root-free soil. Rhizosphere bacteria (RB) can affect plant health and nutrition; however, attempts to manipulate introduced and/or indigenous communities to benefit plants are unreliable. Current evidence indicates that habitat factors strongly influence bacterial communities. In the rhizosphere many processes give rise to a high degree of habitat heterogeneity; therefore, to understand how RB interact with their environment their ecology should be studied at the micro-spatial-scale. The objectives of this research were to develop a method for sampling RB at the microhabitat-scale, and to investigate techniques that can link these samples with key factors, such as substrate availability and pH.

A novel method enabling non-destructive, micro-scale sampling of bacteria was developed. Its efficiency for removing bacteria from the root surface was similar to that of existing methods but offered greater accuracy in estimating RB densities. The novel method revealed that RB density was inversely proportional to distance from the apex of *Brassica napus* roots and that the composition of RB communities was highly variable at the micro-scale. Imaging of ^{14}C-labelled root exudates revealed that RB density was not reflective of exudate availability but attempts to link RB with available C were unsuccessful.

A key outcome of this work was the development of a strategy to combine micro-sampling with microelectrode measurements. Microelectrodes revealed that pH at the root surface was highly variable at the micro-scale which, combined with similar observations for RB density/diversity, highlights the appropriateness of this scale for linking RB communities with their environment.

This thesis considers the link between RB community structure, habitat and function and provides a detailed description of micro-sample analyses as well as a set of methods that will enable for the first time, the interactions between any surface-associated bacteria and their environment to be investigated at a microhabitat-scale.

TABLE OF CONTENTS

LIST OF FIGURES

LIST OF TABLES

ACKNOWLEDGEMENTS

I gratefully acknowledge the Biotechnology and Biological Sciences Research Council (BBSRC) and the Natural History Museum (NHM), London, for providing me with a three-year BBSRC industrial CASE studentship (#10275). I also thank University College London (UCL) and Rothamsted Research (RRes) for hosting me throughout the course of my PhD.

I have really enjoyed working towards this degree and have ended feeling even more enthusiastic about science than when I began. This is largely due to the inspirational characteristics of my primary supervisor and good friend, Dr Penny Hirsch (RRes). Being part of Penny's group has been very special. Ian, Lucy, Lesley and those that have passed through have made the Sun shine irrespective of the weather. I particularly want to say thank you to Ian, not only for the many beers that we enjoyed together, but also for imparting so much of his scientific expertise on me. Thank you as well to my other supervisors: Drs. Tony Miller (RRes), Eva Valsami-Jones (NHM) and Richard Taylor (UCL). Without you all this PhD would simply have never happened. Your advice and help in every way is greatly appreciated and I hope that we will remain in contact.

I wish also to thank: Dr Steve Powers (RRes) for his statistical master classes, Susan Smith (RRes) for her patience and help during my electrophysiology experiments, Professor Chris Grovenor and Dr Matt Kilburn (University of Oxford) for facilitating the nanoSIMS work; Jean Devonshire (RRes) and Drs. Alex Ball and Ben Williamson (NHM) for my basic training in scanning electron microscopy; Drs. Davey Jones (University of Wales, Bangor) and Kim Hammond-Kosack (RRes) for facilitating the ^{14}C-labelling work; and the many friends who have given me such good memories – notably my last house mates, the Grove Road guzzlers: Dennis and Tim, and the Gib gang: Rolo, Simon, Sofia, Keith and Tina. Finally, I want to say a special thank you to those that I love: Mum and Dad, and my sister Faye. This is our achievement, just one of many that gives us all reason to be proud.

CHAPTER 1

INTRODUCTION AND LITERATURE REVIEW

1.1. Introduction

The vast majority of energy that drives Earth's terrestrial ecosystems is derived from the sun and is captured by green plants via the process of photosynthesis. Some plants are able to obtain mineral nutrients above ground; the Venus fly trap (*Dionaea muscipula*) for example, has leaves that are adapted to trapping and digesting small animal prey. However, most terrestrial plants rely on root systems that extract mineral nutrients from soils which are both complex and generally teeming with life.

Due to their lack of sentimental appeal combined with the fact that they are incredibly difficult to study, underground organisms have received far less attention than their above ground counterparts. However, soil communities may constitute the majority of Earth's terrestrial species (Wardle, 2002) and many are involved in major ecosystem functions such as the decomposition of dead organic matter from the above-ground plant-based food web. In recognition of this, increasing attention is being given to soil biodiversity and related questions (Fig. 1.1).

In addition to their role in material cycling, soil organisms have diverse functions; on the one hand their acitivities may promote plant growth, while on the other, they may lead to disease. Table 1.1 summarises the relative size of some of the major groups of soil organisms. After plant roots, bacteria represent the largest fraction of biological material in most arable soils, and along with fungi they are the main primary consumers in the soil food web (Bardgett, 2005). Higher-level consumers, representing a smaller fraction of biological material, can however strongly influence soil physical, biological and chemical properties through their activities. For example, the environment surrounding and affected by the feeding, casting and burrowing activities of earthworms, the 'drilosphere', is distinct from neighboring soil (Bouché, 1975.; Lavelle,

1988). Microbial communties associated with burrow walls have be shown to differ from those in non-drilosphere soil (Tiunov & Scheu, 1999) and drilosphere pH has been reported to be more alkaline than surrounding soil (Schrader, 1994; Tiunov & Scheu, 1999). However, as the focus of this thesis is on bacteria, further consideration of the effects of other organisms on the soil environment are beyond the scope of this review.

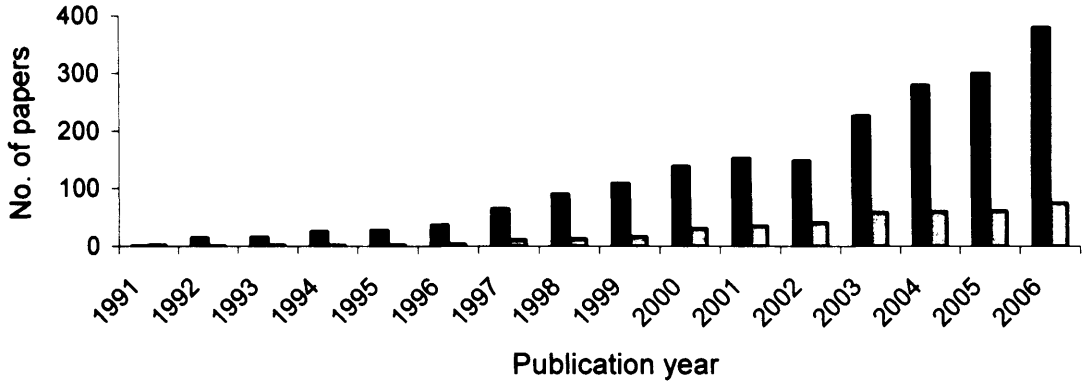

Fig. 1.1 The number of peer reviewed journal papers matching the search terms 'soil, microbial, and diversity' (black), and 'rhizosphere, microbial, and diversity' (grey) (Web of knowledge, 18/12/06).

Table 1.1 Fractions of biological compenents in soil*

Bacteria	30–90 kg C ha^{-1}
Fungi	4–70 kg C ha^{-1}
Protozoa	50 kg C ha^{-1}
Nematodes	0.01–0.24 kg C ha^{-1}
Microarthropods	0.01–0.19 kg C ha^{-1}
Macroarthropods	0–0.1 kg C ha^{-1}
Enchytraeids	0.03 to 0.21 kg C ha^{-1}
Earthworms	0–13.5 kg C ha^{-1}

* Adapted from Zwart & Brussaard (1991) and Watt *et al.* (2006a).

To affect a plant, bacteria must be on the root surface or within the soil that is influenced by the presence and activities of roots (Weller, 1988). Within this zone, known as the 'rhizosphere' (Hiltner, 1904; Curl & Truelove, 1986; Hinsinger, 1998), bacteria are generally present in greater population densities than in root-free soil. This is thought to result primarily from the presence of carbon-containing compounds lost from roots (rhizodeposition), many of which are suitable substrates for bacterial growth (Curl & Truelove, 1986; Griffiths *et al.*, 2004; Dumont & Murrell, 2005). In addition, bacterial communities in the rhizosphere are also generally less diverse than those associated with root-free soil (Marilley *et al.*, 1998; Marilley & Aragno, 1999). This phenomenon is assumed to reflect a difference in the relative capacity for bacteria to metabolise and compete for carbon sources deposited by the root. The factors that ultimately determine the structure of rhizosphere bacterial communities are poorly understood. However, as they are known to influence plant health and nutrition (Cambell & Greves, 1990) it is important that we improve our knowledge to facilitate the manipulation of introduced and indigenous rhizosphere bacterial communities for environmental and/or commercial gain. This goal is challenging because soil architecture and the physical, chemical and biological interactions that occur there within are highly heterogeneous in space and time. Ultimately, rhizosphere bacterial communities are assumed to represent a sub-set of the species that are present in soil; therefore, to understand what structures rhizosphere bacterial communities it is important to first consider the types and relative abundance of species present in soil as well as their distribution in space and time.

This review aims to provide a general framework for exploring how soil bacteria respond to, and influence, the environment on and around plant roots. It begins by discussing patterns of bacterial diversity over space and time and then introduces the nature of soil and rhizosphere environments in relation to the potential habitats of bacteria. It then highlights the need to develop novel methodologies for investigating bacterial communities at the microhabitat scale.

1.2. Bacterial biogeography

1.2.1. What is biogeography?

Biogeography is the study of the distribution of biodiversity over space and time. It aims to reveal which biological entities live where, when, why, and at what abundance. The biogeography of plant and animal species has been extensively studied (Brown & Lomolino, 1998); however, that of microorganisms has received relatively little attention. In any biogeographical study it is important to consider the resolution of the biological entity under investigation as this can affect the trends one may observe. The 'species' is the most commonly used unit, but is difficult to define. A common 'species' definition for prokaryotes is 'a group of strains that have some degree of phenotypic consistency, exhibit at least 70 % DNA–DNA hybridization, and greater than 97 % 16S rRNA gene (small sub-unit ribosomal ribonucleic acid; see section 4.1) sequence similarity' (Gevers *et al.*, 2005). It is argued that this definition is too broad (Horner-Devine *et al.*, 2004a). For example, if this species definition were applied to humans we would be members of the same species as chimpanzees and lemurs (Sibley *et al.*, 1990). Nevertheless, bacterial diversity is unparalleled in the natural world; there may be as many as 10 billion bacterial species (Dykhuizen, 1998) that represent a significant proportion of all evolutionary diversity (Woese, 1987).

Many studies abandon the 'species' as the fundamental unit of diversity and opt for 'operational taxonomic units' (OTUs) instead. These are based on a user-defined depth of sample clustering following some form of discrimination between different prokaryotic types e.g. ribosomal sequences or fingerprints. The level of discrimination between different types of microorganisms is proportional to the taxonomic resolution at which an OTU is defined. For example, Horner-Devine *et al.* (2004b) found that by changing their species definition from 95 to 99 % 16S rRNA gene sequence similarity, the rate at which new species were observed with increasing area was greater.

1.2.2. Do bacteria exhibit similar biogeographical trends to macroorganisms?

In his book on the biogeography of plants, Agustin de Candolle introduced the terms 'habitations' and 'stations' (de Candolle (1820), cited by Hughes-Martiny *et al.*, 2006). A 'habitation', otherwise known as a province, signifies a region in which the biota reflect the legacies of historical events. For instance, the abundance of endemic species in Australia is attributable to its past connection to, and long isolation from other continents (Hughes-Martiny *et al.*, 2006). A 'station', signifies a habitat type – an environment defined by its associated biotic and abiotic characteristics. For example, coastal scrub habitat can be found in Australia but also in other provinces including the Mediterranean, California and South Africa (Hughes-Martiny *et al.*, 2006). Distributions of plant and animal species reflect both habitat type and historical events (Brown & Lomolino, 1998); therefore, similar plant and animal communities are generally found in similar habitat types within provinces. Whether a similar biogeographical trend operates for microorganisms is currently a topic of intense scientific debate (Finlay & Clarke, 1999; Finlay, 2002; Fenchel & Finlay, 2003; Green *et al.*, 2004; Horner-Devine *et al.*, 2004a; Green & Bohannan, 2006; Hughes-Martiny *et al.*, 2006).

Due to their large population sizes, and short generation times, combined with their very small size, microorganisms are advocated by many to be easily distributed worldwide (Glockner *et al.*, 2000; Brandao *et al.*, 2002; Ward & O'Mullan, 2002; Fenchel & Finlay, 2003; Fenchel & Finlay, 2004; Finlay & Fenchel, 2004). In this view of the microbial world, their biogeography is hypothesised to reflect multiple habitat types within a single province (Baas-Becking, 1934). Although current evidence supports the suggestion that environmental factors influence microbial biogeography (Horner-Devine *et al.*, 2004b; Fierer & Jackson, 2006), a number of studies report examples of microorganisms that exhibit provincialism, i.e. species that have a limited geographical range (Table 1.2).

Table 1.2 Studies of distance and environmental effects on microbial composition

Organisms	Approximate scale (km)	Habitat	OTU	Distance effect	Environmental effect	Reference
Synechococcus	20000	Hot springs	16S/ITS sequence	Yes	No	Papke *et al.* (2003)
Sulfolobus	12000	Hot springs	MLS of isolates	Yes*	No*	Whitaker *et al.* (2003)
Bacteria	3000	Coral	16S sequence	No	Yes*	Rohwer *et al.* (2002)
Bacteria	500	Lakes	ARISA	Yes*	Yes*	Yannarell & Triplett (2005)
3-CBD bacteria	500	Soil	ARDRA	No	Yes*	Mantel (1967)
Ascomycetes	100	Soil	ARISA	Yes*	Yes*	Green *et al.* (2004)
Bacteria	100	Aquatic	ARISA	No	Yes	Hewson & Fuhrman (2004)
Bacteria	10	Lakes	DGGE of 16S	Yes*	No*	Reche *et al.* (2005)
Bacteria	0.3	Marsh sediment	16S sequence	No*	Yes*	Horner-Devine *et al.* (2004)
Bacteria	0.1	Soil	TRFLP	No	Yes*	Kuske *et al.* (2002)

*Statistically significant. 3-CBD, 3-chlorobenzoate-degrading; ARDRA, amplified ribosomal DNA restriction analysis; ARISA, automated ribosomal intergenic spacer analysis; DGGE, denaturing gradient gel electrophoresis; ITS, intergenic transcribed space; MLS, multilocus sequencing; OTU, operational taxonomic unit used in the study; TRFLP, terminal restriction fragment length polymorphism. Source: Hughes-Martiny *et al.* (2006).

The examples in Table 1.2 indicate that not all microorganisms are free of dispersal limitations as suggested by the protagonists of the 'everything is everywhere' hypothesis. Drawing on the knowledge of macroorganisms, Hughes-Martiny *et al.* (2006) suggest an alternative view of microbial dispersal. They suggest that microorganisms are unlikely to have the capacity to cross significant geographical distances under their own propulsion; suggesting that the mechanisms that influence their dispersal are largely passive. They hypothesise that as with macroorganisms, the significance of passive dispersal varies between different microbial species. For example, passive dispersal is highly significant for tree ferns but negligible for elephants.

Differences in the passive dispersal of microbial species could result from their respective population size, source habitat, geographic range and propagule number (Plomp *et al.*, 2005; Hughes-Martiny *et al.*, 2006). However, on arriving in a new habitat microbial species will differ in their relative capacity to survive. Survival may relate to the hardiness of individual propagules (Plomp *et al.*, 2005) and/or to their competency and competitiveness in colonising a new environment. In the opinion of Hughes-Martiny *et al.* (2006), microbial biogeography is hypothesised to reflect

multiple habitat types within multiple provinces. If this is the case, the influence of habitat on community structure needs to be understood at a provincial scale. In contrast, if the opinion of Hughes-Martiny *et al.* (2006) is rejected in favour of the Baas-Becking (1934) hypothesis (everything is everywhere – the environment selects), the rules underpinning habitat driven community structuring will be globally relevant.

1.2.3. The influence of habitat on bacterial biogeography

A habitat is an environment that is defined by its abiotic and biotic characteristics. Current evidence suggests the relationship between microbial community similarity and that of their habitat is positively correlated. For example, the composition of bacterial communities has been shown to vary with pH (Fierer & Jackson, 2006) plant species (Grayston *et al.*, 1998; Kuske *et al.*, 2002; Marschner *et al.*, 2004), nutrient status (Broughton & Gross, 2000), contamination with pollutants (Muller *et al.*, 2001), salinity (Nubel *et al.*, 2000), temperature (Ward *et al.*, 1998), predation (Griffiths *et al.*, 1999; Jurgens & Matz, 2002), moisture content (Zhou *et al.*, 2002; Treves *et al.*, 2003), substrate availability and complexity (Marschner *et al.*, 2004) and other variables such as the architecture of their habitat (Ranjard & Richaume, 2001; Sessitsch *et al.*, 2001). However, the relative importance of such variables on the outcome of community composition is poorly understood.

Fierer and Jackson (2006) collected 98 soil samples across North and South America and investigated the relative importance of environmental factors that have been shown to influence bacterial community composition. In each sample they measured temperature, soil moisture deficit, organic carbon concentration, carbon:nitrogen ratio, soil texture and other variables. They found that pH had the greatest influence on community composition. In addition, they assessed the impact of these variables on bacterial diversity. They demonstrated that neutral pH soils were associated with the greatest bacterial diversity and increasingly acidic soils were less diverse. Interestingly, the influence of above-ground taxonomic diversity did not correlate strongly with bacterial diversity despite the fact that many of the acidic soils were associated with tropical forests whereas more neutral soils were associated with desert scrub lands. However, such findings must be treated with caution as comparable studies are limited. For example, Zhou *et al.* (2002) reported that soil moisture content had the greatest

impact on bacterial diversity and another study indicated that particle size has a greater impact on bacterial diversity than soil pH (Sessitsch *et al.*, 2001).

The relative impact of different environmental factors on bacterial community composition and diversity remains unclear but there is a growing body of evidence linking levels of habitat heterogeneity with those of bacterial diversity (Zhou *et al.*, 2002; Treves *et al.*, 2003; Horner-Devine *et al.*, 2004a). This heterogeneity can be thought of as relating to the architecture of their habitats, the patchiness of resources, and/or to the nature and complexity of the physical, chemical and biological factors. Soils are by definition, highly heterogeneous and thus provide a vast array of habitat types in which bacteria and other microorganisms can co-exist. This is thought to explain why bacterial communities in soils are generally more diverse than in other environments such as aquatic environments (Torsvik *et al.*, 2002).

1.2.4. Bacterial function and activity

Determining which species live where, at what abundance and why is central to monitoring patterns of bacterial biodiversity; however, to understand the ecological significance of community composition and diversity it is necessary to characterise their function and activity. Soil bacteria are functionally diverse. Some may benefit plant growth through facilitating the availability of certain nutrients, inhibiting the activities of phytopathogens, or by releasing secondary metabolites such as: plant growth regulators, phytohormones and/or other biologically active substances. On the other hand, bacteria may compete with plants for nutrients or cause disease.

A functional group is a set of biological units that possess common functional attributes. The degree to which bacterial types are functionally related is considered in the bacterial species definition noted in section 1.2 i.e. 97 % rRNA gene similarity yields species that are consistent with pragmatic taxonomy[1] (Gevers *et al.*, 2005). However, 16S rRNA gene sequences often provide little insight into the functional role of each phylogenetic group (Torsvik & Ovreas, 2002). Recent advances in technology have enabled more suitable tools for linking phylogenetic groups to their functions and activities (Borneman, 1999; Manefield *et al.*, 2002a; Griffiths *et al.*, 2004; Dumont &

[1] Pragmatic taxonomy uses characteristics of interest (e.g. phytopathogenicity, nitrogen fixation, among others) to produce species delineations with practical applications.

Murrell, 2005). The suitability of one method over another is, however, highly dependent on the function under investigation (Torsvik & Ovreas, 2002).

Current evidence indicates that 'soil' functions, such as carbon mineralization (Yin *et al.*, 2000; Griffiths *et al.*, 2001; Gray *et al.*, 2003; Nannipieri *et al.*, 2003; Wertz *et al.*, 2006), denitrification and ammonia oxidation (Wertz *et al.*, 2006) are insensitive to changes in bacterial diversity. This insensitivity of processes at an ecosystem level to changes at lower levels of ecological complexity has been largely attributed to 'functional redundancy' - the presence of more than one species performing the same ecological function. Nonetheless, this may be somewhat misleading as the existence of functional redundancy is currently a matter of controversy (Loreau, 2004; Fitter, 2005). It is argued that stable co-existence of species necessitates some degree of divergence. Functional redundancy *senso stricto* can therefore only occur at very small spatial and temporal scales (Loreau, 2004). However, with respect to bacteria in soil, it is likely that functional redundancy may also occur over greater spatiotemporal scales as a result of cell inactivity. To perform a function and to compete with functionally similar species, it is assumed that a bacterial cell must be active. The proportion of soil bacterial biomass that is active is reported to be between 6-56 % (Vandewerf & Verstraete, 1987a; Vandewerf & Verstraete, 1987b; Vandewerf & Verstraete, 1987c; Darrah, 1991a); therefore, it is possible that stable co-existence of functionally similar species could occur where all but one species are inactive. Further research on this topic may be particularly enlightening if directed towards comparisons of the impact of different populations on a particular process over a range of environmental conditions.

1.3. The soil environment

This section will discuss the nature and properties of soils that influence the diversity of bacterial habitats; the influence of plant roots will be discussed in section 1.4. The following text aims to highlight the heterogeneity of these environments and provide evidence to show how this can influence bacterial biogeography at the habitat level.

1.3.1. Pore spaces and water dynamics

Soils are formed by the interplay between climate, topography, organisms and parent material, all operating over time. These factors set the conditions for processes that lead to the development of diagnostic soil properties, such as, structure, texture, and colloidal composition (Bockheim *et al.*, 2005). The soil environment is dominated by solid particles (clay, silt, sand, and organic matter) between which are pore spaces that are more or less filled with gaseous and/or liquid phase constituents. Whereas texture refers the size distribution of these particles, structure refers to how they aggregate. Together, soil structure and texture influence the dimensions and abundance of pore spaces (Fig. 1.2) as well as the size of the entrance and exit routes to and from them.

The pore-size distribution of a soil not only influences the dimensions of potential bacterial microhabitats but also the movement of water and organisms between them. Water movement, retention and evaporation are all energy-related phenomena and involve different kinds of energy including kinetic and potential energy. However, in soils, water movement is generally so slow that kinetic energy is negligible.

Potential energy is dominant and is affected by three main forces: (1) adhesion or attraction to soil particles (matrix) creating a matric force that leads to adsorption and capillarity, (2) attraction to mono- and poly-ionic chemical species creating an osmotic force, and (3) gravity resulting in a gravitational force (Brady & Weil, 1996). These forces generally reduce the potential energy of water in soil solution thereby establishing energy gradients that influence the movement of water from areas of high to low potential energy. The energy status of soil water is generally compared with that of pure water at standard temperature and pressure and the difference is termed the 'soil water potential (Ψ)'[2] (Brady & Weil, 1996).

[2] In saturated pores an additional force (hydrostatic submergence) constitutes the water potential. This is a pressure force that results from the weight of the surrounding water.

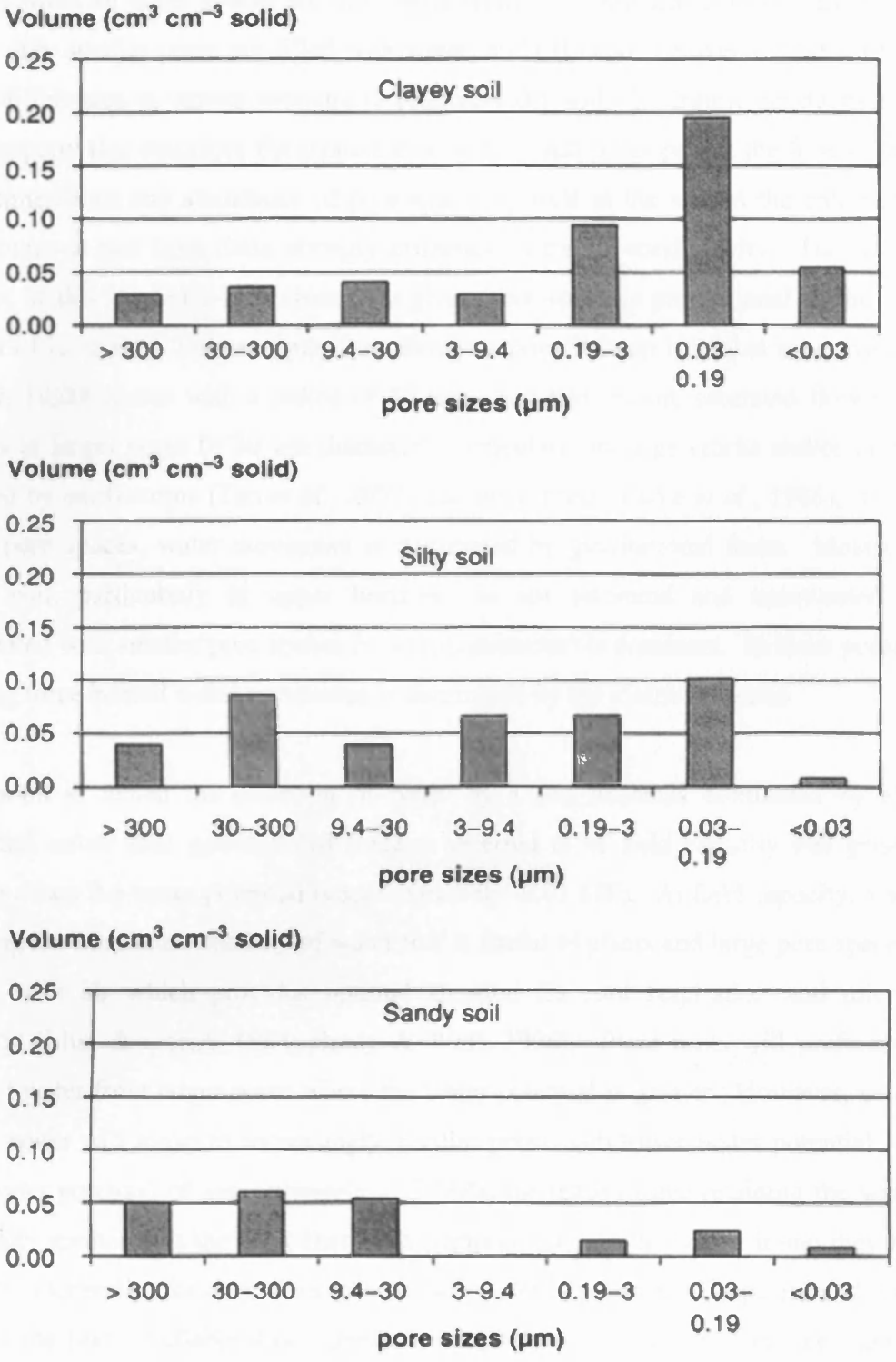

Fig. 1.2 Pore size distribution in soils of contrasting texture. Source: Chenu and Stotzky (2002).

Water movement in soil can be considered in three ways: (1) saturated flow, which occurs when all pores spaces are filled with water, (2) unsaturated flow, which occurs when only smaller pores are filled with water, and (3) vapour movement which results from differences in vapour pressure in relatively dry soil. Hydraulic conductivity is a soil property that describes the relative ease with which pores permit the flow of water. The dimensions and abundance of pore spaces as well as the size of the entrance and exit routes to and from them strongly influence hydraulic conductivity. The resulting impact of this on water flow through a given pore space is proportional to the fourth power of its radius. For example, flow though a pore 500 μm in radius is equivalent to that in 10,000 pores with a radius of 50 μm. For this reason, saturated flow mainly occurs in larger pores (> 30 μm diameter), particularly in large cracks and/or biopores created by earthworms (Tan *et al.*, 2002) and plant roots (Parke *et al.*, 1986). In these large pore spaces, water movement is dominated by gravitational force. Most of the time, soil, particularly in upper horizons, is not saturated and unsaturated flow associated with smaller pore spaces (< 30 μm diameter) is dominant. In these pores, the driving force behind water movement is dominated by the matric potential.

The point at which the retention of water by a soil becomes dominated by matric potential rather than gravitational force is referred to as field capacity and generally occurs when the water potential is approximately -0.01 MPa. At field capacity, a soil is holding the maximum quantity of water that is useful to plants and large pore spaces are filled with air which provides optimal aeration for root respiration and microbial activity (Linn & Doran, 1984; Brady & Weil, 1996). Plant roots will preferentially extract water from larger pores where the water potential is greater. However, as a soil dries, water will move to increasingly smaller pores with lower water potential. At a soil water potential of approximately -1.5 MPa, the matric force retaining the water is generally greater than the force that most plants could exert to extract it and they begin to wilt. Generally, the pore sizes that contain water between field capacity and wilting point - the plant available water, are approximately 30–0.2 μm in diameter (Hanks & Ashcroft, 1980). The relationship between soil moisture content, water potential, texture and structure[3] is illustrated in Figure 1.3. From this, it is apparent that the range of moisture contents that define different pools of water (gravitational, plant available

[3] The relationship between soil water potential and the moisture content differs depending on whether a soil is being dried or wetted. This phenomenon is known as 'hysteresis' and is thought to relate to factors such as the non-uniformity of soil pores, swelling and shrinking during wetting or drying, and trapped air bubbles that restrict capillarity

and plant inaccessible) vary with texture. It should be noted that organic matter has an inherently high capacity to hold water, and helps to stabilise soil structure, increasing both the abundance and size of the pore spaces. Combined, these attributes mean that addition of organic matter to a soil increases its capacity to hold water between field capacity and the wilting point.

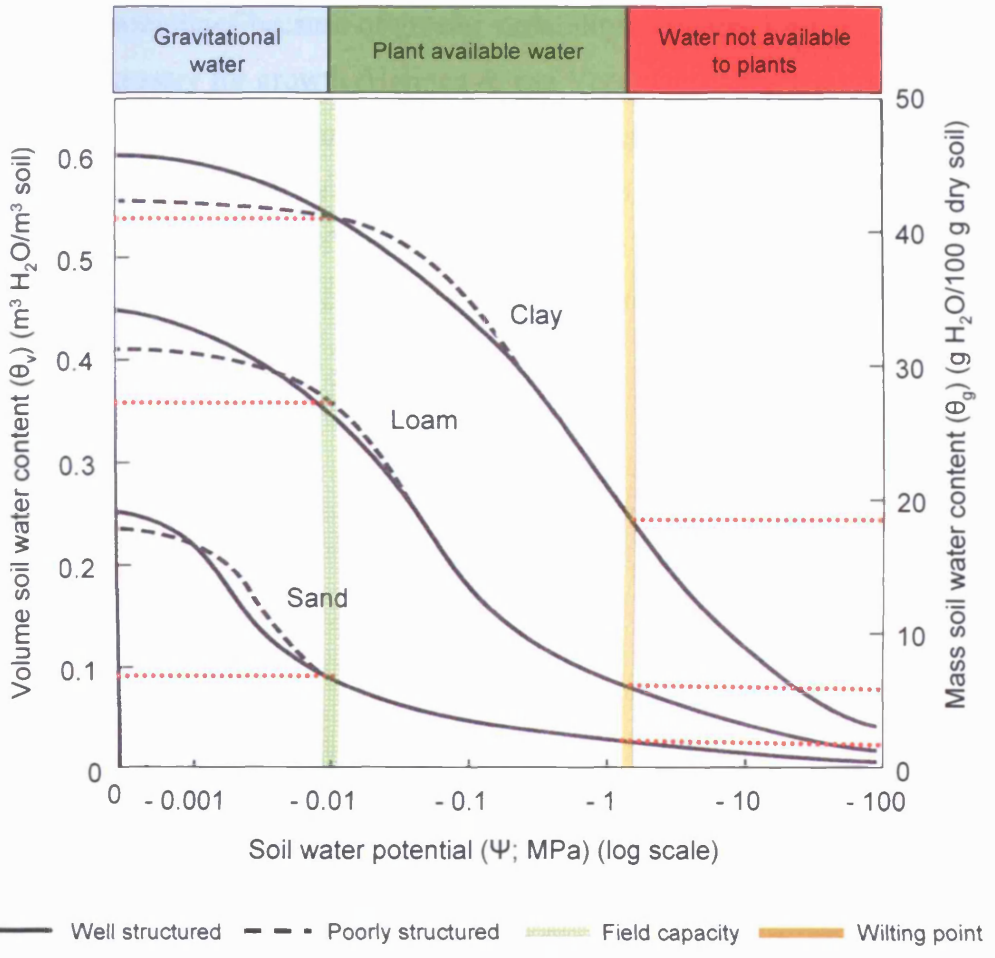

Fig. 1.3 Soil water potential curves for soils with contrasting texture and structure (a loam is a soil with relatively even particle size distribution). Adapted from Brady and Weil (1996).

Soil structure, texture, and water content and potential give rise to an extremely diverse range of microhabitats that may or may not be occupied by soil organisms. Observations using optical (Nunan *et al.*, 2003) and electron microscopy (Kilbertus, 1980; Foster, 1988) have revealed that bacteria preferentially inhabit pore spaces with a diameter of less than 30 μm. This finding has also been shown using a physical

fractionation procedure to separate different soil microenvironments (Heijnen & van Veen, 1991; Ranjard *et al.*, 2000; Ranjard & Richaume, 2001). Using this approach, Ranjard and Richaume (2001) reported that 80 % of bacterial cells are located in pores with a diameter of 1-20 μm, and Heijnen and van Veen (1991) demonstrated that pores with necks < 3 μm and between 3 and 6 μm positively affected the survival of introduced rhizobia whereas pores with necks > 6 μm had a negative effect. It is likely that larger pore spaces are less favourable habitat for the development and persistence of bacterial communities because of greater variability of moisture content and leaching of nutrients necessary for growth (Heijnen & van Veen, 1991; Killham, 1994; Nunan *et al.*, 2003). In addition, the dimensions of the pore spaces that bacteria preferentially inhabit, and the size of the entrance and/or exit routes to and from them, may exclude bacterial feeders on the basis of their body size (Table 1.3; Heijnen & van Veen, 1991; Killham, 1994; Young & Ritz, 1998; Nunan *et al.*, 2006).

Table 1.3 Approximate dimensions of soil components and of water-filled pores and water films at and between field capacity and wilting point.

Feature		Size (μm)
Soil particles	Stones	2000
	Coarse sand	200-2000
	Fine sand	50-200
	Silt	2-50
	Coarse clay	0.2-2
	Fine clay	0.2
Plant material	Root hairs*	7-15
	Fine roots*	50-1000
	Roots*	1000
Microbes	Viruses	0.05-0.2
	Bacteria	0.5-5.0
	Actinomycetes*	1.0-1.5
	Fungi*	0.3-10
Some soil animals	Protozoa	10-80
	Nematodes*	500-2000
	Mites	500-2000
	Earthworms*	2-5000
Pore diameters	Between clay particles	≤ 0.2
	Within microaggregates	1-2
	Between microaggregates	10-30
	Between aggregates in the rhizosheath	6-500
	Created by roots, macroorganisms, wetting, drying and/or freezing	20-2000
Water-filled pores	-0.01 MPa	< 30
	-0.1 MPa	< 3
	-1 MPa	0.2-0.3
Water films	-0.1 MPa	< 0.003
	-1 MPa	Few molecules thick

*Cross-sectional diameter. Adapted from Watt *et al.* (2006a) and Killham (1994).

1.3.2. Connectivity between microhabitats

Soil bacteria can be free or attached to particle surfaces (clay, silt, sand, and organic matter), or biotic surfaces (other soil organisms or plant roots), located in water-filled pores, or in a film of water on the walls of air-filled pores (Chenu & Stotzky, 2002). They may disperse in soils by active propulsion using flagella or cilia, or passively as a result of water movement (Parke *et al.*, 1986; Treves *et al.*, 2003), attachment to and subsequent detachment from more mobile soil organisms (Daane *et al.*, 1996), and/or soil mass movements (which in arable soil includes tillage). Any decrease in soil moisture content between field capacity and wilting point will result in a reduction in the connectivity between microhabitats, and therefore, spatial isolation of bacterial communities. In a field investigation aimed at linking bacterial community composition and diversity with environmental factors, Zhou *et al.* (2002) found that bacterial communities were less diverse in saturated than in unsaturated field soils. They suggested that this resulted from differences in the degree to which communities were spatially isolated. Treves *et al.* (2003) tested this hypothesis by examining the competitive dynamics of two species growing on a single resource in a uniform sand matrix under varied water contents. One species was dominant in well connected treatments, whereas in poorly connected treatments with a lower moisture content the abundance of both species was relatively even (Fig. 1.4). Their results suggest that where microhabitats are well connected, dispersal limitation is low which facilitates community dominance by the most competitive organisms. Where microhabitats are poorly connected, spatial isolation of communities supports greater levels of diversity. Saturated conditions occur in many soils at some point in time. This is particularly the case in lower soil horizons or following periods of intense rainfall. To determine the significance of these events to bacterial diversity, it is necessary that future work concentrates on identifying the temporal scales over which saturated conditions lead to a bacterial community response.

Spatial isolation is also likely to influence levels of functional redundancy. As noted in section 1.4, Loreau (2004) questions whether functional redundancy actually exists. He argues that stable co-existence of species necessitates some degree of divergence; therefore, functional redundancy *senso stricto* can only occur at very small spatial and temporal scales (Loreau, 2004). However, in the soil environment where bacterial

communities may be regularly spatially isolated, competitive interactions between functionally similar species may not be the dominant factor influencing species diversity within a given functional group. Spatial isolation resulting from low moisture content is likely to maintain high levels of functional redundancy. However, under conditions close to field capacity, where the connectivity between microhabitats is greater, competitive interactions between functionally similar species could be highly significant, particularly given that soil microbial activity is maximal at field capacity (Linn & Doran, 1984).

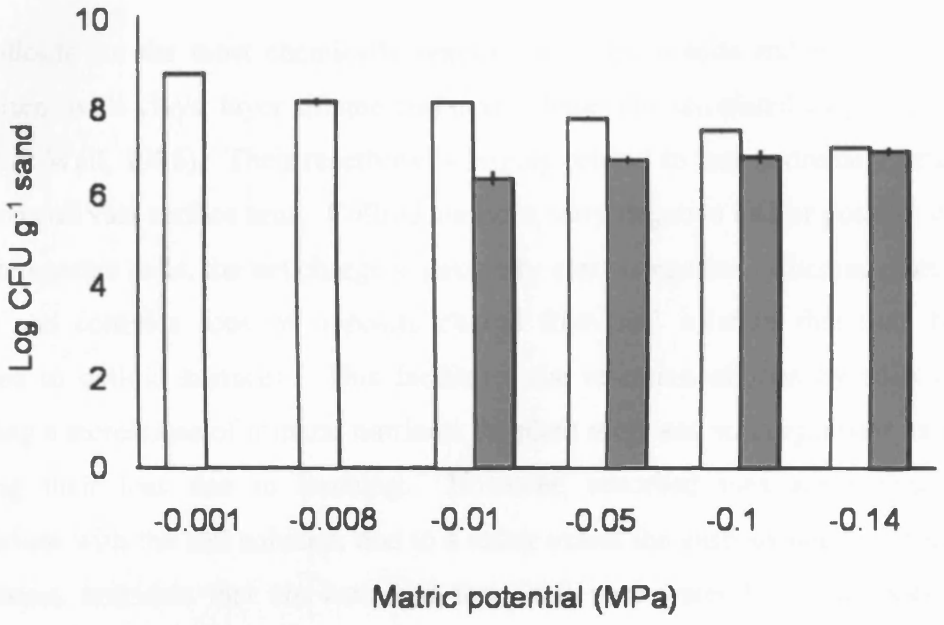

Fig. 1.4 Final population densities for *Ralstonia eutropha* JMP134 (white) and *Sphingomonas* spp. 9256 (grey) maintained at matric potentials ranging from -0.001 to -0.14 MPa in quartz sand for eight days. The number of CFU (colony forming units) refer to the number of bacteria in an original sample that developed into a colony after incubation on a nutrient agar plate. Adapted from Treves *et al.* (2003). Water potential is referred to as the matric potential in recognition of matric force being dominant within the experimental range.

1.3.3. Physicochemical conditions within microhabitats

Although the size, shape and spatial organisation of particles determines the physical architecture of potential bacterial microhabitats in soil, processes that determine their physicochemical properties such as pH and mineral nutrient availability occur in soil solution and at the interface between soil particle surfaces and solution. The gaseous phase is also important here as the availability of oxygen strongly influences oxidation and reduction of chemical species.

Soil colloids are the most chemically reactive surfaces in soils and include iron and aluminium oxide clays, layer silicate clays, allophane and associated clays, and humus (Brady & Weil, 1996). Their reactivity is largely related to their extremely small size (< 2 μm) and vast surface area. Colloid surfaces carry negative and/or positive charges but in temperate soils, the net charge is generally electronegative. Charged sites attract simple and complex ions of opposite charge from soil solution that may become adsorbed to colloid surfaces. This facilitates the retention of ions by soils thereby providing a storehouse of mineral nutrients for plant roots and soil organisms as well as reducing their loss due to leaching. However, adsorbed ions are maintained at equilibrium with the soil solution, and to a lesser extent the gaseous phase as well. For this reason, nutrients that are extracted from soil pore water by plant roots and/or microorganisms are replenished from the solid phase.

The stability of complexes formed between ions and colloid surfaces, depends on the nature of the sorption site and the ionic species, as well as soil pH (Fig. 1.5), and the concentration of an ion in solution relative to that adsorbed to the soils solid phase. For example, at low pH, the great abundance of protons in solution means that other cations are out-competed for negatively charged sites on the colloid surfaces shifting their distribution in favour of the solution phase.

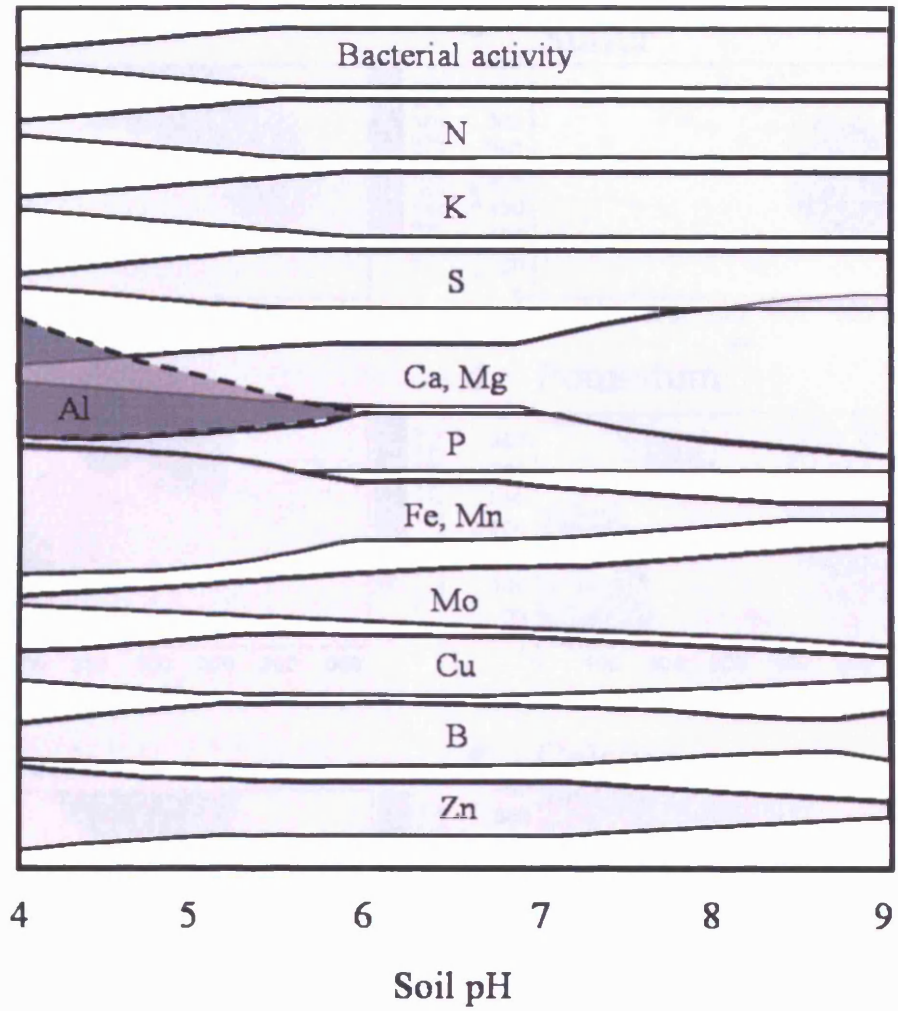

Fig. 1.5 Generalised relationship between pH, bacterial activity, and the availability of mineral nutrients in soil solution. Adapted from Brady and Weil (1996).

Bacteria are aquatic organisms in the sense that they rely on diffusion of organic and inorganic compounds in water for their nutrition. This is probably the main reason for their preference towards pores that are likely to be filled in part or in full for the majority of time. However, between different pore spaces the composition of the pore water is likely to vary in the availability and complexity of resources such as carbon substrates and mineral nutrients as well as in pH and the availability of toxic substances (Fig. 1.6). This heterogeneity between habitats is likely to influence the composition and diversity of bacterial communities within each pore space, and at a larger scale, it is likely to be a major determinant of overall soil biological diversity (Rosenzweig, 1995).

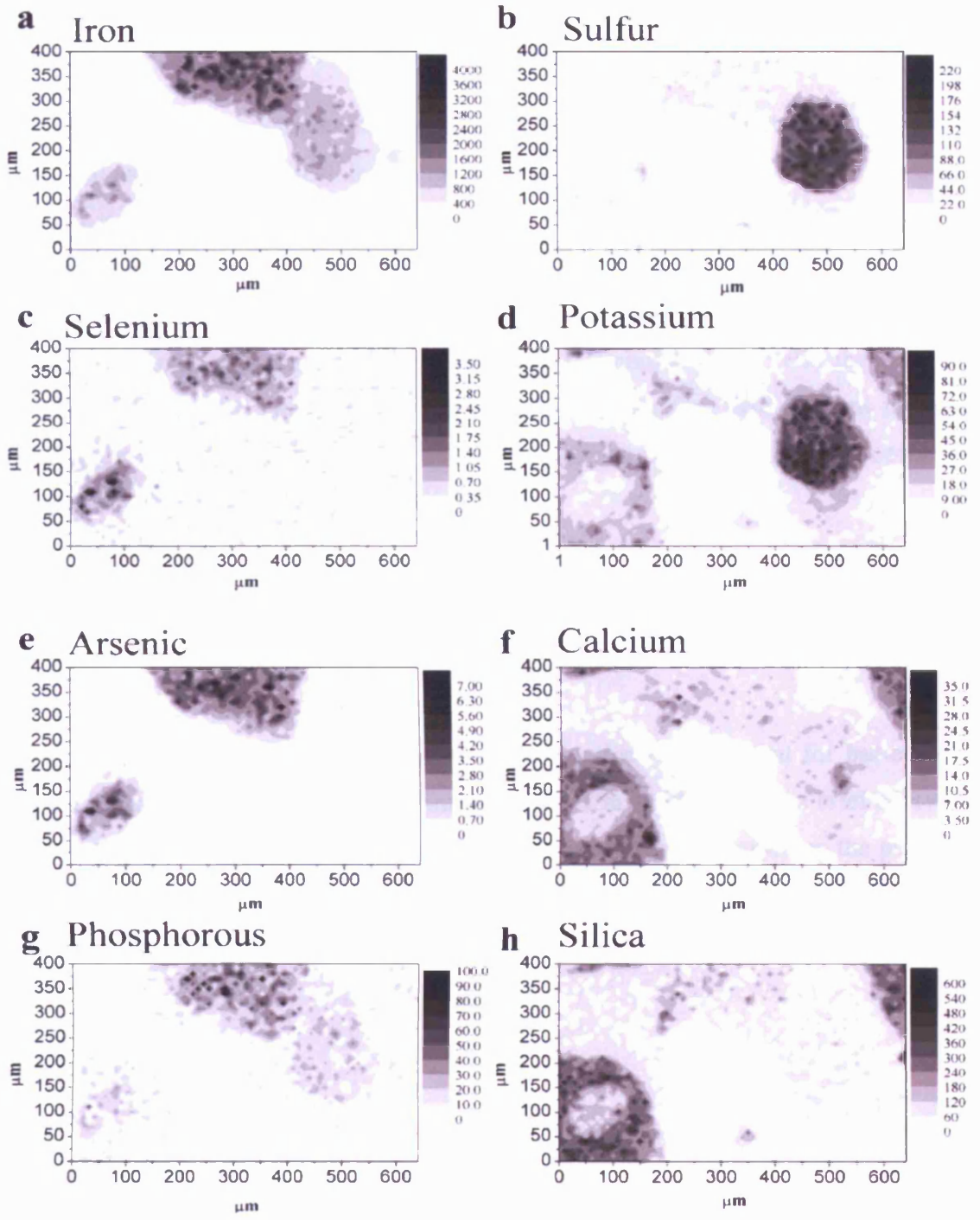

Fig. 1.6 Elemental composition of a 0.4 x 0.6 area on a 3 mm thick ultic haploxeralf soil thin section (concentrations are in µm cm^{-2}). Micro analysis was performed using a synchrontron-based X-ray fluorescence microprobe (µ-XRF). As the soil was dried prior to analysis the images reflect elemental distributions associated with the soils solid phase. It is likely that the elemental distribution of pore water would reflect these patterns to maintain equilibrium between the soil solid/solution phases. Source: Strawn *et al.* (2002).

1.3.4. Summary

In summary, soils are complex and provide a vast diversity of habitats that result from structural aspects such as the size, shape and connectivity of pore networks as well as other factors including the complexity of resources, physicochemical conditions and biological interactions. As roots grow into soil their presence and activities induce biological, physical and physicochemical gradients that exist on both radial and longitudinal axes, and fluctuate over spatial and temporal scales (Hinsinger *et al.*, 2005). Habitats associated with the rhizosphere are therefore distinct from those in root-free soil and generally support less diverse communities with greater population densities that those associated with root-free soil.

1.4. The rhizosphere environment

This section will deal with the nature of the rhizosphere as a habitat for bacteria. It begins by providing an up-to-date definition of the term and then gives a brief overview of the structure and anatomy of roots. The influence of root processes on the physical, chemical and biological properties of rhizosphere microhabitats is then discussed and finally conclusions are drawn about how these properties affect bacterial communities.

1.4.1. Definition

The term 'rhizosphere', from the Greek words: rhizo (root) and sphere (zone of influence) was originally coined by Lorenz Hiltner (1904) to describe the zone of microbial proliferation on and around the roots of *Leguminoseae*. Today, after more than 100 years of rhizosphere research, the term is best defined as the volume of soil that is influenced by the presence and activities of a root. The underlying changes in the biological, physical and chemical characteristics of the rhizosphere, compared with the bulk soil, arise from either processes for which roots are directly responsible, and/or those that may be attributed to the microorganisms that generally proliferate there as a consequence of rhizodeposition. The rhizosphere can be divided into the endorhizosphere (within the root; Lynch, 1990), the rhizoplane (the root surface; Clark, 1949), and the ectorhizosphere (outside the root; Lynch, 1990) (Fig. 1.7).

Throughout this review, rhizosphere soil refers to soil that is within the ectorhizosphere including that in contact with the rhizoplane.

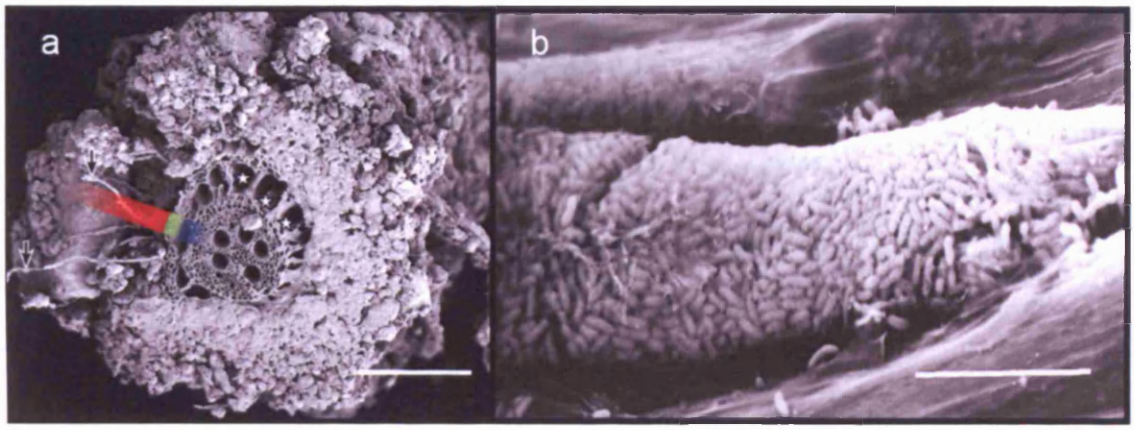

Fig. 1.7 Cryo-scanning electron micrographs of (a) a nodal wheat root grown in soil (scale bar = 1 mm; Watt *et al.*, 2006a) and (b) a microcolony of *Pseudomonas fluorescens* on the tomato rhizoplane (scale bar = 10 μm; Chin-A-Woeng *et al.*, 1997); (a) Arrows indicate root hairs, and blue, green, and red shading highlights the endorhizosphere, rhizoplane, and ectorhizosphere respectively.

1.4.2. Root structure and anatomy

The anatomy of growing roots varies along their longitudinal axes and leads to considerable differences in the physiology of different root zones. Only a brief description of root structure and anatomy will be discussed here. For detailed information the reader is directed to Esau (1977) and Waisel *et al.* (2002) although many other reviews are available. For convenience, the various regions of the root that will be discussed are described as discrete, functional units that are spatially separated from one another (Fig. 1.8). However, in reality, there are no clearly delineated points at which one region becomes distinct from another.

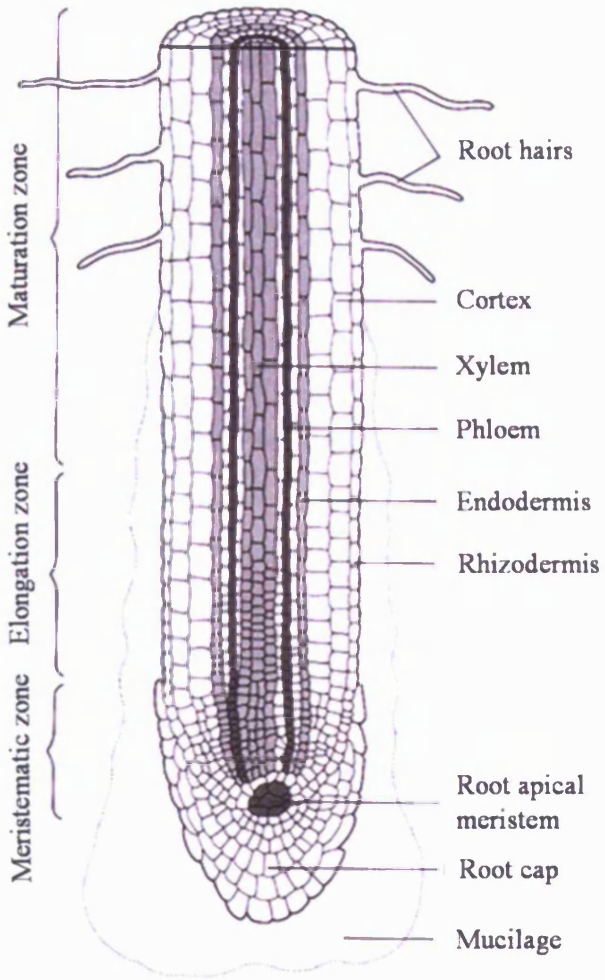

Fig. 1.8 Longitudinal section of the root apex. Adapted from Bloom *et al.* (2002).

1.4.2.1. The root cap

Generally, all angiosperm root cells originate from the divisions of cells known as initials which are part of the root apical meristem (RAM). The root apical meristem is completely undifferentiated and is protected by the most apical structure of the root, the root cap. In addition to its role as a protective barrier between the RAM and the soil, the root cap is involved in sensing gravity and other environmental signals, and cells towards its periphery are involved in the production and secretion of polysaccharide mucilages (Darwin & Darwin, 1880; Juniper *et al.*, 1966; Rougier & Chaboud, 1985; Sievers *et al.*, 1999).

The most common functions attributed to this mucilage include the lubrication of root passage through soil, and the retention of water, thus reducing root desiccation (McCully, 1999). This capacity to retain water is based on the observation that around the tips of washed roots, or root mounted in water, the mucilage appears markedly swollen (McCully & Sealey, 1996). However, the mucilage associated with the tips of soil grown roots, even at field capacity, is not expanded (McCully & Sealey, 1996). Evidence suggests that root cap mucilage, as is generally the case with other biological mucilages, has no capacity to retain water against water potentials significantly lower than 0 MPa (Guinel & McCully, 1986; McCully & Boyer, 1997); therefore, its role in protecting the root or associated microorganisms from desiccation is questionable (McCully & Boyer, 1997). However, mucilage-bound soil around the roots of some species of cacti has been reported to retain water at a greater potential than that of the surrounding root-free soil (Huang *et al.*, 1993; North & Nobel, 1997).

In the rhizosphere, exposure to successive wetting and drying cycles causes mucilage to develop relatively strong adhesive properties (Watt *et al.*, 1993; Watt *et al.*, 1994). This facilitates the aggregation of soil particles that become bound or closely associated with the roots (Oades, 1978; Morel *et al.*, 1991). In some plant species, this leads to the development of a soil sheath that extends along the length of the root, and radiates approximately 400-1000 μm from the root surface (Watt *et al.*, 2006a); this is commonly known as a 'rhizosheath' (McCully, 1999). The improved contact between the soil and the root surface is thought to facilitate better conditions for plant up-take of mineral nutrients (Nambiar, 1976a; Nambiar, 1976b; Uren & Reisenauer, 1988; Uren, 1993; Marschner, 1995) and is likely to be maintained when roots dry in response to water stress. Rhizosheaths have been observed to form on the roots of some cacti, many desert non-grass monocotyledons, some legumes, and a few dicotyledonous crop plants (McCully, 1999). The factors that underpin their absence on some other species are, however, poorly understood.

As mucilage-producing cells reach the cap periphery, they ultimately separate from the cap. This programmed cell separation is achieved through the activity of pectolytic enzymes (Hawes & Lin, 1990; Stephenson & Hawes, 1994) and for most plant species the detached cells are metabolically active, in which case they are known as border cells (Hawes, 1991). These form a physical and biological interface between the root and the soil and have been reported to influence bacterial communties in a variety of ways

including: stimulation of sporulation (Gochnauer *et al.*, 1990), supressing phytopathogens (Hawes *et al.*, 1998; Hawes *et al.*, 2000; Zhao *et al.*, 2000; Gunawardena & Hawes, 2002), species-specific chemoattraction and/or repulsion (Hawes, 1990; Hawes *et al.*, 2000) and competition for resources such as sugars (Stubbs *et al.*, 2004). The number of border cells varies between different plant species and for dicotyledons at least, this variability appears to relate to the organisation of the RAM (Hawes *et al.*, 2003; Hamamoto *et al.*, 2006).

The RAM of monocotyledons is generally of closed-type construction i.e. the root cap is distinct from the root proper (Sievers *et al.*, 1999). For dicotyledons, RAM organisation is more variable and was recently catagorised into three types: closed, basic-open, and intermediate-open (Groot *et al.*, 2004). Species with closed RAM organisation release fewer border cells than those with open organisation (Fig. 1.9; Hawes *et al.*, 2003; Hamamoto *et al.*, 2006). In the case of *Brassica napus* and *Arabidopsis thaliana,* which are members of the *Brassicaceae* and exhibit closed RAM organisation, no border cells are released at all (Hawes *et al.*, 2003; Hamamoto *et al.*, 2006). Instead sheets of dead mucilage-producing cells are sloughed-off (Fig. 1.10), which as with border cells and in combination with mucilages, are thought to act as a lubricant to facilitate ease of root penetration into soil (Bengough & McKenzie, 1997; Hawes *et al.*, 2003). These are conveniently termed border-like cells (Vicre *et al.*, 2005).

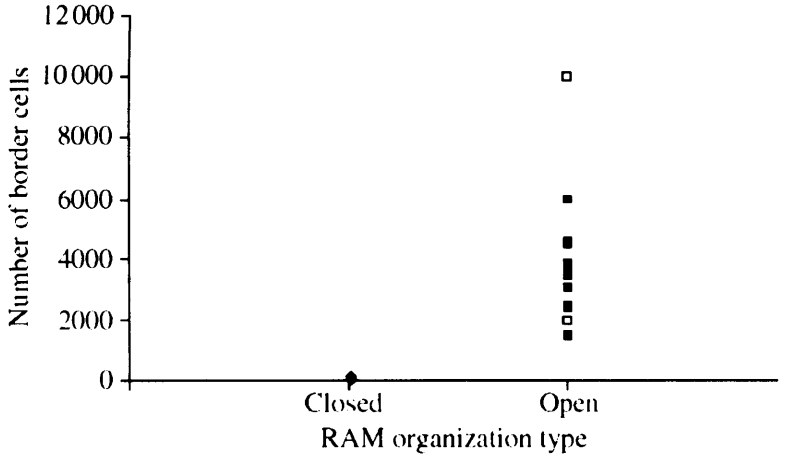

Fig. 1.9 Number of root border cells associated with species exhibiting closed (triangles), intermediate-open (open squares), and basic-open (closed squares) RAM organisation. Source: Hamamoto *et al.* (2006).

Following their release, sloughed-off root cap cells will eventually lyse their contents into the rhizosphere, providing a local hotspot of resources for rhizosphere microorganisms. In the case of border cells, these lysates can represent 10 % of all carbon released by roots (Iijima *et al.*, 2000). It is not known, however, how well this estimate relates to the dead border-like cells associated with the *Brassicaceae* and whether it is influenced by plant and/or environmental factors. In addition, the lag period between detachment from the root cap and lysis has not been charcterised; however, this is likely to significantly influence the spatial availability of soluble carbon compounds in the rhizosphere and thus potentially the distribution of bacteria and other soil organisms.

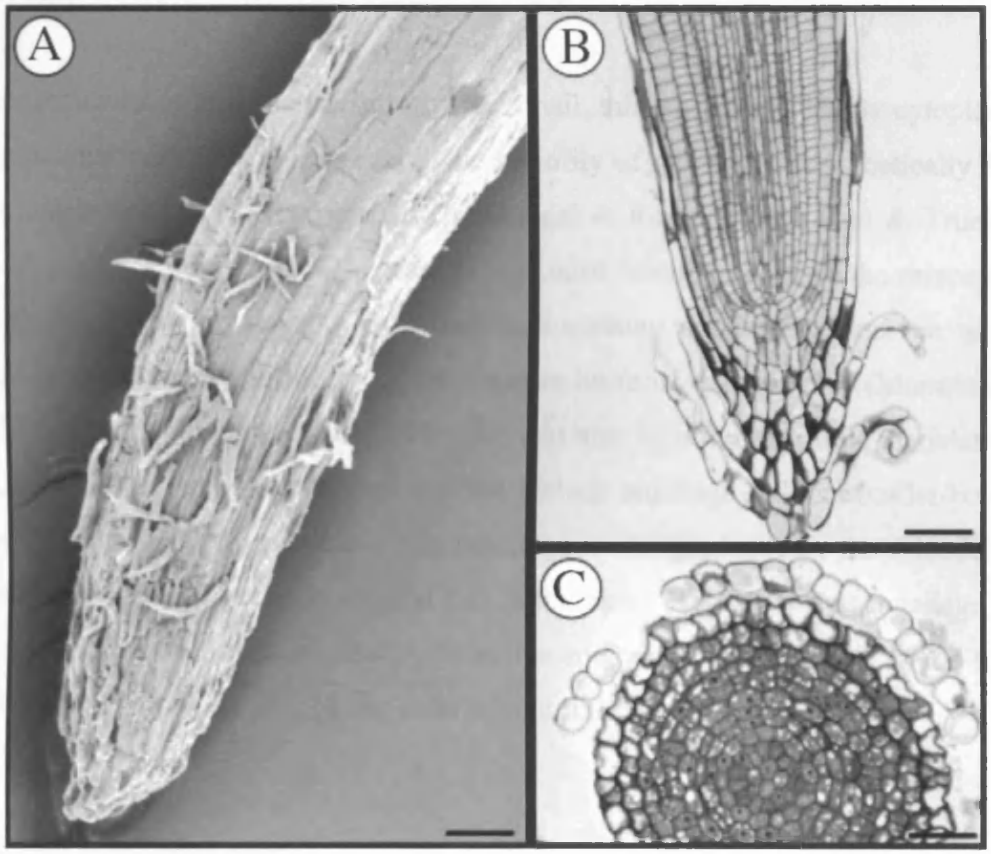

Fig. 1.10 (A) Scanning electron micrograph of a *Brassica napus* root apex showing the root cap. (B) Longitudunal and (C) transverse sections of a closed RAM showing layers of mucilage producing cells peeling off. Source: Hamamoto *et al.* (2006).

1.4.2.2. Meristematic zone

Immediately behind the root cap is the meristematic zone where cells that constitute the root proper originate from the divisions of initial cells in the RAM. This leads to the formation of the three primary meristems: (1) the 'protoderm', which differentiates into the rhizodermis (a single cell thick layer of cells covering the root), (2) the 'ground meristem', which differentiates into predominantly parenchyma cells which fill the space between the epidermis and the stele, known as the cortex (these tissues are used for storage of materials and are also active in the uptake and transport of mineral nutrients that enter the root in solution), and (3) the 'procambium', which differentiates into the stele where the xylem and phloem develop.

As a consequence of this intense activity, the small, thin walled and highly cytoplasmic cells associated with this region receive the majority of recent photosynthetically fixed carbon that is allocated below ground (McDougal & Rovira, 1970; Curl & Truelove, 1986). A significant fraction of this carbon is exuded from the root into the rhizosphere in the form of low-molecular-weight carbon-containing compounds that are widely reported to exert a major influence on rhizosphere bacterial communities (Marschner *et al.*, 2004). Other pools of root-derived carbon that may be observed in the meristematic region, as well as in more mature root regions, include mucilage and root border/border-like cells. This gives the appearance that mucilage is also produced by the rhizodermal cells but there is no evidence to suggest that is the case. It is likely that mucilage and root border/border-like cells originating from the root cap are left behind as the tip is pushed through soil by the elongating cells behind it (McCully, 1999).

1.4.2.3. Cell elongation zone

The meristematic zone graduates into of the zone of elongation where, approximately 0.5 mm behind the meristematic zone, rhizodermal cells expand to 10-20 times their original length. The process of elongation facilitates root growth rates that are typically in the range 20-90 mm per day (Foster, 1986), which means that cells in the elongation and meristematic zones as well as those associated with the root cap, move through soil at an approximate rate of 0.2-1.0 μm per second. The rapid movement of the root apex though soil creates very hostile conditions for microorganisms on the rhizoplane and is

likely to be an important factor underpinning the scarcity of bacteria at the root apex (Chin-A-Woeng *et al.*, 1997).

1.4.2.4. Root hair zone

When a rhizodermal cell has fully extended, root hairs (Fig. 1.11) may develop in great abundance. These hairs significantly increase the root surface area that is in contact with the soil, and have been demonstrated to greatly increase a plant's capacity to take up sparingly soluble mineral nutrients such as phosphate (Gahoonia *et al.*, 1997). As they extend, root hair tips tend to secrete mucilage which helps to bind soil particles thereby improving the root-soil contact (Scott *et al.*, 1958; Curl & Truelove, 1986). In legumes, lectins (which are used for detecting specific sugar molecules), are known to be involved in the recognition of rhizobia in the early stages of nodulation (Hirsch, 1999); however, their role in other plant-microbe interactions is not clear. At the surface of root hairs of legumes and some *Brassicaceae*, sugars that bind to specific lectins have been reported (Ridge & Rolfe, 1986; Ridge *et al.*, 1998), and some evidence suggests that glycoproteins found at the surface of the root hairs of various species including maize are also involved in plant-microbe signalling (Samaj *et al.*, 1999).

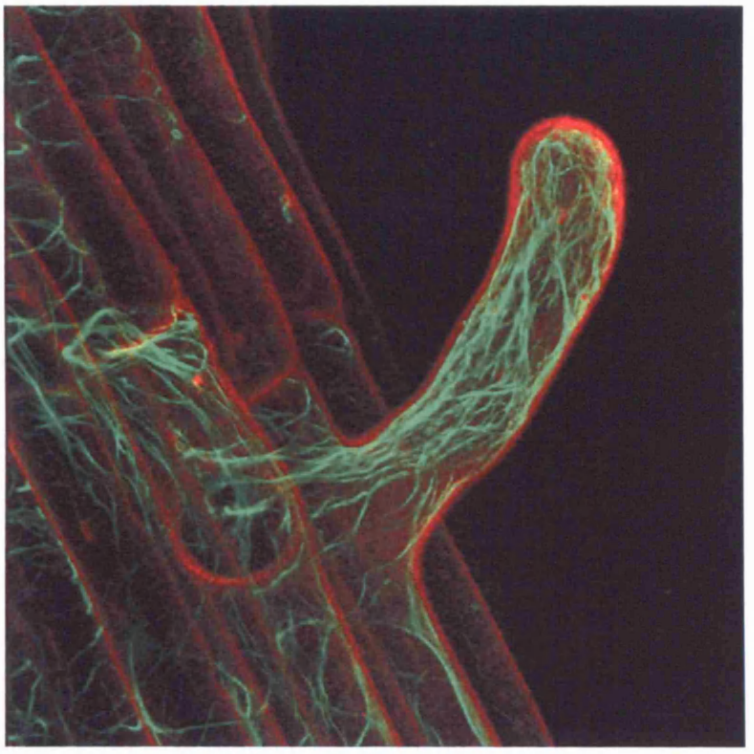

Fig. 1.11 Root hair of *A. thaliana* expressing GFP (green fluorescent protein) fused to the actin binding domain of talin (GFP-mTalin; green). The root was counter stained with propidium iodide to reveal the outline of the cell walls (red). Source: http://www.noble.org/webapps/imagegallery/image.aspx?imageid=33&searchresults=33,34,37,12.in. (accessed 02/02/07).

1.4.2.5. Mature zone

The external face of rhizodermal cells bulges-out into the rhizosphere creating a network of depressions at the junctions between cells (Fig. 1.11). Rhizoplane bacteria are commonly observed to inhabit these depressions, and are often covered in a thin transparent membrane (Chin-A-Woeng *et al.*, 1997). Whether this membrane is of root or microbial origin is not clear; however, similar membranes have been observed on the roots of axenically grown plants (Foster, 1986). In reality, both roots and microorganisms are involved. It has been proposed that the membrane surface may be a site of lectin mediated plant-microbe interactions (Lalonde & Knowles, 1975); however, it is possible that specific sugars and glycoproteins also play an important role.

Rhizodermal and cortical cells of most plants autolyse with increasing age (Watteau *et al.*, 2002). As the rhizodermal cells autolyse, their cell walls become impregnated with suberin (Esau, 1977); however, the lysed cells rapidly become invaded by microorganisms. When the flow of lysates ceases, bacteria attack the primary wall of the rhizodermis and may eventually form a continuum from the ectorhizosphere to the stele (the central part of the root, containing the vascular tissue; Foster, 1982).

1.4.3. Influence of root processes on environmental conditions in the rhizosphere

Root processes such as growth, water and nutrient uptake, respiration and rhizodeposition markedly alter the physical, chemical and biological properties of rhizosphere soil and its associated microhabitats (Hinsinger *et al.*, 2005). These changes result in microbial communities, that when compared with root-free soil, differ in their composition, diversity and population sizes. This section will provide an overview of our current understanding of these interactions and highlight knowledge gaps and misconceptions.

1.4.3.1. Root growth and water uptake

The root processes that are likely to have the greatest influence on the physical properties of the rhizosphere and associated microhabitats are root growth and water uptake. Root growth can exert considerable forces (Bengough & Mackenzie, 1994) that generally cause an increase in soil bulk density and strength (Dexter, 1987; Bruand *et al.*, 1996; Clemente *et al.*, 2005). Porosity of rhizosphere soil has also been reported to decrease by approximately 25 % as a result of the removal of mesopores and decrease in larger micropores (Bruand *et al.*, 1996). As roots grow into soil they tend to move into pores of sufficient diameter to accommodate them (Brady & Weil, 1996; Tinker & Nye, 2000) and are known to shrink and swell during the diurnal cycle (Weller, 1988) particularly in response to wetting and drying of the soil. These processes create a channel surrounding the root through which water can flow rapidly during times of rainfall. Such flow, simulated by watering plants, has been shown to carry bacterial cells from the basal towards apical root regions, substantially modifying their distribution pattern when compared to plants that were not watered (Parke *et al.*, 1986).

Another process that influences rhizosphere physical properties is the release of mucilages of both root and bacterial origin, which help to bind soil particles and in some plant species lead to the formation of rhizosheaths (section 1.5.2.1; Watt *et al.*, 1993; Watt *et al.*, 1994; Amellal *et al.*, 1998; Amellal *et al.*, 1999; McCully, 1999). Other soil organisms are also likely to influence the physical properties of rhizosphere soil through the release of compounds that influence soil aggregation or by burrowing activities. These processes may feed-back to the functioning of roots or the dynamics of bacterial communities (e.g. by facilitating or retarding the movement of water, nutrients and gases such as oxygen and carbon dioxide) although we can only speculate on the effects that this may have.

Water uptake results in substantial and rapid changes in water potential around roots (Doussan *et al.*, 2003). This is likely to influence not only the radial transfer of water into the plant but also the connectivity of rhizosphere soil microhabitats occupied by bacteria. However the magnitude of these effects varies in space and time. The uptake of water is non-uniform with respect to location on the root (Fig. 1.12), with apical regions being more active than older portions of the root (Doussan *et al.*, 2003).

The decline in water uptake by basal zones is caused mainly by formation of suberin in the rhizodermis and endodermis which provides an obstacle to apoplasmic flow – the transport of water and solutes in the spaces between cells (Marschner, 1995). Water uptake may, however, be increased where lateral roots penetrate the cortex and temporarily disrupt these barriers (Marschner, 1995). The consequence of this pattern of water uptake is likely to result in greater connectivity between microhabitats at the root base when compared to the apex. Differences in the composition of bacterial communities associated with these root zones have been reported (Semenov *et al.*, 1999; Duineveld *et al.*, 2001; Marschner *et al.*, 2002) but I am not aware of a study that has compared the diversity of communities.

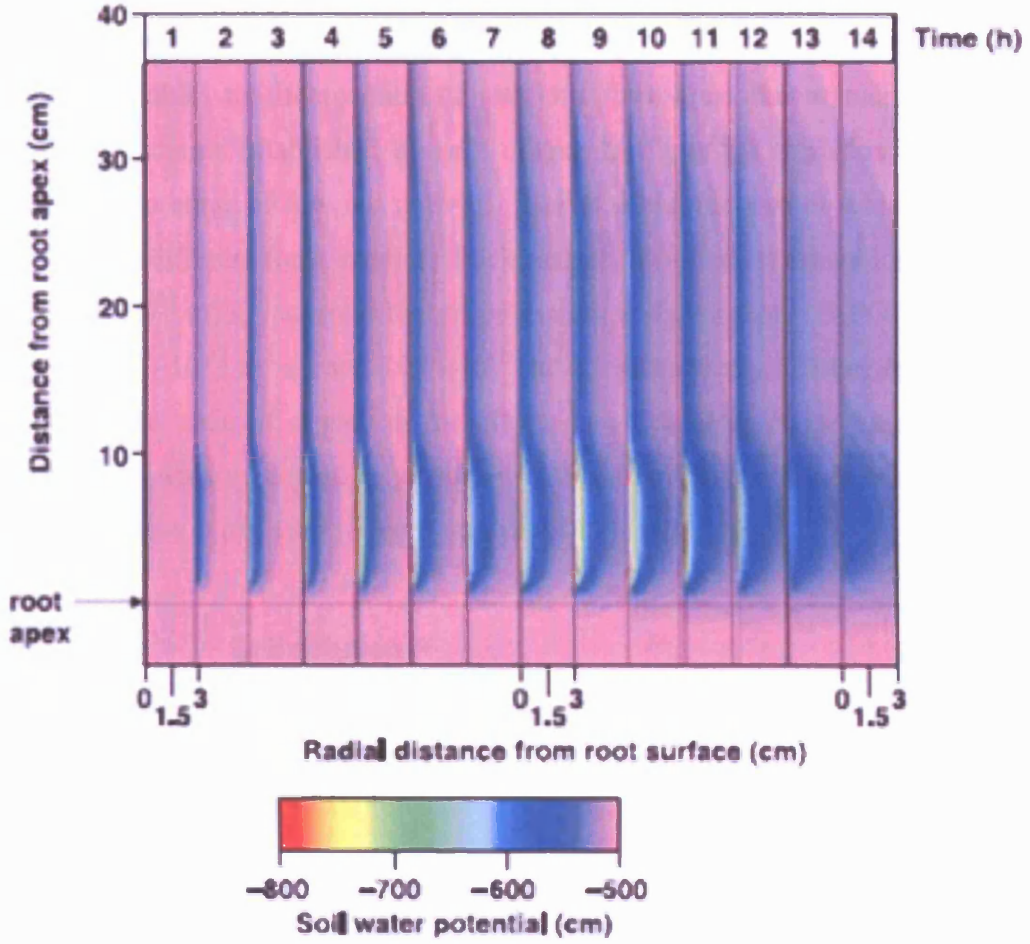

Fig. 1.12 Model simulation of changes in water potential over a 14-hour period in the rhizosphere of maize (*Zea mays*). The plant was grown in a clay–loam soil at initial potential of −0.05 MPa (500 cm = 50 KPa). Source: Doussan *et al.* (2003).

1.4.3.2. Nutrient uptake

1.4.3.2.1. General uptake trends

When at the root surface, and in a soluble form, ions may be taken up by plant roots. Uptake is generally mediated by active metabolic processes that allow regulation of the quantities and relative proportions of ions taken up. This is important because although the uptake of ions such as nitrate or phosphate is essential for plant growth, other ions may be toxic if absorbed in sufficient concentrations (e.g. heavy metal ions).

The removal of ions from soil solution by root uptake can quickly lead to their depletion. However, mass flow can deliver nutrients from root-free soil and continued root growth enables the interception of nutrients from areas that remain un-depleted. In addition, gradients established by root uptake facilitate the diffusion of ions from areas of high to areas of low ion activity. Nonetheless, the rate at which this occurs varies between different ionic species. For example, diffusion of nitrate ions occurs at a rate of 10^{-10}–10^{-11} m^2 s^{-1}, whereas that of potassium and phosphate ($H_2PO_4^-$) ions occurs at rates of 10^{-11}–10^{-12} m^2 s^{-1} and 10^{-12}–10^{-15} m^2 s^{-1} respectively (Tinker & Nye, 2000). As a result, the zone of depletion for nitrate can extend up to several centimetres, whereas for phosphate, depletion generally extends no further than a millimetre from the root (Hendriks *et al.*, 1981; Tinker & Nye, 2000) (Fig. 1.13).

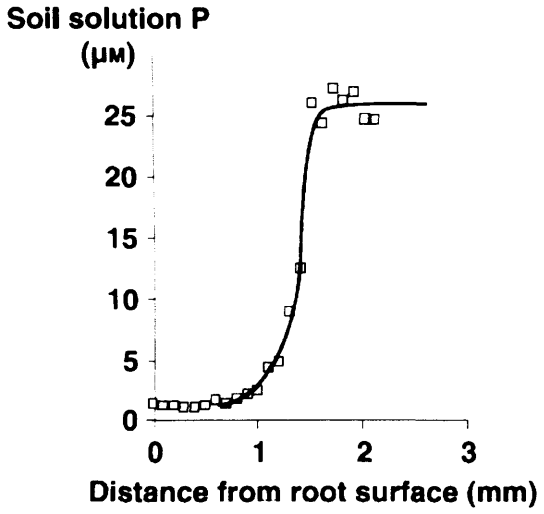

Fig. 1.13 Phosphate depletion zone in the rhizosphere of maize (*Zea mays*). Source: Hendriks *et al.* (1981).

In conditions where the transport of a certain ion to the root surface by mass flow exceeds the actual amount taken up by the root, the concentration of that ion may become elevated in rhizosphere relative to root-free soil. Under certain conditions, ion accumulation has been reported for calcium, magnesium, cadmium and chloride ions in the rhizospheres of *Lolium perenne*, *Brassica juncea*, and *Zea mays* respectively (Hinsinger & Gilkes, 1996). However, ion accumulation in the rhizosphere is likely to occur for any mobile ion for which the plant has low demand.

So far I have discussed patterns of ion availability and uptake along radial root axes. These findings are generally based on methods that treat the rhizosphere as a single experimental compartment against which average bulk soil measurements can be compared. However, when the rhizosphere is considered at greater spatial resolution it becomes apparent that uptake rates of mineral nutrients are non-uniform with respect to position along the longitudinal root axis. The spatial and temporal patterning of root uptake is perhaps the least well documented aspect of plant nutrition. Of the studies reported in the available literature, most have used plants grown in solution culture, and often in sterile conditions. Consequently, the findings may poorly reflect the trends that may occur in soils under ecologically realistic conditions. These studies have generally relied on the detection of isotopic tracers in different parts of roots after a period of exposure to a solution containing the tracer (Russell & Sanderson, 1967; Raven & Smith, 1976; Rubio *et al.*, 2004). More recently ion-selective microelectrodes have also been used (Henriksen *et al.*, 1990; Henriksen *et al.*, 1992; Colmer & Bloom, 1998; Taylor & Bloom, 1998; Papeschi *et al.*, 2000; Garnett *et al.*, 2001; Plassard *et al.*, 2002) and bacteria-based nutrient reporter assays are in use and being developed (Kragelund *et al.*, 1997; Dollard & Billard, 2003; Standing *et al.*, 2003; Taylor *et al.*, 2004).

It is often considered that the uptake of mineral nutrient ions generally decreases with increasing distance from the root apex. This assumption is logical in light of the fact that: (1) the apex is the first part of the root to come into contact with un-depleted soil; (2) replenishment of ions by mass water flow is likely to be greatest toward the root apex as a consequence of trends in water uptake (Fig. 1.12); (3) the rhizodermis and endodermis of older root regions may be suberised and therefore inhibit apoplastic movements of certain nutrient ions; and (4) nutrient demands are generally greatest at the root apex as a consequence of meristematic activity and cell elongation. With respect to the latter, mineral nutrients may be supplied not only by uptake from the external solution but also via delivery along phloem vessels either from basal root zones or from the shoot. Phloem tissues at the root apex are, however, relatively immature when compared with older root regions. As a consequence, transport of ions such as nitrate and ammonium along the phloem at root apices is impaired (Bloom *et al.*, 2002). For this reason, the nitrogen requirements of the meristematic and elongation zones are likely to be satisfied predominately by direct uptake by the root apex itself (Bloom *et al.*, 2002).

Despite the simple logic of the assumption outlined above, experimental evidence indicates that spatial and temporal patterns of mineral nutrient uptake are more complicated and highly variable. Uptake of magnesium (Grunes *et al.*, 1993), copper (Papeschi *et al.*, 2000), cadmium (Pineros *et al.*, 1998), and particularly calcium (Ryan *et al.*, 1990) is characterised by maximal influx in the elongation zone and the root apex appears to be the principal site of iron uptake (Clarkson & Sanderson, 1978). Evidence suggests that magnesium and calcium ions are taken up by an apoplastic route; therefore, their uptake is impeded in older root regions by the formation of suberin in the rhizodermal and endodermal cell layers which effectively blocks apoplastic flow (Robards *et al.*, 1973; Ferguson & Clarkson, 1975; Ferguson & Clarkson, 1976). For iron, however, greater uptake is thought to occur at the root apex because greater quantities of compounds that are associated with its uptake are released there (Clarkson & Sanderson, 1978; Marschner, 1995).

In contrast, phosphate (Rubio *et al.*, 2004), potassium (Marschner, 1995), nitrate and ammonium (Henriksen *et al.*, 1992; Colmer & Bloom, 1998; Taylor & Bloom, 1998; Garnett *et al.*, 2001) are reported to be taken-up more uniformly along the root. However, uptake of phosphate has been observed to be greater in basal than in apical root regions when barley plants are experiencing phosphate deficiency (Clarkson *et al.*, 1978). This is probably related to lower internal phosphorus concentrations in the basal zones which deliver phosphorus to apical zones under deficiency conditions (Marschner, 1995). Also, fluxes of ammonium and nitrate into the first seven centimetres of seven day-old barley roots varied both in space and time; however, the variations were not consistent between plants - each plant showed a unique uptake pattern (Henriksen *et al.*, 1990; Henriksen *et al.*, 1992). Garnett *et al.* (2001) reported similar variation in the uptake of ammonium, nitrate and protons within the region 20-600 mm from the root cap of *Eucalyptus nitens* roots.

It is worth restating that the findings summarised above are based on studies that used plants grown in solution culture. Under these conditions, nutrient ions are well dispersed, and zones of ion accumulation and depletion are less likely to develop. Therefore, while these studies demonstrate that roots have the capacity to take up poorly mobile ions such as phosphate or ammonium more or less anywhere along the longitudinal root axis, it is likely that in soil, their uptake at the root base would be greatly reduced due to their depletion in the surrounding soil. On the other hand, uptake

trends observed in plants grown in solution culture for highly mobile ions such as nitrate are likely to be more representative of those associated with soil grown plants.

Other root processes also influence rhizosphere soil solution ion activities such as the release of H^+ or HCO_3^- ions (and CO_2) which change the pH (Hinsinger *et al.*, 2003); or O_2 consumption or release which may alter the redox potential (Mancuso *et al.*, 2000). In addition, low molecular weight root exudates can mobilise mineral nutrients directly, by processes such as acidification, chelation, ligand exchange and/or enzymatic hydrolysis; or indirectly, by providing a substrate for microorganisms that release exudates that directly mediate nutrient availability or enhance the mineralization of soil organic matter.

1.4.3.2.2. The influence of rhizosphere microorganisms on nutrient uptake

Barber (1967) compared the nutrient uptake of barley plants grown under (a) sterile, and (b) non-sterile conditions in hydroponics. The presence of bacteria was found to decrease phosphate and ammonium uptake and increase nitrate and metal uptake. Decreased phosphate uptake was thought to be due to competition and was most apparent at low total phosphate concentration at higher pH. The root systems of many plant species form mutualistic associations with mycorrhizal fungi (Marschner, 1995). This association is established when individual hyphae extend from the fungal mycelium and colonise the roots of a host plant either intracellularly or extracellularly. Those that colonise intracellularly are known as endomycorrhizal fungi whereas those that colonise extracellularly are known as ectomycorrhizal fungi. The fungi obtain carbon from the plant that they use to proliferate throughout the soil exploring for nutrients such as phophorus, and the plant benefits from this activity through enhanced phophorus acquisition (Marschner, 1995). Mycorrhizal symbiosis also exerts a strong influence on rhizosphere bacterial communities (Andre *et al.*, 2003), although this will be discussed in section 1.5.

1.4.3.3. Rhizodeposition

1.4.3.3.1. Terms and definitions

Of all root-mediated processes that influence bacterial communities, rhizodeposition (the loss of carbon from roots) has received the greatest attention. In soils, carbon availability is often a factor that limits bacterial population sizes (Nunan *et al.*, 2003); therefore, elevated concentrations of organic carbon compounds, resulting from rhizodeposition, are thought to be key to the establishment of greater bacterial densities in the rhizosphere when compared with root-free soil (Semenov *et al.*, 1999; Marschner *et al.*, 2004). Prior to exploring this phenomenon further, it will be useful to describe the nature of rhizodeposits in more detail.

In this discussion, a rhizodeposit is defined as any root-derived product that contains carbon. Rhizodeposits are extremely diverse and differ in their relative recalcitrance and function; therefore, it is useful to adopt some additional terms that help to identify characteristics such as their mode of arrival, their function and/or their availability to microorganisms (Table 1.4).

Table 1.4 Definitions of terms that are use to classify rhizodeposits and processes relating to rhizodeposition.

Root exudates	A plethora of soluble compounds that are released from roots (Table 1.6). These fall into two categories: (1) those that are lost by passive diffusion and over which the plant is able to exert little control (basal exudation), and (2) those which are released for a specific purpose and over which the plant is able to exert a high degree of control (Jones *et al.*, 2004).
Root exudation	The process by which root exudates are released. This is thought to be largely passive; however, in contrast to the first category of exudates (above) over which the plant is able to exert little control, diffusion of exudates in the second category (above) is thought to be regulated by membrane pores such as anion channels (Jones, 1998; Jones *et al.*, 2004).
Leakages	Exudates release without the expenditure of energy (Whipps, 1990).
Secretions	Exudates that require energy expenditure for release (Whipps, 1990).
Mucilages	Mucilages are generally composed of hydrated, complex polysaccharides such as pectin and hemicellulose (Samstevich, 1968; Floyd & Ohlrogge, 1970; Miki *et al.*, 1980) and in the rhizosphere they derive from peripheral root cap cells, epidermal cells with only a primary cell wall (e.g. root hairs), bacterial degradation of old epidermal cells (Curl & Truelove, 1986).
Mucigel	Mucilaginous sheets that may cover sections of the root and typically bacteria inhabiting the junctions between epidermal cells.
Sloughed-off cells and dead tissues	Includes root border cells and root border-like cells associated with root apices, but also cells that may be lost due to damage and eventually whole dead roots. The number of root border cells produced per root in a 24 h period varies from approximately a hundred for the nightshade family, to several thousand for cereals and legumes, to 10,000 for pine and cotton (Hawes *et al.*, 2003).
Lysates	Cell contents leaked from sloughed-off cells and dead tissues upon lysis or from cortical and rhizodermal cells upon autolysis or physical damage.
Volatiles	Compounds including alcohols, fatty acids, alkyl sulfides, and carbon dioxide (Curl & Truelove, 1986) that are volatile upon release. These may diffuse over greater distances than liquid and solid phase rhizodeposits.

1.4.3.3.2. How large are different pools of rhizodeposits?

Estimates for total allocation of photosynthates to roots range between 30-50 % for pasture plants and 20-30 % for cereals such as wheat and barley (Kuzyakov & Domanski, 2000). For cereals, roughly half of this carbon remains in the roots, while approximately one third is released from the rhizosphere by root or microbial respiration within a few days; the remaining fraction of carbon allocated below ground is incorporated into the microbial biomass and soil organic matter (Kuzyakov & Domanski, 2000). In a comparison of four methods used to separate and quantify root and microbial respiration in the rhizosphere, Kuzyakov *et al.* (2001) concluded that the most reliable technique indicated that root respiration contributes about 40-50 % of the CO_2 flux from the rhizosphere, while microbial respiration relating to the assimilation of rhizodeposits contributes the remaining 50-60 %. However, estimates of carbon economies within plants are controversial and vary considerably between different workers (Fig. 1.14). This is largely due to methodological problems that limit the determination of the relative sizes and origins (root or microbial) of various pools of rhizodeposits (e.g. exudates, lysates, mucilages, volatiles, sloughed-off cells and tissues).

In the case of non-volatile rhizodeposits, analytical techniques generally require that soil solution is filtered prior to any measurements; therefore, carbon compounds contained within sloughed-off root cells and tissues are likely to be neglected. This pool may represent a considerable fraction of total rhizodeposition; for example, as noted previously, carbon contained within the root border cells of maize, may represent 10 % of all rhizodeposition (Iijima *et al.*, 2000). Further research is necessary to improve our understanding of the fate of such cells in the rhizosphere which is likely to follow one of three scenarios: (1) cell dies immediately, resulting in cessation of metabolic activity and a more or less immediate release of all carbon and nutrients; (2) cell remains metabolically active and may contribute to rhizodeposition by releasing carbon-containing exudates, volatiles and/or mucilages before carbon reserves are eventually depleted or leaked by cell lysis; and (3) prior to detachment from the root, carbon and nutrient reserves are re-translocation to other growing areas of the plant.

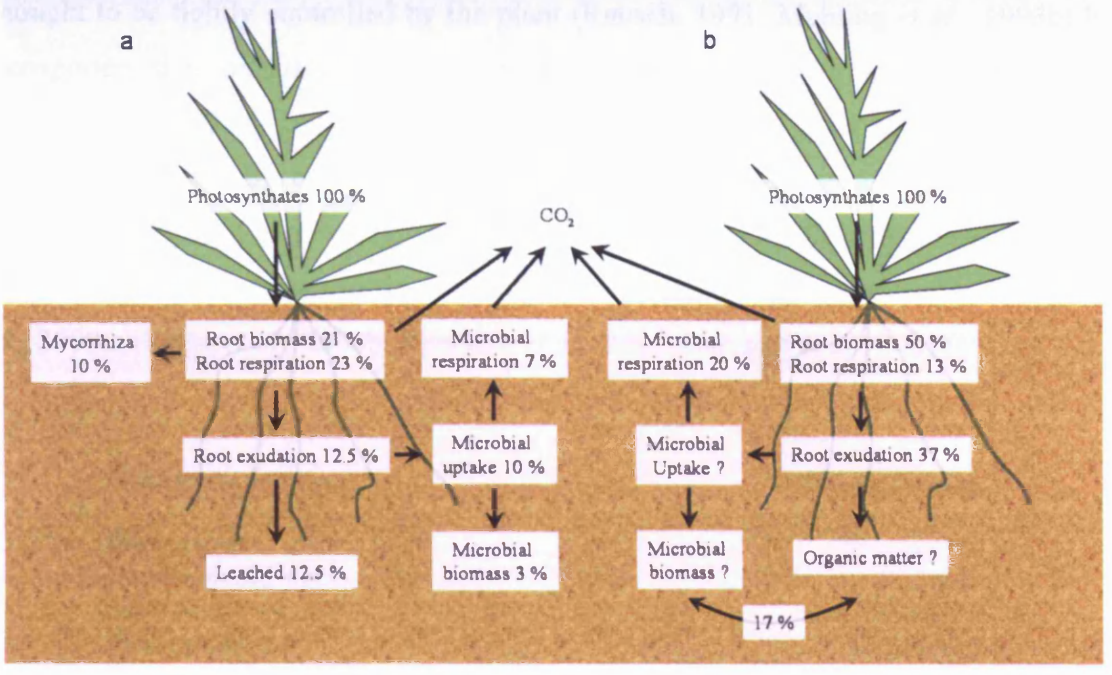

Fig. 1.14 The partitioning of carbon within a plant and the distribution of root exudates within the soil according to (a) Farrar *et al.* (2003), and (b) Kuzyakov & Domanski, (2000).

A further methodological problem results from the fact that the quantity and composition of rhizodeposition varies in time and in space with respect to position on the root (McDougal & Rovira, 1970; Vanegeraat, 1975; Jaeger *et al.*, 1999; Darwent *et al.*, 2003). Current methods fail to allow measurements at high spatial resolution and, as is the case with most soil solution sampling approaches, enable only a snapshot in time. Furthermore, rhizodeposition is influenced by many factors (Fig. 1.15). Despite this, most rhizosphere carbon-flow research has been undertaken in laboratory microcosms, often under sterile conditions and in the absence of soil. This is a problem because in addition to changes in its composition, rhizodeposition appears to be increased in the presence of solid rooting media as opposed to solution culture, and also by environmental stress (e.g. phosphate or iron deficiency) and the presence of microorganisms (Jones & Darrah, 1992; Jones & Darrah, 1993a; Jones & Darrah, 1993b; Muhling *et al.*, 1993a). In addition, current evidence suggests that a number of root-derived carbon-containing compounds can be actively reabsorbed along the length of the root (Jones *et al.*, 2004). Reabsorption is particularly relevant for those compounds that are released in the greatest quantities such as sugars and amino acids (Farrar *et al.*, 2003) which, in absence of a microbial, and soil colloidal sink, leads to

their underestimation in sterile, solution culture. In contrast to exudation, recapture is thought to be tightly controlled by the plant (Rausch, 1991; Muhling *et al.*, 1993b) by transporters that are also used for mineral nutrient uptake such as H^+-cotranporters (Jones *et al.*, 2005). Generally, recapture is likely to be of little significance to net carbon acquisition by photosynthetic plants but its significance as a mechanism of nitrogen acquisition is now being investigated (Jones *et al.*, 2004). It should be noted that the plant is also in competition with microorganisms for these resources (Hodge *et al.*, 2000a; Hodge *et al.*, 2000b; Korsaeth *et al.*, 2001; Bardgett *et al.*, 2003).

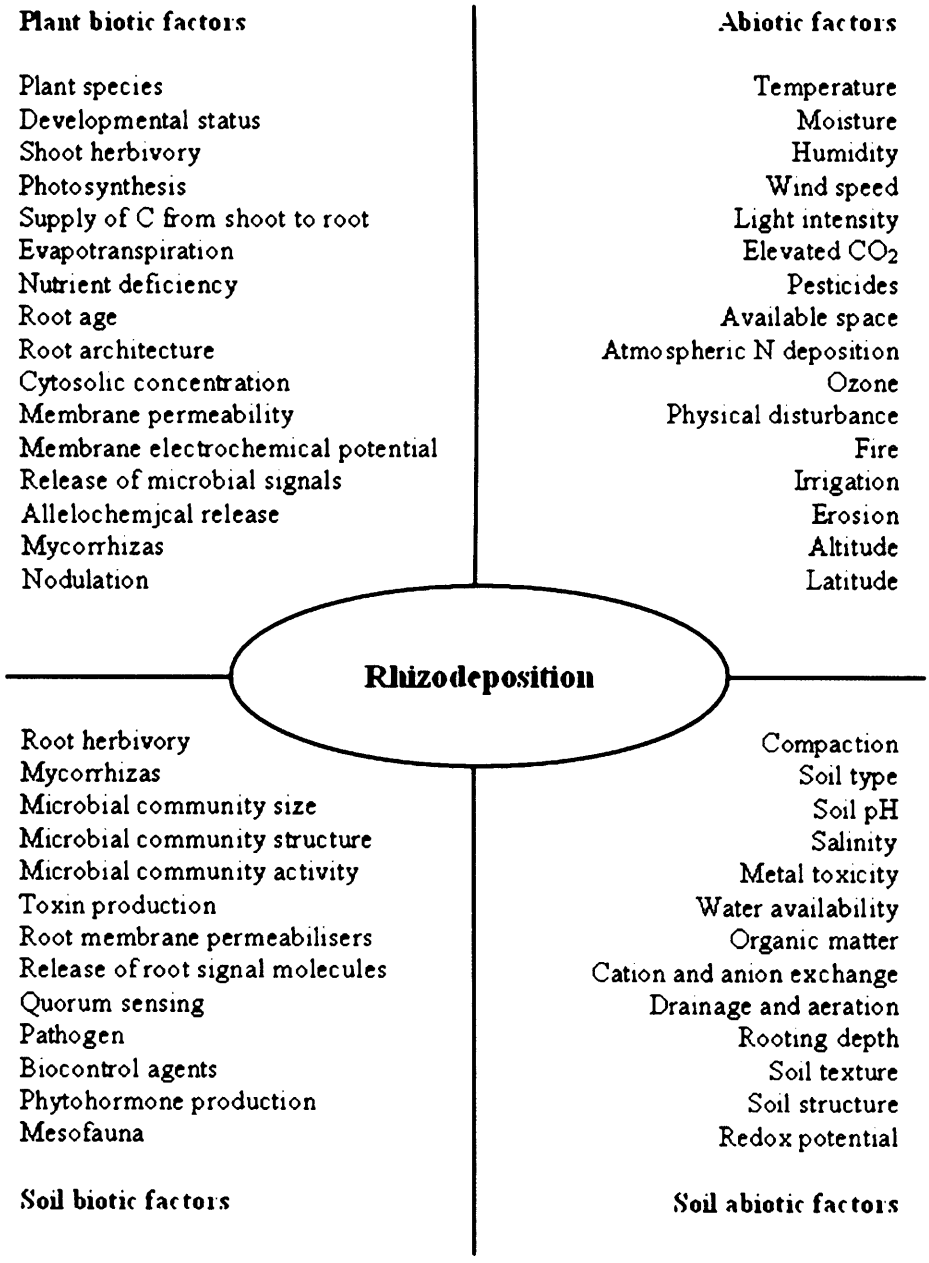

Fig. 1.15 Factors influencing rhizodeposition. Source: Jones *et al.* (2004).

1.4.3.3.3. What compounds are usually found in rhizodeposits and what do they do?

The constituents of rhizodeposits often found in rhizosphere soil solution are summarised in Table 1.5. As discussed in the last section, most studies have involved the analysis of rhizodeposits in filtered solutions recovered from sterile, hydroponic cultures at coarse spatial and temporal resolution (Jones, 1998; Abadia *et al.*, 2002; Neumann & Martinoia, 2002); therefore, most previous work can be viewed as being qualitative rather than quantitative.

In addition to stimulating microbial proliferation in the rhizosphere, there is a wealth of literature implicating various rhizodeposits in different roles or functions. Few suggestions have been established and the majority remain ambiguous. Table 1.6 summarises the possible functions attributed to various rhizodeposits. Many of these compounds are released in greater quantities under conditions where their presence may confer a benefit to the plant. For example, the exudation of organic acids, which are thought to help mobilise sparingly soluble phosphates, is increased in response to phosphate deficiency (Uren, 2001).

The composition of rhizodeposits is purported to influence bacterial communities as a result of the competitive interactions between populations that differ in their affinity to utilise the available carbon compounds (Marschner *et al.* 2004). Factors that influence the quantity and composition of rhizodeposits may therefore indirectly affect bacterial community composition and diversity. However, the extent to which bacterial communities respond to shifts in rhizodeposition is poorly understood.

Table 1.5 Organic compounds release by plant roots*.

Sugars:

Arabinose, fructose, galactose, glucose, maltose, mannose, mucilages of various compositions, oligosaccharides, raffinose, rhamnose, ribose, sucrose, xylose, desoxyribose

Amino acids:

α-Alanine, β-alanine, γ-aminobutyric, α-aminoadipic, arginine, asparagine, aspartic, citrulline, cystathionine, cysteine, cystine, deoxymugineic, 3-epihydroxymugineic, glutamine, glutamic, glycine, histidine, homoserine, isoleucine, leucine, lysine, methionine, mugineic, ornithine, phenylalanine, praline, proline, serine, threonine, tryptophan, tyrosine, valine

Organic acids:

Acetic, aconitic, ascorbic, aldonic, benzoic, butyric, caffeic, citric, p-coumaric, erythronic, ferulic, formic, fumaric, glutaric, glycolic, lactic, glyoxilic, malic, malonic, oxalacetic, oxalic, p-hydroxybenzoic, piscidic, propionic, pyruvic, succinic, syringic, tartaric, tetronic, valeric, vanillic

Fatty acids:

Linoleic, linolenic, oleic, palmitic, stearic

Sterols:

Campesterol, cholesterol, sitosterol, stigmasterol

Growth factors and vitamins:

p-amino benzoic acid, biotin, choline, N-methyl nicotinic acid, niacin, pathothenic, thiamine, riboflavin, pyridoxine, pantothenate,

Enzymes:

Amylase, invertase, peroxidase, phenolase, acid/alkaline phosphotase, polygalacturonase, protease

Flavonones and purines/nucleotides:

Adenine, flavonone, guanine, uridine/cytidine

Miscellaneous:

Auxins, scopoletin, hydrocyanic acid, glucosides, unidentified ninhydrin-positive compounds, unidentifiable soluble proteins, reducing compounds, ethanol, glycinebetaine, inositol and myo-inositol-like compounds, Al-induced polypeptides, dihydroquinone, sorgoleone, isothiocyanates, inorganic ions and gaseous molecules (e.g. CO_2, H_2, H^+, OH^-, HCO_3^-), some alcohols, fatty acids and alkyl sulphides.

*Adapted from Uren (2001), Curl and Truelove (1986), and Dakora and Phillips (2002).

Table 1.6 Functional role of rhizodeposits in the rhizosphere*

Component	Rhizosphere function
Sugars	Nutrient source for microorganisms
Amino acids and phytosiderophores	Nutrient source for microorganisms; chelators of poorly soluble mineral nutrients; chemoattractant signals to microbes
Organic acids	Nutrient source for microorganisms; chemoattractant signals to microbes; chelators of poorly soluble mineral nutrients; acidifiers of soil; detoxifiers of Al; nod gene inducers
Phenolics	Nutrient source for microorganisms; chemoattractant signals to microbes; microbial growth promoters; nod gene inducers/inhibitors in rhizobia; resistance inducers against phytoalexins; chelators of poorly soluble mineral nutrients (e.g. Fe); detoxifiers of Al; phytoalexins against soil pathogens
Vitamins	Promoters of plant and microbial growth; nutrient source for microorganisms
Purines	Nutrient source for microorganisms
Enzymes	Catalysts for P release from organic molecules; biocatalysts for organic matter transformation in soil
Root border cells	Produce signals that control mitosis; produce signals controlling gene expression; stimulate microbial growth; release chemoattractants; synthesize defence molecules for the rhizosphere, act as decoys that keep root cap infection free; release mucilage and proteins

*Adapted from Dakora and Phillips (2002).

1.4.3.3.4. Range of influence of various rhizodeposits

As with nutrient ions, soluble rhizodeposits differ in their relative mobility in soil; therefore, the radial distance that they travel from the root surface before adhering to soil colloidal surfaces is dependant on their species (Fig. 1.16). This results in every position in the rhizosphere being chemically unique.

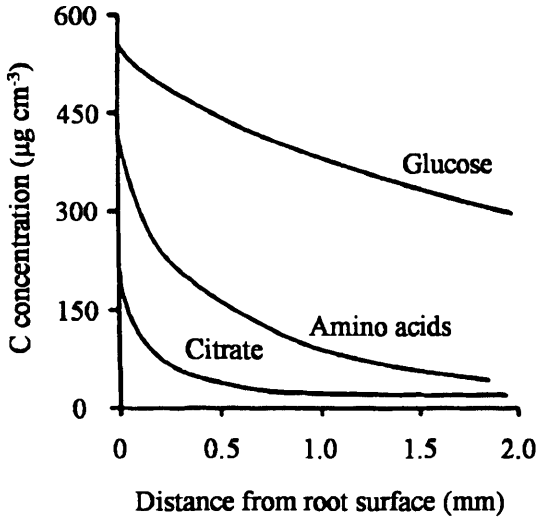

Fig. 1.16 Gradients of three rhizodeposits with increasing distance from the rhizoplane, showing that each position in the rhizosphere is unique. Source: Jones *et al.* (2004).

In comparison to other soluble pools of rhizodeposits (e.g. lysates and secretions), root exudates are well documented. Current evidence suggests that root exudation occurs primarily from the meristematic regions of roots (McDougal & Rovira, 1970; Vanegeraat, 1975; Jaeger *et al.*, 1999; Darwent *et al.*, 2003) and most researchers hold the opinion that exudates are rapidly mineralised by microorganisms (Nguyen *et al.*, 1999; Kuzyakov & Cheng, 2001). For example, Ryan *et al.* (2001) reported that most amino acids, sugars and organic acids are mineralised with a half-life of between thirty minutes and two hours when added to the rhizosphere at ecologically realistic concentrations. However, these estimates were arrived at by adding exudates to a root mat – a dense population of roots formed at the base of a container in which a plant is grown as a consequence of spatial constraint. For this reason, the measured mineralization rates were averages for the whole rhizosphere and were likely to have been overestimated. This is because the density of bacteria at the apex of roots growing

'naturally' in soil is low when compared with the root base (Semenov *et al.*, 1999; Duineveld *et al.*, 2001; Marschner *et al.*, 2002). Further work is necessary to elucidate the mineralization rates of various root exudates in more natural systems.

Once assimilated by the microbial biomass, carbon contained in the rhizodeposits may be rapidly lost by respiration; however, part will return to the rhizosphere in the form of microbial excretions or lysates upon cell death. The temporal scales over which these events occur are yet to be determined as are the effects of microbial transformations of carbon-containing compounds on bacterial community structure. However, given that current evidence suggest that very subtle changes in the rhizosphere environment or the plant can induce rapid shifts in the quality and quantity of exudative fluxes (Dilkes *et al.*, 2004), it is necessary to develop methods that facilitate the measurement of root exudates and characterisation of bacterial communities at high spatial and temporal resolution.

1.4.3.3.5. Influence of rhizodeposition on bacterial distribution

To date, spatiotemporal patterns of rhizosphere bacteria have primarily been described in relation to root exudation using computer models (Newman & Watson, 1977; Darrah, 1991b; Darrah, 1991a; Scott *et al.*, 1995; Semenov *et al.*, 1999; Zelenev *et al.*, 2000). These models generally describe microbial growth using classic bacterial growth equations (Monod, 1942) coupled with equations describing how growth substrates are transported from the root surface through the soil (Darrah & Roose, 2001). Newman and Watson (1977) modelled bacterial dynamics along the radial axis of a root in relation to the concentration of soluble carbon compounds exuded from it. Darrah (1991a) later modified these equations to account for microbial death, carbon recycling, and the deposition of insoluble rhizodeposits, while in a follow-up paper Darrah (1991b) reported a model that investigated bacterial dynamics along the longitudinal axis of a root. This model predicted bacterial biomass and necromass carbon along the length of a root in response the release of 62.8 μg soluble C per cm root. Two strategies of exudate release were simulated: in the first simulation (S1), the exuding surface was assumed to be confined to a region extending 0.5 cm basipetally along the rhizoplane from the root tip, while in the second simulation (S2) this region extended for 5 cm. These strategies were designed to simulate experimental evidence

indicating that exudation is greatest at the root apex (McDougal & Rovira, 1970; Norton *et al.*, 1990). Figure 1.17 illustrates the simulated bacterial biomass and necromass associated with the S1 simulation over time. The trend observed for the S2 simulation was similar although the radial extent of the rhizosphere extended just 0.9 mm from the root surface and the peak biomass C lagged considerably further behind the peak C concentration, with a lag of approximately 3.75 cm as apposed to 0.6 cm for the S1 simulation. The model clearly demonstrates a wave of peak bacterial density following the root tip through the soil and predicts lower numbers of bacteria at the root base. This is in contrast with the findings of other authors which indicate that bacterial density follows the general trend: basal region > bulk soil > apical region (Parke *et al.*, 1986; Olsson *et al.*, 1987; Liljeroth *et al.*, 1991; Chin-A-Woeng *et al.*, 1997; Duineveld & Van Veen, 1999). There are very few examples where bacterial densities at the root apex are reported to be greater than those at the base. The study by Naim (1965) is one example; however, this study investigated the distribution of bacteria on the roots of *Aristida coerulescens* grown in the Libyan Desert. As a result it is likely that the scarcity of bacteria at the root base reflects a low abundance of bacteria in the soil of upper horizons that is likely to occur as a consequence of environmental factors (e.g. high temperatures, very low water content, ultraviolet irradiation, and high salinity) rather than a trend that is in direct agreement with the modelled predictions of Darrah (1991b). Another example where high numbers where found at the root apex is the study by van Vuurde and Schippers (1980); however, these workers observed a peak of bacterial density at the root base as well as at the apex. They suggested that this may reflect two sources of rhizodeposits: (1) exudates which are thought to be released predominately at the root tip, and (2) lysates which they deduced from observations of cell integrity to be more prevalent around the root base. This clearly demonstrates the need to consider the effects of other sources of rhizodeposits as well exudates. The group of Ariena van Bruggen at Wageningen in the Netherlands have reported two investigations designed to demonstrate a link between the spatial distribution of bacteria and total organic carbon (TOC) concentrations in the rhizosphere of wheat plants grown in rhizotrons containing soil (Maloney *et al.*, 1997; Semenov *et al.*, 1999). In both studies, their results indicated that spatial patterns of rhizosphere bacteria were not linked to the concentration of water soluble carbon along the roots; however, given the difficulty of such investigations (section 7.1), further evidence to either support or reject these findings is currently unavailable.

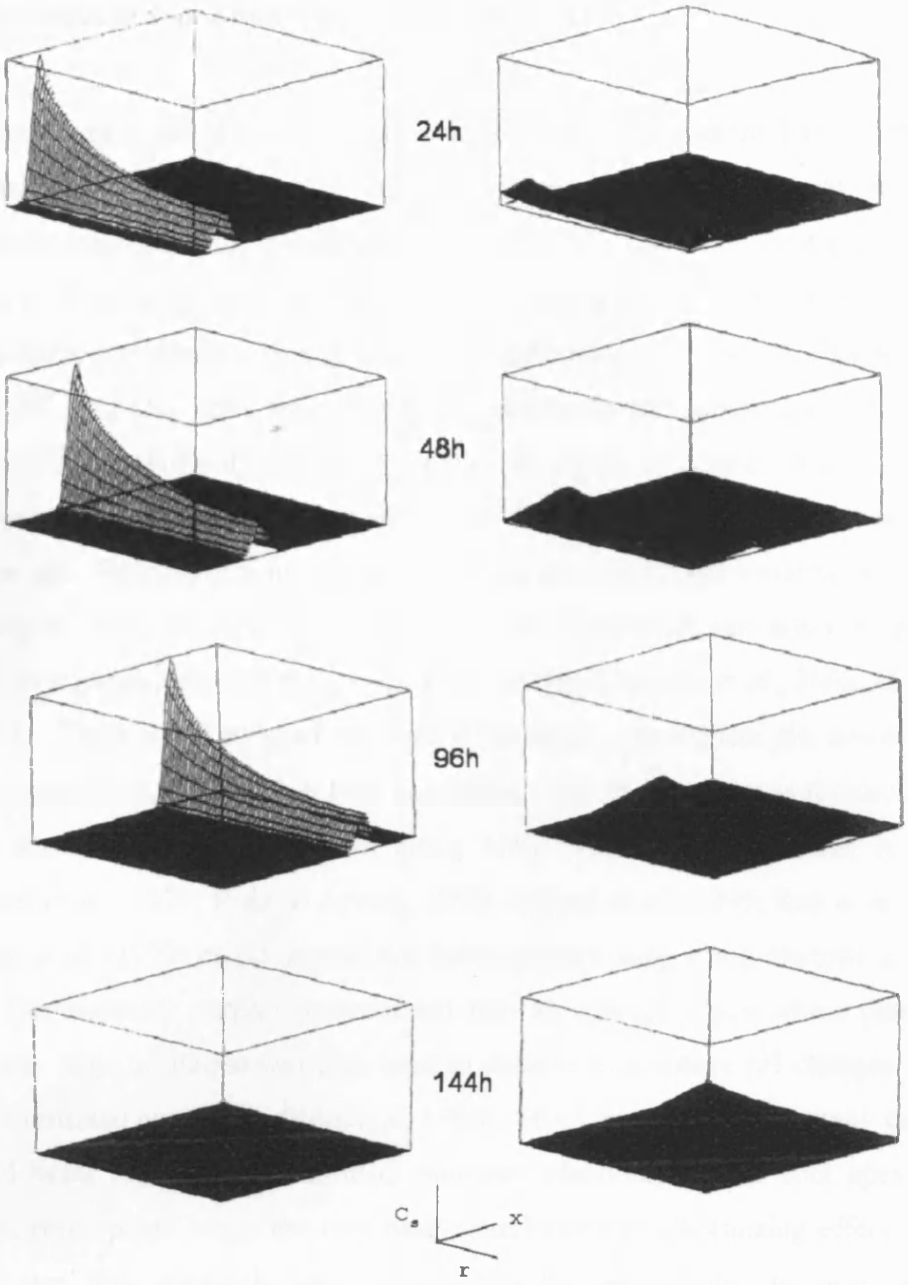

Fig. 1.17 Spatiotemporal pattern of bacterial biomass C (left) and necromass C (right) (μg C cm^{-3}) within a 5 cm cylinder of rhizosphere soil at different times for the S1 simulation. The direction of the axes, r (radial distance from the rhizoplane; cm), x (longitudinal distance from root tip), C_m and C_n (microbial biomass C and necromass C repectively) are shown in the diagrams at the bottom of each column. Source: Darrah (1991b).

1.4.3.4. Influence of root processes of rhizosphere pH

As noted previously, soil pH is a critical parameter that influences the bioavailability of many nutrients (Fig. 1.5) and strongly influences the physiology of roots and rhizosphere microorganisms (Hinsinger *et al.*, 2003). Therefore, root-mediated pH changes are of considerable importance to the ecology of the rhizosphere and its associated flora and fauna. A key process contributing to these pH changes is the release of H^+ and OH^- ions from roots to compensate for unbalanced cation-anion uptake, or rhizodeposition (Marschner, 1995). However, in neutral to alkaline soils, carbon dioxide released by respiring roots may form carbonic acid, contributing to a decrease in pH. Rhizosphere microorganisms can also contribute towards pH changes by releasing H^+ and OH^- ions to to compensate for unbalanced cation-anion uptake or release, or as a consequence of their respiratory activity (Carrillo *et al.*, 2002; Hinsinger *et al.*, 2003). There are many methods used to determine rhizosphere pH; however, few allow for spatial mapping of pH at high resolution. This is necessary as rhizosphere pH has been shown to differ greatly in along both radial and longitudinal root axes (Weisenseel *et al.*, 1979; Ruiz & Arvieu, 1990; Jaillard *et al.*, 1996; Rao *et al.*, 2002). Weisenseel *et al.* (1979) demonstrated this heterogeneity using a non-phytotoxic pH dye indicator (bromocresol purple) incorporated into an agar gel upon which plant roots were grown. This technique was then used to observe rhizosphere pH changes under a range of nutritional conditions (Römheld, 1986), which revealed that in many cases the apical and basal root regions exhibited opposite behaviour, i.e. the root apex would acidify the rhizosphere while the root base would exert an alkalinising effect, or *vice versa.* Later this approach was combined with densitometry to provide more quantitative information (Ruiz & Arvieu, 1990; Jaillard *et al.*, 1996). However, the technique was designed to measure pH changes in gels rather than soils; therefore, the information provided may poorly represent 'real' trends. Jaillard (1987) tried to overcome this problem by placing a gel over the surface of roots grown in rhizotrons containing soil; however, problems with root/soil – gel contact meant that the approach was unreliable. Another approach involves the use of pH microelectrodes. These have been successfully applied to the roots of spruce seedlings grown in soil for which alkalisation was observed predominantly at the root apices (Haussling *et al.*, 1985). An additional advantage of this technique is that it is non-destructive, thus facilitating repeated measurements over time.

1.4.4. Summary

The presence and activities of roots in soil give rise to a unique environment that is distinct from that of root-free soil. Along both longitudinal and axial root axes, soil physical, chemical and biological conditions are highly heterogeneous at a range of spatiotemporal scales. This gives rise to a vast array of microhabitats in which rhizosphere microorganisms may or may not proliferate. The following section deals with the factors that enable bacteria to colonise and compete within this environment, and will lead on to the objectives of this thesis.

1.5. Rhizosphere bacteria

The impact of rhizosphere bacteria on plant growth was highlighted by the study of Cambell and Greves (1990) in which 150 *Pseudomonas* spp. were isolated from the wheat rhizosphere and then reintroduced separately on wheat seedlings. Root growth was stimulated by 40 % of the isolates, while 40 % inhibited it and 20 % had no significant effect. Rhizosphere bacteria can affect plant growth by causing or suppressing disease, by producing phytohormones, plant growth regulators, or other biologically active substance, or by modulating the availability of nutrients or toxic elements (Lugtenberg *et al.*, 2002). Rhizosphere bacteria that exert beneficial effects on plant productivity are referred to as plant growth promoting rhizobacteria (PGPR) (Kloepper & Schroth, 1978) and many have been isolated from the rhizosphere of different plant species (Zahir *et al.*, 2004); however, their exploitation has resulted in mixed successes. Further work is necessary to improve our understanding of the factors that influence the competency and competitiveness of different bacterial species in the rhizosphere of environmentally or economically interesting plant species.

1.5.1. Bacterial competency and competitiveness in the rhizosphere

To establish themselves in the rhizosphere, bacteria should be able to survive there, make use of rhizodeposits, be able to effectively colonise the root or the rhizosphere soil, proliferate and be able to compete with other organisms. Over the past twenty years, considerable progress has been made in understanding the traits and genes that

facilitate effective rhizosphere colonisation. Although not established in some studies (Howie *et al.*, 1987), motility appears to be an important trait for rhizosphere colonisation (Deweger *et al.*, 1987; Simons *et al.*, 1997). Motility requires the use of flagella and the expenditure of energy; therefore, colonisation ability can be decreased if either flagella or ATP production is disrupted. For example, Dekkers *et al.* (1998a, 1998b) screened a library of random transposon mutants of *P. fluorescens* WCS365 for colonisation traits. In one colonisation defective mutant they found an insertion in a member of the lambda integrase family of site-specific recombinases (*xer*C/*sss*) which in *Salmonella typhymurium* regulates the production of flagella (Dekkers *et al.*, 1998a). In another colonisation defective mutant they found an insertion in the *nuo*4 gene encoding one of the subunits of NADH:ubiquinone oxidoreductase, NADH dehydrogenase which is involved in the generation of proton motive force that is used for synthesis of ATP, active transport of various nutrients and ATP-dependent rotation of flagella (Anraku & Gennis, 1987). Another trait that is important in effective root colonisation by bacteria is their growth rate. Growth rate is partly dependent on an organisms ability to obtain components that are essential for growth and/or maintenance. Therefore, it is not surprising that growth rate has been linked with the ColR/S two-component system for uptake of certain root exudates (de Weert *et al.*, 2006), the proton motive force generated by NADH dehydrogenase encoded by the *nuo*4 gene, and the ability to synthesise amino acids and vitamin B1 (Simons *et al.*, 1997), and utilise organic acids (Wijfjes *et al.* unpublished data, cited in Bloemberg & Lugtenberg, 2001). Evidence suggests that the O-antigen of lipopolysaccharide (LPS) is also important in regulating growth rates (Dekkers *et al.*, 1998b). In summary, the ability for a bacterial cell to move towards a root in response to rhizodeposition (chemotaxis) and grow rapidly are important traits that enable a bacterial species to be competitive within the rhizosphere environment.

Rhizosphere bacteria include species that are adapted to growth in carbon rich as well as carbon poor environments. Species that are generally more competitive in carbon rich environments are known as copiotrophs (Poindexter, 1981; Semenov, 1991); while those that favour carbon poor environments are called oligotrophs (Poindexter, 1981). Soil and even rhizosphere environments can be considered as oligotrophic with carbon concentrations ranging from 10-100 μg C per gram of dry soil (Darrah, 1991a); therefore, oligotrophs may be quite common due to carbon limitation inherent in the environment or due to depletion by microorganisms as a consequence of competition

(Morita, 1988). In the rhizosphere of lettuce, Maloney *et al.* (1997) found that the ratio of copiotrophic to oligotrophic bacteria was high at the root apex and declined towards the root base. However, for tomato they found the opposite pattern and suggested that their observations may reflect differences in the quantity and quality of rhizodeposits. The idea that rhizosphere bacteria are selected by the plant through the nature of its rhizodeposits has also been expressed by Marschner *et al.* (2004) who found that the composition of rhizosphere bacterial communities differed with plant species. This has contributed to the assumption that a greater proportion of bacteria are likely to be cultivable in the rhizosphere when compared with those in root-free soil which current evidence would appear to support (van Veen, 2004).

1.5.2. Rhizosphere bacterial distribution patterns

In the rhizosphere, spatial patterns in the structure of bacterial communities have been demonstrated at scales of several centimetres (macro-scale) to several micrometers (micro-scale). At the macro-scale, microscopic or culture based investigations have revealed that bacterial densities generally decrease with increasing distance from the root base to the root apices (Parke *et al.*, 1986; Olsson *et al.*, 1987; Liljeroth *et al.*, 1991; Chin-A-Woeng *et al.*, 1997; Duineveld & Van Veen, 1999), and the species that form these communities have been shown, by culture dependent and independent methods, to differ along longitudinal root axes (Semenov *et al.*, 1999; Duineveld *et al.*, 2001; Marschner *et al.*, 2002). At the micro-scale, scanning electron microscopy has revealed that bacteria at the root base are clustered, whereas at the root apices, bacteria are present as single cells (Chin-A-Woeng *et al.*, 1997). However, further information at this scale is limited, due to a lack of appropriate experimental techniques. While microscopic observations can provide useful information about the distribution of bacteria at the micro-scale, investigations of other features, such as bacterial diversity, require that samples are taken. Chapter three of this thesis concerns the development of a novel method that addresses this problem.

The influence of rhizodeposition on rhizosphere bacterial distribution trends was discussed in section 1.4.3.3.5, which highlighted the problems associated with investigating this relationship. It is likely that this is due, at least in part, to a lack of consideration of other factors that influence the distribution of bacteria in this complex

environment. For example, increased nitrate concentrations have been shown to increase bacterial numbers on roots (Griffiths *et al.*, 1992; Elliott *et al.*, 2003). Additional evidence in support of this observation is provided by Marschner *et al.* (1999) who used *P. fluorescens* 2-79RLI containing *lux* genes driven by a constitutive promoter to compare root colonisation of wheat plants grown in hydroponics under different nitrogen concentrations and nitrogen sources. Nitrogen deficiency decreased root growth and root colonisation at the root tip while it had no effect on root colonisation in the lateral zone. Ammonium nutrition increased root colonisation at the root tip and lateral zones when the pH was allowed to change according to the nitrogen form provided; however, when maintained at pH 6.5, nitrogen source had no effect on root colonisation. They concluded that the increase in bacterial colonisation under ammonium nutrition may be due to enhanced exudation at low pH. This idea is supported by Mahmood *et al.* (2002; 2005) who found that bacteria density was increased in the rhizosphere of nitrate and ammonium fertilised maize plants but unaffected in bulk or unplanted soil.

Rhizosphere bacterial distributions are also influenced by biological interactions. For example, bacterial densities have been observed to oscillate along the longitudinal axes of roots with population densities of predators (Semenov *et al.*, 1999; Zelenev *et al.*, 2004). In addition, the composition of microbial communities associated with roots infected with mycorrhizal fungi differs greatly from those associated with non-infected roots (Katznelson *et al.*, 1962; Garbaye & Bowen, 1989; Garbaye, 1991). This is thought to relate to specific relationships between mycorrhizal fungi and mycorrhizophere[4] bacteria, such as competition and inhibition (André *et al.*, 2003); for instance, population densities of rhizosphere fluorescent pseudomonads can be decreased by mycorrhizal infection of roots (Meyer & Linderman, 1986; Andrade *et al.*, 1997; Filion *et al.*, 1999).

It is generally assumed that bacterial densities at root apices are low as a result of rapid root elongation. The best example of this interaction can be observed on the roots of directly drilled crop plants. The agricultural practice of 'direct drilling', which involves planting seeds in narrow drill holes created in non-tilled soil, is designed to minimise erosion and preserve soil structure; however, the practice generally leads to reduced

[4] The mycorrhizophere is a term used to describe the soil influenced by a root infected with a mycorrhizal fungus Pinton *et al.* (2001).

crop yield when compared to inversion tillage (Chan *et al.*, 1987). A number of studies have demonstrated that root growth rates are lower in non-tilled soils than in tilled soils as a consequence of soil strength - relatively hard non-tilled soil impedes root growth (Chan *et al.*, 1987). Current evidence suggest that poor crop yields under direct drilling relate to the interaction between root growth rate and the accumulation of rhizosphere bacteria, particularly those belonging to the genus *Pseudomonas* (Chan *et al.*, 1987; Simpfendorfer *et al.*, 2001; Simpfendorfer *et al.*, 2002). Watt *et al.* (2003) investigated this interaction using wheat roots grown in field soils that differed in strength. Strong soils resulted in slower growing roots when compared with those growing in weaker soil. They found that the density of *Pseudomonas* spp. at root apex was inversely proportional to the rate of root elongation; however, for total bacteria, this trend was only observed on the roots of plants grown in the field.

1.5.3. Potential consequences of rhizosphere bacterial distribution patterns

The spatial distribution of rhizosphere bacteria is likely to be of great importance when considering processes such as plant-bacterial nutrient competition, bacterial mediated modifications to root development (Costacurta & Vanderleyden, 1995), and plant disease (Weller, 1988; Zahir *et al.*, 2004). In addition, current evidence suggests that the effect of bacteria within the rhizosphere is density dependant (Persello-Cartieaux *et al.*, 2003) and that cell density may influence bacterial gene expression and cell to cell communication by quorum sensing (Savka *et al.*, 2002; Bauer & Mathesius, 2004; Schuhegger *et al.*, 2006). Bacteria at the root apex may have a negative effect on plant growth by competing with roots for nutrient ions, consuming nutrient-mobilising rhizodeposits, or exhibiting phytopathogenic behaviour. However, they may also benefit plant growth by mobilising nutrients through the release of nutrient-mobilising compounds or by transforming ions to species that require less energy expenditure for uptake (e.g. nitrate to ammonium). In addition, they may also provide protection against phytopathogens that infect at the apex.

1.6. Research objectives and thesis overview

1.6.1. Objectives of research

Root activities vary greatly along the longitudinal root axis, which combined with the inherent variability of soil gives rise to a high degree heterogeneity between habitats within the rhizosphere. In order to relate bacterial communities with these habitats it is necessary to develop methods that enable investigations to be undertaken at the micro-spatial-scale.

The objectives of this research were to develop a novel method for sampling bacteria at a spatial-scale that approximates that of a microhabitat and to investigate methods that could be used in combination with the micro-sampling technique to facilitate a better understanding of how bacteria interact with their environment at the micro-spatial-scale. Key interactions to be investigated were the link between bacteria and habitat factors, such as substrate availability and pH.

1.6.2. Summary of chapters

Chapter two reports the choice of plant used throughout this thesis. It also describes the growth substrates and propagation systems used. Chapter three reports the development and testing of a novel method that facilitates non-destructive micro-spatial-scale sampling of bacteria. Chapter four investigates methods that could be used to estimate total bacterial yield in micro-samples. In Chapter five, the micro-sampling method is used to investigate bacterial density and diversity at the root apex and base of four, six and eight day old *B. napus* plants grown in compost. In the same chapter, spatial trends in rhizosphere bacterial density were also investigated using a bioluminometric colonisation assay. Chapter six also reports spatiotemporal trends in rhizosphere bacterial density; however, these measurements were taken from roots grown for up to 26 days in soil. The dynamics of root growth were also monitored in this system and enabled the interaction between root growth rate and bacterial densities at the root apex to be investigated. Chapter's seven to nine concern methods that enable micro-samples to be linked with habitat factors such as substrate availability and pH. Chapter seven

investigates methods for mapping root exudation and bioavailable carbon in the rhizosphere of soil grown plants. Chapter eight reports the use of pH microelectrodes and Chapter nine reports the potential for using imaging mass spectrometry to trace the fate of introduced isotopic markers in micro-samples. Finally, Chapter ten discusses the achievement of the research objectives and highlights the ways in which this research could be taken forward to contribute to our understanding of microbial ecology at a relevant spatial-scale.

CHAPTER 2

GENERAL MATERIALS AND METHODS

2.1. Introduction

This chapter describes the systems used for preparing plants. Experiment-specific details, such as ammonium nitrate applications or watering regimes post planting are discussed in each chapter and will not be mentioned here.

2.2. Plants

2.2.1. Choice of plant species and cultivar

Interactions between bacterial communities and roots are highly complex and poorly understood. It was hypothesised that this level of complexity would be even greater when mycorrizal fungi were present; therefore, the experiments detailed in this thesis were conducted on the roots of a non-mycorrhizal plant species. *Brassica napus*, commonly known as oil seed rape, is non-mycorrhizal and is an important agriculture crop. The cultivar "Pronto" was found to have seeds with a high germination rate and was selected for this series of investigations.

2.2.2. Seed germination

Prior to planting, *B. napus* cv. Pronto seedlings were always pre-germinated for 16 h on tissue paper dampened with 0.2 mM $CaSO_4$. The germination rate of the seeds was found to be improved by $CaSO_4$ (Susan Smith, Rothamsted Research, *pers. comm.*).

2.3. Growth substrates

2.3.1. Compost

The compost was that prepared for Rothamsted Research by Petersfield Products (Leicester, UK) since November 1994. It is composed of 75 % medium grade peat, 12 % heat sterilised loam (≤ 8 mm particle size), 3% medium grade vermiculite, and 10 % grit (≤ 5 mm particle size, lime free). The mix also contained: a) 3.5 kg m^{-3} Osmocote Exact (Scotts Professional, Ipswich, UK) which released nutrients over a 3 - 4 month period (Table 2.1), b) 0.5 kg PG mix (Yara UK Ltd., Immingham, UK) per m^3 which was a quick release nutrient mix (Table 2.1), c) and a wetting agent (Vitax Ultraflo; Richard Aitken Ltd., Glasgow, UK) that contained an anionic surfactant which improved the distribution of water in the compost by reducing surface tension. The compost mix was finally amended with lime to pH 5.5 - 6.0.

	Osmocote Exact (% composition)	PG mix (% composition)
N	16	14
P_2O_5	11	16
K_2O	11	18
MgO	3	0.7
Bo	0.02	0.03
Mo	0.02	0.2
Cu	0.05	0.12
Mn	0.06	0.16
Zn	0.015	0.04
Fe(chelated)	0.2	0.09

Table 2.1 Nutrient composition of fertiliser amendments

2.3.2. Soil

2.3.2.1. Site description and sampling regime

Approximately 500 kg of soil was sampled from the Road Piece field at Woburn Farm, Bedfordshire, England (Fig. 2.1.). The sampling process involved removing 15 blocks of soil of approximately 30 x 30 cm to a depth of 25 cm using a stainless steel spade. The soil was from the Stackyard series which is characterised as brown earth on sandy colluvium (Catt *et al.*, 1975). To homogenise the soil, it was initially passed through a 10 mm gauge stainless steel sieve to remove large stones and then passed through a 4 mm gauge stainless steel sieve. The sieved soil was stored at 4 °C throughout the duration of this research.

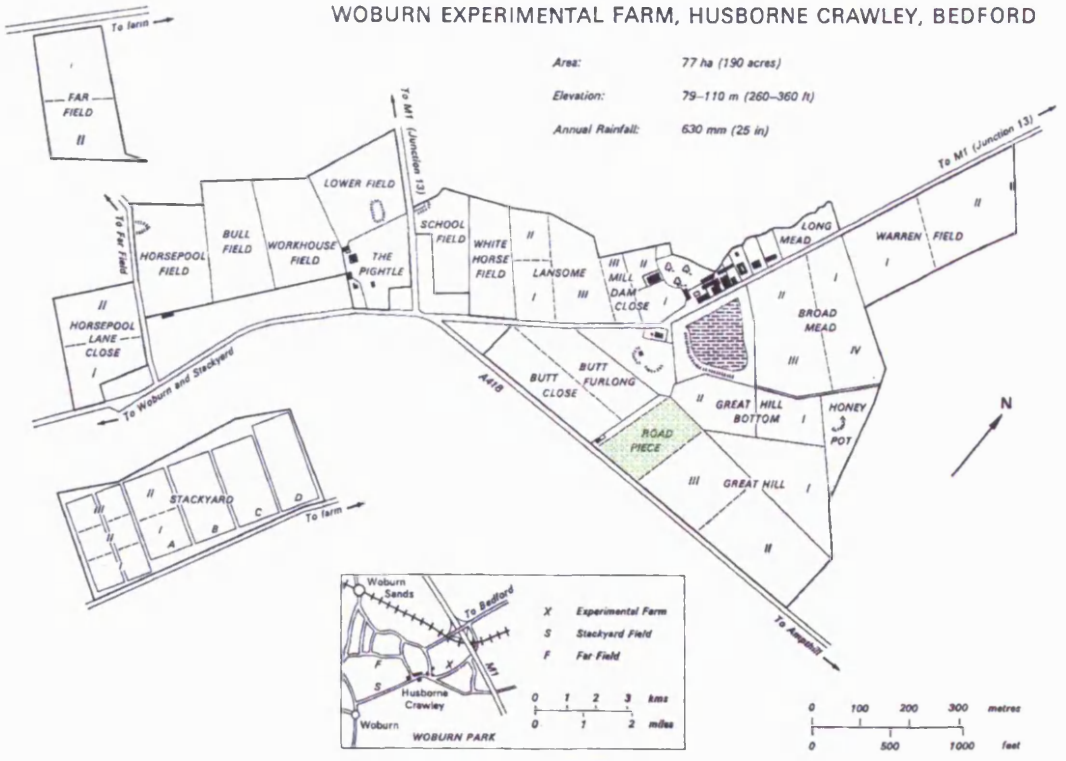

Fig. 2.1 Map of Woburn Experimental Farm indicating the location of the Road Piece field (green). Adapted from Catt *et al.* (1975).

2.3.2.2. Summary of the physicochemical properties of the soil

Details of analytical methods are given in Annex 1. Tables 2.2 and 2.3, summarise the physicochemical properties of the soil.

Parameter		Value	Unit
pH		7.33	
Total	N	0.11	%
	C	1.15	%
Available	NO_3^- - N	3.43	mg kg^{-1}
	NH_4^+ - N	1.49	mg kg^{-1}
	PO_4^-	55.2	mg kg^{-1}
Moisture content (MC)		10	%
Dry matter content (DM)		90	%
Water holding capacity (WHC)		43	ml 100 g^{-1} oven dry soil

Table 2.2 Physicochemical characteristic of the soil. Total N and C were determined by complete combustion using a LECO CNS200. The available NO_3^- and NH_4^+ pools were measured colourimetrically following extraction with 2M KCl. Available phosphate was extracted with sodium bicarbonate (pH 8.5) and measured colourimetrically. Refer to Appendix 1 for further details.

Element	Total (mg kg^{-1})	Available (mg kg^{-1})	Element	Total (mg kg^{-1})
K	2148	132.2	Zn	47.15
Mg	2033	270.7	Fe	25146
Ca	3274	1888	Al	7661
Na	39.36	6.100	Co	7.940
Mn	222.4		Cu	10.46
Ni	17.48		Pb	24.72
P	766.7		Cr	39.13
S	164.4		Cd	< 0.000

Table 2.3 Concentrations of total and available cations in soil. Total cations were measured using an ICP-AES following hot acid digestion. Available cation pools were measured by ICP-AES following extraction with ammonium acetate. Refer to Appendix 1 for further details.

2.4. Plant growth systems

To relate rhizosphere bacterial communities to the factors that influence them it is necessary to allow access to the root while preserving the spatial organisation of the rhizosphere. Sampling techniques that involve root excavation, such as the classical 'pull and shake' method (Katznelson *et al.*, 1948) are therefore inappropriate.

The rhizotron, in its classic sense, is a subterranean laboratory with glass walls that facilitate the visualisation of root systems in the field. The mini-rhizotron, which is commonly termed a rhizobox, is a scaled down adaptation of this concept that is suited to pot experiments. It consists of two transparent panels, between which is sandwiched a monolith of soil in which a plant can be grown. By tilting the rhizobox during the plant growth period, roots can be encouraged to grow along the surface of the soil

which enables their visualisation. By removing the transparent panel, the plant-soil profile can be exposed to facilitate the sampling of microbial communities and/or the measurement of a range of physicochemical factors. All plants used in the experiments reported in this thesis were grown one of two types of rhizotron: CYG plastic growth pouches (Mega International, Minneapolis, MN, USA) and Perspex rhizotrons that I designed and manufactured myself.

2.4.1. CYG plastic growth pouches

CYG plastic growth pouches (145 x 155 mm) are made from gas permeable transparent plastic sheeting and contain a brown paper wick that is folded at the top (Fig. 2.4). They were filled with 100 g of compost and 50 ml of reverse osmosis water and a pregerminated seedling was placed in a hole that was pierced in the centre of the folded wick. Each pouch was placed in an envelope to protect the roots from light and maintained in a controlled environment (section 2.5). Plants were grown at a 45° angle to ensure root growth occurred along the surface of the soil. In this system, the root growth rate was approximately 1.8 cm per day.

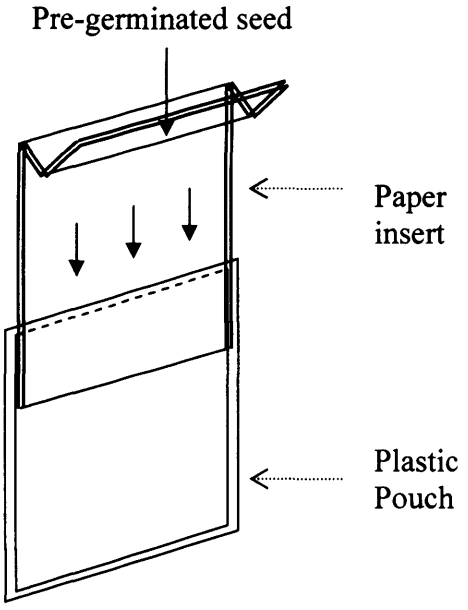

Fig. 2.2. Schematic diagram of CYG rhizotron.

Use of CYG plastic growth pouches in combination with compost was an excellent system for producing well nourished plants in a reproducible manner. The system imposed, however, a number of limitations that restricted its use. For instance, Mega International produce CYG growth pouches in one size only, which given that the roots of *B. napus* cv. Pronto grew to the bottom of the pouch in just over eight days, limited the length of time course experiments. Attempts to heat-seal two pouches together were successful; however, as these larger pouches were flimsy and unable to support the weight of the growth substrate. As a result compost and particularly soil tended to fall to the bottom of these extended pouches. For soil, this problem was also experienced with the normal sized CYG pouches. It was possible to stop the soil from falling to the bottom of the pouch by compacting it to a point at which it could support itself. However, this led to uneven densities of soil across the profile which would have increased the heterogeneity of the system, making it more difficult to resolve significant effects that were imposed by experimental treatments. To facilitate experiments with soil that could be run over a greater time period larger and more rigid rhizotrons were constructed using Perspex.

2.4.2. Perspex rhizotrons

Perspex rhizotrons were constructed in three sizes (Fig. 4.1). The largest facilitated the growth of plants that were up to a month old. The smallest rhizotrons could be placed inside the light-tight chamber of a low light imaging system at Rothamsted Research (section 5.2.2.4). This facilitated bioluminescence assays with plants that were up to eight days old.

A sheet of chromatography paper equal in dimension to that of the soil monolith was placed between the soil and the rhizotron to act as a wick for moisture. Rhizotrons were loaded with the appropriate amount of fresh soil (Table 2.4) to achieve a standardised bulk density of 2.27 g^{-1} cm^3. A rolling pin was then used to flatten the soil in to the recess to produce a monolith that was flush with the surface of the rhizotron. Sterile distilled water or a sterile nutrient solution was then added to the soil monolith using a spray gun to ensure a homogenous distribution. Immediately after this application the rhizotron was wrapped in cling film. The upper most edge of the soil monolith was left exposed such that a pregerminated seedling could be planted between

the soil and the cling film. Each pouch was placed in a plastic envelope to protect the roots from light and maintained in a controlled environment (section 2.5). Plants were grown at a 45° angle to ensure root growth occurred along the surface of the soil. Root growth rates of plants grown in this system were monitored over a 26-day period and are summarised in section 6.3.

Table 2.4 The quantity of soil that was added to each rhizotron to achieve a standardised bulk density. *Fresh soil contained 10 % moisture.

Rhizotron	Dimensions of soil monolith (mm)	Quantity of soil (g dry weight)	Quantity of soil (g fresh weight*)	Bulk density (g^{-1} cm^3)
Large	400 x 200 x 3	545	605	2.27
Intermediate	250 x 200 x 3	340	378	2.27
Small	150 x 120 x 3	123	136	2.27

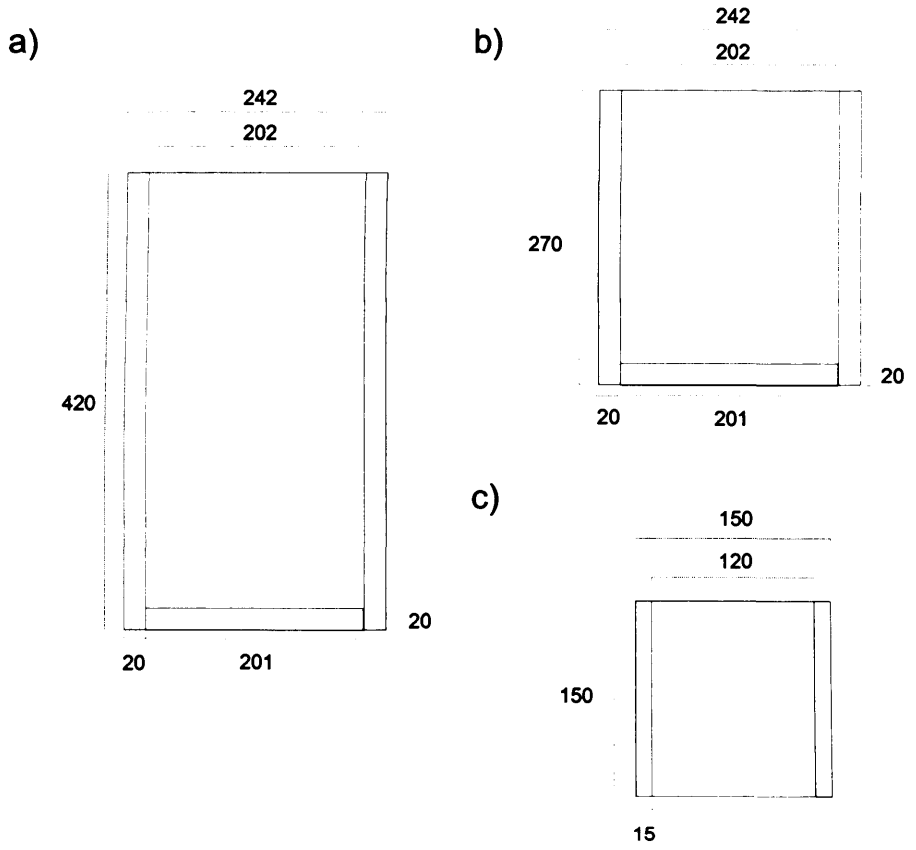

Fig. 2.3 Schematics of Perspex rhizotrons. All Perspex sheeting was 3 mm thick and all measurements are in mm.

2.5. Plant growth conditions

All plants were maintained in a controlled environment chamber with the following conditions: day length 16 h; photon flux density 300 μmol m^{-2} s^{-1}; temperature 20 °C; humidity 70 %; night length 8 h; temperature 18 °C, humidity 80 %.

CHAPTER 3

DEVELOPMENT OF A NOVEL TECHNIQUE TO FACILITATE BACTERIAL SAMPLING AT THE MICRO-SPATIAL-SCALE

3.1. Introduction

This chapter describes the development of the first method to facilitate quantitative and non-destructive micro-spatial-scale sampling of bacteria. The sampling process involves touching a surface with the tip of a laser-cut metal rod (Ø 130 μm) controlled by a micro-manipulator; bacteria adhere to the sampling tip on contact and can be recovered for microbiological analyses. If plants are grown in rhizotron systems, root and soil surfaces can be exposed and sampled. The efficiency with which the rods are able to remove bacteria from the root surface is compared to that with which bacteria are recovered from dissected root segments by washing.

3.1.1. Current methods for sampling bacteria from root and soil surfaces

The necessity to preserve the spatial organisation of the rhizosphere in order to relate bacterial communities to factors that influence them means that sampling techniques involving root excavation are inappropriate. As previously mentioned, the alternative is to grow plants in rhizotrons. Transfer of bacteria from the root or soil into a suitable medium for microbiological analyses can be achieved directly by washing bacteria from a sample surface, or indirectly, by washing bacteria from a surface previously used to blot the sample.

To investigate spatial distributions of rhizosphere bacteria using direct washing techniques, it is necessary to section the root. Bacteria recovered from these segments are then related to a reference unit. For example, colony-forming units (CFU) have been expressed as: CFU cm^{-1} of root (Liljeroth *et al.*, 1991), CFU g^{-1} root fresh weight (Bennett & Lynch, 1981; Scher *et al.*, 1984) or CFU g^{-1} dry weight rhizosphere soil

(Miller *et al.*, 1990; Semenov *et al.*, 1999). Duineveld and van Veen (1999) measured bacterial numbers in the basal and apical regions of chrysanthemum roots and compared their conclusions according to the reference units listed above. They found that different reference units led to different estimates of bacterial numbers and recommended the use of root surface area as the most reliable. For investigations of bacterial communities at the micro-scale, however, excision of sub-millimetre root sections presents a significant technical challenge. In addition, the resulting sections are of variable size, and prone to desiccation and contamination. The destructive nature of direct washing techniques also means that temporal dynamics on the same plant cannot be monitored.

Resolving many of these issues, Marschner and Crowley (1996) developed a novel method in which filter paper cut-outs, of a standardised surface area (2 x 10 mm) were used to sample bacteria in a non-destructive manner from roots or soil. Their technique offers clear advantages over destructive methods and facilitates expression of bacterial numbers and diversity per unit area. They reported, however, that due to the comparatively small diameter of the roots (0.5 – 1 mm), their filter papers also covered adjacent soil. This coupled with the large axial transect along the root surface in contact with the filter paper (10 mm) means that a wide range of micro-habitats with potentially contrasting physicochemical conditions and their associated bacterial communities can be encompassed in a single sample. This problem limits the method to sampling at the macro-spatial-scale as the preparation and handling of filter papers of standardised size at the sub-millimetre scale is not feasible.

3.1.2. Development of a novel technique for sampling at the micro-spatial-scale

The motivation for developing a novel method that would enable sampling of bacteria at the micro-spatial-scale was to facilitate a better understanding of how rhizosphere bacterial communities respond to and influence their environment. It was important, therefore, that the method should complement techniques that facilitate the measurement of physicochemical factors within the sample area. In addition, the method had to be non-destructive so that temporal dynamics on same plant could be monitored over time. For this reason, the root dissection approach was not investigated; instead, a blotting style technique was developed.

3.1.2.1. Bacterial sampling with micro ion-selective electrodes

The original concept for this micro-scale blotting technique arose from discussions between Drs Penny Hirsch and Tony Miller (Rothamsted Research, UK). They hypothesised that micro-ion-selective electrodes (micro-ISEs) could swab bacteria from root or soil surfaces, thus facilitating the characterisation of bacterial communities and their physicochemical environment at a scale that is appropriate for microorganisms. The capacity for micro-ISEs to pick up and release bacteria was demonstrated using PCR to detect bacterial 16S rDNA in a buffer used to wash adhered bacterial cells from a tip that had been touched on a root surface (Cryer N, Laboratory note book No. 1350, Rothamsted Research, UK). However, the diameter of an unbroken micro-ISE tip is approximately 1 μm and is, therefore, too small to be used to sample bacteria, which are on average 1 μm^3 (Grundmann & Gourbiere, 1999). For this reason, the edge of the tip was used for sampling which lead to a variable surface area in contact with the sample surface. This problem was exacerbated by the fact that micro-ISEs are extremely fragile, thus liable to break, and meant that quantitative comparisons between bacterial samples were not possible.

These issues required that an alternative approach was developed. The prerequisites for the sampling system were for a robust and non-toxic material providing a standardised surface area (sub-millimetre range), able to pickup and release bacterial samples without bias to specific groups. Due to the fact that ion-selective electrodes that met these requirements were not available, it was decided that the design of the new technique would focus solely on meeting the criteria needed for micro-scale sampling. To link bacterial communities with their physicochemical environment, ion concentrations would be measured using micro-ISEs at the same position on a root or soil surface from which bacterial samples had been removed.

3.1.2.2. Bacterial sampling with tungsten rods

Tungsten is a metal with low toxicity compared to most other metals, high tensile strength, the highest melting point of all metals, and excellent corrosion resistance reacting only slightly to most mineral acids. Tungsten rods are cheap and readily available in sub-millimetre diameter sizes. Its properties provide excellent durability

and facilitate a wide range of sterilisation techniques. It is, therefore, a good material with which to design a sub-millimetre scale bacterial sampling probe.

To enable comparison of bacterial samples it was necessary to standardise the surface area used for sampling; this was achieved by laser cutting the tips of the rods. The rods were then mounted in glass capillary tubes to provide support and enable them to be attached to a micromanipulator. In combination with a microscope this allowed the tips to be accurate positioned on a sample surface such as the rhizoplane or a soil crumb. This chapter describes the preparation of micro-sampling rods discusses their ability to pickup and release bacteria.

3.1.2.3. Pickup efficiency

During sampling, the nature of surface interactions between the bacterial cells, the surface upon which they are present, and the micro-sampling tip, influence the efficiency of the sampling process. Bacterial adhesion to a root or soil surface involves: (a) transport to the surface, (b) contact and initial adhesion, (c) firmer attachment, and then (d) growth to form micro-colonies or biofilms (van Loosdrecht *et al.*, 1990). It is possible that bacteria which are more firmly attached to a root or soil surface will be sampled less efficiently than those that are weakly adhered (Fig. 3.1). The efficiency with which the rods are able to remove bacteria from the root surface was compared to that with which bacteria are recovered from dissected root segments by the conventional technique of washing.

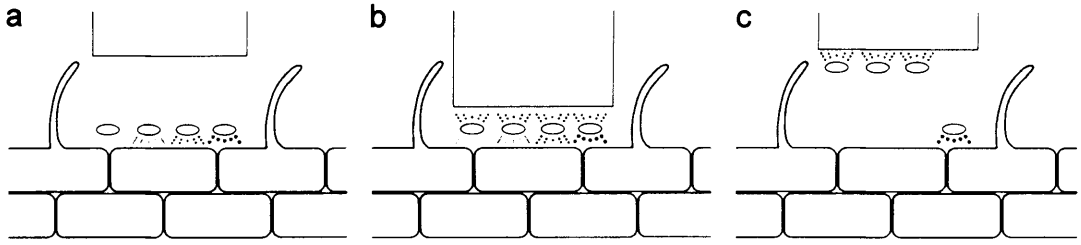

Fig. 3.1 Competitive adhesion between a sampling tip and a root surface. (a) Bacterial cells on a root surface prior to sampling. Thickness of dotted lines represents increasing strength of adhesion. (b) Sampling tip makes contact with root surface and exerts a specific adhesive force on bacterial cells. (c) Sampling tip is moved away from the root surface. Cells that are adhered to the root with greater force that that exerted by the sampling tip, remain on the root surface.

3.2. Materials and methods

3.2.1. Preparation of micro-sampling rods

The ends of tungsten rods (diameter 130 μm; Science Products, Hofheim, Germany) were laser-cut at the Laser Micromachining Centre IBMM (Bangor, Wales, UK), to achieve sampling tips of standardised surface area. Cut rods were mounted in single-barrelled borosilicate glass capillary tubes, each with an outer diameter of 1.0 mm and an inner diameter of 0.58 mm (Hilgenberg Glass, Malsfeld, Germany) with a pointed tip produced by heating and pulling the glass using a PE-2 vertical micropipette puller (Narishige, Tokyo, Japan). The pointed tips of the glass tubes were blunted to allow the cut rod to be inserted and fixed in place with Loctite® Easy Brush Super Glue (Henkel Consumer Adhesives, Cheshire, UK) (Fig. 3.2).

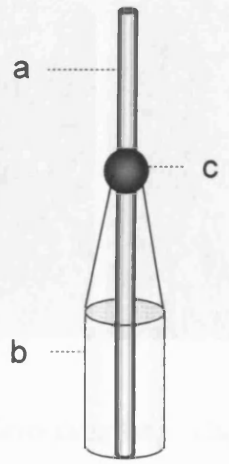

Fig. 3.2 Micro-sampling rod (a) embedded in a borosilicate glass capillary tube (b) using super glue (c). Mounting the micro-sampling rods in this manner provided them with support and enabled them to be used with a micro-manipulator.

Tips were sterilised by the following procedure: 30 min submersion in 10 % SDS, 30 s sonication at high power (Ultrasonik 300; JM Ney, Bloomfield, CT, USA) in sterile distilled water, 30 min submersion in 5 % HCl, and 30 s sonication at high power in sterile distilled water. Tips were then irradiated with UV light at 254 nm for 45 min in a laminar flow cabinet.

3.2.2. Plants and growth conditions

Plants were grown in CYG plastic growth pouches containing compost. For further details refer to Chapter two.

3.2.3. The ability for micro-sampling rods to pick up and release bacteria

A micro-sample was taken from the root apex (0 - 10 mm from the root cap) and the root base (0 - 20 mm from the root-shoot junction) of five, four-day old, plants. Roots were viewed with a dissecting microscope; this coupled with the use of a micro-manipulator (Prior Scientific, Cambridge, UK) to which the micro-sampling rods were attached, enabled finely controlled navigation toward target sites (Fig. 3.3).

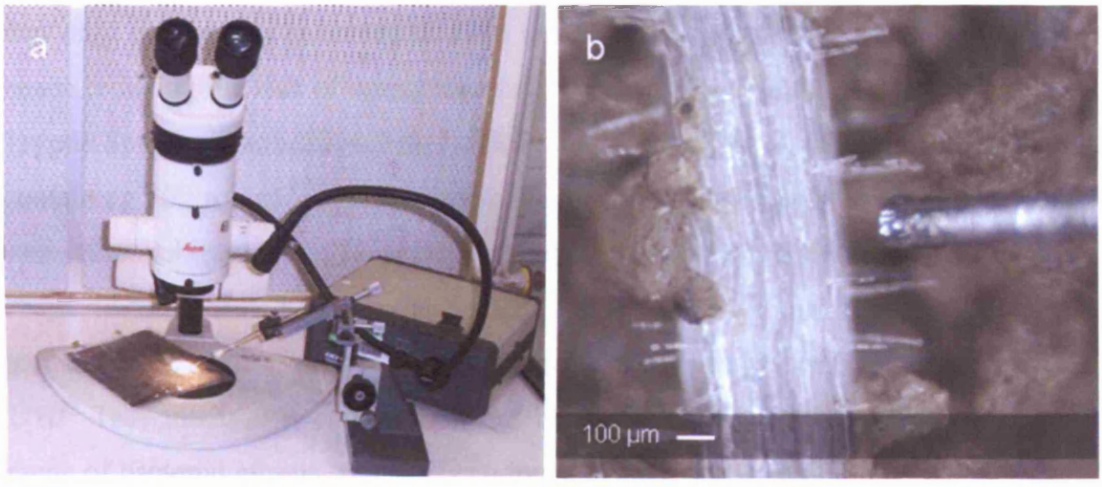

Fig. 3.3 (a) Equipment used for micro-sampling. The image shows *B. napus* plants in a CYG growth pouch. A hole was cut in the plastic to enable a micro-sampling rod to be directed towards a sampling site on the rhizoplane using a micro-manipulator. (b) Using a microscope to target sites on root or soil surfaces makes it possible to see when contact has been made or if the sides of the rod have made contact with other surfaces during sampling.

Care was taken to avoid touching the sides of the micro-sampling rods on any surfaces during sampling. Contact between the sampling tip and the root or the soil was maintained for ten seconds. This process did not damage the root surface e.g. leakage of cell contents; however, had this occurred both the sample and the plant would have

been discarded. After making contact, the tip was withdrawn from the sample specimen and removed from the manipulator. Bacteria adhered to the tip were recovered in a microtube containing 10 µl phosphate buffered saline (PBS; 137 mM NaCl, 1.5 mM KH_2PO_4, 6.5 mM $Na_2HPO_4 \cdot H_2O$, 2.7 mM KCl, pH 7.2) by sonicating for 60 s at low power in a sonicating water bath (Ultrasonik 300; JM Ney, Bloomfield, CT, USA) containing ice and water. The microtube was supported by a polystyrene float. This approach facilitated the recovery of bacteria from multiple samples simultaneously. In addition, as it involved less manual handling, the risk of contamination was reduced.

Following this primary wash, rods were placed in new microtubes each containing 10 µl sterile PBS and the washing process was repeated. This process enabled the efficiency with which bacteria were recovered by washing to be assessed. To ensure that the samples could be spread evenly over the surface of an agar plate they were made up to a final volume of 200 µl sterile PBS. The starting volume was 10 µl because this ensured that only the tip was submerged when the sampling rod was placed in the microtube hence reducing the risk of contamination. Samples were plated on $1/10^{th}$ TSA (3 g L^{-1} Tryptic Soy Broth solidified with 1.5% Technical Agar No. 3, Oxoid, Basingstoke, UK) containing 100 µg ml^{-1} cycloheximide (Sigma, UK). Three unused micro sampling rod were also subjected to this procedure and were considered to be negative controls. Plates were incubated for ten days at 28 °C and CFU were recorded after three, seven and ten days. The maximum count for each plate was used as the final result. The $1/10^{th}$ TSA media was chosen as it has been shown to support the growth of a wide range of bacterial groups, and has been found to give rise to more CFU than other media (O'Flaherty *et al.*, 2001).

3.2.4. Comparison of the sampling efficiency between sampling methods

3.2.4.1. Enumeration of culturable rhizoplane bacteria by root dissection

Four days after planting, a sterile scalpel blade was used to cut 1 cm segments from the root base and apex of 24 plants. To remove adhered rhizosphere soil, each root segment was gently agitated using sterile forceps in sterile PBS for 5-10 s. After this initial washing process root segments were transferred to vials containing 15 ml of sterile PBS

buffer. Rhizoplane bacteria were extracted at 4 °C for 45 min by vigorous shaking at 2200 rpm using a IKA-Vibrax-VXR shaker (Janke & Kunkel, Staufen, Germany).

Samples were diluted and then plated on $1/10^{th}$ TSA containing 100 μg ml^{-1} cycloheximide. Plates were incubated for ten days at 28 °C and CFU were recorded after three, seven and ten days. The maximum count for each plate was used as the final result.

3.2.4.2. Enumeration of culturable bacteria by micro-sampling

Four days after planting, two samples per plant were taken from the root apex (0 – 10 mm from the root cap) and one from the root base (0 - 20 mm from the root-shoot junction). Twenty eight plants were sampled in total. Bacteria adhered to the tip were recovered in a microtube containing 10 μl sterile PBS and processed as described in section 3.2.3.

3.2.4.3. Statistical analysis

For both sampling methods, bacterial densities (i.e. CFU tip^{-1} for micro-samples and CFU cm^{-1} of root) four days after planting, were expressed as CFU mm^{-2} of root. The surface area of each root segment was assumed to be that of a 10 mm long cylinder with a diameter of 1 mm. Differences in bacterial densities (CFU mm^{-2} root) (x) between the two sampling methods within the apical and basal root zones were then investigated using the method Residual Maximum Likelihood (REML) (Patterson & Thompson, 1971). This method took account of the unbalanced design structure (unequal numbers of plants between sampling methods) and a data transformation (square root (x + 1)) ensured that the assumption of Normality was fulfilled. A mixed model was fitted with random effects due to nested design terms (plants, and zones within plants) and fixed effects due to the treatment terms (zone, method and their interaction). The effects of treatment terms were tested for significance using the Wald test (Welham & Thompson, 1997). When these were significant (chi-squared, $P < 0.05$), it was possible to determine which treatment combinations significantly differed from one another using 2-tailed t-tests on the residual degrees of freedom for the model (df = 125).

3.3. Results

3.3.1. Laser cutting

Laser cutting produced rods with flat tips that were perpendicular to their length and therefore of adequately standardised surface area (Fig. 3.4).

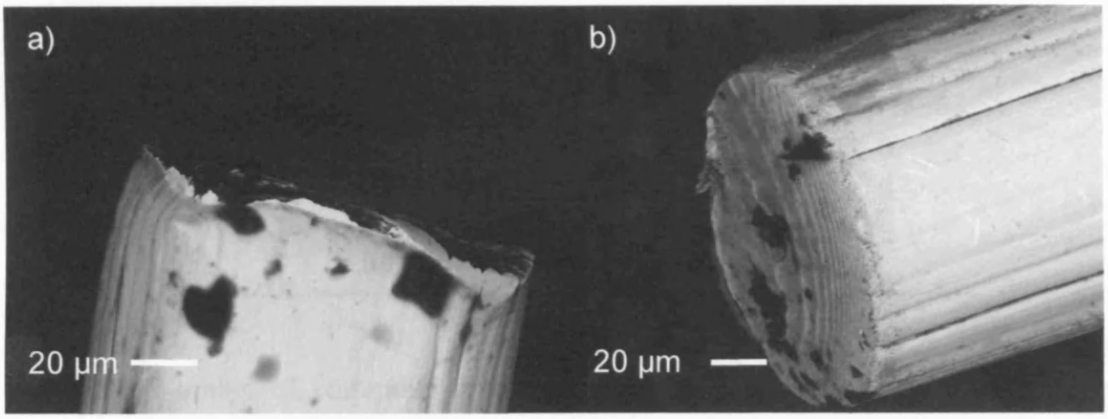

Fig. 3.4 Scanning electron micrographs of un-washed sampling rods a) before and b) after laser cutting.

3.3.2. The ability for micro-sampling rods to pick up and release bacteria

Table 3.1 displays the number of culturable rhizoplane bacteria in each sample after one or two washes. It is clear that the micro-sampling rods were able to pick up bacteria and that the washing procedure was very effective in recovering bacteria that became adhered to the tip during sampling. In addition, the absence of contamination in the controls indicates that the sterilisation protocol was adequate. Using the standard errors, the mean bacterial densities for the root base and apex were significantly different. The mean bacterial densities with their associated standard errors were: 6.8 ± 2.7 CFU^{-1} tip at the root apex and 40.0 ± 16.4 CFU^{-1} tip at the base.

Root zone	Plant/Replicate	First wash	Second wash
Apical region	1	2	0
	2	3	0
	3	17	0
	4	5	0
	5	7	0
Basal region	1	1	0
	2	80	0
	3	71	1
	4	44	0
	5	4	0
Negative control	1	0	0
	2	0	0
	3	0	0

Table 3.1 Number of culturable rhizoplane bacteria recovered from micro-sampling rods after one or two washing cycles. Samples were from the root apex or base of four day old *B. napus* plants.

3.3.3. Investigation of sampling efficiency

3.3.3.1. Comparison of the sampling efficiency between sampling methods

The treatment terms (zone, method and their interaction) all had a significant effect (Wald tests, $P < 0.05$) on bacterial densities. Figure 3.5 shows the REML predicted means and standard errors for each treatment combination. Using the micro-sampling approach, bacterial densities were approximately 1 x 10^3 CFU mm^{-2} root at the base and 4 x 10^2 CFU mm^{-2} root at the apex. The corresponding figures using the root dissection approach were 6 x 10^4 CFU mm^{-2} root at the base and 2 x 10^3 CFU mm^{-2} root at the apex. Two-tailed t-tests revealed that between methods, there was no difference in bacterial densities at the root apex ($P > 0.05$), but, at the root base bacterial density was greater when using the dissection method ($P < 0.05$). This may be related to differences in root surface area (RSA) between the two zones (Fig. 3.6; see discussion). Both

methods revealed greater bacterial density at the root base than at the apex (2-tailed student t-test, $P < 0.05$).

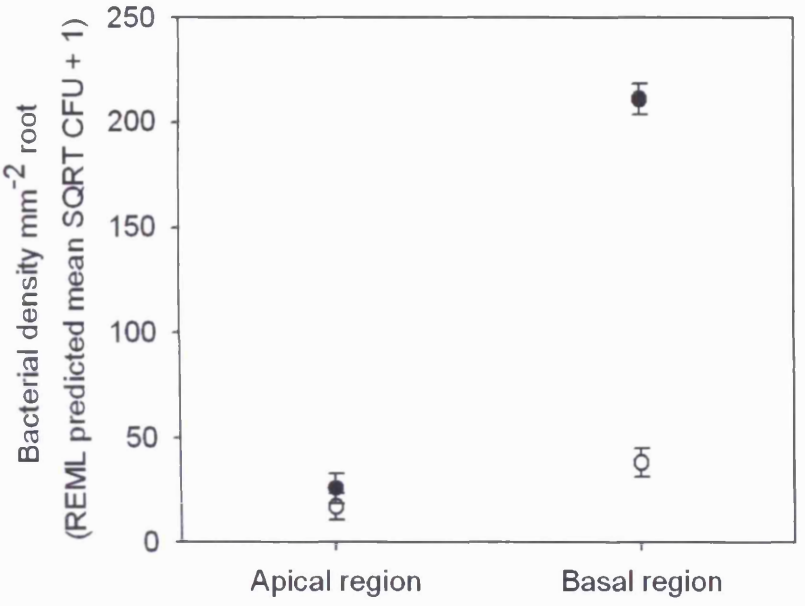

Fig. 3.5 REML predicted mean bacterial density mm^{-2} root (SQRT CFU + 1) within each zone by sampling method combination: root dissection method (●), micro-sampling method (○). Error bars represent standard errors of means.

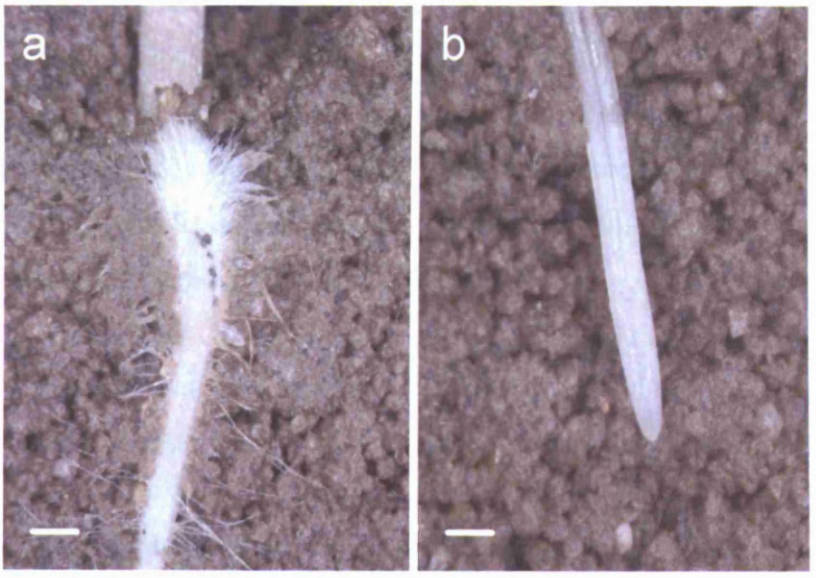

Fig. 3.6 Basal region (a) and apical region (b) of a 4 day old *B. napus* root growing in compost. High densities of root hairs and attached soil particles were associated with the root base but were absent at the root apex. Scale bar equals 1 mm.

3.4. Discussion

The laser cutting resulted in tips of standardised surface area (Fig. 3.4). By mounting the laser cut rods in glass capillaries they were compatible with the micro-manipulator. This in conjunction with the microscope made it easy to achieve finely controlled movement towards targeted sampling sites on the rhizoplane. It was possible to observe when the tip had made contact with the root and control the pressure with which the tip pressed against the root surface; this process avoided the tip penetrating the root tissues.

Micro-sampling tips were clearly able to pick up bacteria; however, the density of culturable bacterial cells per tip was very low (Table 3.1). This is to be expected as approximately 800-100 bacterial cells would be present if they formed a dense monolayer over the surface of the tip (assuming standardised cell dimensions of 1 x 0.5 μm). Nonetheless, the micro-sampling technique was found to be as efficient as washing dissected root segment (see below). The results indicate that the tip washing process was highly effective at recovering adhered bacterial cells from the surface of the micro-sampling tips and that the sterilisation protocol was effective (Table 3.1).

Recovery of bacteria from the surface of a root segment by vigorous washing was assumed to be highly efficient, and therefore a good reference with which to compare the sampling efficiency of our new micro-sampling technique. The comparison revealed that bacterial density (CFU mm^{-2} root) at the root base was greater when measured using the root dissection technique. At the root apex however, there was no difference between the methods (Fig. 3.5).

The apparent disparity between sampling methods at the root base may reflect an overestimation of bacterial density that could have resulted from the harvesting of bacteria from a greater RSA than that accounted for when calculating bacterial density. As aforementioned, the RSA of each segment was assumed to be that of a 10 mm long cylinder with a diameter of 1 mm. While this provided reasonable estimates for the RSA of apical segments, high densities of root hairs meant that the RSA of basal root segments was underestimated (Fig. 3.6). This problem was further exacerbated by the presence of soil particles that had become trapped between the root hairs, as these were not removed efficiently by the primary washing step. By underestimating RSA, a

problem that is intrinsic to the root dissection method, an overestimation of bacterial density was inevitable. Such inaccuracies could be highly significant – for example, Macduff *et al.,* (1986) reported that root hairs increased *B. napus* RSA by approximately 200 %. However, given that the density of root hairs differed along the length of the roots in our study, this estimate could have varied accordingly. Almost no root hairs were observed at the root apex, and any soil particles that were attached to dissected apical root segments were easily removed during the initial washing step. For this reason, RSA and bacterial density estimation was reasonably accurate at the root apex. Estimation of the sampled RSA was not a problem when using the micro-sampling tips, as these were of standardised dimensions. Bacterial density at the root apex was similar when measured by either method indicating that the micro-sampling tips were efficient at sampling a diverse range of bacteria with little or no bias to particular groups.

A better understanding of how rhizosphere bacterial communities respond to and influence their environment is likely to be obtained through investigations at an appropriate scale. This chapter reported the development of a novel method that facilitates non-destructive bacterial sampling at the sub-millimetre spatial scale; this was previously not possible. The prerequisites for the sampling system were for a robust and non-toxic material providing a standardised surface area (sub-millimetre range), able to pickup and release bacterial samples without bias to specific groups. The results indicate that all of these criteria have been met; however, as the numbers of bacteria per micro-sample are low, unique problems arise in estimated their numbers. These issues will be discussed in the next chapter.

CHAPTER 4

ENUMERATION OF TOTAL BACTERIA YIELD

4.1. Introduction

In Chapter three I demonstrated that a micro-sample from the rhizoplane of a four-day old *B. napus* plant contained approximately 0-100 culturable bacteria per tip. In light of a wealth of literature reporting that standard cultivation methods result in the underestimation of both bacterial density and diversity (Weisburg *et al.*, 1991), it is likely that this estimate should be greater. In this chapter I investigate methods that facilitate the enumeration of bacterial cells in micro-samples independently of cultivation methods. Throughout the introduction I aim to describe the reasons why certain techniques were chosen above others and present sufficient detail to understand the theory behind them. It was necessary that the approaches tested were non-destructive so that bacterial DNA/RNA could be extracted and analysed post enumeration if desired.

4.1.1. Direct microscopic counts

4.1.1.1. Light microscopy

The proportion of bacteria that are cultivable is commonly reported to be less than 1 % of all species in the domain. In soil, estimates vary from < 1-10 % of the species present (Janssen, 2006) and are usually calculated by comparing plate counts with direct counts using a light microscope. Standard microscopic counting involves the use of a haemocytometer, which is a glass slide marked with a microscopic grid. A known volume of a bacterial suspension is dispensed onto the surface of the haemocytometer and the number of bacteria within a set number of grid squares can be counted. The average bacterial density per grid square can then be extrapolated to estimate the density

of cells in the original aliquot. It is likely that, because they contain such low numbers of cells, this approach would be unsuccessful for micro-samples. I investigated whether this problem could be overcome by concentrating cells in the recovery buffer prior to microscopic examination.

4.1.1.2. Direct counts of bacteria on the surface of a tip using scanning electron microscopy

As an alternative to light microscopy of bacterial cells recovered from a tip, I investigated whether scanning electron microscopy (SEM) could be used to count bacteria on the surface of a tip directly. To investigate diversity post enumeration it was necessary that the microscope could image bacterial cells without any pre-treatment that may have a damaging effect on the DNA or inhibit the recovery of cells from the surface of the tip post enumeration. In addition, as the surface of the rod would need to be facing the on-coming electron beam, it was necessary to use a microscope that could accommodate the rod in an upright position. The LEO 1455VP SEM operated at the Natural History Museum, London, has a large chamber capable of accommodating samples up to 150 x 150 x 150 mm, and at short working distances, it is capable of obtaining images at magnifications in excess of 10,000 X, giving sub-micron resolution. In addition, the microscope is able to image uncoated fresh samples. As such, it was suitable for the intended application.

4.1.2. A molecular approach to the determination of bacterial numbers

By extracting DNA from bacterial cells recovered from a micro-sampling tip, it may be possible, using molecular methods (Torsvik *et al.*, 1998) to determine their abundance while preserving a means of investigating their diversity. As molecular methods are culture-independent, they have enabled a more comprehensive picture of bacterial communities to be developed; this has constituted a revolution in microbial ecology.

The particular approach that I investigated involved using real-time quantitative polymerase chain reaction (PCR) to enumerate the number of copies of a target DNA sequence in an original micro-sample (see below). The prerequisites for the target DNA sequence were that it contained regions that were ubiquitous and conserved among

bacteria, and that it should have a similar copy number per cell in all bacterial species. Also, it would be useful if the target DNA sequence contained a region that varied between bacterial species, as this would facilitate determination of bacterial diversity following bacterial enumeration. The following section describes the theory behind the method and the selection of the DNA target molecule.

4.1.2.1. Polymerase chain reaction

PCR allows the amplification of a specific region of DNA that lies between two regions of known DNA sequence (Saiki *et al.*, 1985). PCR amplification uses short oligonucleotide primers which are complementary to the two regions of known DNA sequence. The target DNA is heat-denatured to obtain two single-stranded DNA templates to which the primers hybridise as the mixture cools. The primers are then extended along the singled-stranded DNA templates in the presence of deoxynucleoside triphosphates (dNTPs) using DNA polymerase at a temperature suitable for enzyme activity. This results in the synthesis of new DNA strands (target amplicons) that are complementary to the template sequence between the two primers. Target amplicons act as additional templates when a reaction cycle of heating and cooling is repeated; therefore, if repeated over many cycles the target amplicon yield will increase exponentially. In practice the yield increase of target amplicons is not quite exponential. This results from a variety of factors including: the presence of PCR inhibitors in environmental samples, differences in the thermodynamic stability of primers, the formation of dimer-primers, and changes in the concentration of dNTPs and/or the activity of the DNA polymerase (Kidd & Ruano, 1995; Nolan *et al.*, 2006). Many techniques can be used to detect and confirm the identity of target amplicons following PCR (Newton & Graham, 1994). The simplest and most commonly used is, however, electrophoretic size separation in an agarose gel. The size-separated target amplicons are then generally stained with ethidium bromide - a fluorescent dye that binds to DNA, thus enabling bands to be visualised by transillumination with ultra-violet light.

Due to the exponential nature of optimized PCR there is a log-linear relationship between the quantity of target amplicons and the number of PCR cycles. This phenomenon enables PCR to be used in a quantitative manner (Ferre, 1992; Heid

et al., 1996). To determine the number of copies of a target DNA sequence that were in an original sample, the number of target amplicons in a sample following PCR can be compared with those in standards that contained known copy numbers. Using this approach, quantification occurs at the end-point of the PCR series (Ferre, 1992; Newton & Graham, 1994). However, as aforementioned, PCR efficiency is inversely proportional to cycle number; therefore, in the latter cycles of a PCR series, amplification is unlikely to be exponential. For this reason, end-point quantification of target amplicons is semi-quantitative at best. Improved quantification is achieved using real-time quantitative PCR (Heid *et al.*, 1996), where the dynamics of the amplification are monitored in real-time.

4.1.2.2. Real-time quantitative PCR

Real-time PCR (RT PCR; not to be confused with reverse transcriptase PCR) enables the yield of target amplicons to be measured after every PCR cycle. Provided that standards containing known copy numbers of the targeted DNA sequence are run alongside the samples, it is possible to extrapolate the number of target amplicon copies present in an original sample. This is the basis of real-time quantitative PCR (RT qPCR; Heid *et al.*, 1996).

As noted above, the degree to which target DNA sequences are amplified in an exponential manner is influenced by factors that affect the efficiency of the PCR (Nolan *et al.*, 2006). In addition, the number of target amplicons despite further PCR cycles reaches a plateau. For this reason, the data used to quantify the starting copy number of a target DNA molecule in a sample, are collected in the early stages of a PCR series as soon as the reaction becomes log-linear.

The numbers of copies of a target amplicon in samples at successive PCR cycles is determined fluorimetrically. Typically this involves the use of SYBR Green, a dye that becomes fluorescent once bound to doubled-stranded DNA, or a TaqMan probe which is a short oligonucleotide sequence that hybridises to a complementary sequence between the forward and reverse priming sites of a PCR. The probe is conjugated to a fluorophor on the 5' end and a quenching molecule on the 3' end. When the fluorophor and the quencher are in proximity to one another, fluorescence is quenched.

On encountering the DNA polymerase, however, the 5' to 3' exonuclease activity cleaves the TaqMan probe, separating the reporter from the quencher, which leads to the generation of a fluorescence signal (Fig. 4.1). As fluorescence is generated only when a target amplicon has been produced, the TaqMan approach is not susceptible to overestimation of PCR yield as non-target DNA does not give a fluorescence signal. SYBR Green on the other hand will bind to any doubled-stranded DNA; therefore, fluorescence will also be detected from non-target DNA.

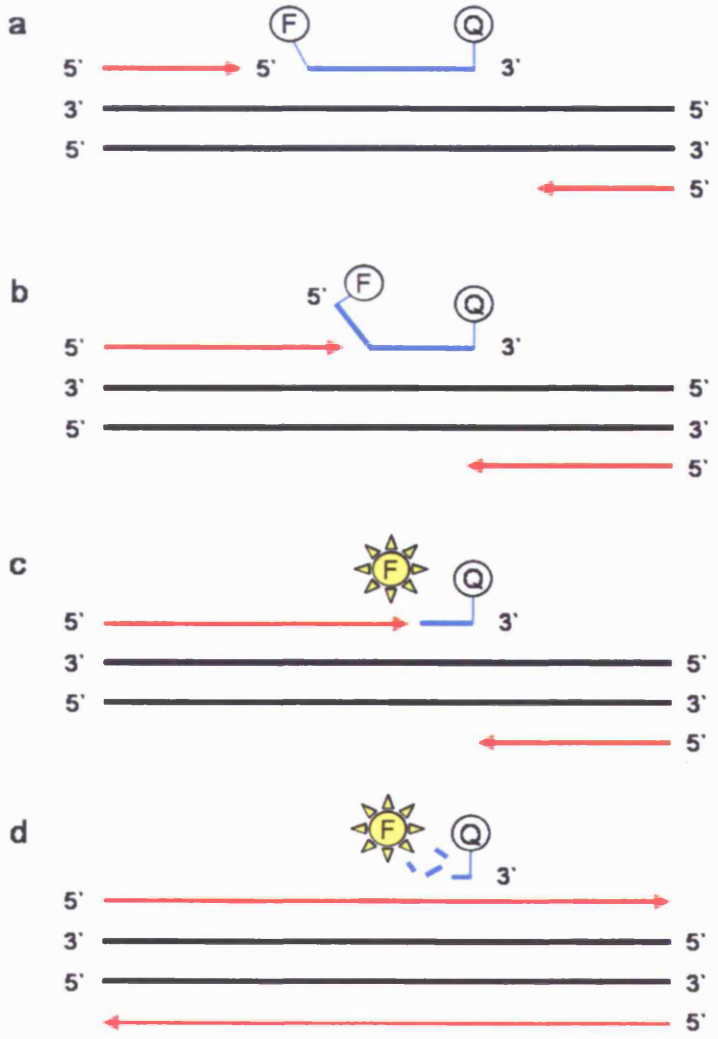

Fig. 4.1 Detection of PCR amplicons using a TaqMan probe. (1) Primers and a probe (conjugated to a flourophor and a quenching molecule) anneal to complementary sequences on the target DNA. (2) As the polymerase extends the primers, the probe is displaced. (3) exonuclease activity cleaves the TaqMan probe, separating the reporter

from the quencher (4) After release of the reporter dye from the quencher, a fluorescent signal is generated.

The degree of fluorescence for any sample during RT qPCR is related to the amount of target present in the original sample. The PCR cycle number which corresponds to a point at which the increase in fluorescence (and therefore amplification of target DNA strands) is log-linear and rises above a defined background fluorescence threshold is known as the cycle threshold (C_t). By plotting the C_t values of unknown samples against those generated by known standards the copy number of the target gene within the original samples can be extrapolated.

4.1.2.3. Selecting a DNA target molecule for bacterial enumeration using RT qPCR

To quantify the number of bacteria in an original micro-sample using RT qPCR while maintaining the facility to investigate bacterial diversity post enumeration, it is necessary that the sites in the target DNA sequence to which primers and hybridisation probes anneal are present and conserved in all bacteria and flank regions of DNA sequence that vary between bacterial types. Ideally the target DNA sequence would also have a similar copy number per cell in all bacterial species as this would mean that the number of copies of target DNA amplicons would be directly proportional to the number of bacterial cells. It is not likely that a DNA target sequence will be found that fulfils these criteria in 100 % of bacterial species; however, if an appropriate target could be identified in a high proportion of bacterial species this approach would represent a great improvement over culture-based methods.

Sequences that are highly conserved between bacterial species are generally associated with genes that confer critical life functions. One such example is *gyr*B a single-copy gene that is ubiquitous throughout the bacterial domain (Wantanabe *et al.*, 2001). This gene would be an ideal target for the proposed application; however, the database of bacterial DNA sequences containing *gyr*B is currently too small to be able to design universal primers and probe sets. An alternative is the 16S rRNA gene, encoding a constituent of prokaryotic ribosomes, which are small protein-RNA complexes, vital to cell function as the sites of protein synthesis. Significant alterations to rRNA gene sequences at locations relating to their secondary structure affect the conformation of the subunits and therefore the function of the ribosome. For this reason, sections of

rRNA gene sequences are highly conserved across broad phylogenetic distances. However, between these conserved regions lie sections that have little or no effect on the function of the ribosome. These regions are variable between different bacteria because they have evolved at rate that is disproportionate to that of those that are constrained by the requirement to maintain ribosome function.

The fact that rRNAs are found in all bacteria, are functionally consistent, and contain conserved as well as variable domains makes them good targets for molecular microbial ecology studies (Woese, 1987; Weisburg *et al.*, 1991). Sequences from such studies have been submitted to on-line databases such as the Ribosomal Database Project II (http://rdp.cme.msu.edu/, 14/12/06) and the National Centre for Biotechnology Information (http://www.ncbi.nlm.nih.gov/, 14/12/06) which has resulted in a substantial volume of sequence data. The most widely studied prokaryotic rRNA gene is 16S for which the Ribosomal Database Project II contains 107,136 sequences (10/01/07). These data facilitate the design of oligonucleotide primers and hybridisation probes that may be used for PCR amplification of target DNA sequences within 16S rDNA. The main drawback of using 16S rRNA genes for quantification of total bacterial yield is the fact that bacteria harbour multiple rRNA operons containing the 16S, 23S and 5S rRNA genes (Rainey *et al.*, 1996; Klappenbach *et al.*, 2000). It has been shown that the copy number of rRNA operons varies between 1-15 (Rainey *et al.*, 1996); therefore, bacterial load may be overestimated.

4.1.2.4. RT qPCR amplification using universal primers and SYBR Green

By analysing 16S rRNA gene sequences from multiple genera within each bacterial phylum, Muyzer *et al.* (1993) were able to design universal bacterial primers that flanked a region of DNA sequence that varied between different bacterial types. This variable region facilitates a range of techniques to be used to determine the diversity of the amplicons. Using the function 'probe match' in the Ribosomal Database Project II the proportion of 16S rRNA gene sequences that perfectly matched the forward and reverse primers reported by Muyzer *et al.* (1993) was 92.3 % and 88.8 % respectively (30/03/07) thus highlighting that they have the capacity to detect a high proportion of bacterial species. I investigated whether RT qPCR using non-GC

clamped versions of the primers reported by Muyzer *et al.* (1993; section 4.2.2.1) and SYBR Green could be used to accurately quantify bacterial numbers.

4.1.2.5. Design of a 16S rDNA-based TaqMan probe RT qPCR system for enumeration of total bacteria

Using the Ribosomal Database Project II, I arbitrarily selected multiple 16S rRNA sequences from each genus within each bacterial phylum and constructed a multiple sequence file. I then surveyed the 16S rRNA sequences to determine whether a suitable region of DNA sequence could be found for enumeration of total bacteria using a TaqMan probe RT qPCR system. At the time that I conducted this research (Jan, 2004) I was unaware that a number of peer-reviewed journal papers had already reported RT qPCR methods for enumerating total bacterial loads (Corless *et al.*, 2000; Lyons *et al.*, 2000; Takai & Horikoshi, 2000; Khan *et al.*, 2001; Nadkarni *et al.*, 2002; Yang *et al.*, 2002; Maeda *et al.*, 2003; Tseng *et al.*, 2003). This was because the nature of the paper was not instantly obvious from the title and/or because they were exclusive to medical journals. Consequently, I abandoned this work when it became apparent that the DNA target sequences that met the conditions for TaqMan technology were poorly conserved between different bacterial species. This is in contrast to the authors noted above, who tested suboptimal primer and probe sets; however, some of these methods appear promising (Nadkarni *et al.*, 2002; Maeda *et al.*, 2003; Tseng *et al.*, 2003; Horz *et al.*, 2005). In this chapter I will describe the challenges that I experienced during the testing of a SYBR Green RT qPCR protocol for enumeration of total bacterial yield and in the design of a 16S rRNA-based TaqMan probe RT qPCR system for universal bacterial enumeration.

4.2. Materials and methods

4.2.1. Direct microscopic counts

4.2.1.1. Direct counts of bacteria recovered from a tip using light microscopy

A micro-sample was taken from the root apex (0 - 10 mm from the root cap) and the root base (0 - 20 mm from the root-shoot junction) of three, four day old, plants grown in CYG plastic growth pouches containing compost. For a positive control, a micro-sampling rod was touched on a three day old colony of *P. fluorescens* SBW25::*gfp* cells growing on 1/10th TSA (3 g L^{-1} Tryptic Soy Broth solidified with 1.5% Technical Agar No. 3, Oxoid, UK) containing 100 µg ml^{-1} cycloheximide (Sigma, UK) at 28 °C. This strain was a kind gift from Dr Tracy Timms-Wilson (Centre for Ecology and Hydrology, UK) who is the contact for further information. Bacteria adhered to the tips were recovered by sonicating at low power in 10 µl sterile water stored in a microtube supported by a polystyrene float in a water bath (Ultrasonik 300; JM Ney, Bloomfield, CT, USA) containing ice and water.

A small incision was made in the lids of the tubes to allow water to evaporate during the concentrating step. Samples containing bacterial cells and negative controls containing 10 µl sterile water were concentrated to a final volume of approximately 0.5 µl using a centrifugal evaporator (GeneVac SF50; Sales Development Ltd., Ipswich, England) with an RV5 high vacuum pump (BOC Edwards, Sussex, UK) and then transferred to wells on a sterile multi-spot glass slide (Flowlabs, Hertfordshire, UK). The remaining water was left to evaporate at room temperature and then bacterial cells were viewed under a 100x oil immersion lens using an Olympus BH-2 microscope. Photomicrographs were obtained using a Nikon Coolpix 5700 (Nikon, Tokyo, Japan).

4.2.1.2. Direct counts of bacteria on the surface of a tip using SEM

A stainless steel sample stub was smeared with *P. fluorescens* SBW25 *gfp* cells from a three day old colony growing on 1/10th TSA containing 100 µg ml^{-1} cycloheximide at

28 °C. This enabled clarification of the capacity for the LEO 1455VP SEM to image fresh bacterial cells. In addition, a micro-sampling rod was touched on a colony from the same plate. The rod was detached from the glass capillary and then mounted upright on a stainless steel sample stub using Loctite® Easy Brush Super Glue (Henkel Consumer Adhesives, Cheshire, UK). After imaging the stainless steel sample stub smeared with *P. fluorescens* SBW25 *gfp* cells using the LEO 1455VP SEM, the stub was coated with 60% gold-palladium using a Polaron E5100 coater (Polaron, Watford, UK), and then viewed in a Philips XL-30 field emission SEM. This microscope provides greater resolving power than the LEO 1455VP SEM and is likely to have comparatively little difficulty in imaging individual bacterial cells. For this reason it can be used as a control to check if bacteria are present on the sample stub in the event that the LEO 1455VP SEM fails to image bacterial cells.

4.2.2. RT qPCR quantification of total bacteria

4.2.2.1. Testing universal bacterial primers with SYBR green

RT qPCR was performed using an ABI 7700 Sequence Detection System (PE Applied Biosystems) and SYBR® Green for detection. Concentrations for the forward and reverse primers[5] reported by Muyzer *et al.* (1993) were optimized at 300 nM. RT qPCR consisted of 1-2 µl pooled soil gDNA ranging from neat genomic preparations to 10^{-2} dilution, in a total volume of 25 µl with SYBR® Green Jumpstart™ Taq ReadyMix™ (Sigma) and 60 nM ROX dye. RT qPCR amplification was performed using 94 °C 15 s denaturing, 53°C 15 s annealing and 72°C 30 s extension for 55 cycles in duplicate for all standards. In addition, two no-template controls, and two no-template controls without primers were included.

[5] Muyzer *et al.* (1993) report three primers. Primer one (5' – CCTACGGGAGGCAGCAG – 3') is the forward primer; however, the published nucleotide sequence is incorrect and the revised primer is 5' – CCTACGGGAGGGAGCAG – 3' (Ian Clark, Rothamsted Research, *Pers comm.*). Primer two (5'- ATTACCGCGGCTGCTGG – 3') is the reverse primer, and Primer three is the same as the revised primer one but has at its 5' end an additional 40-base GC rich sequence (GC clamp).

4.2.2.2. Design of a TaqMan system

4.2.2.2.1. Acquisition and alignment of 16S rRNA gene sequences

Multiple 16S rRNA gene sequences from type strains within each genus within each bacterial phylum were acquired from the Ribosomal Database Project II using the hierarchical browser function. Sequences were then imported into the BioEdit program (Hall, 1999) and aligned using ClustalW (Thompson *et al.*, 1994).

4.2.2.2.2. DNA sequence analysis and design of the universal primers and probe

Multiple sequences from arbitrarily selected type strains were analysed individually using the Primer Express software provided by PE Applied Biosystems (ABI; Wolverhampton, UK). This software designs probes and primers suitable for the thermo-cycling conditions specified by ABI. The main selection criteria are that the selected primers and probes should be close together in a region with G/C contents between 20-80 % and should amplify a DNA segment between 50-150 base pairs. The regions within the multiple sequence file in BioEdit corresponding to the best fit suggestions for universal probe and primers sets were then assessed manually.

4.3. Results

4.3.1. Direct microscopic counts

4.3.1.1. Direct counts of bacteria recovered from a tip using light microscopy

P. fluorescens SBW25 *gfp* cells recovered from a micro-sampling tip were clearly visible using the light microscope (Fig. 4.2a). However, bacterial cells recovered from micro-sampling tip touched on the rhizoplane could not be distinguished from other debris that may have been picked up by the tip on contact with the root (Fig. 4.2c, d). Bacterial cells were absent from the negative control but a number of marks were apparent on the microscope or camera lens (Fig. 4.2b). These are consistent between the samples and should not be confused with possible bacterial cells.

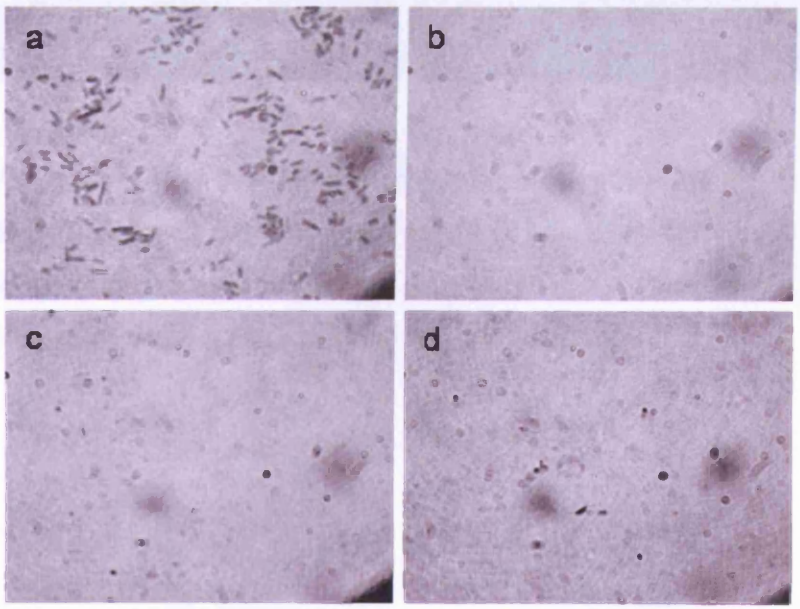

Fig. 4.2 Photomicrographs showing (a) a control sample containing *P. fluorescens* SBW25 *gfp* cells, (b) a control sample containing no bacteria, (c) a sample containing bacteria recovered from the tip of a micro-sampling rod that had been touched on the rhizoplane at the root base, and (d) a sample containing bacteria recovered from the tip of a micro-sampling rod that had been touched on the rhizoplane at the root apex. Note that the marks in b are associated with the microscope and are present in all samples.

4.3.1.2. Direct counts of bacteria on a tip using SEM

Using the LEO 1455VP SEM, *P. fluorescens* SBW25 *gfp* cells smeared on the surface of a stainless steel sample stub were indistinguishable (Fig. 4.3a). Bacterial cells could also not be distinguished on the surface of a micro-sampling tip that had been touched on the surface of a *P. fluorescens* SBW25 *gfp* colony. This was clearly related to the resolving power of the LEO 1455VP SEM as the Philips XL-30 field emission SEM was able produce clear images of the *P. fluorescens* SBW25 *gfp* cells that were smeared on the surface of the stainless steel sample stub (Fig. 4.4).

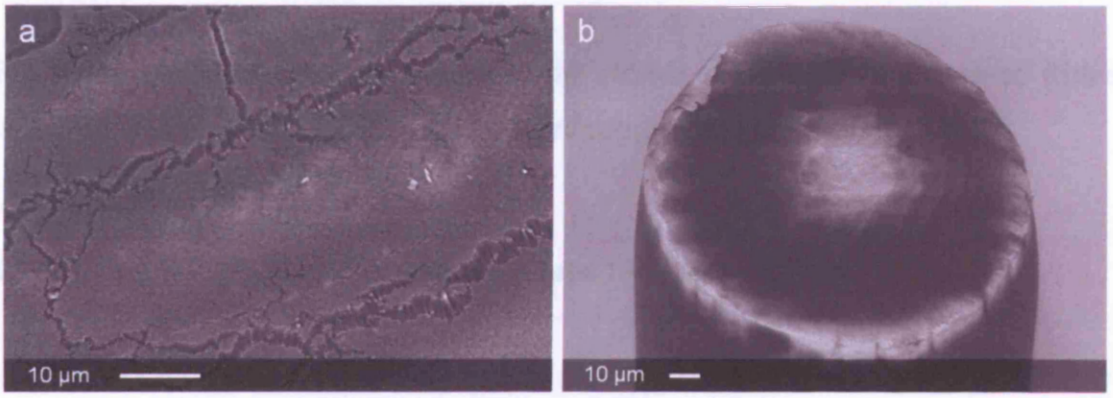

Fig. 4.3 Scanning electron micrographs showing (a) the surface of a sample stub smeared with a colony of *P. fluorescens* SBW25 *gfp*, and (b) the tip of a micro-sampling rod that had been touched on a colony of *P. fluorescens* SBW25 *gfp*. Images were captured using a LEO 1455VP SEM.

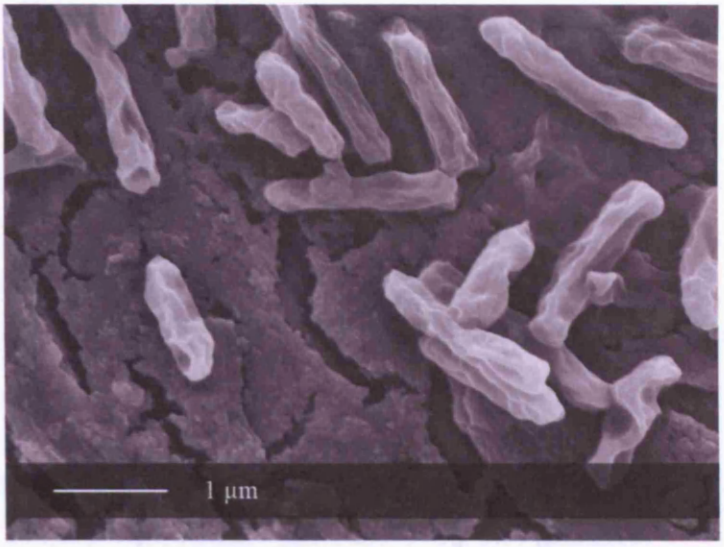

Fig. 4.4 Scanning electron micrograph of the surface of a sample stub smeared with a colony of *P. fluorescens* SBW25 *gfp* captured using a Philips XL-30 FEG SEM.

4.3.2. Using RT qPCR to determination total bacterial numbers

4.3.2.1. SYBR Green

RT qPCR amplification of samples containing a two concentration of pooled soil gDNA was successful; however, a signal was also generated from the no-template controls. The melt curve analysis revealed that this was not due to the presence of contaminating bacterial DNA but a consequence of the generation of primer dimers (Fig. 4.5). The production of primer dimers will decrease the efficiency of PCR and as they are double stranded they also lead to SYBR Green fluorescence. This will contribute towards to the fluorescence signal and interfere with the interpretation of the results; therefore, a high-degree of optimisation would be required to develop a reliable RT qPCR protocol. As fluorescence is only detect from specific hybridised target amplicons using the TaqMan system, this approach may be preferable.

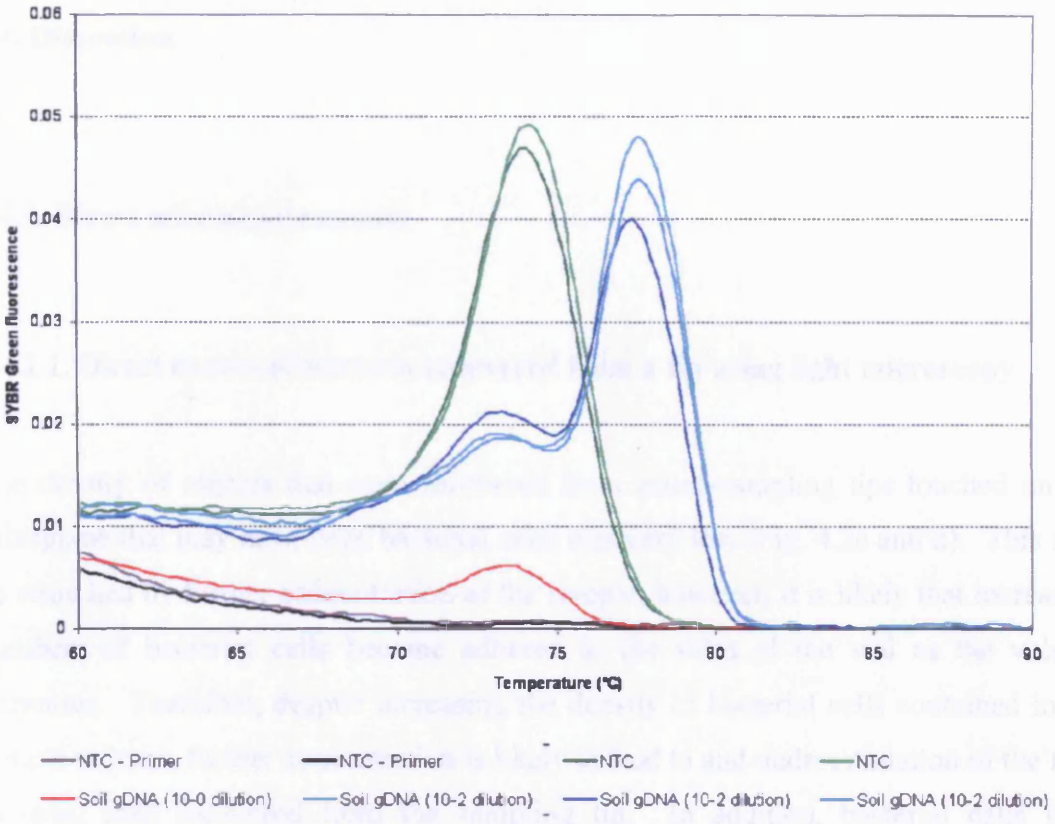

Fig. 4.5 Melt curve analysis of samples containing pooled soil gDNA (undiluted and 10^{-2} dilutions) using primers reported by Muyzer *et al.* (1993). The peak around 77.8 °C corresponds to the target amplicons while the peak around 74.3 °C is likely to correspond to a primer dimer. The use of high concentrations of pooled soil gDNA was also observed to inhibit PCR. This is likely to result from the presence of humic acids and other PCR inhibitors (von Wintzingerode *et al.*, 1997).

4.3.2.2. DNA sequence analysis and design of the universal primers and probe

The Primer Express software resulted in a series of best fit suggestions for the universal probe and primers set that lead to unsatisfactory sequence homology for many of the bacterial genera (see Appendix 2).

4.4. Discussion

4.4.1. Direct microscopic counts

4.4.1.1. Direct counts of bacteria recovered from a tip using light microscopy

The density of objects that were recovered from micro-sampling tips touched on the rhizoplane that may have been bacterial cells was very low (Fig. 4.2c and d). This may be remedied by further concentration of the sample; however, it is likely that increasing numbers of bacterial cells become adhered to the sides of the vial as the volume decreases. Therefore, despite increasing the density of bacterial cells contained in the sample volume, further concentration is likely to lead to and underestimation of the total bacterial load recovered from the sampling tip. In addition, bacterial cells were indistinguishable from other debris that may have been picked up on contact with the root. This problem may be remedied by using fluorogenic stains. For example, Griebler (2001) was able to differentiate between bacterial-like particles and bacterial cells in aquatic sediments by staining with DAPI and then counter-staining with SYBR Green II. Despite this it is unlikely that light microscopy will be effective for enumerating bacterial cells in micro-samples.

4.4.1.2. Direct counts of bacteria on a tip using SEM

The prerequisites for enumeration of bacterial cells on a sampling tip using SEM were that bacterial cells could be imaged effectively without any pre-treatment that may have a damaging effect on the DNA or inhibit the recovery of cells from the surface of the tip post enumeration. In addition, to view the sampling tip it was necessary to that the microscope could accommodate the rod in an upright position. The LEO 1455VP SEM fulfilled the latter criterion but failed to image individual bacterial cells clearly. This was related to the resolving power of the microscope rather than a problem with the samples themselves as using the Philips XL-30 field emission SEM, individual bacterial cells were imaged clearly. In absence of a microscope that fulfils both criteria

SEM is not a feasible option for enumerating bacterial cells in micro-samples. The method is also very expensive when compared with other approaches such as RT qPCR.

4.4.2. RT qPCR enumeration of total bacteria

4.4.2.1. Testing universal bacterial primers with SYBR green

The melt curve analysis for the no-template control indicated that the fluorescence signal was generated from primer dimers. This may be overcome with significant PCR opimisation; however, contaminating bacterial DNA is widely reported to occur in commercial PCR-grade consumables including the SYBR Green mix (Shen *et al.*, 2006), water, primers, and reaction vessels (Corless *et al.*, 2000; Shen *et al.*, 2006). This represents a major obstacle for PCR amplification using primers that target a broad-range of bacterial species, and may be particularly problematic when samples contain very low quantities of bacterial DNA, such as is the case with micro-samples. For example, Nadkarni *et al.* (2002) found that contaminating bacterial DNA in a range of PCR reagents from different suppliers limited the detection limit of their universal TaqMan RT qPCR system to approximately 50 bacterial cells. Numerous efforts have been made to eliminate contaminating bacterial DNA, including exposure to ultraviolet radiation (Maiwald *et al.*, 1994; Corless *et al.*, 2000; Sleigh *et al.*, 2001), digestion with *Ava*I, *Hae*III, *Hin*fI, *Sau*3AI, and *Sma*I restriction endonucleases (Carroll *et al.*, 1999; Corless *et al.*, 2000), and treatment with the DNase I enzyme (Rochelle *et al.*, 1992; Steinman *et al.*, 1997; Corless *et al.*, 2000). However, while these treatments may be effective for conventional PCR, they generally lead to a decrease in PCR efficiency and therefore affect the sensitivity of RT qPCR (Corless *et al.*, 2000). Having said this, a more recent report has demonstrated that treatment of 2 X SYBR Green PCR master mixture with DNase I (10^{-3} U/µl) at 37 °C for 60 min followed by heat inactiviation at 90 °C for 30 min before running RT qPCR can effectively remove contaminating bacterial DNA with little loss of efficiency (Tseng *et al.*, 2003).

Tseng *et al.* (2003) also demonstrated that they could differentiate between target amplicons from different bacterial types based on their melting peak profiles. This is particularly interesting as their primers have been shown to perfectly match 71% of 16S rRNA genes out of 41,000 sequences analysed using the ARB software (Horz *et al.*,

2005). This is a vast improvement on coverage of bacterial species over culture-based techniques.

As bacterial numbers in micro-samples are likely to be very low, any loss in PCR efficiency is likely to result in substantial underestimation by RT qPCR. Therefore, the effect of DNase I pre-treatment of 2 X SYBR Green PCR master mixtures on RT qPCR sensitivity requires considerable investigation before applying this step to RT qPCR of micro-samples.

4.4.2.2. Design of a TaqMan system

The suggestions for universal probe and primers sets provided by the Primer Express software were associated with regions of 16S rDNA that exhibit too low a level of homology between different bacterial types. For this reason, I decided to abandon the development of a TaqMan system for enumerating bacteria in micro-samples.

Nadkarni *et al.* (2002) also reported the limited value of the Primer Express software in determining a universal primers and probe set for enumeration of total bacteria numbers. As a result they investigated suitable locations within 16S rRNA gene sequences manually, using the Primer Express software to check for primer dimer or internal hairpin configurations, melting temperature, and the percentage of G/C contents within possible primers and probes. Their final primers and probe set amplifies a region 466 bp (50-150 bp is the size recommended by ABI) and has been shown to perfectly match 63 % of 16S rRNA genes out of 41,000 sequences analysed using the ARB software (Horz *et al.*, 2005).

Horz *et al.* (2005) also investigated the proportion 16S rRNA gene sequences out of a total of 41,000, that perfectly matched most other reported universal primers and probe sets (Corless *et al.*, 2000; Lyons *et al.*, 2000; Takai & Horikoshi, 2000; Khan *et al.*, 2001; Nadkarni *et al.*, 2002; Yang *et al.*, 2002; Maeda *et al.*, 2003; Tseng *et al.*, 2003; Labrenz *et al.*, 2004; Siqueira *et al.*, 2004). The TaqMan primers and probes designed by Nadkarni *et al.* (2002) and the universal primers for use with SYBR Green designed by Maeda *et al.* (2003) and Tseng *et al.* (2003) appear to be the best and deserve further investigation.

4.4.3. General comments

Issues relating to contamination and the universality of probe and/or primers sets are of great importance to both TaqMan and SYBR Green based RT qPCR detection systems and have been discussed above. Other issues that affect the quantitative capacity of RT qPCR include the method of DNA extraction (Zucol *et al.*, 2006) and the number of copies of the 16S rRNA gene per bacterial cell (Klappenbach *et al.*, 2000). With respect to the latter, the interpretation of total bacterial load is complicated by the fact that bacteria harbour multiple rRNA operons containing the 16S, 23S and 5S rRNA genes (Rainey *et al.*, 1996; Klappenbach *et al.*, 2000). It has been shown that the copy number of rRNA operons varies between 1-15 (Rainey *et al.*, 1996); therefore, bacterial load may be overestimated.

This is likely to be particularly problematic when analysing the relative abundance of different bacterial types post-PCR, as organisms with greater copy numbers of 16S rRNA genes will appear more abundant than those with lower copy numbers and may out compete 16S rDNA from rarer species during PCR (von Wintzingerode *et al.*, 1997). A further issue relating to diversity analysis based on 16S rRNA genes is that they can vary up to several percent between operons within the same species (Mylvaganam & Dennis, 1992; Wang *et al.*, 1997; Yap *et al.*, 1999; Tourova *et al.*, 2001; Acinas *et al.*, 2004). Any investigation of bacterial diversity based on discrimination between amplified sequences of 16S rDNA can therefore lead to significant overestimation of the number of different bacterial types (Crosby & Criddle, 2003).

Currently, there is not a single method that enables bacterial numbers to be enumerated accurately while maintaining the facility to investigate bacterial diversity post enumeration. While microscopic techniques appear to be unsuitable for determining bacterial numbers in micro-samples, further investigation of molecular based approaches is likely to be fruitful. This would be particularly advantageous if the approach developed could provide both the total number of bacteria and the relative abundance of different bacterial types. This would enable valid comparisons of diversity between samples (Chapter 5).

CHAPTER 5

SPATIOTEMPORAL TRENDS IN CULTURABLE BACTERIAL DENSITY AND DIVERSITY

5.1. Introduction

Spatiotemporal trends in rhizosphere bacterial density and diversity were discussed in section 1.5.2., which highlighted that while microscopic observations can provide useful information about the distribution of bacteria at the micro-spatial-scale, investigations of other features, such as bacterial diversity, require that samples are taken. In this chapter I report the application of the micro-sampling method (Chapter 3) to investigating culturable bacterial density and diversity at the root base and apex of four, six and eight day old *B. napus* roots. To further validate the findings of the microsampling assays, trends in rhizosphere bacterial density were also investigated using a bioluminometric colonisation assay (section 5.1.2). This enabled trends to be observed at a whole root system scale.

Before proceeding to the experimental details it is important to discuss the issues surrounding diversity estimation in micro-samples. Here, diversity is considered to be the rate at which new species (OTU) are encountered with increasing numbers of individuals observed. This is in recognition of the fact that the sampling effort necessary to count all species in the soil and on the rhizoplane is beyond practical limits.

5.1.1. Measuring bacterial diversity

As mentioned in section 4.1, standard cultivation methods are widely reported to underestimate both bacterial density and diversity (Weisburg *et al.*, 1991). However, given that root exudates are thought to underpin the proliferation of bacteria in the

rhizosphere (Marschner, 2002), and that simple sugars, and other compounds common to most cultivation medias are reported to be the main constituents of exudates, it is likely that a greater proportion of bacteria in the rhizosphere are culturable when compared with bulk soil. Therefore, with respect to the rhizosphere, it is assumed that culture-related bias leads to less deviation from the real trends in community structure than would be apparent in more oligotrophic environments. In this sense it is worth emphasising that in the rhizosphere, culture-dependent techniques may provide insights into microbial ecology that are currently not possible with molecular-based approaches.

It is widely recognised that for bacteria inhabiting the soil/rhizosphere it is currently not possible to measure asymptotic richness (absolute richness) due to the number of samples that would be need to be analysed to observe all species. Therefore, asymptotic richness is inferred in a qualitative manner, using a range of techniques such as rarefaction (Colwell *et al.*, 2004), or richness/diversity estimators (Magurran, 2004). As the number of individuals in a sample may vary, sample-based diversity analyses are technically a measure of the species density rather than species richness. For this reason, in molecular studies, it is standard protocol to extract DNA from bacterial communities present in one gram of soil and then standardise the concentration of bacterial DNA added to a PCR. It is assumed that this process enables taxonomic richness to be assessed at equal densities of bacteria such that diversity can be compared between treatments at equal numbers of replicates. For micro-samples, however, low concentrations of bacterial DNA present an obstacle to the standardisation of DNA concentrations between samples. Therefore, given that bacterial density has been shown to be heterogeneous at the micro-spatial-scale, an alternative approach to sample-based comparisons is necessary. This is not a problem provided that individual bacteria can be enumerated and identified. Culturing enables the numbers of bacteria to be counted, and by fingerprinting each colony it is possible to identify both the richness and evenness of a sample. Given that micro-samples contain low bacterial densities this approach is feasible and allows diversity to be compared on an individual basis.

In Chapter three the number of culturable rhizoplane bacteria recovered from micro-sampling rods after one or two washing cycles varied between 1-80 CFU per tip at the root base and 1-17 at the root apex (table 3.1). This heterogeneity must be accounted for when determining the bacterial diversity of a micro-sample as the diversity of a sample containing three bacteria consisting of two species is quite different to one

containing a hundred bacteria, ninety nine of which belong to one species and only one belonging to another. This problem can be overcome using the technique, 'rarefaction'. Rarefaction enables the calculation of richness (the number of OTU) for a given number of sampled individuals and allows the construction of a rarefaction curve for each community analysed. To understand the general principle behind rarefaction curves is is useful to first consider accumulator curves.

An accumulator curve is a plot of the cumulative number of operational taxonomic units (OTU) versus the cumulative number of individuals within a sample inventory. As more individuals are sampled, more OTU will be observed; therefore, accumulator curves rise rapidly at first and then more slowly as increasingly rare OTU are observed. Theoretically, an asymptote will be reached and no further OTU will be observed, a point which is representative of the richness of the community under investigation. For diverse taxa in complex environments, such as bacteria in soil, asymptotic richness is elusive as the sampling effort is beyond the scope of current feasibility. Instead, richness can be inferred in a qualitative manner, as can evenness (equality of OTU abundances), from the slope of the curve – the steeper the slope the greater the richness and evenness. As accumulator curves are constructed by sequential accumulation of individuals within a sample or sample set the resulting curves are not smooth, but jagged, reflecting the spatial and temporal patchiness inherent in the environment that they represent. Individual-based rarefaction can be used to produce a smooth curve that may be viewed as the statistical expectation of the corresponding accumulator curve over different reorderings of individuals (Hurlbert, 1971; Heck *et al.*, 1975).

5.1.2. Bioluminometric colonisation assay for spatial mapping of rhizosphere bacterial colonisation

Beauchamp *et al.* (1993) reported a technique for imaging the colonisation of maize roots by a bioluminescent bacterial mutant. The technique involved inoculating maize seedlings with Tn5-*lux*AB *Pseudomonas* sp. that were then grown in rhizotrons containing soil. The *lux*AB genes produce bacterial luciferases which catalyse bioluminescence reactions that involve the oxidation of a reduced riboflavin phosphate and a long chain fatty aldehyde (Meighen & Dunlap, 1993). In addition to the reaction

products there is also a concomitant emission of blue green light which can be detected to monitor the bioluminescence reaction. Using a sensitive low-light camera, Beauchamp *et al.* (1993) were able to image the spatial distribution of their mutants *in-situ* following the addition of decyl aldehyde to fulfil the requirements for the bioluminescence reaction. I modified this approach such that *P. fluorescens* SBW25::*lux*CDABE cells would colonise the root from inoculated soil, rather than from the seed. This mutant, produced by Wiles (2001), was a kind gift from Tracy Timms-Wilson (Centre for Ecology and Hydrology, UK). The *lux*CDE genes encode enzymes that are responsible for the synthesis of the long-chain aldehyde substrate that is required in the bioluminescence reaction; therefore, by using a mutant containing the full bacterial luciferase operon (*lux*CDABE) it was not necessary to add the aldehyde prior to imaging. This is advantageous as it avoids any re-distribution of cells that may occur as a consequence of the aldehyde application.

5.2. Materials and methods

5.2.1. Micro-sampling approach

5.2.1.1. Plants and growth conditions

Twenty eight plants were grown in CYG plastic growth pouches containing compost. For further details refer to Chapter two.

5.2.1.2. Micro-sampling and enumeration of culturable bacteria

Four, six and eight days after planting, two samples per plant were taken from the root apex (0 - 10 mm from the root cap) and one from the root base (0 - 20 mm from the root-shoot junction) (Fig. 5.1). In addition, two samples per plant were taken from randomly selected points in the bulk soil by touching the tip on a soil crumb (Fig. 5.1).

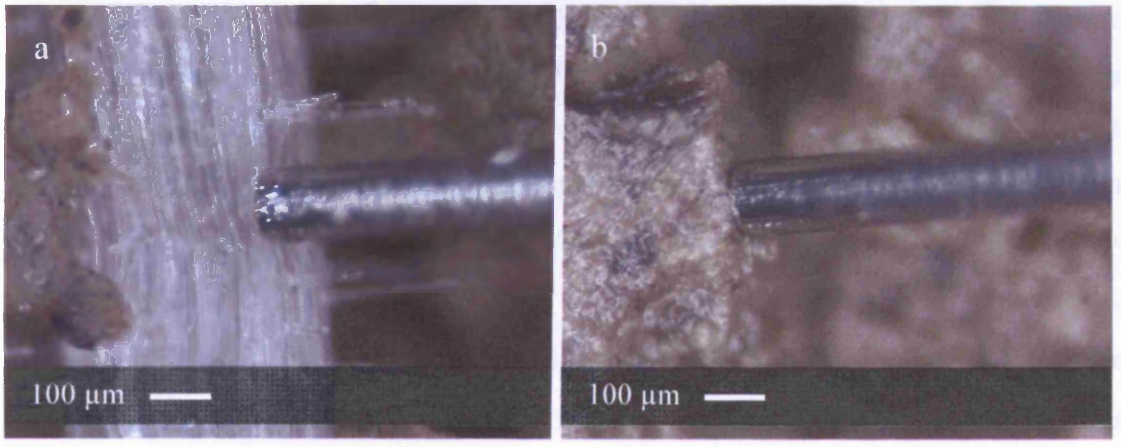

Fig. 5.1 Micro-sampling rod touching a) the rhizoplane and b) a soil crumb.

Bacteria adhered to the tip were recovered in a microtube containing 10 µl PBS by sonicating for 60 s at low power in a sonicating water bath containing ice and water. Samples were then made up to 200 µl with sterile PBS and plated on $1/10^{th}$ TSA

containing 100 μg ml^{-1} cycloheximide. Plates were incubated for ten days at 28 °C. CFU were recorded after three, seven and ten days; the maximum count for each plate was used as the final result.

5.2.1.3. Colony picking and DNA extraction

Bacterial numbers in the basal region were most numerous and least variable. They were therefore considered the most reliable counts upon which to select plants that best represented the mean bacterial population trends observed within the experiment. Five plants were selected with CFU in basal region micro-samples that were closest to the mean of all plants measured, both four and six days after planting. The selection provided 716 colonies from which DNA was extracted by the method of Klimyuk *et al.*, (1993).

5.2.1.4. DNA fingerprinting of culturable bacteria using ERIC-PCR

PCR fingerprinting, using Enterobacterial Repetitive Intergenic Consensus (ERIC) primers that bind to repeated sequences present in many bacterial genomes and thus provide arbitrary fingerprints (Versalovic *et al.*, 1991), was routinely performed using 1 μl DNA sample, 12.5 μl REDTaq™ 2X ReadyMix™ PCR Reaction Mix (Sigma, UK), 1 μl 10 μM μl^{-1} R1CIRE (5'- CAC TTA GGG GTC CTC GAA TGT A-3'), 1 μl 10 μM μl^{-1} ERIC2 (5'- AAG TAA GTG ACT GGG GTG AGC G-3'), 1 μl 2.5 mM $MgCl_2$ and 8.5 μl molecular biology grade water per reaction. The following thermocycler (T Gradient; Biometra, Göttingen, Germany) conditions were used: 30 cycles of 94 °C 1 min, 46 °C 1 min, 72 °C 1 min, final step 72 °C 5 min, then maintained at 4 °C. PCR reactions and size markers (100 bp DNA ladder; Fermentas Life Sciences, York, UK) were run on 1.5 % agarose gels and stained with ethidium bromide prior to image capture using a transilluminator.

ERIC profiles were analysed using Phoretix 1D analysis software v. 2003.02 (Phoretix International, Newcastle upon Tyne, UK). Lanes were identified; then bands were assigned and matched by comparison with molecular size ladders (100 bp). Results were summarised in a dendrogram which allowed sample profiles to be divided

into clades; each clade was designated an operational taxonomic unit (OTU) for diversity analyses.

5.2.1.5. Statistical analyses

5.2.1.5.1. Bacterial density

Differences in bacterial density, i.e. CFU tip^{-1} (x) within treatment combinations (plant ages within zones) were compared using the REML method which accounted for the unbalanced design structure (unequal numbers of replicates between zones) and any correlation between plant ages given the repeated measures on plants. Data were transformed (log_{10} (x + 0.5)); this ensured that the assumption of Normality was fulfilled. A mixed model was fitted with random effects due to nested design terms (plants, zones within plants, and plant ages within zones within plants) and fixed effects due to the treatment terms (zones, plant ages and their interaction). All REML analyses were implemented using the GenStat statistical system (GenStat 8th edition, Lawes Agricultural Trust; VSN International, Hemel Hampstead, UK).

5.2.1.5.2. Bacterial diversity within micro-samples

5.2.1.5.2.1. Individual-based rarefaction

Individual-based rarefaction curves were used to investigate the effect of plant ages and zones on taxonomic diversity. These were computed by EstimateS (Colwell, 2005) using the method of Colwell *et al.* (2004). This method estimates rigorous confidence intervals that enable straightforward comparisons between different curves.

5.2.1.5.2.2. Correspondence between different samples and groups of samples

It was not possible to detect correspondence between bacterial types within the treatment combinations as too little of the variation was accounted for in the first three

inertias (23 %; implemented using the GenStat statistical system). Therefore, the number of bacterial types that appeared in more than one sample within each treatment combination was assessed manually.

5.2.2. Bioluminometric colonisation assay

5.2.2.1. Bacterial growth conditions

Liquid cultures were initiated by inoculating 20 ml Tryptic Soy Broth (TSB; Oxoid, UK) with a single colony of *P. fluorescens* SBW25::*lux*CDABE that had been isolated on 1/10 TSA (3 g L^{-1} TSB solidified with 1.5 % Technical Agar No. 3, Oxoid) containing 50 μg ml^{-1} kanamycin (to select for the maintenance of the *lux*CDABE operon) and maintained for 16 h at 28 °C, 200 rpm on an orbital shaker. Cells were then harvested by centrifugation (15 min, 4000 X g), the supernatant was removed and the pelleted cells were re-suspended in an equal volume of sterile reverse osmosis water (RO H_2O). This washing process was repeated three times and the cell suspension was then returned to 28 °C, 200 rpm for 24 h to precondition the cells for the relatively low-nutrient conditions in the compost when compared with the 1/10 TSB.

5.2.2.2. Compost inoculation procedure

Starved cells were harvested by centrifugation (15 min, 4000 X g), the supernatant was removed and the cells were re-suspended in 15 ml of sterile RO H_2O by vigorous shaking. Starved cell suspensions containing approximately 10^8 cells per millilitre were thoroughly mixed with 100 g compost per growth pouch to achieve the intended inoculation density of 10^7 cells per gram of compost (fresh weight). An inoculation density of 10^7 cells per gram of compost was considered to be appropriate for visualisation of bacterial rhizosphere colonisation as the population size of the mutant would vastly out number that of other species, thereby increasing its likelihood to establish. Inoculated soil was equilibrated for 72 h in a sterile light-tight ventilated container at 28 °C.

5.2.2.3. Plants and growth conditions

Fourteen plants were grown in seven CYG plastic growth pouches each containing 115 g of inoculated compost and 35 ml of reverse osmosis purified water. Other details relating to plant growth were the same as those described in Chapter two.

5.2.2.4. Image capture

The imaging equipment consisted of a CCD camera (Roper Scientific, Tucson, AZ, USA and Princeton Instruments, Trenton, NJ, USA) with a Nikkor 50 mm f 1:1.2 lens (Nikon, Japan) connected to a computer operating the MetaMorph V.4.5r6 software package (Universal Imaging Corporation™, Downingtown, PA, USA). The camera, cooled to -120 °C with liquid nitrogen, was mounted in a light-tight box that contained a lamp that could be switched on and off to capture bright or dark field images. Prior to placing a CYG rhizotron in the light-tight box, the roots were exposed by cutting back the plastic fascia. Once in the box the working distance was fixed (350 mm), as was the aperture setting (f 1.2), and then the roots were brought into focus. Two images were then captured: (a) a bright field image (light on) (52 milliseconds), and (b) a dark field image (light off) (40 min). The dark field image was then converted to pseudo-colour and overlaid on the bright field image (Fig. 6.1); the software overlay settings were fixed throughout the experiment (bright field: 560 – 7400; dark field: 65 – 114). Roots were imaged four and six days after planting.

5.3. Results

5.3.1. Micro-sampling approach

5.3.1.1. Bacterial density within micro-samples

Figure 5.2 displays the number of culturable bacteria in each micro-sample. Bacterial density was highly variable between samples indicating a high degree of patchiness at the micro-scale.

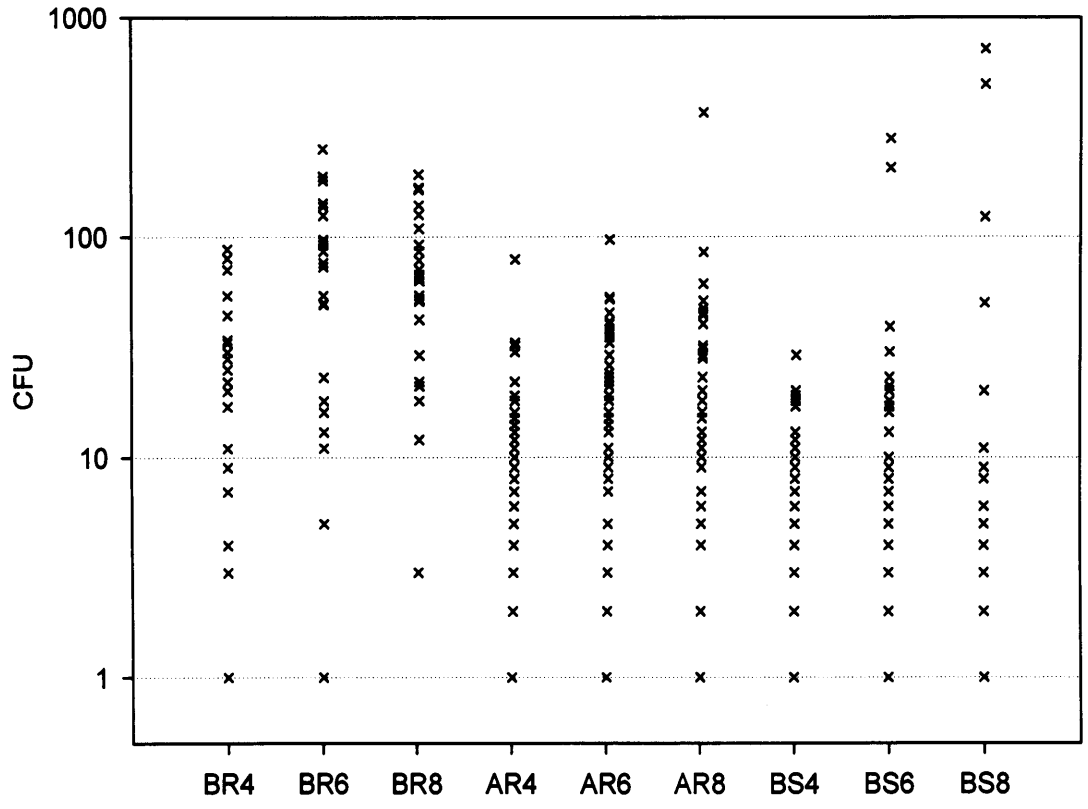

Fig. 5.2 Numbers of bacteria (CFU) in micro-samples within treatment combinations: BR (basal region), AR (apical region), BS (bulk soil), 4, 6, and 8 d after planting.

The treatment terms (zones, plant ages and their interaction) all had a significant effect (Wald tests, $P < 0.05$) on bacterial densities. Although there were repeated measures within plants, there was no significant autocorrelation between plant ages within zones within plants ($P > 0.05$). Figure 5.3 shows the REML predicted means and standard errors for each treatment combination. The density of culturable bacteria followed the order: basal region > bulk soil > apical region. Using standard errors, with the exception of the basal region and bulk soil four and eight days after planting, all zones were significantly different from one another. A significant temporal effect on bacterial density was observed only in the basal region between four and six days.

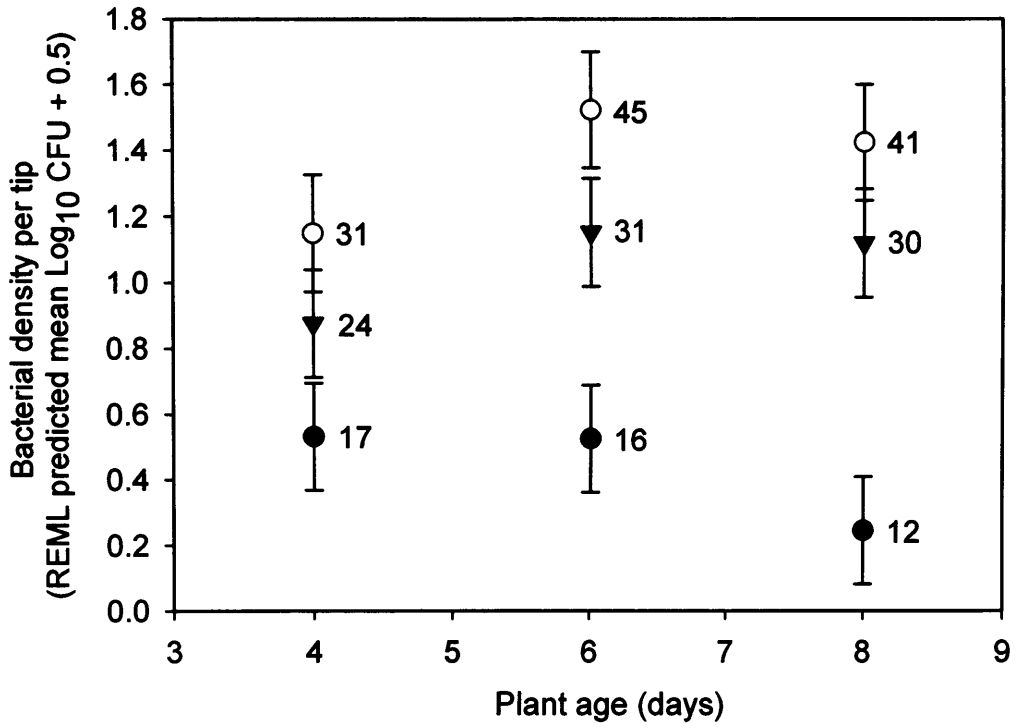

Fig. 5.3 REML predicted mean bacterial densities per tip (Log_{10} CFU + 0.5) within each zone by plant age combination: apical region (●), basal region (○), bulk soil (▼). Error bars represent standard errors of means. Numbers represent REML predicted means back-transformed to the original scale.

5.3.1.2. Bacterial diversity

5.3.1.2.1. ERIC-PCR fingerprinting

ERIC profiles were obtained from 40 % (262/655) of the colonies that were analysed (Fig. 5.4). These colonies represented 135 OTU.

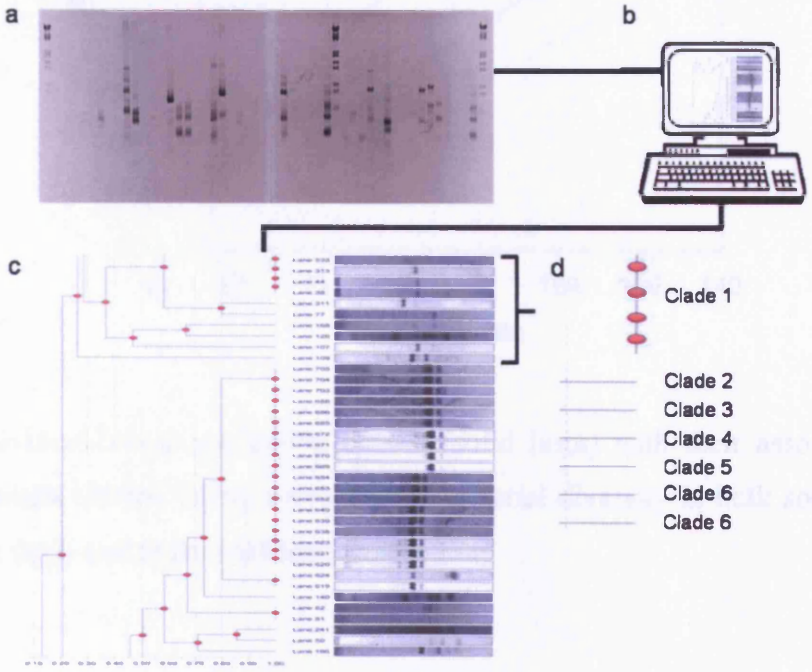

Fig. 5.4 ERIC profiles from colonies in microsamples ran on a 1.5 % agarose gel with 100 bp ladders (a). Gel images are analysed using specialist computer software (b) that organises ERIC fingerprints into a dendrogram (c). The final branches of the dendrogram represent the clade or bacterial type (d).

5.3.1.2.2. Individual-based rarefaction

Plant age at the time of sampling was found to have a significant effect on bacterial diversity. Differences between zones were not significant but followed the order: bulk soil > apical region > basal region (Fig. 5.5). Differences in bacterial diversity between zones within plant ages, or between plant ages within zones were not

significant; however, the order bulk soil > apical region > basal region was observed in both plant age categories, and increasing dominance was more apparent in root samples than in soil samples.

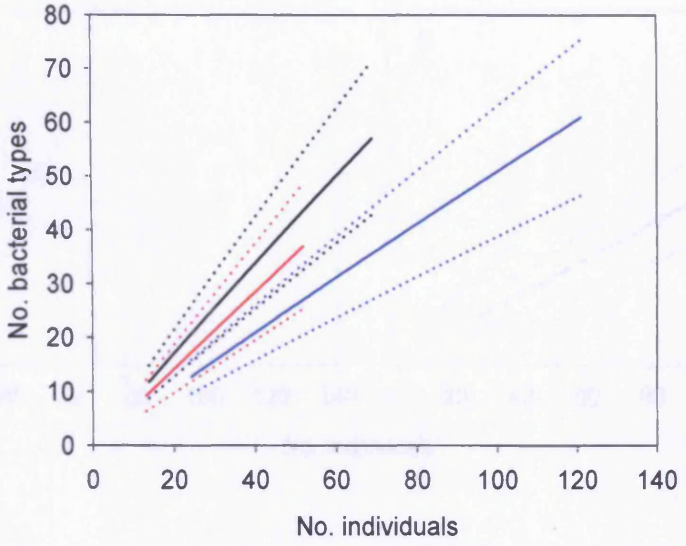

Fig. 5.5 Individual-based rarefaction curves (solid lines) with their associated 95 % confidence limits (dotted lines), representing bacterial diversity in bulk soil (black), at the root apex (red) and at the root base (blue).

In pooled root samples, bacterial diversity decreased significantly between four and six days, whereas in the bulk soil there was no change. The difference between root samples and bulk soil samples became significant six days after planting (Fig. 5.6).

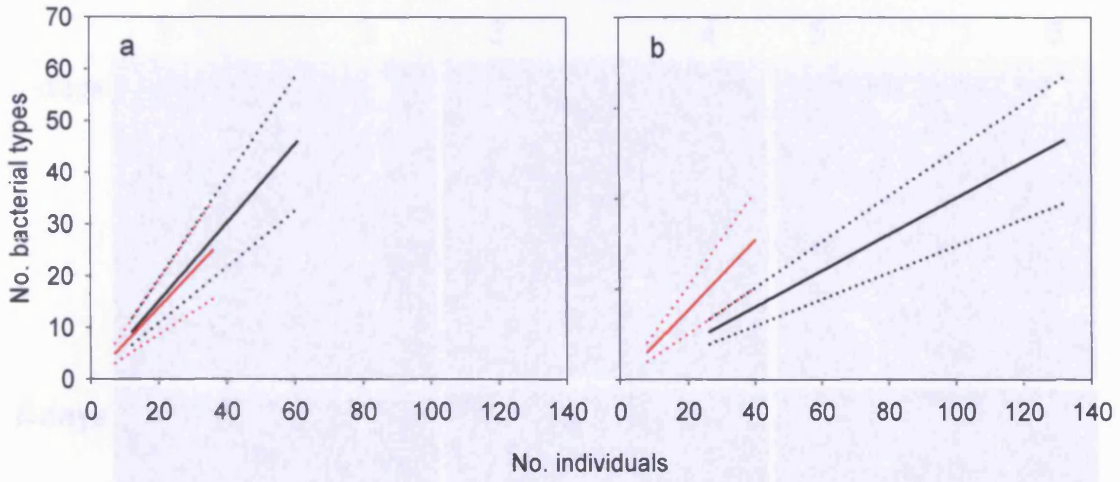

Fig. 5.6 Individual-based rarefaction curves (solid lines) with their associated 95 % confidence limits (dotted lines), representing bacterial diversity: 4 (a) and 6 (b) days after planting, on the rhizoplane (black) or in bulk soil (red).

5.3.1.2.3. Correspondence analysis

A manual comparison of the bacterial types that were found in each micro-sample revealed that just 4.6 % of OTU were observed on more than one plant within each zone within plant age category. This may reflect the very high diversity associated with the soil and the rhizosphere.

5.3.2. Bioluminometric colonisation assay

Luminescence, indicative of the presence of active *P. fluorescens* SBW25::*lux*CDABE cells within the rhizosphere, was detected on approximately 30 % of four day old root systems, and approximately 14 % of six day old root systems (Fig. 5.7). Of the root systems from which bioluminescence was detected, the signal was generally absent in the apical root region but was always detected in the root base. Figure 5.8 shows an overlay as well as the bright and dark field images from which it was generated it is

clear from the dark field image that bioluminescence decreased with increasing distance from the apical region. This was the case for all root systems from which bioluminescence was detected.

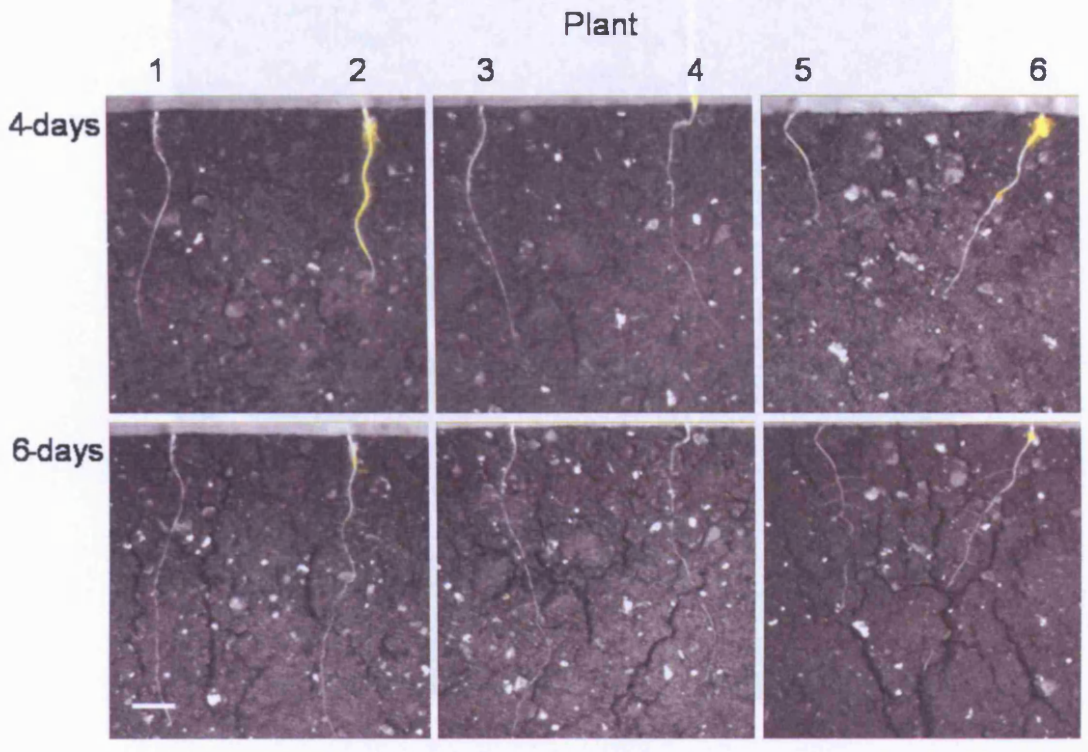

Fig. 5.7 Colonisation patterns of the bioluminescent mutant *P. fluorescens* SBW25::*lux*CDABE (yellow) on the rhizosphere of *B. napus*. Scale bar (bottom left) = 2 cm.

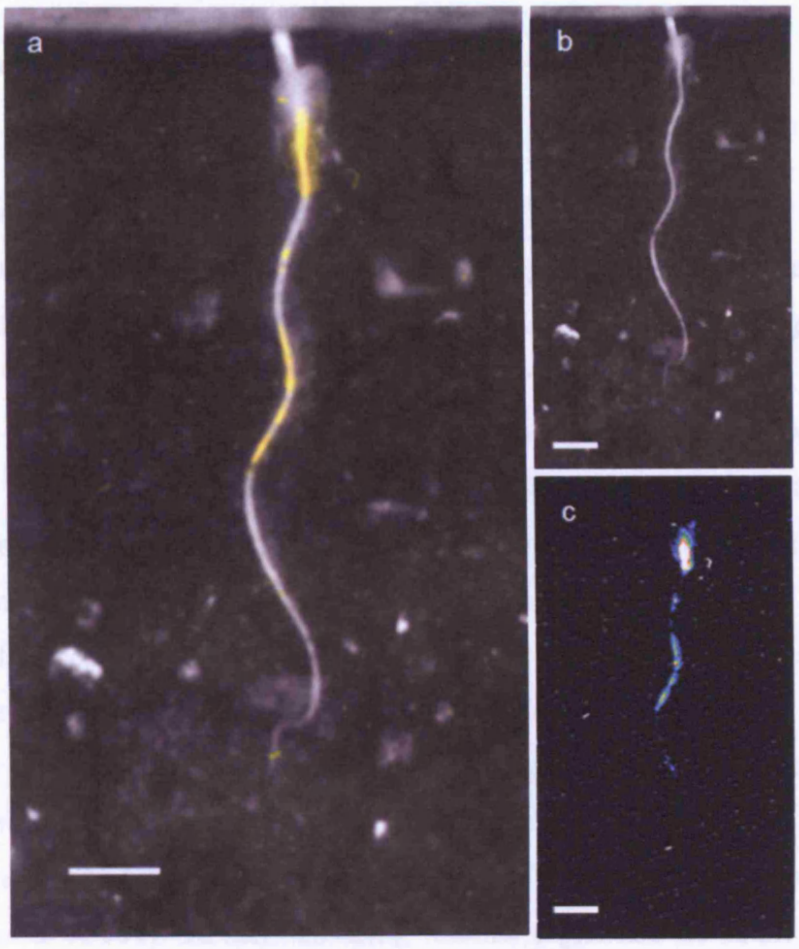

Fig. 5.8 Colonisation pattern of *P. fluorescens* SBW25::*lux*CDABE in the rhizosphere of a four day old *B. napus* root; (a) overlay, (b) bright field, and (c) dark field image. Scale bars = 1 cm.

5.4. Discussion

As the micro-sampling technique was non-destructive it was possible to take repeated samples from the same plants, four, six and eight days after planting. Results were in agreement with the bioluminometric colonisation assay and other investigations (Parke *et al.*, 1986; Olsson *et al.*, 1987; Liljeroth *et al.*, 1991; Chin-A-Woeng *et al.*, 1997; Duineveld & Van Veen, 1999) demonstrating that bacterial density followed the order: basal region > bulk soil > apical region. This is hypothesised to reflect a lag period between bacterial assimilation of rhizodeposits and their subsequent proliferation: due to the rapid rate of root growth, bacteria are less able to colonise the root apex than the root base. In addition, the root apex may release anti-bacterial agents that further decrease the opportunities for colonisation (Walker *et al.*, 2003). The spatial distribution of rhizosphere bacteria is likely to be of great importance when considering processes such as plant-bacterial nutrient competition, bacterial mediated modifications to root development (Costacurta & Vanderleyden, 1995), and plant disease (Weller, 1988; Zahir *et al.*, 2004). In fact, assessing whether organisms are in the right place at the right time to fulfil their beneficial niche could improve the exploitation of bacterial species that display beneficial attributes.

Between samples within each zone by plant age, bacterial density was highly variable (Fig. 5.2). High density samples (CFU > 50) were considerably more abundant in the basal region than in the apical region or bulk soil. This finding is in general agreement with SEM observations at the micro-scale, which indicate that bacteria at the root base are clustered, whereas, at root apices bacteria are present as single cells (Chin-A-Woeng *et al.*, 1997). However, the presence of high densities at the root apex suggests that whilst they are smaller and less abundant than at the root base, bacterial clusters are still present there. These are likely to represent colonies that were present in the soil and were picked up by the passing root tip.

As previously mentioned, ERIC profiles were obtained from 40 % (262/655) of the colonies that were analysed. Failure to obtain an ERIC-PCR fingerprint from colonies may relate to the age of the colony when picked, insufficient cell lysis of certain groups of bacteria, damage of DNA or inhibition of PCR due to insufficient neutralisation during the DNA extraction process, or to the absence of sites within a specific

organisms genome for hybridisation with ERIC primers under the reaction conditions. Nonetheless the ERIC-PCR fingerprinting yielded sufficient data for rigorous comparisons of diversity using individual-based rarefaction curves. These curves showed no sign of reaching an asymptote and were highly linear, indicating that the sampled communities were very diverse. They showed that in contrast to soil samples, bacterial diversity within pooled root samples decreased over time. While no difference was observed 4 days after planting, bacterial diversity in pooled root samples became significantly less than that of the bulk soil six days after planting. These observations clearly support other studies in which bacterial diversity was found to decrease with increasing proximity to a root (Marilley *et al.*, 1998; Marilley & Aragno, 1999). In addition bacterial diversity within root zones was observed to follow the trend bulk soil > apical region > basal region, although these differences were not significant. This order is interesting in that the oldest zone of the root is the least diverse. This and the decrease in diversity toward the root may reflect root-mediated selection (Grayston *et al.*, 1998; Smalla *et al.*, 2001; Clark *et al.*, 2002; Kowalchuk *et al.*, 2002; Marschner *et al.*, 2004) of rhizosphere competitive-species that are expected to increase in dominance within their associated community over time.

The novel micro-sampling technique has proved to be robust and reproducible, enabling for the first time, non-destructive, micro-spatial-scale sampling of diverse bacterial communities that can be recovered for further analyses. The fact that bacterial density varied between 0 – >200 CFU mm^{-2} of root highlights the appropriateness of this scale for linking bacterial communities with factors that influence them. This is further supported by Grundmann & Debouzie (2000) who found that NO_2^--oxidisers were absent in some soil samples of approximately 250 μm diameter, and Nunan *et al.* (2001; 2002), who revealed a correlation between bacterial distribution patterns and soil structure at the micro-scale by microscopic analysis of soil thin sections. This study has demonstrated that bacterial communities are diverse even within a very small area. The results confirmed previously published trends thereby demonstrating its reliability as a sampling method. In the next chapter I investigate whether these trends can be observed using soil rhizotrons. In addition, I investigate the effect of root growth rate on bacterial densities associated with the root apex.

CHAPTER 6

SPATIOTEMPORAL PATTERNS OF RHIZOSPHERE BACTERIAL DENSITY IN SOIL AND THE INTERACTION BETWEEN ROOT GROWTH RATE AND THE DENSITY OF BACTERIA AT ROOT APICES

6.1. Introduction

In this chapter, the micro-sampling technique was applied to determining bacterial densities at the root base and apex of plants grown in soil for up to twenty six days. Following each sampling session, images of the roots were captured and root lengths determined. These observations enabled the interaction between the rate of root growth and colonisation of bacteria at the root apex to be explored.

As mentioned in section 1.5.2, Watt *et al.* (2003) found that the density of *Pseudomonas* spp. at root apex of directly drilled wheat plants was inversely proportional to the rate of root elongation. However, for total bacteria, this relationship was apparent on the roots of field grown wheat plants, but not on the roots of those grown in a controlled environment chamber. Bacteria at the root apex may have a negative effect on plant growth by competing with roots for nutrient ions, consuming nutrient-mobilising rhizodeposits, or exhibiting phytopathogenic behaviour (Zahir *et al.*, 2004). However, they may also benefit plant growth by mobilising nutrients through the release of nutrient-mobilising compounds or by transforming ions to species that require less energy expenditure for uptake (e.g. nitrate to ammonium; Marschner, 1995; Zahir *et al.*, 2004). In addition, they may also provide protection against phytopathogens that infect at the apex. In this chapter, I test whether variation in the rate of root growth of *B. napus* plants grown under similar conditions leads to differences in bacterial density at the root apices.

6.2. Materials and methods

6.2.1. Plants and growth conditions

Ten plants were grown in large Perspex rhizotrons (see Chapter two). Prior to planting the seedlings, each soil monolith was amended with 50 ml 5 mM NH_4NO_3 using a spray gun. Before the plants reached 8 days old, four were lost due to the roots burrowing below the exposed soil surface and another was damaged after sampling the 20 day old roots. This resulted in an unbalanced design structure, where the number of plants (*n*) varied throughout the sampling period as shown in table 6.1.

Plant age (days)	Number of plants (*n*)
4	10
8	6
12	6
16	6
20	6
26	5

Table 6.1 Number of plants that were sampled in each plant age category.

During the growth period water was added by removing the cling film fascia and spraying evenly over the surface. When the plants looked nutrient starved (pale green) 5 mM NH_4NO_3 was added. These additions are summarised in Table 6.2. Any effect that these additions may have had on bacterial densities was tested statistically.

Table 6.2 Details of nutrient and watering regime.

Days after planting	Addition	Volume (ml)
0	5 mM NH_4NO_3	50
2	5 mM NH_4NO_3	35
4	H_2O	8
6	H_2O	10
8	H_2O	10
10	H_2O	10
12	5 mM NH_4NO_3	10
14	H_2O	20
16	H_2O	10
19	H_2O	10
20	5 mM NH_4NO_3	20
25	H_2O	10

6.2.2. Micro-sampling and enumeration of culturable bacteria

Four days after planting, two micro-samples were taken per plant from the root apex (0 - 10 mm from the root cap) and the root base (0 - 20 mm from the root-shoot junction); two samples were also taken from the bulk soil. The same sampling strategy was employed for 8, 12, 16, 20 and 26 day old plants. Bacteria adhered to the tip were recovered in a microtube containing 10 µl PBS by sonicating for 60 s at low power in a sonicating water bath containing ice and water. Samples were then made up to 200 µl with sterile PBS and cultivated as described in section 3.2.3.

6.2.3. Image capture and analysis for root growth measurement

After removal of the clingfilm fascia, but prior to the addition of nutrients or water, rhizotrons were placed on a level surface and illuminated from above. A Nikon Coolpix 5700 digital camera (Nikon, Tokyo, Japan) was used to photograph the whole rhizotron from an angle perpendicular to the level surface. Root length was measured using the image analysis software, ImageJ 1.36v (Rasband, WS, U.S. National Institute of Health, Bethesda, Maryland, USA, http://rsb.info.nih.gov/ij/, 1997-2006).

6.2.4. Statistical analysis

All analyses were implemented using the GenStat statistical system (GenStat 8th edition, Lawes Agricultural Trust; VSN International, Hemel Hampstead, UK).

6.2.4.1. Root lengths within each plant age category

Due to the unbalanced design structure, root lengths were analysed using the REML method. A mixed model was fitted with random effects due to the nested design terms (plants, plant ages, and plant ages within plants) and fixed effects due to the treatment term, plant age. Root lengths within each plant age category fulfilled the assumption of Normality in the REML method.

6.2.4.2. Determining whether nitrogen additions had an effect on bacterial densities

It was possible to test whether the nitrogen additions had an effect on bacterial densities using the REML method. The days on which sampling occurred fell within three time periods (periods of time between NH_4NO_3 additions) which were included as a factor in the fixed model. Within these time periods, sampling days were assigned a variable 'days after last NH_4NO_3 addition'. This combination allowed the acute effect of nitrogen addition to be investigated after having considered the cumulative effect of nitrogen additions given preceding time periods. If a sampling session was on the same

day a as water or nutrient addition, the sampling was conducted first; therefore, the data generated from that sampling day was considered to be the last part of the previous time period rather than the first part of the next. Data were transformed (Log_{10} (x + 0.5)) as this ensured that the assumption of Normality was fulfilled. A mixed model was fitted with random effects due to nested design terms (plants, zones within plants, and plant ages within zones within plants) and fixed effects due to the treatment terms (zones, 'days after last NH_4NO_3 addition' within time periods, root length (a covariate) and the interaction between zones and 'days after last NH_4NO_3 addition' within time periods) (Table 6.3).

Table 6.3 Fixed and random effects for REML mixed model.

Fixed model	Zone + (Time periods / Days after last NH_4 addition) + Root length + Zone·(Time periods / Days after last NH_4NO_3 addition)
Random model	Plants/Zones/Plant ages

6.2.4.3. Bacterial density

Differences in bacterial density, i.e. CFU tip^{-1} (x) within treatment combinations (plant ages within zones) were compared using the REML method which accounted for the unbalanced design structure (unequal numbers of replicates between zones) and any correlation between plant ages given the repeated measures on plants. Data were transformed (log_{10} (x + 0.5)); this ensured that the assumption of Normality was fulfilled. A mixed model was fitted with random effects due to nested design terms (plants, zones within plants, and plant ages within zones within plants) and fixed effects due to the treatment terms (zones, plant ages and their interaction).

6.2.4.4. Interaction between root growth rate and bacterial densities at the root apex

The effect of root growth rate on bacterial density (CFU tip^{-1}) (x) at the root apex within each plant age category was compared using the REML method. Data were transformed (Log_{10} (x + 0.5)) as this ensured that the assumption of Normality was fulfilled. A mixed model was fitted with random effects due to nested design terms (plants, and plant ages within plants) and fixed effects due to the treatment terms (plant ages, root length (a covariate) and their interaction).

Predictions of bacterial numbers were produced at the minimum, the maximum, and the REML predicted mean root lengths within each plant age category using the VPREDICT directive after the REML directive. Predictions were plotted with the standard error of each estimate.

6.3. Results

6.3.1. Root growth dynamics

The root systems of younger plants were simple and were dominated by the tap root; however, older plants were characterised by complex root systems with a high degree of branching (Fig. 6.1).

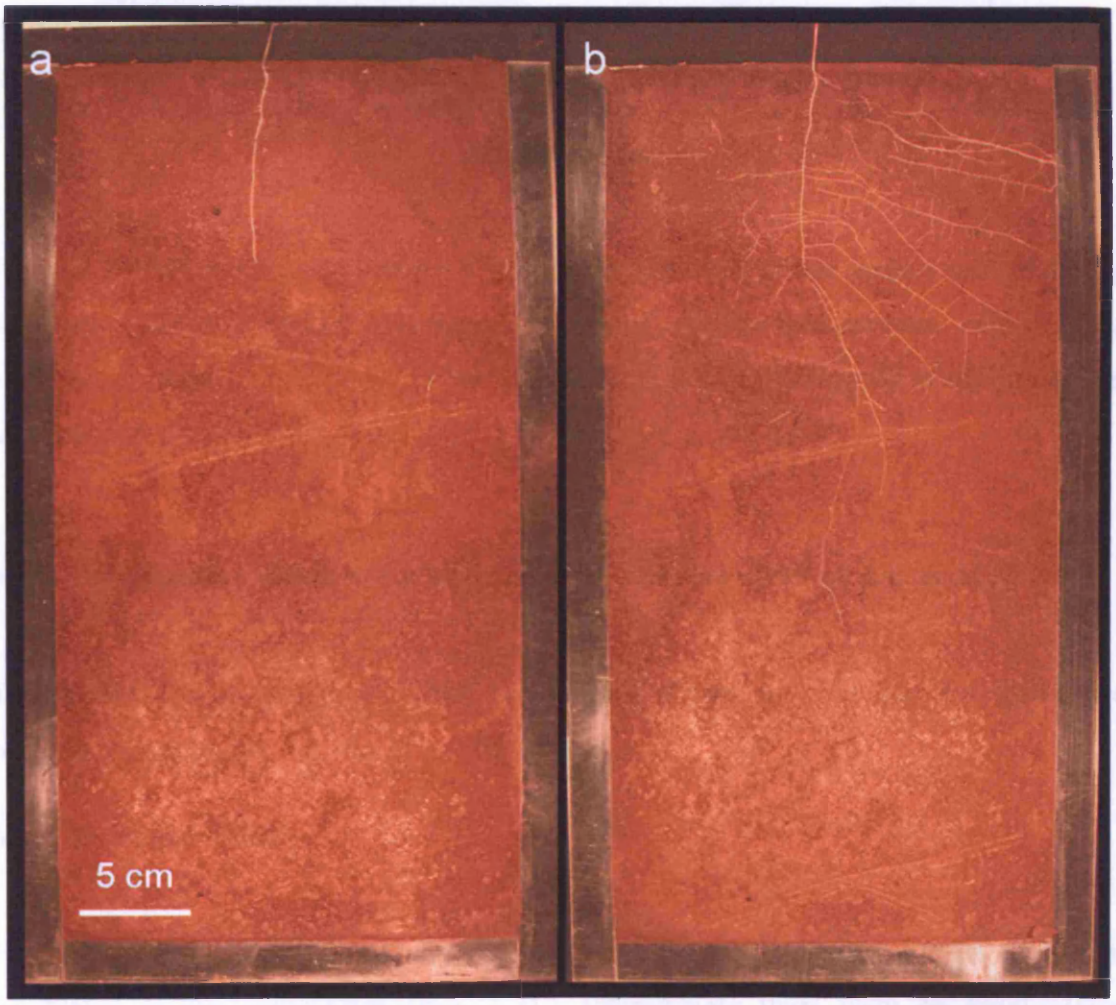

Fig. 6.1 Four day (a) and sixteen day (b) old *B. napus* plants grown in soil.

Generally root length increased over time (Wald tests, $P < 0.05$; Fig. 6.2) but between 12 and 16 days this increase was not significant (2-tailed student t-test, $P < 0.05$).

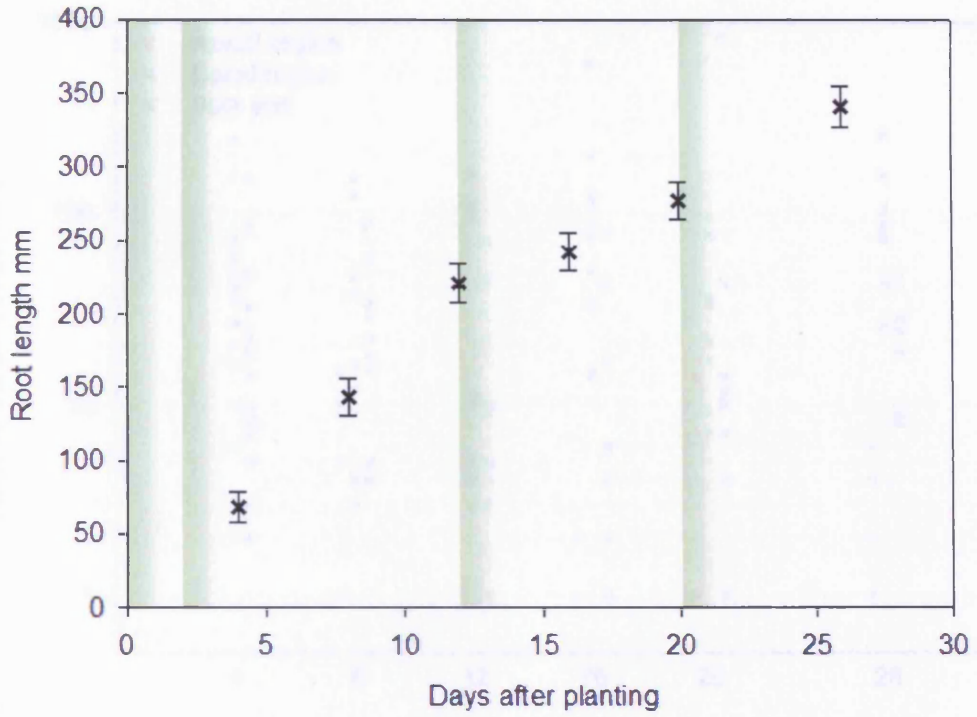

Fig. 6.2 REML predicted mean root lengths and standard errors within each plant age category. Green shading represents occasions within the growing period when ammonium nitrate was supplied. For more information regarding these additions refer to Table 6.2.

6.3.2. Determining whether nitrogen additions had an effect on bacterial densities

The REML analysis indicated that ammonium nitrate addition had not influenced bacterial densities (Walds test, $P > 0.05$).

6.3.3. Bacterial density

Bacterial density was highly variable between samples indicating a high degree of patchiness at the micro-scale (Fig. 6.3). Interestingly there were no basal region samples with less than two bacteria.

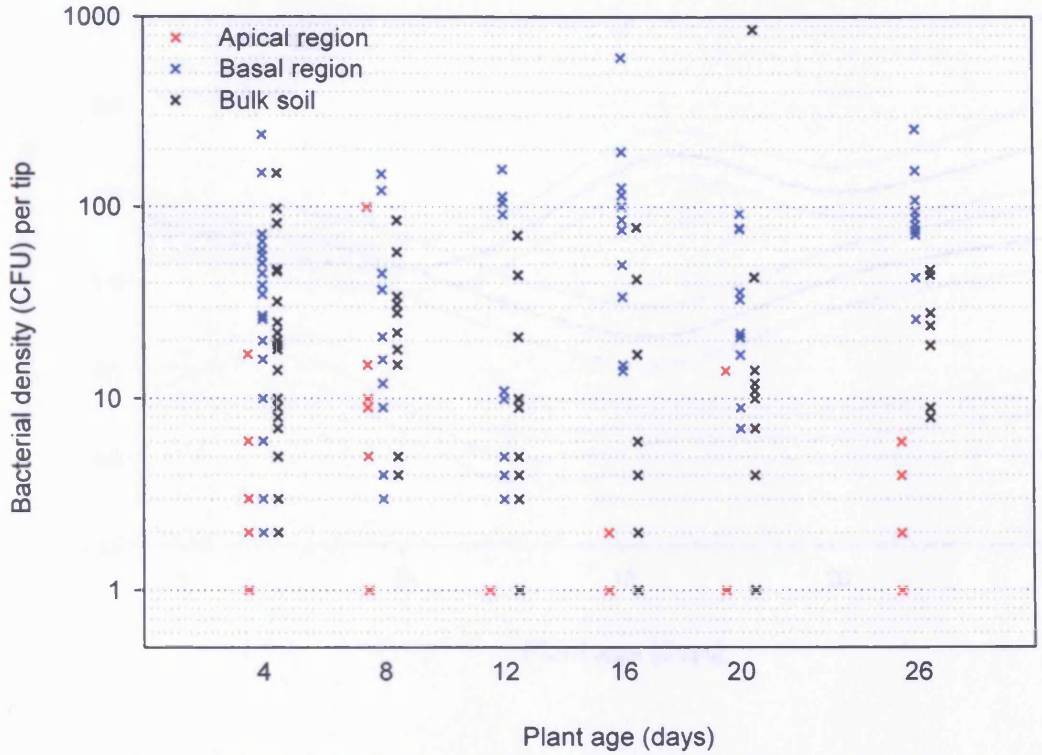

Fig. 6.3 Numbers of bacteria within micro-samples within treatment combinations 4, 8, 12, 16, 20 and 26 days after planting.

The treatment terms zone and plant age had a significant effect on bacterial densities (Wald tests, $P < 0.05$). Although there were repeated measures within plants, there was no significant autocorrelation between plant ages within zones within plants ($P > 0.05$). Figure 6.4 displays REML predicted mean bacterial densities per tip (Log_{10} CFU + 0.5) within each plant age category. The density of culturable bacteria followed the general order: basal region > bulk soil > apical region. Using standard errors, with the exception of the basal region and bulk soil four, eight and twelve days after planting, all zones were significantly different from one another.

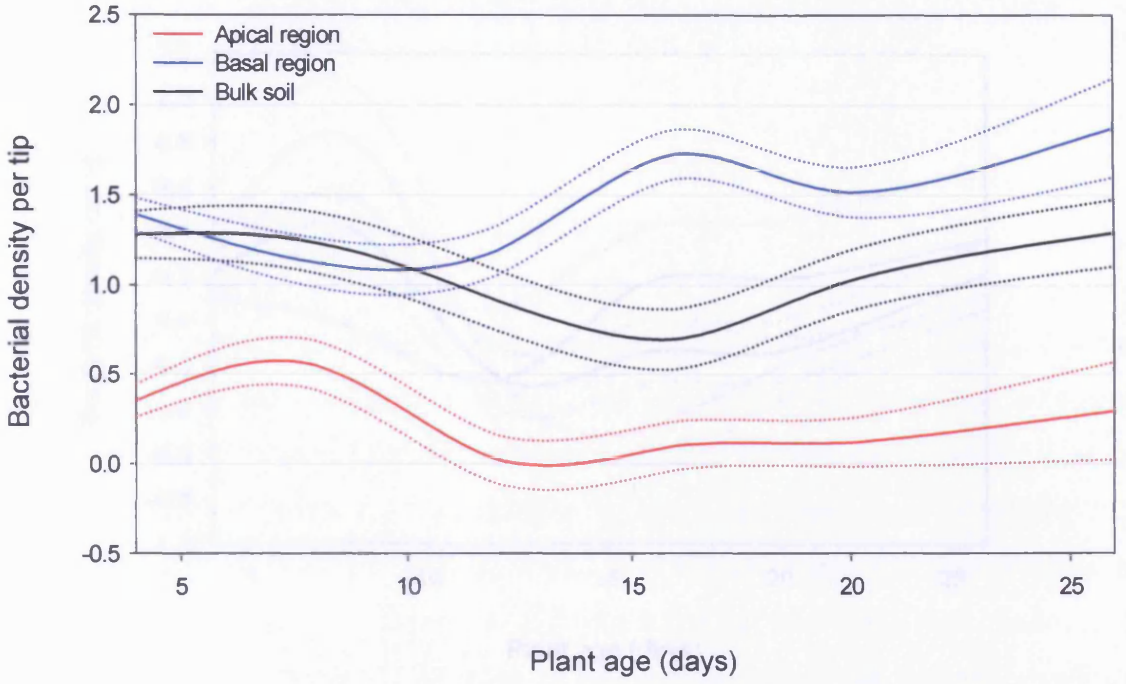

Fig. 6.4 REML predicted mean bacterial densities (Log_{10} CFU + 0.5 per tip) within each treatment combination. Dotted lines represent standard errors of means.

6.3.4. Interaction between root growth rate and bacterial density at the root apex

Generally root growth rate did not affect bacterial densities at the root apex (Wald tests, $P > 0.05$); however, within some plant age categories bacterial numbers did interact with root growth rate. Figure 6.5 displays REML predicted mean bacterial densities at the root apex of the slowest, the average, and the fastest growing roots. Using the standard errors, root growth rate had a significant effect on bacterial density on eight and sixteen day old root apices. On eight day old roots all root growth rate categories where significantly different from one another; however, on sixteen day old roots, the extremes were different from one another but not from the average growth rate.

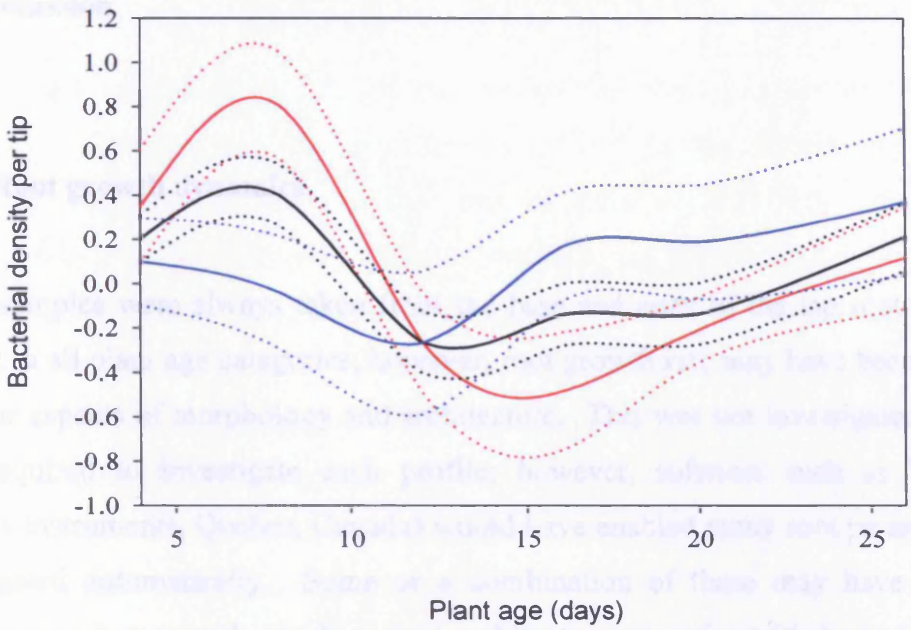

Fig. 6.5 REML predicted mean bacterial densities (Log_{10} CFU + 0.5 per tip) at the root apex of the slowest (red), the average (black), and the fastest (blue) growing roots. Dotted lines represent standard errors of means.

6.4. Discussion

6.4.1. Root growth dynamics

Micro-samples were always taken from the base and apex of the tap root as this was present in all plant age categories; however, root growth rate may have been influenced by other aspects of morphology and architecture. This was not investigated due to the time required to investigate each profile; however, software such as WinRHIZO (Regent Instruments, Quebec, Canada) would have enabled many root parameters to be investigated automatically. Some or a combination of these may have been more appropriate when considering how root architecture co-varies with bacterial densities. For example, proliferation of lateral roots may have altered the nature of rhizodeposits as well as the locations of their release.

As aforementioned, root length increased over time; however, between 12 and 16 days this increase was not significant (Fig. 6.2). It is tempting to speculate that this may be related to the previous ammonium nitrate addition. It is has been demonstrated that plant roots will grow rapidly until they encounter a nitrogen-rich patch in soil (Farley & Fitter, 1999; Hodge *et al.*, 1999). The addition of ammonium nitrate may have satisfied the nutrient demands of the plant and temporarily reduced it necessity to forage. However, this must remain speculation as the data set is insufficient to justify these claims.

6.4.2. Bacterial densities

Spatiotemporal trends in bacterial densities were in agreement with those observed in compost (Chapter 5) demonstrating that bacterial density followed the general trend: basal region > bulk soil > apical region (Fig. 6.4). However, bacterial densities at the root base only became greater than those in soil after twelve days of root growth. This may be reflective of how slowly bacteria in the soil/rhizosphere environment divide.

6.4.3. Interaction between root growth rate and bacterial density at the root apex

In most plant age categories root growth rate had no effect on bacterial density at the root apex. This was not the case, however, for eight and sixteen day old plants (Fig. 6.4). Bacterial densities at the apex of eight day old roots were inversely proportional to the rate of root growth; however, at the apex of sixteen day old roots, bacterial densities were proportional to root growth rate. These findings suggest that the variation in root growth rates between plants of the same species grown in similar conditions does not result in predictable differences in colonisation of root apices by bacteria. Expressed in another way, the data suggest that between plants grown in the same soil, other factors are more important than root growth rate in determining the density of bacteria at root apices. The most obvious factor is rhizodeposition.

Interestingly, between 4 and 8 days after planting, root systems developed many lateral roots (Fig. 6.1). It is likely that during this developmental stage the quantity and quality of carbon released at the root apex changed as a consequence of the plant allocating carbon to the new meristems of the laterals. We may speculate that if this resulted in enhanced exudation, bacterial densities may have increased accordingly. However, at the apices of sixteen day old plants we might assume that low bacterial densities reflect the release of fewer and more complex exudates or even the release of antimicrobial agents by the root. Alternatively, the temporal variation in bacterial densities at the root apices may reflect the feeding activities of other soil organisms that predate on bacteria.

CHAPTER 7

INVESTIGATION OF METHODS THAT ENABLE MICRO-SAMPLES TO BE LINKED WITH RHIZODEPOSITION

7.1. Introduction

It is generally assumed that bacteria proliferate in the rhizosphere as a consequence of rhizodeposition (Lynch & Whipps, 1990; Marschner *et al.*, 2004) and that the density and composition of rhizosphere bacterial communities reflect the quantity and quality of rhizodeposits that they are most closely associated with in space and time (McDougal & Rovira, 1970; McCully & Canny, 1985; Lynch & Whipps, 1990; Norton *et al.*, 1990). This chapter outlines the difficulty in linking bacterial communities with carbon dynamics in the rhizosphere and explores various methods that facilitate spatial mapping of root exudates and available carbon compounds in the rhizosphere. The prerequisite for the methods explored were that they had the potential to provide data at a sufficiently fine spatial resolution to enable carbon dynamics to be linked with micro-samples.

7.1.1. Current methods for spatial analysis of rhizosphere carbon dynamics

7.1.1.1. Root exudation

There is currently a lack of suitable methods that enable the spatial distribution of different pools of rhizodeposits to be mapped, and as such, it is difficult to understand the links between rhizodeposition and rhizosphere bacterial distribution patterns. Exudation is the easiest pool to examine, and as well as being the largest pool of

rhizodeposits (Meharg & Killham, 1988) it is widely reported to underpin the rhizosphere effect[6] (Lynch & Whipps, 1990; Marschner *et al.*, 2004).

By growing plants in an atmosphere containing either $^{13}CO_2$ or $^{14}CO_2$ it is possible to isotopically label recent photosynthates, a portion of which are translocated below ground. In the roots, photosynthates are predominately allocated to the meristematic regions of individual root apices (McDougal & Rovira, 1970; Norton *et al.*, 1990) where many may be lost due to passive diffusion along steep electrochemical gradients (Farrar *et al.*, 2003). These labelled compounds can be sampled from the rhizosphere using a variety of techniques including extraction from soil in a solution, or by collecting soil solution using filter papers or micro-suction cups (Curl & Truelove, 1986; Gottlein *et al.*, 1996; Neumann *et al.*, 1999; Neumann & Romheld, 2001). However, these sampling methods are limited to the macro-spatial-scale. An alternative is to image the distribution of ^{14}C-labelled compounds using autoradiography. However, as with the methods mentioned above, the patterns are likely to be partially obscured by the loss of labelled-CO_2 as a consequence of root respiration or microbial mineralization of recent root exudates (Farrar *et al.*, 2003). Autoradiography involves exposing X-ray films or phosphor storage plates to the roots of radiolabelled plants. By scanning these exposures, intensity maps consisting of millions of pixels can be stored and analysed using a computer. The high spatial resolution of such images means that this approach has the potential to provide information that may be used to complement micro-sampling data.

7.1.1.2. Available carbon

As noted in Chapter one, pools of rhizodeposits other than root exudates, are more difficult to investigate. As the root penetrates the soil and a rhizosphere effect develops, it may be assumed that rhizodeposits fuel microbial proliferation; however, rhizosphere microorganisms can mobilise carbon substrates from protected soil organic matter and particularly in older root regions, the turnover of microbial cells provides an additional source of carbon for microbial growth – the necromass (Meharg, 1994). This is a further complication when attempting to determine the source of microbial substrates in

[6] The 'rhizosphere effect' could be considered as any root-induced change in any soil variable (e.g. chemical, physical and/or biological); however, it is generally used to describe the presence of greater bacterial population densities in the rhizosphere when compared with root-free soil.

the rhizosphere. In light of these problems it is perhaps more sensible to link bacterial distributions with total available carbon concentrations; however, few investigators that have adopted this approach.

In Chapter one I mentioned two investigations designed to demonstrate a link between the spatial distribution of bacteria and total organic carbon (TOC) concentrations in the rhizosphere of wheat plants grown in rhizotrons containing soil (Maloney *et al.*, 1997; Semenov *et al.*, 1999). In these studies, soil was sampled within a three millimetre radial axis from the rhizoplane at different distances along the longitudinal root axis and then shaken with water for one hour to extract water soluble carbon; suspensions were then centrifuged and filter sterilised prior to TOC analysis. Their results indicated that spatial patterns of rhizosphere bacteria were not linked to the concentration of water soluble carbon along the roots; however, I am not aware of any similar studies with which to compare these findings. The approach used in these studies presents a number of problems that may have obscured the observation of a relationship between water soluble carbon concentrations and bacterial distribution patterns. These include the fact that not all carbon compounds in the extract will be suitable substrates for bacteria, and that the extraction process may introduce contaminating carbon sources through damage to non-lysed root or microbial cells (Neumann & Romheld, 2001). In addition, filter sterilisation of the extract prior to analysis will remove any large components that may be suitable substrates for microbial growth (e.g. sloughed-off root cells, dead microbial cells and mucigels). Finally, the necessity to acquire sufficient soil (3 g) to enable detection of carbon in a water extract means that the spatial resolution of the technique is inappropriate for studies concerning carbon availability at the microhabitat scale. As previously mentioned, other techniques for extracting rhizosphere soil solution, such as the application of filter papers or micro-suction cups are also limited to macro-spatial-scale analyses.

Recently, a number of bacterial isolates have been genetically modified, such that environmentally responsive gene promoters drive the expression of reporter genes (Amin-Hanjani *et al.*, 1993; van Overbeek & van Elsas, 1995; Jaeger *et al.*, 1999; Standing *et al.*, 2003). By using an appropriate detection system, the expression of such reporter genes in bacteria deployed *in vitro/vivo* can be related to the quantity and/or quality of appropriate effector molecules. If used *in vivo* this approach may facilitate detailed mapping of available carbon compounds in the rhizosphere while avoiding

many of the pitfalls of the rhizosphere soil solution extraction methods described above. For example, by fusing the ice nucleation gene, *inaZ*, to promoters from genes involved in sucrose catabolism as well as tryptophan-induced indoleacetic acid production in the outer membrane of two strains of bacteria, Jaeger *et al.* (1999) were able to use the bacteria to detect areas of sugar and tryptophan availability within the rhizosphere of soil-grown *Avena barbata* plants. They observed peak ice nucleation activity corresponding to tryptophan availability 12-16 cm from the root tip, while that corresponding to sucrose availability was associated with the root tip. Interestingly, these peaks also corresponded with the locations of the root that were found to have the greatest densities of indigenous rhizosphere bacteria; however, this may have been a coincidence as the reporter bacteria were designed to detect just two of more than two hundred compounds released by roots.

Other workers have described a biosensor in which a reporter gene is fused to a promoter that is induced by the presence of a broad range of wheat root exudates (van Overbeek & van Elsas, 1995); however, the response to exudates from other plant species was more variable. Amin-Hanjani *et al.* (1993) constructed a bioluminescent strain of *P. fluorescens* for which light production was apparently proportional to metabolic activity. Yeomans *et al.* (1999) tested the bioluminescence response of this biosensor to a range of rhizodeposits including sugars, amino acids, and organic acids as well as wheat root exudates of complex composition. They found that the biosensor provided a characteristic bioluminescence response to a sugar, an amino acid and an organic acid, demonstrating the potential for the system to discriminate between different forms of carbon. The bioluminescence response to the wheat exudate was similar to that of glucose, sucrose and fructose indicating that the composition of the exudate was predominantly sugars. Chemical analysis of the wheat root exudate confirmed this assumption, highlighting the potential for the biosensor to both qualify and quantify rhizodeposition. More recently, this biosensor was applied to the roots of barley plants grown in rhizotrons containing carbon-free sand (Darwent *et al.*, 2003). These workers monitored bioluminescence at 15 min and 24 h after application of the biosensor and found that bioluminescence was always greater 15 minutes after application than after 24 hours. They suggested that peak bioluminescence was detected at 15 minutes post application as a consequence of the biosensor utilising exudates from previous plant growth. This was supported by the observation that after 24 hours bioluminescence was isolated to the root apices reflecting the sites of

exudation of recent photosynthates. Their aim was to map exudation patterns, and in this they appear to have been successful; however, despite their comment on bioluminescence at 15 min post application they did not discuss the possibilities of applying their method to mapping available carbon concentrations. This was suggested by Patterson (2006), who indicated that it may also be used in real soils in which the biosensor would report on carbon availability rather than just root exudation. By combining the technique with low-light camera equipment to detect bioluminescence, data values can be collected for each pixel. Therefore, as with the phosphor imaging, the method is likely to provide high-spatial-resolution data that could be linked with micro-samples.

7.1.1.3. Preliminary trial of a bioluminometric assay for available carbon concentrations

Using *P. fluorescens* SBW25::*lux*CDABE[7], I conducted a preliminary investigation to determine whether the bioluminescence peak at 15 min post application reported by Darwent *et al.* (2003) was, as they suggested, due to the catabolism of exudates from previous plant growth. If this was the case then their method could be used as a bioluminometric assay for available carbon in the rhizosphere. Briefly, *P. fluorescens* SBW25::*lux*CDABE[8] cultures were prepared as described in section 5.2.2.1 except that after washing, the cells were starved for three hours as recommended by Darwent *et al.* (2003). Starved cells were then sprayed evenly over the roots of plants grown in CYG growth pouches and imaged 15 min post application using the equipment and settings described in section 5.2.2.4.

Figure 7.1a displays the overlaid bright and dark field images. Bacterial luminescence is represented in pseudocolour, using the colour orange. Luminescence, indicative of active *P. fluorescens* SBW25::*lux*CDABE cells, was detected ubiquitously in the rhizosphere and was generally greatest in the basal region (Fig. 7.1b). This may infer a

[7] It should be noted that the Amin-Hanjani *et al.* (1993) reporter was a different strain of *P. fluorescens*. These authors engineered *P. fluorescens* 10586 with pucD607. Strain SBW25::luxCDABE is assumed to be functionally similar to strain 10586 and therefore valid for use in similar applications.

[8] As the bioluminescence reaction requires energy from cell metabolism the metabolic state of cells affects its bioluminescence activity. Assuming that the metabolic state of a cell is proportional to the availability of growth substrates, it should be possible, as suggested by Amin-Hanjani *et al.* (1993) and Yeomans *et al.* (1999), to use the bioluminescence response as an indicator of carbon availability in the rhizosphere.

greater availability of carbon at the root base than at the apex; however, by imaging the biosensor on a carbon-free plastic surface it was possible to detect considerable bioluminescence (Fig. 7.1c and d). This suggests that three hours starvation was insufficient to deplete the internal carbon reserves of the biosensor cells to a level at which bioluminescence was indicative of external substrate availability. Therefore, it is likely that greater bioluminescence was detected at the root base as a consequence of it providing a greater exposed surface area upon which the biosensor landed than that of the apex. This is further evidenced by the fact that very little bioluminescence was detected from root-free soil where biosensor cells may have been absorbed or occluded by the soil matrix. In summary, it would appear likely that the bioluminescence peak at 15 min post application reported by Darwent *et al.* (2003) was reflective of high intracellular carbon reserves post propagation of biosensor cells in carbon-rich media.

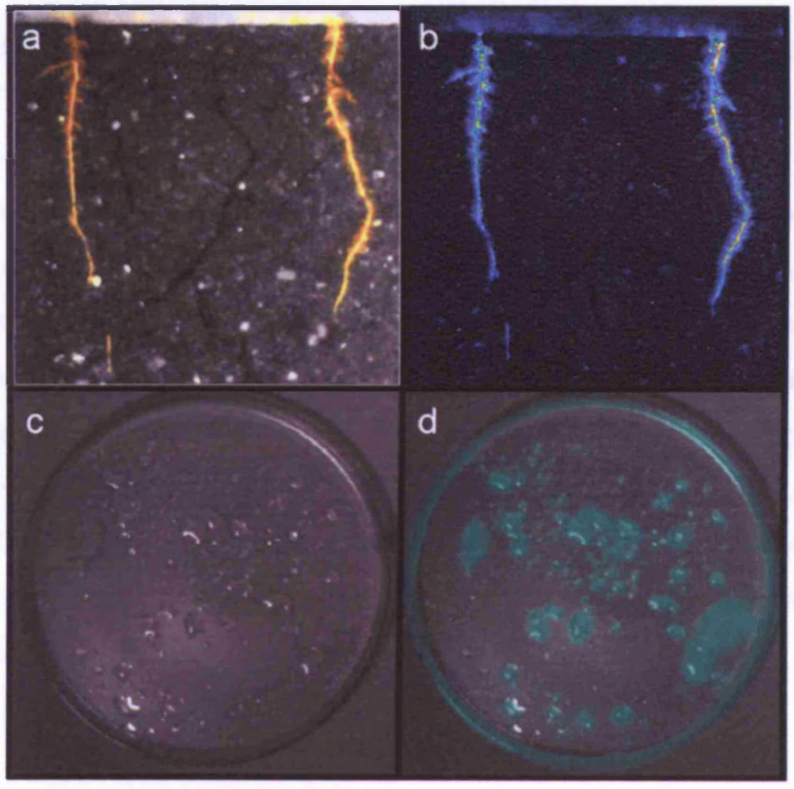

Fig. 7.1 Bright- (grey) and dark-field (orange) overlay image showing bioluminescence of *P. fluorescens* SBW25::*lux*CDABE cells applied as a biosensor for available carbon (a). Intensity map of dark-field image showing bioluminescence of *P. fluorescens* SBW25::*lux*CDABE (b); the gradient from black to white represents low to high bioluminescence intensity. Petri dish containing a sample of the 3 h starved *P. fluorescens* SBW25::*lux*CDABE culture; (c) bright-field image and (d) bright- (grey) and dark-field (green) overlay image.

7.1.1.4. Methods selected for investigation

Given that current evidence indicates that exudation occurs primarily at root apices (McDougal & Rovira, 1970; Norton *et al.*, 1990) and that a large proportion of exudates will be mineralised or become adhered to soil colloids within 0.5-2 h after being released (Ryan *et al.*, 2001) it seems apparent that root locations associated with high levels of exudate availability are not spatial correlated with those that are most densely colonised by bacteria. To check that exudation was occurring primarily at the root apices of plants used throughout this thesis, I used a ^{14}C pulse-labelling technique combined with phosphor-imaging to generate images of the allocation of recent photosynthates within the roots as well as their distribution within the rhizosphere.

With regards to the spatial distribution of available carbon, I investigated whether the method of Darwent *et al.* (2003) could be modified such that the bioluminescence response of *P. fluorescens* SBW25::*lux*CDABE was representative of extra-cellular carbon concentrations. This involved testing the bioluminescence response of cells exposed to a concentration gradient of glucose over time and after different starvation durations and enabled the conditions that gave the greatest near linear response to the glucose gradient to be identified. These conditions (starvation and exposure period) were then applied to biosensor cells that were applied to a root-soil profile and the bioluminescence activity was monitored using a low-light imaging camera. It should be emphasised that to link this method with micro-sampling data, the biosensor must be applied after micro-samples have been taken and that due to the introduction of the biosensor cells temporal trends can not be monitored.

7.2. Materials and methods

7.2.1. Spatial mapping of the allocation and exudation of recent photosynthates

The following general method was used with specific adaptation where mentioned.

7.2.1.1. Construction of the labelling sheaths

A lidless 200 µl micro-tube was adhered to the face of one of two 50 x 90 x 0.2 mm sheets of Mylar. The Mylar sheets were heat sealed together on three edges leaving one of the 50 mm edges open (Fig. 7.2). High density urethane foam adhesive tape was stuck around the inner rim of the opening. Care was taken to ensure that when the foam was pressed together the resulting seal was air-tight. A hole was created in the Mylar sheet facing the micro-tube as this allowed liquids to be dispensed into the micro-tube.

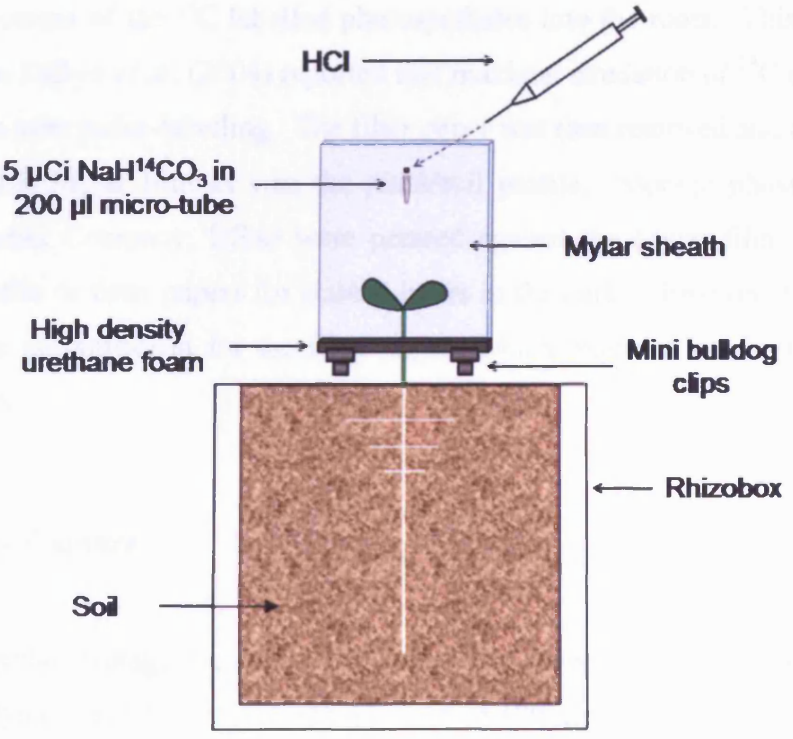

Fig. 7.2 Diagram of the pulse labelling set-up

7.2.1.2. ^{14}C pulse-labelling

To image the spatial distribution of root exudates containing recent photo-assimilates a piece of filter paper was placed over the root/soil profile which absorbed exuded compounds. A Mylar sheath (15 cm^3) was then placed over the shoots and the ring of high density foam was pressed together with mini bulldog clips to form an air-tight seal. Taking care not to contaminate the outer rim of the injection hole, 5 μCi $NaH^{14}CO_3$ (Sercon Ltd., Stapeley, UK) in 150 mM TRIS buffer (pH 8) was dispensed into the micro-tube. To generate a $^{14}CO_2$ atmosphere within the sheath, an excess of concentrated HCl (8 μl) was injected into the micro-tube. The injection hole was then sealed immediately to prevent $^{14}CO_2$ escaping. All liquid transfers and the sealing of the injection port where conducted in a fume cupboard. The quality of the seal was then carefully monitored using a Geiger counter to detect $^{14}CO_2$ leakage.

Given that the seal was efficient, plants were then placed under growth lamps for the one hour duration of pulse-labelling. This duration was sufficient to ensure maximal $^{14}CO_2$ uptake. Any $^{14}CO_2$ remaining after this period was exhausted in a fume cupboard. Post labelling, plants were left to photosynthesise for a further two hours to allow translocation of the ^{14}C labelled photosynthates into the roots. This time period was chosen as Dilkes *et al.* (2004) reported that maximal exudation of ^{14}C occurred two to three hours after pulse-labelling. The filter paper was then removed and covered with a 0.8 μm thick Mylar film as was the plant/soil profile. Storage phosphor screens (Eastman Kodak Company, USA) were pressed against the Mylar film covering the plant/soil profile or filter papers for sixteen hours in the dark. However, this length of exposure was not sufficient for the filter papers which required ten days to obtain a good exposure.

7.2.1.3. Image Capture

Exposed phosphor storage plates were scanned on a Typhoon 8600 phosphor imager (Molecular Dynamics, USA) at a pixel resolution of 100 μm using the Typhoon Scanner Control v.1.0 software package (Molecular Dynamics, USA). In addition, a colour photograph of the root/soil profile was captured using a Nikon Coolpix 5700 (Nikon, Tokyo, Japan).

7.2.1.4. Image processing

The photograph and phosphor images were opened in Adobe Photoshop 7.0. By dragging a phosphor image over a photograph an overlay image was generated. The overlay could then be blended by selecting 'Linear Burn' in the 'General Blending' options within the 'Layer Styles' menu.

7.2.2. Development of a bioluminometric assay for available carbon

7.2.2.1. Optimisation of biosensor cells for available carbon reporting

7.2.2.1.1. Bacterial strains and growth conditions

P. fluorescens SBW25::*lux*CDABE cells were isolated on 1/10 TSA containing 50 μg ml^{-1} kanamycin and maintained at 28 °C for 48 h. Three tubes each containing 20 ml $1/10^{th}$ TSB were then inoculated with single colonies and incubated at 28 °C, 200 rpm. This process was repeated for *P. fluorescens* SBW25 *gfp*, which was used as a *lux*-free (non-luminescent) control; however, only one 20 ml culture was prepared as opposed to three which was the case for the *lux* strain.

7.2.2.1.2. Bacterial starvation conditions

Cells, at the late exponential growth phase, were harvested by centrifugation (15 min, 4000 X g), the supernatant was removed and the pelleted cells were re-suspended in an equal volume of PBS. This washing process was repeated three times, after which the cells were re-suspended in a final volume of 25 ml PBS and maintained at 28 °C, 200 rpm. Cells were starved for a period of eight days, during which, cells were sub-sampled each day so that their bioluminescence response to a range of glucose concentrations could be assessed. Also, after each sub-sampling, the parent culture was washed using the process outlined above. This was intended to help reduce the accumulation of extra-cellular carbon in the starvation media as a consequence of cellular lysis or exudation.

7.2.2.1.3. Preparation of glucose solutions

Glucose solutions: 10, 7.5, 5, 2.5, 1, 0.75, 0.5, 0.25, 0.1, 0.01, 0 mM, were prepared with PBS buffer to a final volume of 30 ml and then filter sterilised.

7.2.2.1.4. Bioluminescence assay

The bioluminescence response of cells within the test cultures on exposure to a range of glucose concentrations was assessed after: 0, 1, 2, 3, 4, 5, 6, 7, and 8 days of starvation. On each of these test days, 1 ml of each test culture was sub-sampled, and then returned to the incubator at 28 °C, 200 rpm. Bioluminescence assays were conducted in sterile 96-well black wall/clear bottom plates (Packard ViewPlate™-96; Packard Instrument Co., Meriden, CT) using 10 µl of test culture and 90 µl of glucose solution. In addition to the *lux*-free control (*gfp*) a bacteria-free control (sterile PBS) was also included in the assay. Each glucose concentration was duplicated within each test culture or control. Plates were read using a Multilabel Counter 1420 Victor^2 (Perkin Elmer Life Sciences) with a constant temperature of 28 °C. The reader was programmed to repeat the measurement cycle of 30 s orbital shaking, and luminescence reading without a filter for one second per well, once at zero hours exposure (approximately 15 min after the biosensor addition) and then every hour for a total of five hours.

7.2.2.1.5. Statistical analyses

7.2.2.1.5.1. Checking the controls

Differences in the average light emission from test cultures and controls were assessed using a one-way ANOVA. The effects of starvation duration and exposure time where not considered in the analysis.

7.2.2.1.5.2. Effect of starvation duration on the nature of bioluminescence response to glucose

The dose response of cells within the test cultures to glucose was assessed with increasing exposure times and starvation conditions using general linear regression (GLR), implemented in Genstat 8th edition. GLR was used to fit a dose response surface for each starvation duration category. The response variate - light emission (cps), was modelled in terms of glucose concentrations (Log_{10}) and exposure to glucose (h) having considered the *P. fluorescens* SBW25::*lux*CDABE cultures as a blocking term.

The method of forward selection of significant terms was used to obtain a parsimonious model for each starvation duration category, sequentially adding terms of higher order (linear, linear interaction, quadratic, cubic, quartic). The significance of each term was assessed at the p = 0.05 level, using the F-test. Fitted values for light emission were plotted as a 3-D surface against glucose concentration (Log_{10}) and exposure times using SigmaPlot 9.01 (Systat software Inc.); the observed data values were superimposed as points. Given the model for each starvation duration category, the difference in estimated light emission between 0-10 mM glucose was calculated at each exposure (0-5 h). These values represent the response range of the cells to glucose given the fitted models and were plotted to identify which starvation and exposure duration gave the greatest response to glucose.

7.2.2.2. Optimised bioluminometric assay for available carbon in the rhizosphere

7.2.2.2.1. Bacterial growth conditions

P. fluorescens SBW25::*lux*CDABE cells were prepared and washed using the procedure described in section 7.2.2.1. Cells were starved for two days (the optimal starvation duration; see results) and each day the washing process was repeated to avoid an increase of extra-cellular carbon as a consequence of cell lysis or exudation.

7.2.2.2.2. Plant growth conditions

Plants were grown in 150 x 120 mm Perspex rhizotrons containing soil as described in Chapter two. Each rhizotron was amended with 10 ml 5 mM NH_4NO_3 before planting the seedling.

7.2.2.2.3. Biosensor application procedure and calibration solutions

Six days after planting, the roots were exposed and *P. fluorescens* SBW25::*lux*CDABE cells were sprayed evenly over the surface of the soil and root system. The density of cells applied to the root-soil profile was approximately 19.6 cell mm^2; this was equal to that contained in each well (of a 96-well plate) during the optimisation experiment. Assuming an initial density of about 10^8 cells ml^{-1} in the parent culture, this was achieved by applying a 10 ml cell suspension containing 9 ml of the parent culture and 1 ml sterile RO H_2O per rhizotron. A multi-well plate containing the series of glucose concentrations noted above (90 µl/well) was also inoculated with the biosensor (10 µl/well). These samples were run in duplicate and were intended for use as a calibration reference.

7.2.2.2.4. Image capture

Five hours after applying the biosensor, the multi-well plate containing the calibration references, and the plant soil profile were imaged using the equipment and settings described in section 5.2.2.4.

7.3. Results

7.3.1. Carbon-14 pulse labelling and phosphor imaging

Figure 7.3 illustrates the spatial pattern of ^{14}C allocation within and exudation from a six day old *B. napus* root system grown in soil contained in a 150 x 120 mm Perspex rhizotron. Prior to planting the seedling, the soil was amended with 15 ml 5 mM $NH_4NO_3^-$. The plant was maintained in a controlled environment chamber with the same conditions as those summarised in Chapter two. Figure 7.3a is a scan of the phosphor storage plate exposed against the root/soil profile for 16 h. It shows the allocation pattern of ^{14}C within the root system 3.5 h post labelling. Figure 7.3b is a pseudo-colour representation of figure 7.3a generated using Adobe Photoshop 7. It shows that the apical regions of the tap and lateral roots were hotspots for the allocation of ^{14}C-containing compounds. Figure 7.3e is a scan of the phosphor storage plate exposed to the filter paper for 10 days. When overlaid on figure 7.3a it shows that ^{14}C-labelled soluble compounds absorbed by the filter paper were spatially correlated with the apical root regions (Fig. 7.3d); no ^{14}C-labelled soluble compounds were detected at the root base. Interestingly, the quantity of absorbed ^{14}C-labelled soluble compounds was lower around the root cap than just behind (Fig. 7.3e and f), and the pattern of exudation with increasing distance from the apices of the lateral roots differed from that of the tap root. These findings indicate that exudation can be inferred from allocation images and suggest that exudation of recent photosynthates does not occur at the root base.

After completing the sampling of the 26 day old root systems reported in Chapter six, I maintained the plants under the same growth conditions until they were pulse-labelled at 35 days old. No filter paper inserts were included in this run to absorb exudates; however, the results from younger plants indicated that exudation could be inferred from allocation patterns within the roots. Interestingly the allocation pattern in older root systems was slightly different to that observed in younger root systems (Fig. 7.3). Allocation of recent photosynthates appears to have been ceased or considerably reduced in some but not all higher order roots (Fig. 7.4).

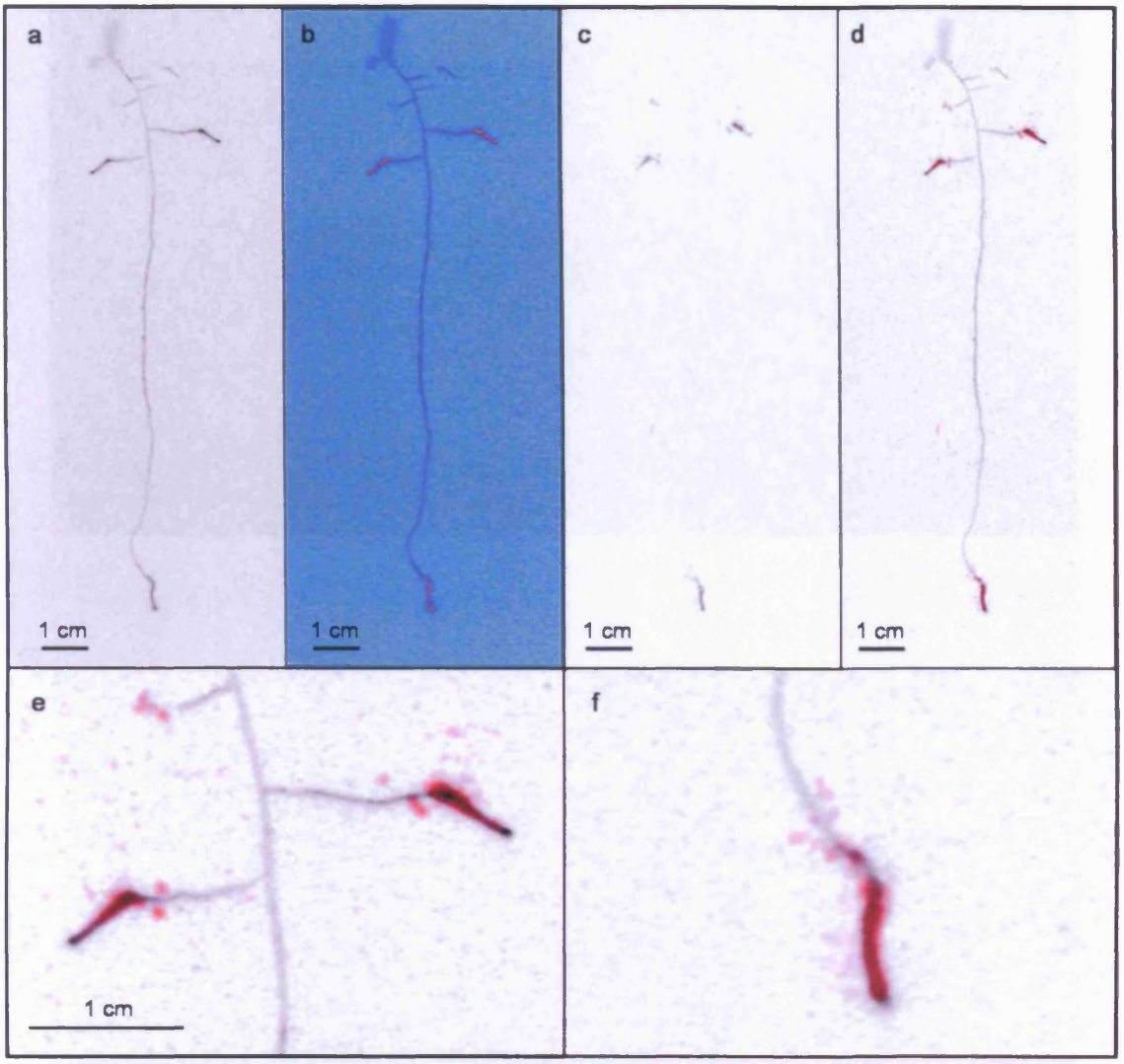

Fig. 7.3 Scanned images of phosphor storage plates used to map recent photo-assimilate allocation within and exuded from a 6-day old *B. napus* root system: (a) allocation pattern of compounds containing recently photo-assimilated ^{14}C within the root system, (b) pseudo-colour representation of 'a' highlighting that the apical regions of the tap and lateral roots were hotspots for the allocation of ^{14}C-containing compounds, (c) spatial distribution of soluble compounds (root exudates) containing recently photo-assimilated ^{14}C that were absorbed by a filter paper pressed against the root, (d) overlay of 'a and c' highlighting that hotspots of ^{14}C allocation within the root were spatially correlated with areas that released the greatest quantities of ^{14}C-containing exudates, (e and f) close-ups of 'd'.

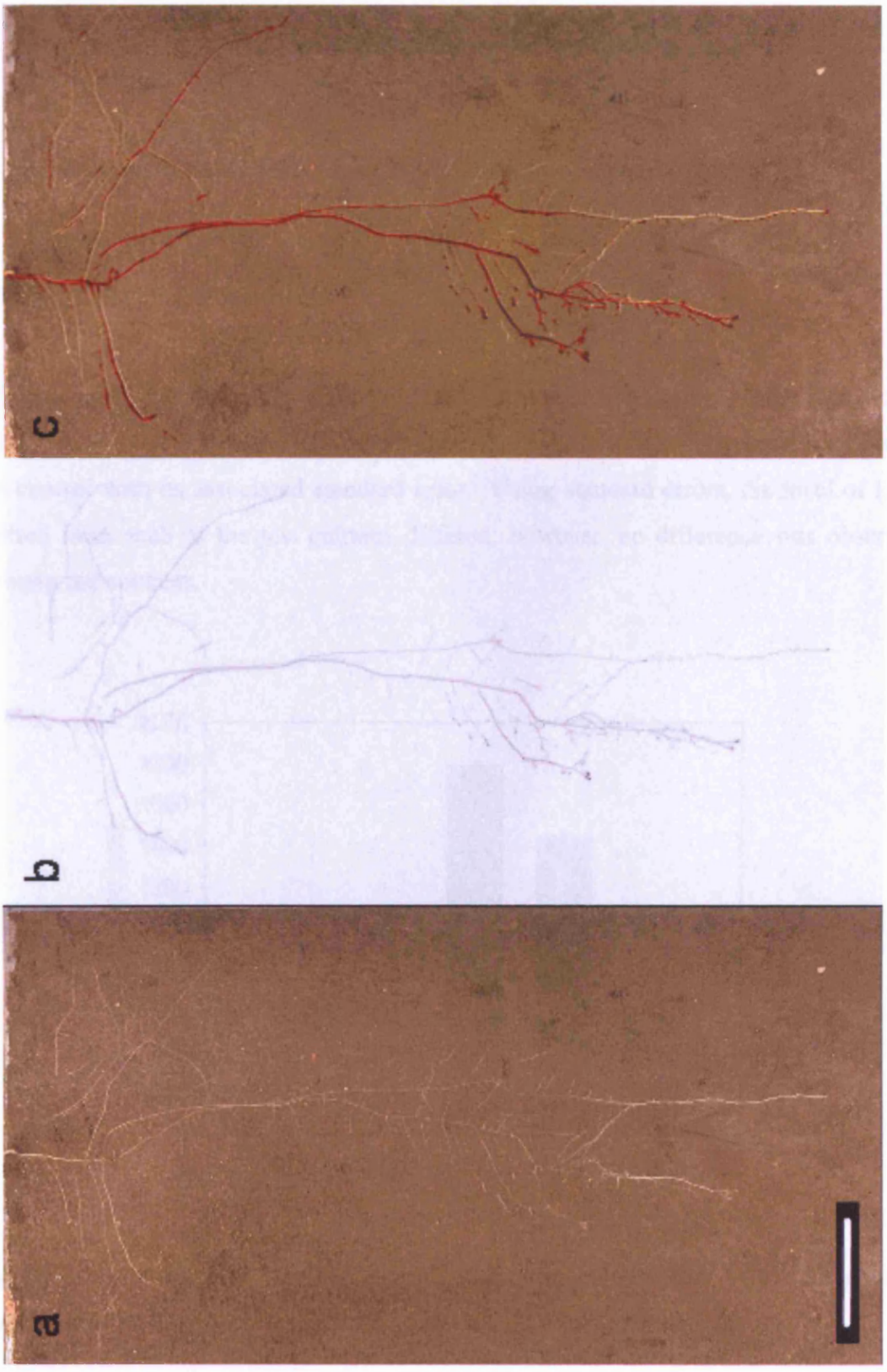

Fig. 7.4 Distribution of ^{14}C labelled compounds in the roots of a 35 day old *B. napus* plant. Photograph of root system (a), scanned phosphor storage screen showing allocation pattern of recent radio-labelled photosynthates (b), and an overlay image of the photograph and the phosphor image (c). Scale bars represent 5 cm.

7.3.2. Development of a bioluminometric assay for available carbon

7.3.2.1. Optimisation of biosensor cells for available carbon reporting

7.3.2.1.1. Checking the controls

Differences in light emission from the test cultures and the controls were significant (ANOVA, $P < 0.05$). Figure 7.5 shows the mean light emission from each test culture and control with its associated standard error. Using standard errors, the level of light emitted from each of the test cultures differed; however, no difference was observed between the controls.

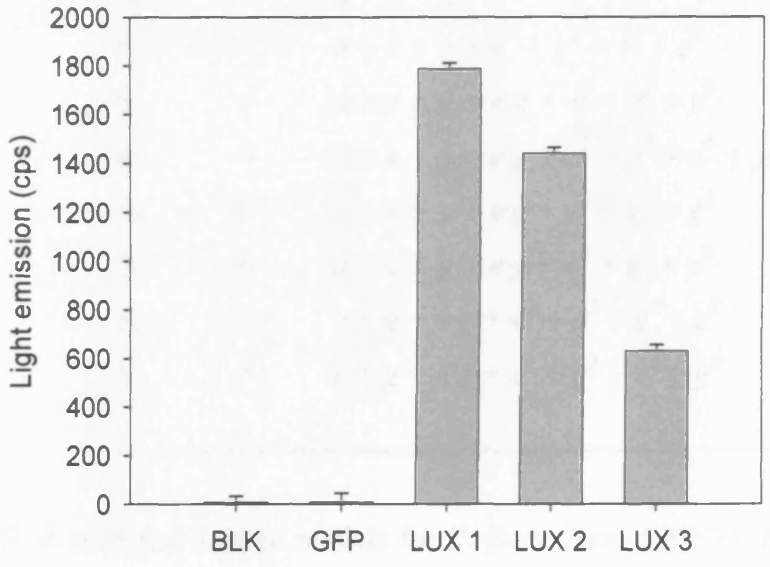

Fig. 7.5 Mean average light emission from each test culture (*lux* 1-3) and control (no-bacteria (BLK); no-*lux* (gfp)) with its associated standard error.

7.3.2.1.2. Effect of starvation duration on the nature of bioluminescence response to glucose

Table 7.1 shows the parsimonious GLM model terms for luminescence data collected from *P. fluorescens* SBW25::*lux*CDABE cells exposed to a range of glucose concentrations (0-10 mM) for 0-5 h within each starvation duration category (0-8 d). They show that the bioluminescence response of *P. fluorescens* SBW25::*lux*CDABE cells when exposed to a range of glucose concentration for 0-5 h was not a simple linear relationship. Figure 7.6 shows model fitted values for light emission. These are plotted as 3-D response surfaces against glucose concentration (Log_{10}) and exposure times; observed data values are superimposed as points. They show the shape of the bioluminescent response and thus facilitate the determination of light emission peaks.

S_0	=	$a + g + g^2$
S_1	=	$a + e + g + e^2 + g^2 + e^3 + e^4$
S_2	=	$a + e + g + e{\cdot}g + e^2 + g^2 + e^3$
S_3	=	$a + e + g + e{\cdot}g + e^2 + g^2 + e^3 + g^3 + e^4$
S_4	=	$a + e + g + e{\cdot}g + e^2 + g^2 + g^3$
S_5	=	$a + e + g + e{\cdot}g + e^2 + g^2 + e^3$
S_6	=	$e + g + e{\cdot}g + e^2 + g^2 + e^3 + e^4$
S_7	=	$e + g + e{\cdot}g + e^2 + g^2 + e^3 + g^3$

Table 7.1 GLR response surface models for *P. fluorescens* SBW25::*lux*CDABE cells exposed to a range of glucose concentration for 0-5 h after different durations of starvation: a = *lux* culture (1-3); e = exposure (h); g = glucose (Log_{10} mM); S = starvation duration (d).

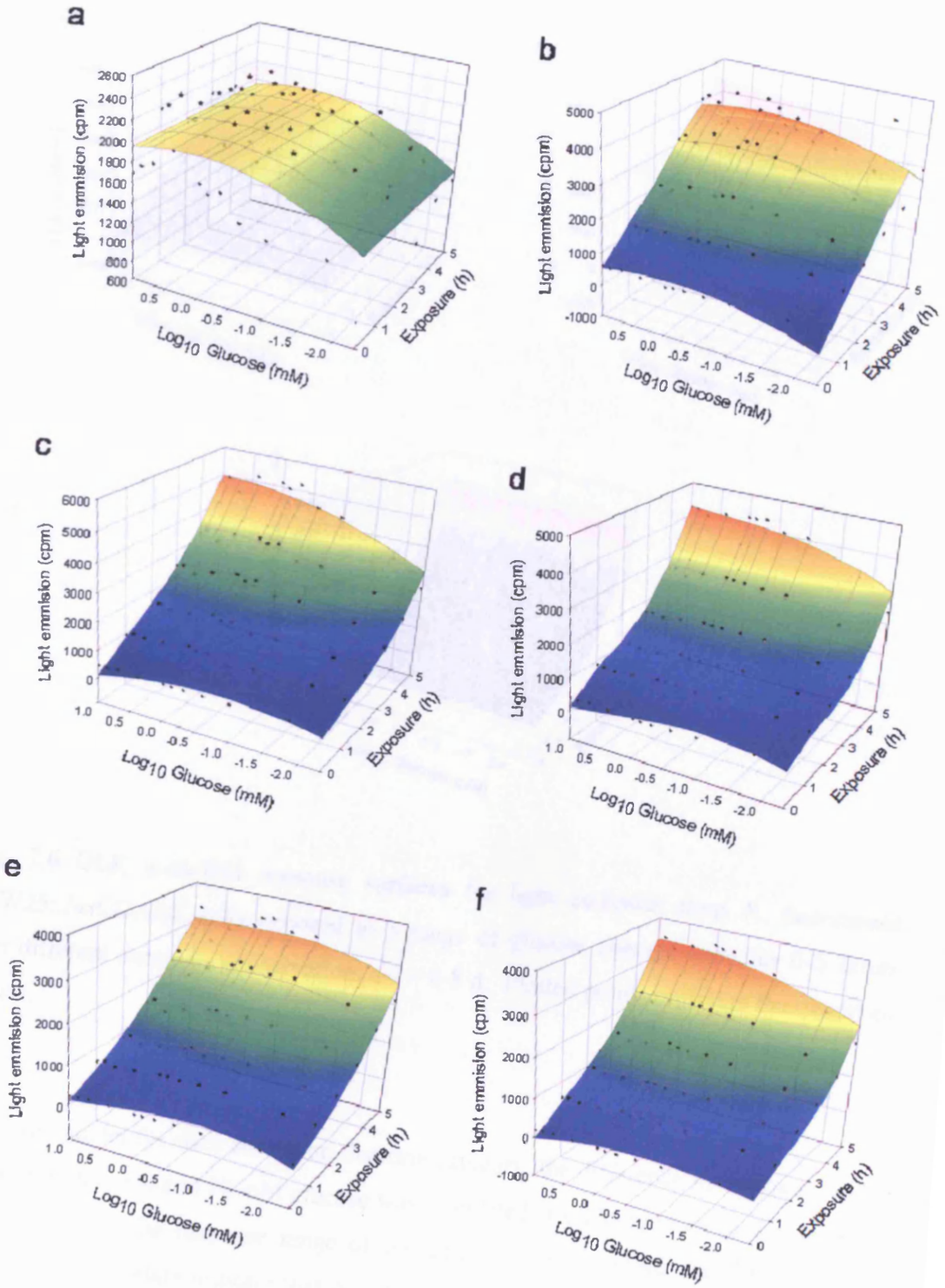
a
Light emmision (cpm)
2600
2400
2200
2000
1800
1600
1400
1200
1000
800
600
0.5 0.0 -0.5 -1.0 -1.5 -2.0
Log10 Glucose (mM)
0 1 2 3 4 5
Exposure (h)
b
Light emmision (cpm)
5000
4000
3000
2000
1000
0
-1000
0.5 0.0 -0.5 -1.0 -1.5 -2.0
Log10 Glucose (mM)
0 1 2 3 4 5
Exposure (h)
c
Light emmision (cpm)
6000
5000
4000
3000
2000
1000
0
1.0 0.5 0.0 -0.5 -1.0 -1.5 -2.0
Log10 Glucose (mM)
0 1 2 3 4 5
Exposure (h)
d
Light emmision (cpm)
5000
4000
3000
2000
1000
0
1.0 0.5 0.0 -0.5 -1.0 -1.5 -2.0
Log10 Glucose (mM)
0 1 2 3 4 5
Exposure (h)
e
Light emmision (cpm)
4000
3000
2000
1000
0
1.0 0.5 0.0 -0.5 -1.0 -1.5 -2.0
Log10 Glucose (mM)
0 1 2 3 4 5
Exposure (h)
f
Light emmision (cpm)
4000
3000
2000
1000
0
-1000
0.5 0.0 -0.5 -1.0 -1.5 -2.0
Log10 Glucose (mM)
0 1 2 3 4 5
Exposure (h)

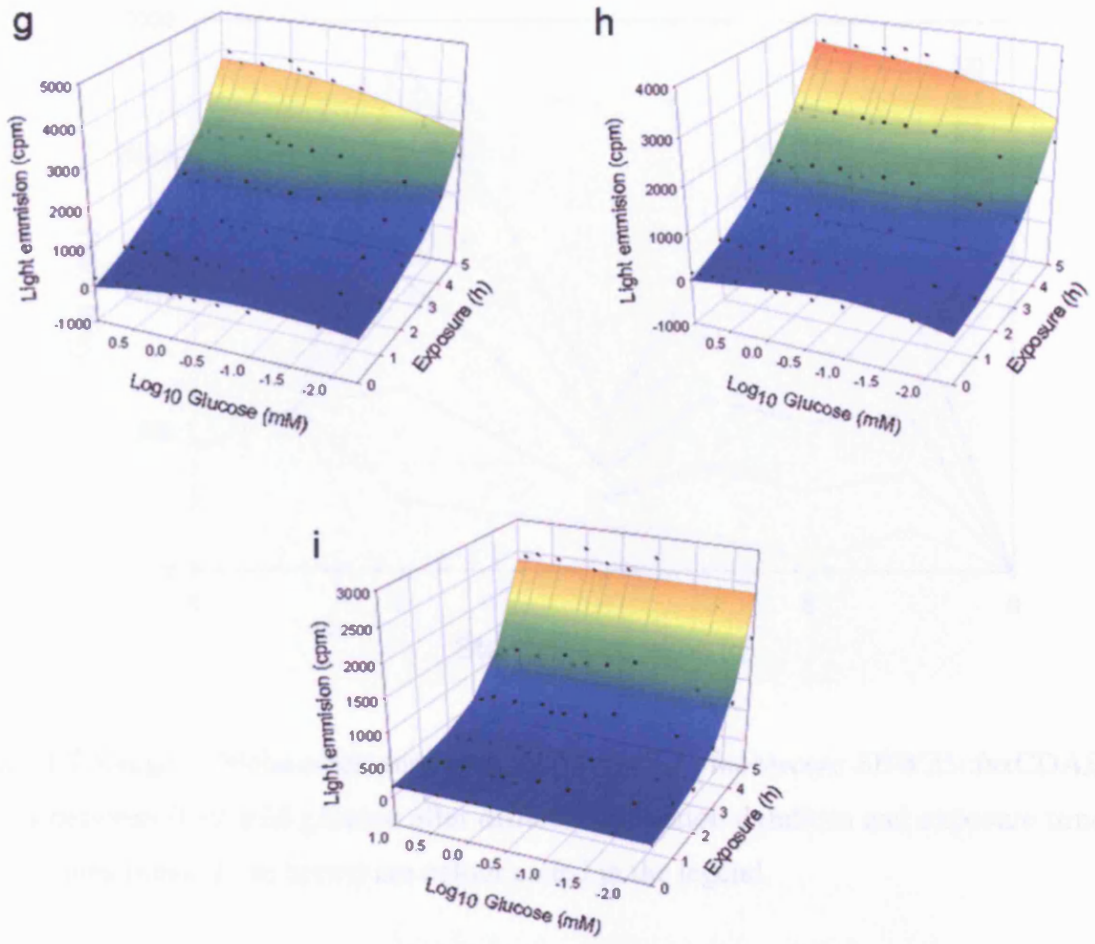

Fig. 7.6 GLR modelled response surfaces for light emission from *P. fluorescens* SBW25::*lux*CDABE cells exposed to a range of glucose concentration for 0-5 hours after different durations of starvation: a-i = 0-8 d. Plotted points represent the observed values.

Given the model for each starvation duration category, the difference in estimated light emission between 0 and 10 mM glucose was calculated at each exposure (0-5 h). These values represent the response range of the cells to glucose given the fitted models (Fig. 7.7). The results indicate that two days starvation and five hours exposure gave the greater response range to the glucose concentrations.

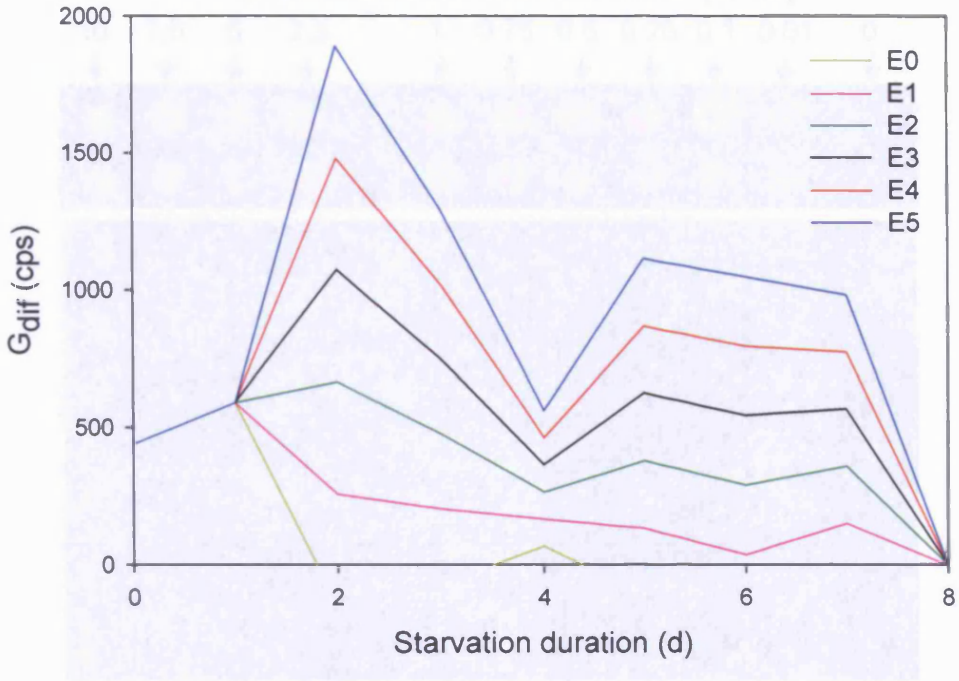

Fig. 7.7 Range of bioluminescence activity (G_{dif}) of *P. fluorescens* SBW25::*lux*CDABE cells between 0-10 mM glucose after different starvation durations and exposure times. Exposures times (E; in hours) are colour coded in the legend.

7.3.2.2. Optimised bioluminometric assay for available carbon in the rhizosphere

Despite the optimised conditions, peak bioluminescence was observed within the range of glucose calibration solutions (0-10 mM; Fig. 7.8); therefore, within the tested range of glucose doses, the bioluminescence response was not pseudo-linear and could be related to carbon concentration. However, the biosensor cells did not emit light in absence of carbon. Therefore, when exposed to the root/soil profile the bioluminescence report is qualitative but not quantitative.

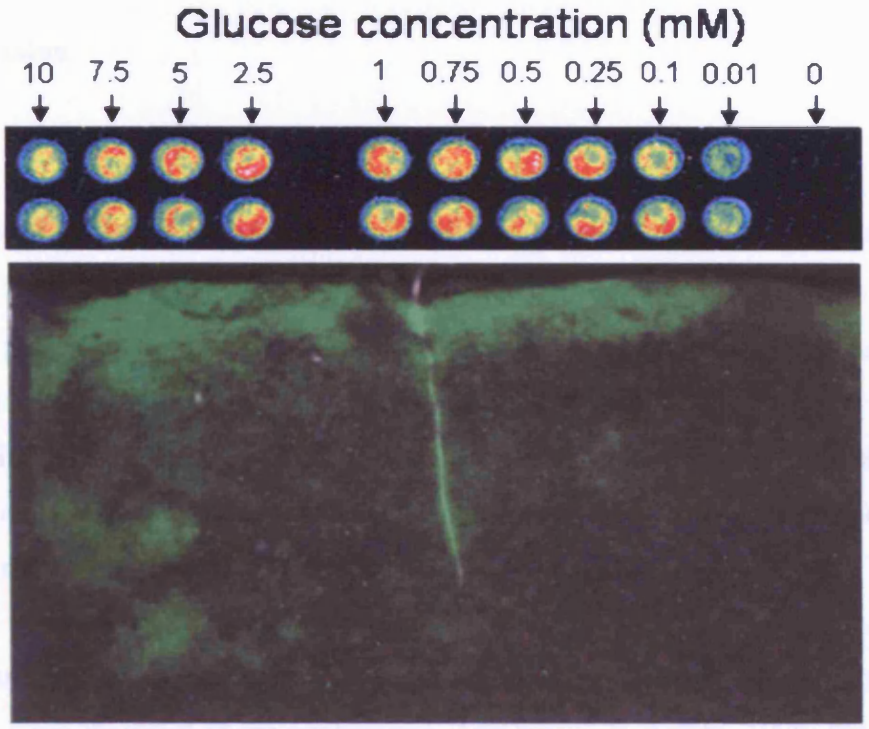

Fig. 7.8 Bioluminescence detected from *P. fluorescens* SBW25::*lux*CDABE cells that were starved for two days and then exposed to a range of glucose concentrations for five hours (top). Bioluminescence is represented by a colour gradient representing low to high activity (black < purple < blue < green < yellow < red < white). The bottom image shows biosensor cells applied to the root-soil profile of a six day old *B. napus* plant.

7.4. Discussion

7.4.1. Spatial mapping of the allocation and exudation of recent photosynthates

The ^{14}C pulse-labelling technique was successful and used in combination with rhizotrons and phosphor storage plates, enabled the spatial allocation of recent photosynthates to be mapped at high spatial-resolution. In addition, by applying filter paper sheets to the root-soil profile it was possible to map the distribution of root exudates in the rhizosphere.

The results were in agreement with other workers in demonstrating that allocation and exudation were maximal at the root apices (McDougal & Rovira, 1970; Norton *et al.*, 1990). As mentioned in section 1.4.3.3.5, Darrah (1991b) modelled bacterial densities along the longitudinal axis of a root in response to two contrasting exudation patterns. In the first simulation (S1) exudation was confined to a region 0.5 cm from the root tip while in the second (S2), exudation was confined to a 5 cm region. The trend observed for the S2 simulation was similar that of the S1 simulation (Fig. 1.18) although the radial extent of the rhizosphere extended just 0.9 mm from the root surface and the peak biomass carbon lagged considerably further behind the peak carbon concentration, with a lag of approximately 3.75 cm as apposed to 0.6 cm for the S1 simulation. The results presented here indicate that the size of the exuding surface for young *B. napus* plants grown in soil was less than one centimetre irrespective of root type; however, the bioluminometric colonisation assays indicate that peak bacterial densities occur within the basal region (0 - 20 mm from the root-shoot junction). Given that other workers have also reported peak bacterial densities at the root base (Parke *et al.*, 1986; Olsson *et al.*, 1987; Liljeroth *et al.*, 1991; Chin-A-Woeng *et al.*, 1997; Duineveld & van Veen, 1999), it would appear that the spatial distribution of rhizosphere bacteria is poorly predicted using current modelling approaches (Darrah 1991b). The results presented in this chapter do not support the idea that the density of rhizosphere bacterial communities reflects the quantity of root exudates along longitudinal root axes.

7.4.2. Spatial mapping of soluble/available carbon in the rhizosphere

General linear modelling revealed that the bioluminescence response of *P. fluorescens* SBW25::*lux*CDABE cells exposed to a range of glucose concentrations was not a simple linear relationship. In addition the parsimonious models indicated that the relationship differed between biosensor populations starved for different durations (Table 7.1). By comparing the range of the bioluminescence response at different exposure times within populations starved for different durations it was possible to determine that the best parameters for biosensor reporting of carbon were two days starvation and five hours exposure. However, when these conditions were applied to a biosensor population that were sprayed on to the surface of a root/soil profile the expected bioluminescence response was not observed – peak bioluminescence was observed within the range of concentrations used for calibration. Therefore, the biosensor was not able to report in a quantitative manner on the availability of carbon. Nonetheless, as bioluminescence was not observed when cells were placed in carbon-free media, the biosensor may be used in a qualitative manner to report on the presence of carbon.

In retrospect, it has occurred to me that the non-linear relationship between *P. fluorescens* SBW25::*lux*CDABE bioluminescence activity and glucose concentration may have resulted from the way in which the bioreporter cells were starved. As mentioned in section 7.2.2.2.1 the cells were starved in PBS buffer (137 mM NaCl, 1.5 mM KH_2PO_4, 6.5 mM $Na_2HPO_4 \cdot H_2O$, 2.7 mM KCl, pH 7.2), which is indeed carbon-free; however, this media is also replete in other essential nutrients such as nitrogen. Therefore, it is likely that the observed bioluminescence response was complicated by the fact that the bioreporter cells were also starved of other nutrients as well as carbon. It is interesting to note that other workers who reported linear responses to a range of carbon concentrations starved their bioreporter strains in carbon-free M9 minimal media which is sufficient in all essential nutrients (Yeomans *et al.*, 1999; Darwent *et al.*, 2003). It is likely therefore, that if this experiment were repeated using carbon-free M9 minimal media, the bioluminescence response of *P. fluorescens* SBW25::*lux*CDABE would be more suitable for the proposed application. However, it seems apparent that to detect bioluminescence in a standardised manner, cells must be applied to a surface of even topography; therefore, while this method may be suitable for carbon reporting on the root surface it is likely that in soil, cells are absorbed and

occluded by the soil matrix. In addition, assuming that bioluminescence is proportional to the metabolic activity of the biosensor, it is important that the surface to which the biosensor is applied does not influence the biosensor directly. For example, differences in pH or temperature between the calibration solutions and the sample surface would lead differences in the metabolic activity of the biosensor that would confound quantitative aspects of carbon reporting. This problem may also be experienced on the sample surface itself due to the heterogeneity of biological, physical and chemical factors inherent to the test environment. A further problem is that carbon-containing compounds differ in their relative availability as substrates for bacterial growth. Therefore, for biosensors in which the bacterial luciferase operon is constitutively expressed, bioluminescence, indicative of metabolic activity, differs depending on substrate quality as well as quantity. Given that the quality of rhizodeposition is known to vary along the root, further research is necessary to determine to what extent this limits the quantitative capacity of such biosensors for broad-range carbon reporting.

CHAPTER 8

LINKING BACTERIAL DENSITY WITH pH AT THE MICRO-SPATIAL-SCALE

8.1. Introduction

As discussed in Chapter one, pH strongly influences the chemical composition of potential microhabitats by mediating the availability of a wide range of nutrient ions. In addition, all bacterial species have a pH range within which growth is possible and usually each have a defined pH optimum. Nonetheless, regardless of the extracellular pH at which the growth of a particular species is optimal, the intracellular pH remains near neutrality. Therefore, most species exhibit optimum growth close to neutrality (Madigan *et al.*, 2000). For example, Fierer and Jackson (2006) demonstrated that the diversity and richness of bacterial communities from 98 soil samples taken from North and South America could be largely explained by soil pH (r^2 = 0.70 and r^2 = 0.58, respectively) with a trend of decreasing diversity with pH.

The aim of this chapter was to determine whether the heterogeneous distribution of bacteria observed on the rhizoplane of *B. napus* (Chapters 5 and 6) could be related to pH measurements taken with microelectrodes.

8.1.1. Microelectrodes

Currently, microelectrodes represent the only reliable method for determination of soil pH at the micro-spatial-scale as imaging techniques using pH indicator dyes are designed to measure pH changes in gels rather than soils (section 1.4.3.4). Jaillard (1987) tried to overcome this problem by placing a gel over the surface of roots grown in rhizotrons containing soil; however, problems with root/soil to gel contact meant that the approach was unreliable.

The theory behind microelectrodes has been extensively reviewed elsewhere (Ammann, 1986); therefore, here, I will outline only the most basic concepts. The term 'microelectrode' generally refers to a glass micropipette which is pulled into a fine tip and filled with a liquid electrolyte (Miller, 1995). The connection between the electrolyte inside the microelectrode and the input of an electrometer amplifier is provided by a half-cell, which is usually a Ag/AgCl wire. When used in conjunction with a reference ground electrode, a complete electrical circuit is achieved and can be used to measure the voltage (contact potential) of a sample solution (Fig. 8.1).

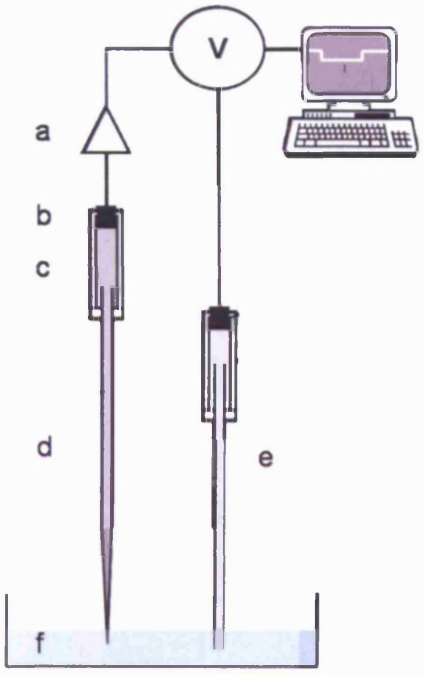

Fig. 8.1 Diagram of a simple microelectrode (d) connected to a microelectrode holder filled with the same electrolyte as the microelectrode. The half cell (b) of the microelectrode holder (c) provides the connection between the electrolyte and the head-stage amplifier (a) of a high impedance electrometer (V). When in contact with a sample solution (f) the circuit is completed by a reference ground electrode (e). The electrometer output is interfaced using a computer

By casting an ion-selective membrane into a microelectrode tip, both the contact potential and the activity of the ion sensed by the selective membrane can be measured in a sample solution. The ideal relationship between electrode output (mV) and the

activity of the ion of interest is log-linear and should yield a slope of 59 mV (at 25 °C) per decade change in the activity of a monovalent ion (Miller 1995). To determine the concentration of the sensed ion in a sample solution, the ion activity (mV) is related to that in a series of calibration solutions containing known activities of the ion. However, as the ion-selective electrode will sense the contact potential of a solution in addition to voltage due to the activity of the ion of interest, the contact potential must be subtracted from the electrode measurement to obtain the output for the ion alone. This can be achieved using either two single barrelled electrodes or a double-barrelled electrode in which the ion-sensing electrode is combined with a contact-potential-measuring electrode (Fig. 8.2). Both output voltages are measured against a reference ground electrode in the measured solution.

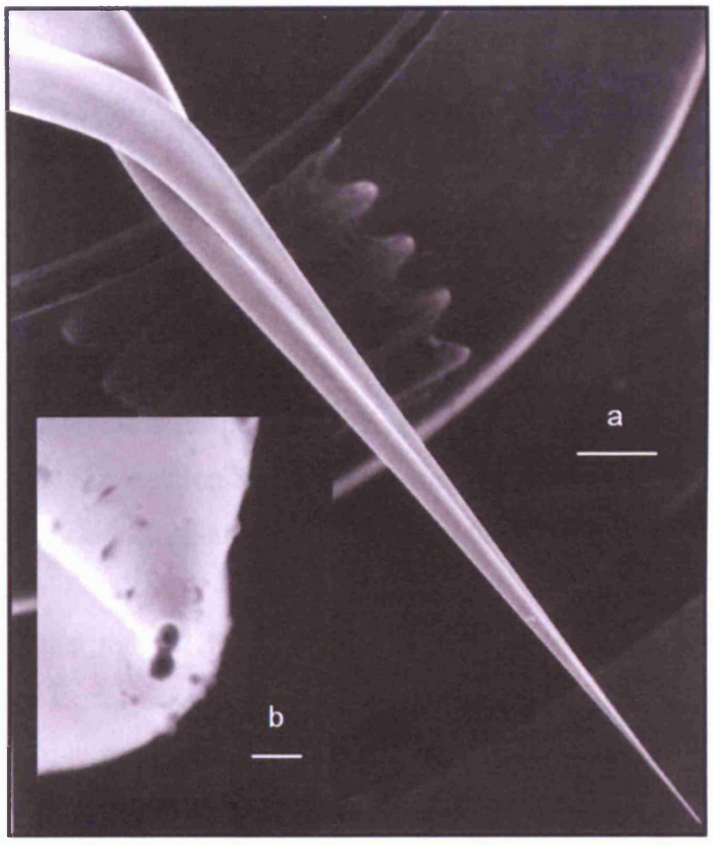

Fig. 8.2 Scanning electron micrographs of a double barrelled micropipette (courtesy of D. J. Walker). Scale bars: a = 500 μm, b = 0.6 μm.

In a preliminary experiment, using single-barrelled microelectrodes back-filled with 200 mM KCl, I demonstrated that the contact potential in the pH calibration solutions differed significantly from that in the unstirred layer of the *B. napus* rhizoplane (Fig. 8.3). Therefore, to determine accurate rhizoplane pH values, differences in contact

potentials between the calibration solution and the root surface must be accounted for. As the contact potential in the unstirred layer of the *B. napus* rhizoplane is variable (Fig. 8.3) it must be monitored throughout the duration of a pH measurement. This was achieved using double-barrelled microelectrodes that consisted of a pH selective barrel and a contact-potential-measuring barrel.

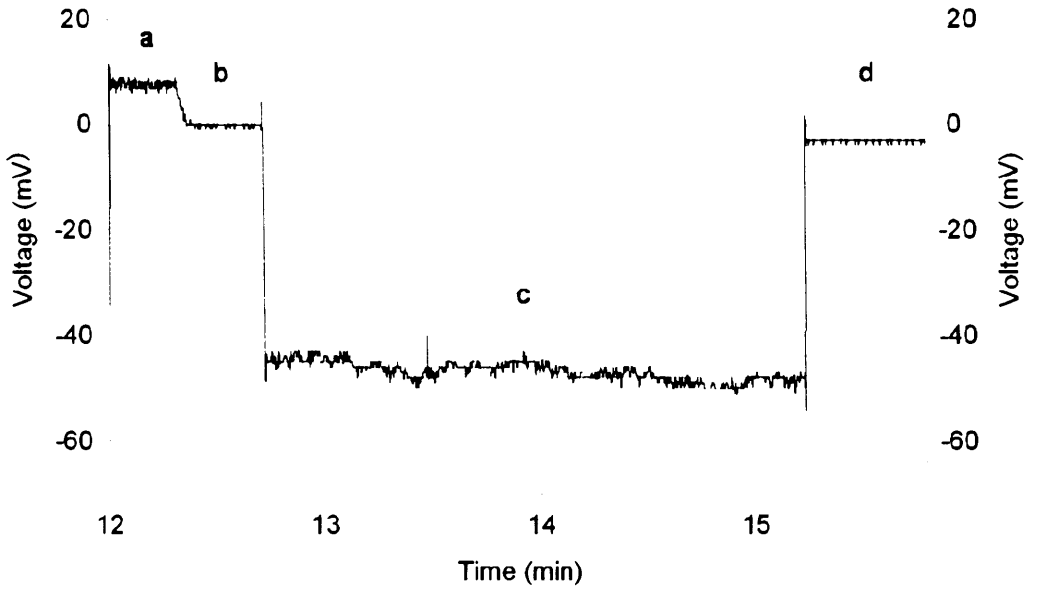

Fig. 8.3 Contact potential measurements using a KCl filled microelectrode: (a) in the pH 6 calibration solution (section 8.2.2) before, and (b), after adjustment to 0 mV, (c) in the unstirred layer of the rhizoplane, and (d) back in the pH 6 solution.

To investigate whether the patchy distribution of bacteria observed on the rhizoplane of *B. napus* could be explained by local differences in pH, the density of bacteria was determined in micro-samples taken from the same positions as those at which pH was measured.

8.2. Materials and methods

8.2.1. Plant growth conditions

Plants were grown in 150 x 120 mm Perspex rhizotrons containing soil (Chapter 2). Each rhizotron received 20 ml NH_4NO_3 via a spray gun, one day before planting. One seedling was planted per rhizotron. Growth conditions were as described in Chapter two.

8.2.2. Preparation of pH calibration solutions

The following solutions were prepared and stored at 4 °C until required: pH 3 (20 mM potassium hydrogen phthalate, 120 mM KCl, 10 mM $NaH_2PO_4 \cdot 2H_2O$; adjusted to pH 3 with 2M NaOH); pH 4 (same as pH 3, but adjust to pH 4 with 2M NaOH); pH 6 (20 mM MES, 120 mM KCl, 10 mM $NaH_2PO_4 \cdot 2H_2O$; adjusted to pH 6 with 2M NaOH); pH 7 (20 mM MOPS, 120 mM KCl, 10 mM $NaH_2PO_4 \cdot 2H_2O$; adjusted to pH 7 with 2M NaOH.

8.2.3. Production of double-barrelled pH microelectrodes and setup of experimental apparatus

The method of Miller and Smith (1992) was used to produce double-barrelled pH microelectrodes and setup the experimental apparatus. This section outlines the relevant details.

8.2.3.1. Production of double-barrelled pH microelectrodes

8.2.3.1.1. Fabrication of doubled-barrelled micropipettes

Doubled-barrelled micropipettes were produced from double-barrelled filamented borosilicate glass capillaries with an outer diameter of 1.0 mm and 0.75 mm, and an

inner diameter of 0.58 mm and 0.35 mm respectively (Hilgenberg GmbH, Malsfeld, Germany) using a PE-2 vertical micropipette puller (Narishige, Tokyo, Japan) with a motor connected to the upper chuck (Fig. 8.4). The motor was set to rotate through 360° in 60 seconds and enabled the two barrels of glass to be twisted into a double helix during heating and pulling (Fig. 8.2). The pulling process was executed as follows. Ten-centimetre lengths of glass were fed through the heating element and then clamped in place using the upper and lower chucks. The graduated metal block was positioned to stop the lower chuck from falling greater than four millimetres during pulling. The puller was then activated, and when the lower chuck made contact with the metal block, the glass was heated for a further 30 seconds prior to switching on the motor. After the 360° turn, the motor stopped automatically at which point the metal block was removed, enabling the lower chuck to fall and complete the pulling process.

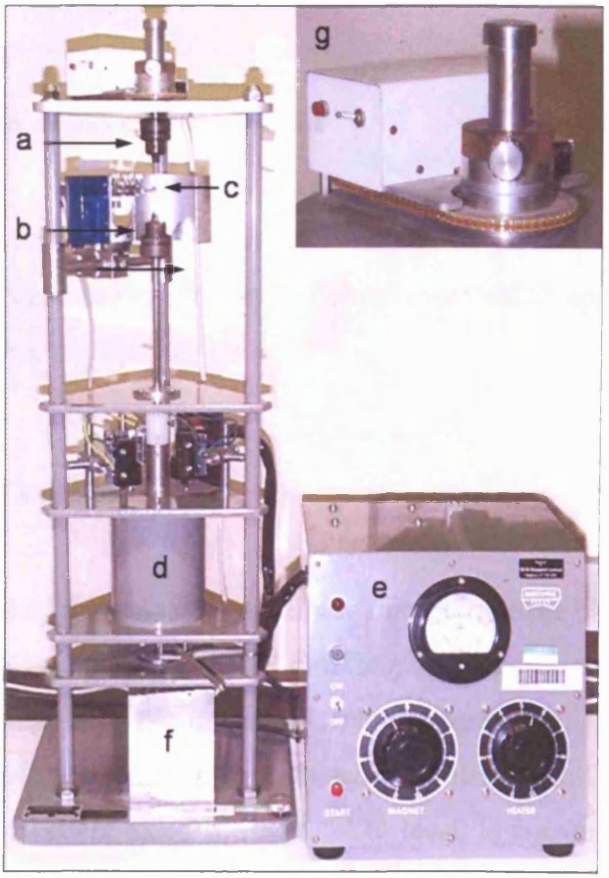

Fig. 8.4 Modified PE-2 vertical micropipette puller; a: upper chuck; b: lower chuck; c: heating element; d: magnet; e: control unit (for adjusting the magnet and heater settings); f: graduated metal block to allow the lower chuck to fall through known increments; g: motor attached to the upper chuck.

8.2.3.1.2. Silanisation of the pH sensitive barrel

After pulling, the narrower barrel was broken away from the wider barrel using a razor blade until the narrow barrel extended two centimetres from the tip of the micropipette. The wider barrel was then silanised* to facilitate a high-resistance seal between the internal surface of the micropipette and the pH sensitive membrane once cast. This process was performed in a fume cupboard by introducing two droplets of 2 % (v/v) dimethyldichlorosilane (DCDMS; Fluka 40140) dissolved in chloroform (AnalR grade, BDH Laboratory Supplies, Poole, UK) into the blunt end of the wider barrel of the micropipette which was still hot from being dried for one hour at 140 °C using a heat lamp. The DCDMS boils at 60 °C and thus vaporised on contact with the micropipette and the vapour coated its internal surfaces. To complete the silanising process, the micropipette was maintained at 140 °C under the heat lamp for a further one hour.

8.2.3.1.3. Production of pH sensor cocktail

The pH sensor was composed of 35 mg Hydrogen Ionophore II Cocktail A (Fluka), 16 mg polyvinylchloride and 6 mg nitrocellulose dissolved in approximately 1 ml of tetrahydrofuran (THF).

8.2.3.1.4. pH sensor casting

Approximately 10 µl of the sensor cocktail was injected into the blunt end of the wider barrel using a 1 ml glass syringe and a 38 mm long 29 gauge stainless steel hypodermic needle (Scientific Laboratory Supplies Ltd., Nottingham, UK). Filled micropipettes were then stored tip-down in an air-tight container containing self-indicating silica gel until required. The filament aided the cocktail to reach to micropipette tip and over a period of 48-72 hours the THF evaporated leaving a semi-solid pH sensitive membrane.

*Silanisation is the process by which hydrophilic hydroxyl groups at the glass surface are replaced by chlorosilanes (Ammann, 1986).

8.2.3.2. Production of the reference ground electrode

The reference ground electrode was produced as follows: one end of a 6 cm length of plastic tubing (outer/inner diameter 2/1.25 mm) was filled with a plug of 10 % agarose, 90 % 200 mM KCl and then the tube was backfilled with 200 mM KCl.

8.2.3.3. Experimental apparatus and microelectrode calibration

Using a plastic syringe and a MicroFil™ flexible needle (World Precision Instruments Inc. (WPI), Stevenage, UK), the pH-measuring barrel was filled with pH 4 calibration solution, and the contact-potential-measuring barrel was filled with 200 mM KCl. The blunt end of the pH-measuring barrel was inserted into a ESP-F10N microelectrode holder (Harvard Apparatus Ltd., Edenbridge, UK) filled with pH 4 calibration solution. The microelectrode holder contained a Ag/AgCl pellet linked to a 2 mm socket that was connected to the head-stage amplifier of a high impedance differential electrometer (F223, WPI). A second microelectrode holder was filled with 200 mM KCl and connected to the same head-stage amplifier. A length of silver wire was then introduced into the KCl filled microelectrode holder and the other end was inserted into the blunt end of the contact-potential-measuring barrel. The microelectrode/holder/head-stage amplifier assembly was mounted on a micromanipulator assembly which used in combination with a binocular dissecting microscope facilitated accurate positioning of the microelectrode tip. The micromanipulator assembly was composed of a course (Prior, Bishop's Stortford, UK) and a fine control manipulator (Goodfellow Cambridge Ltd., Cambridge, UK) enabling movement along the x, y and z planes.

The reference ground electrode was back-filled with 200 mM KCl solution and then inserted into a microelectrode holder containing the same solution. The reference ground electrode provided the connection between the ground of the electrometer and the measured solution and was maintained in position using a clamp. The microscope, micromanipulator and electrodes where all housed in a Faraday cage to minimise electrostatic interference. In addition, all equipment was electro-grounded to a common earth. The output from the electrometer was passed to an IBM-compatible personal computer via an analogue to digital converter and data acquisition card (PC-LabCard

PCL-818H, Advantech Co. Ltd., Taipei, Taiwan) and interfaced using the VISER software program.

8.2.4. Linking bacterial density and pH on the rhizoplane of *B. napus*

8.2.4.1. Electrode calibration and rhizoplane pH measurements

Microelectrodes were calibrated by submerging the tips into calibration solutions contained in a glass funnel (Soham Scientific, Cambridge, UK). The shank of the funnel was shaped in a U-bend which facilitated the retention of a sufficient solution volume during calibration but allowed solutions to be changed without moving the microelectrode tip by adding an excess of solution which caused the funnel to flush-out its contents. An aperture in the U-bend made it possible to for the reference ground electrode to be maintained in the calibration solution at all times. Microelectrode measurements were recorded at stable voltage for approximately two minutes using the VISER software (Version 4.0, I. R. Jennings, University of York, UK) prior to changing the pH calibration solution.

A plant was placed under the microscope and a point at the root base (0 - 20 mm from the root-shoot junction) was brought into focus. The reference ground electrode was then positioned in the soil close to the right hand side of the root, and using the micromanipulator and the microscope, the microelectrode tip was positioned in the unstirred layer of the rhizoplane to the left hand side of the root. Due to the very sharp and fragile nature of the ultra-fine microelectrode tip it was necessary to ensure that during positioning, the tip did not puncture the root, or become damaged. To avoid this, the microelectrode tip was first positioned close to the root surface using the microscope. Contact with the unstirred layer was conducted with the assistance of the electrometer. When the microelectrode was not in contact with the sample solution the circuit was open and the alarm of the electrometer sounded accordingly. Using this feature it was possible to determine when the microelectrode tip had made contact with the unstirred layer as the alarm stopped when the circuit was closed.

Three pH measurements per plant were taken from a total of eight plants and the microelectrode was calibrated before and after each set of three measurements.

The mean ion activity (output – contact potential [mV]) corresponding to each pH calibration solution before and after any soil measurement were then plotted and fitted using a linear model. If the voltages corresponding to the calibration solutions differ by more than 5 mV before and after a soil measurement, the measurement was discarded. Absolute pH values were taken as the mean of the estimate given by the pre and the post-soil measurement calibrations. Each measurement was taken one millimetre apart from the other. This distance was measured using an eye piece graticule. After each measurement, a short length of wire was placed in the soil adjacent to the root to mark the sample location.

8.2.4.2. Micro-sampling bacteria from locations of known pH

Given a successful pH measurement, the plant was transferred from the Faraday cage to a bench top where the micro-sampling was performed. Micro-samples were taken from locations on the root surface that were adjacent to the wire markers placed after each pH measurement. Micro-samples were taken and processed (i.e. plated on nutrient agar, then incubated prior to colony counting) as described in Chapter three.

8.2.4.3. Statistical analysis

As one of the three pH measurements from two of the eight plants was unsatisfactory; the data featured an unbalanced design structure (i.e. unequal number of pH measurements per plant). For this reason, the pH data were analysed using the REML method. A mixed model was fitted with random effects due to the plant (1-8), and fixed effects due to the treatment term bacterial numbers (CFU; a covariate).

8.3. Results

8.3.1. Double-barrelled pH microelectrode calibration

Figure 8.5 shows the response of a typical pH microelectrode to the calibration series detailed in section 8.2.2 before and after a series of rhizoplane measurements. Recalibration was generally less reliable at pH 7 and could differ by up to 10 mV. However, most root measurements ranged between pH 3-5 where recalibration was satisfactory (i.e. measurement in calibration solution before and after a root measurement differed by less than 5 mV).

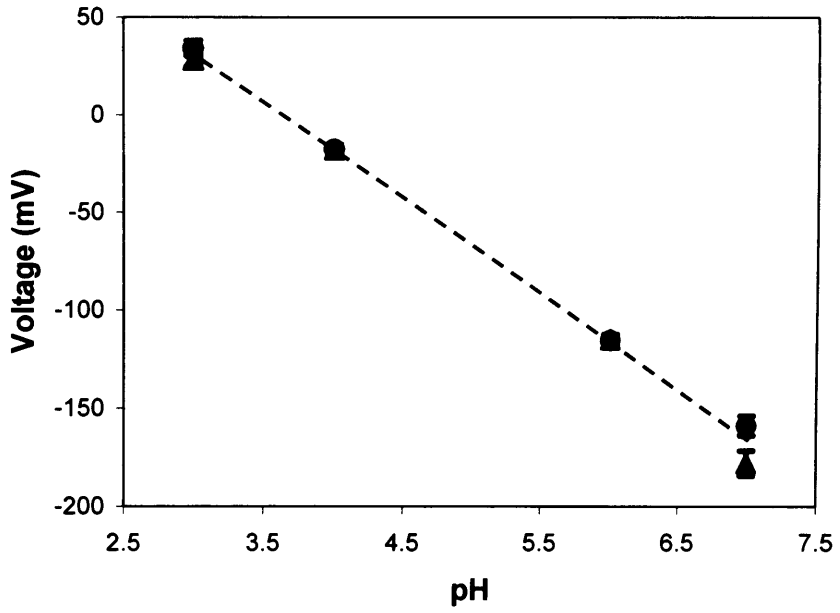

Fig. 8.5 pH microelectrode calibration before (●) and after (▲) a measurement in the unstirred layer of the *B. napus* rhizoplane.

8.3.2. Linking bacterial density and pH on the rhizoplane of *B. napus*

Figure 8.6 shows a typical set of three measurements in the unstirred layer of the rhizoplane after correcting for the contact-potential difference.

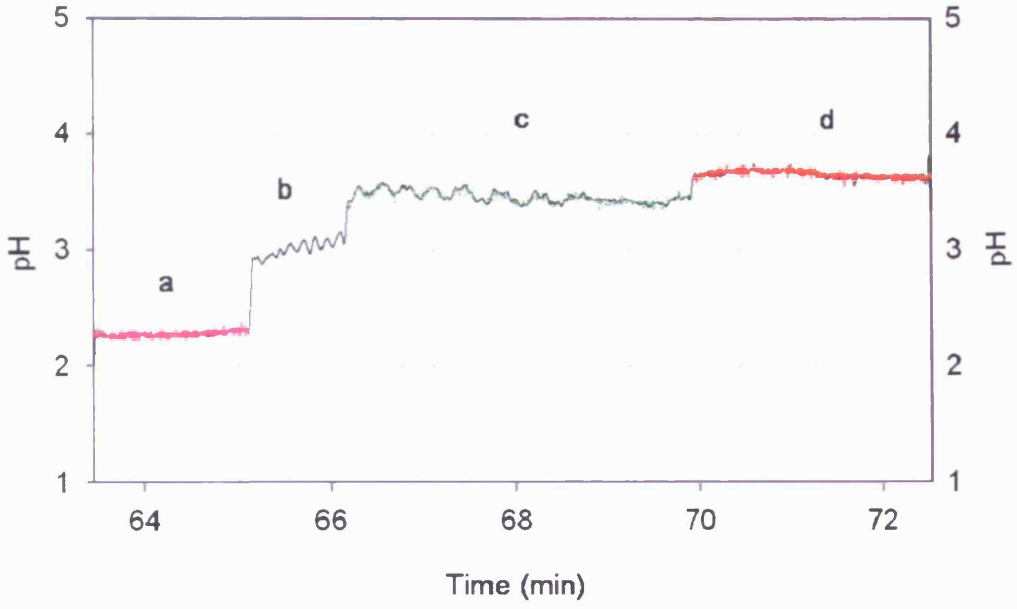

Fig. 8.6 Typical set of measurements in the unstirred layer of the rhizoplane at four different locations (a-d) after correcting for the resting potential difference. The electrode response at location b was unstable; therefore the tip was repositioned at location c. Coloured lines represent the data used for calculating the means for each root location.

The mean pH at the basal region was found to be significantly different between plants (Wald tests, $P < 0.05$), and within plants, measurements taken one millimetre apart varied by up to one pH unit (Fig. 8.7). In addition, significant co-variation between the pH and bacterial density was detected within samples (Wald test, $P < 0.05$). This relationship indicated that bacteria numbers increased with decreasing pH (Fig. 8.8).

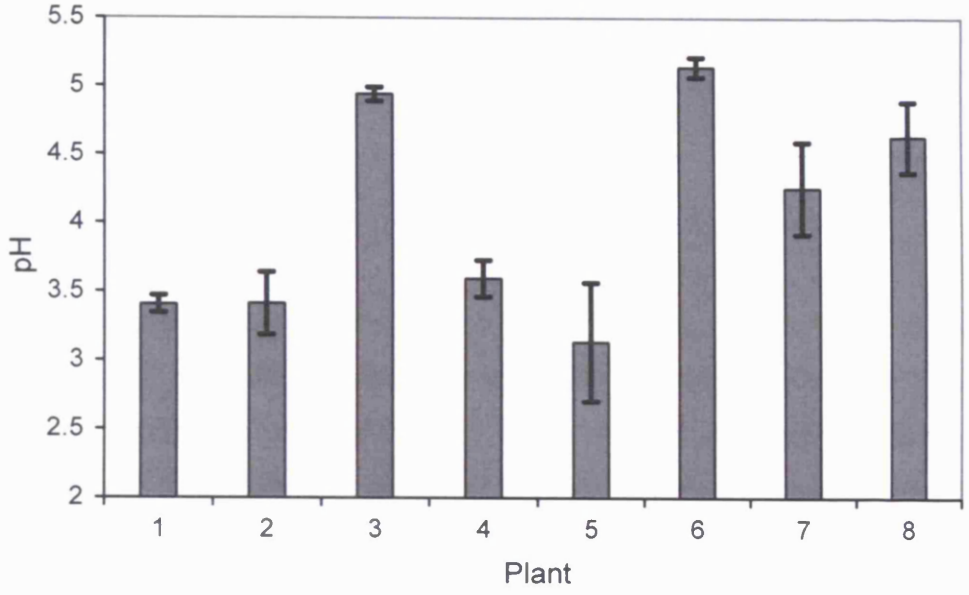

Fig. 8.7 REML predicted mean pH at the basal region of eight *B. napus* plants. Error bars represent the standard error of the estimates.

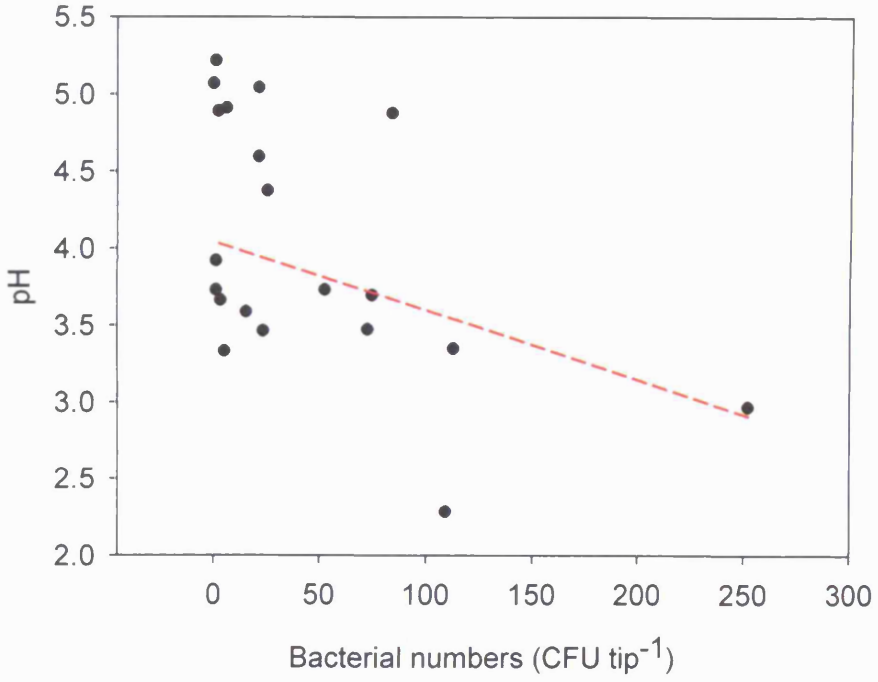

Fig. 8.8 Data points representing a pH value and the corresponding number of bacteria at the location from which the pH was measured. The line of best fit shows the REML predicted trend.

8.4. Discussion

8.4.1. Rhizoplane pH

The microelectrodes responded well to the calibration solutions and could be recalibrated after rhizoplane measurements. The pH microelectrode measurements revealed that rhizoplane pH can vary by up to one unit between positions just one millimetre apart. This finding is important because this level of heterogeneity has been speculated but actual observations have not been reported. In addition, such large difference over small-spatial-spaces highlights the appropriateness of investigating links between bacterial communities and their environment at a sub-millimetre scale. The underlying causes of these pH differences are unknown; however, from the perspective of rhizosphere bacteria, low pH may result from high respiratory activity or ion uptake. Alternatively, acidification may occur as a result of localised plant uptake of particular nutrient ions such as ammonium or the inherent variability of soil pH.

8.4.2. Linking rhizoplane bacterial density and pH

The REML analysis revealed that bacterial densities associated with root locations of low pH were generally greater than those associated with more neutral pH. These are the first measurements of their kind and as such it is not possible to compare these findings with other workers. However, as previously mentioned, greater bacterial densities may be associated with low pH conditions as a consequence of their respiratory or ion uptake activities. On the other hand, given that most bacterial exhibit optimum growth at neutral pH, is possible that species that favour acidic conditions may achieve relatively greater population densities as a consequence of reduced competition for resources. Nonetheless, the findings presented here should only be considered as demonstrative of the capacity for micro-sampling and microelectrode measurements to be combined. The reason for this is that given the level of heterogeneity observed for pH, it is critical that micro-samples are taken from exactly the same locations as the microelectrode measurements. While the wire markers were effective in indicating the approximate location of each pH measurement, I am not convinced that they were

sufficiently accurate at the micro-spatial-scale. In addition, as the diameter of a microelectrode tip is approximately 1 μm, while that of a micro-sampling rod is 130 μm, it may be necessary to take multiple pH measurements within the sample area of a micro-sampling rod. This would enable the derivation of the pH mean corresponding with each micro-sample.

Towards the end of my PhD I began to make some progress in developing strategies to alleviate these problems. The first, and most readily deployed, involved a rearrangement of the experimental apparatus to enable microelectrode calibration/rhizoplane measurements and micro-samples to be taken without moving the plant from the Faraday cage. This allowed the targeted sample location on the rhizoplane to be maintained within the cross-hairs of the microscope viewing plane between measurements, thus vastly improving the accuracy with which the sample location was marked (the modifications are shown in figure 8.9). However, it must be emphasised that this strategy does not overcome the problem related to the size difference between the microelectrode and the micro-sampling tips. Therefore, as mentioned above, multiple pH measurements within the sample area of a micro-sampling rod must be taken. It is likely that pH measurements taken at such short distances apart will be less variable than those taken at 1 mm intervals. However, it is important that this variation is assessed prior to linking pH with micro-samples.

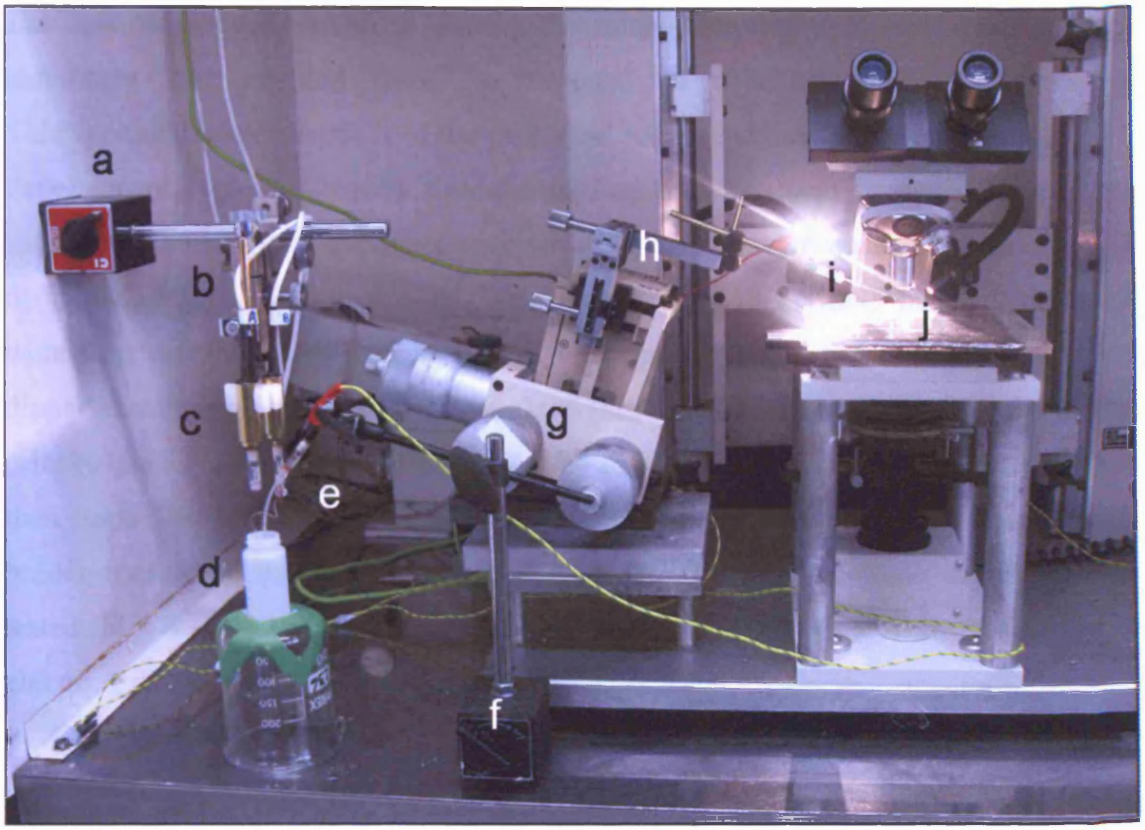

Fig. 8.9 Modified arrangement of the experimental apparatus to enable microelectrode measurements and micro-sampling without moving the plant. A magnetic stand (a) was attached to the side of the Faraday cage to support a micromanipulator (b) which allowed the microelectrode/holder/head-stage amplifier assembly to be moved in and out of the calibration solutions (d). The reference ground electrode (e) was attached to a magnetic clamp stand (f) which could be moved from its current position (for calibration) to the right hand side of the microscope base during rhizoplane measurements. After calibration component c could be removed from the micromanipulator (b) and attached to the coarse (h) and fine control (g) micromanipulator assembly for rhizoplane measurements. The reverse process enabled the microelectrode to be repositioned in the calibration solution for recalibration. Prior to measuring pH, a rhizotron (j) was placed under the microscope and the sampling location on the rhizoplane was targeted using the crosshairs of the microscope view plane. After a successful pH measurement, the micro-sampling rod/holder was attached to component g/h and directed towards the targeted sample.

The second strategy, involved coating the micro-sampling rods with a pH sensitive membrane that enabled them to be used as solid-state pH microelectrodes. This approach alleviates both of the problems outlined above; however, it is still in the developmental stage. Briefly, micro-sampling rods mounted in pulled and blunted single-barrelled borosilicate glass capillaries (Chapter 3) were washed by sonicating the tip in 1M HCl (1 min), then THF (1 min) and finally 18.5 MΩ (5 min). Washed tips were then dried for one hour at 140 °C under a heat lamp, and once cool, tips were dipped three times in the pH sensor cocktail (section 8.2.3.1.3) and dried for 30 minutes prior to use. The capillary tubes housing the solid-state micro-sampling electrodes were then back-filled with the pH 4 calibration solution and inserted into a microelectrode holder containing the same solution. The response of the electrode to pH was then tested (Fig. 8.10). The results indicate that the electrode response drifts (towards more electronegative) with increasing usage.

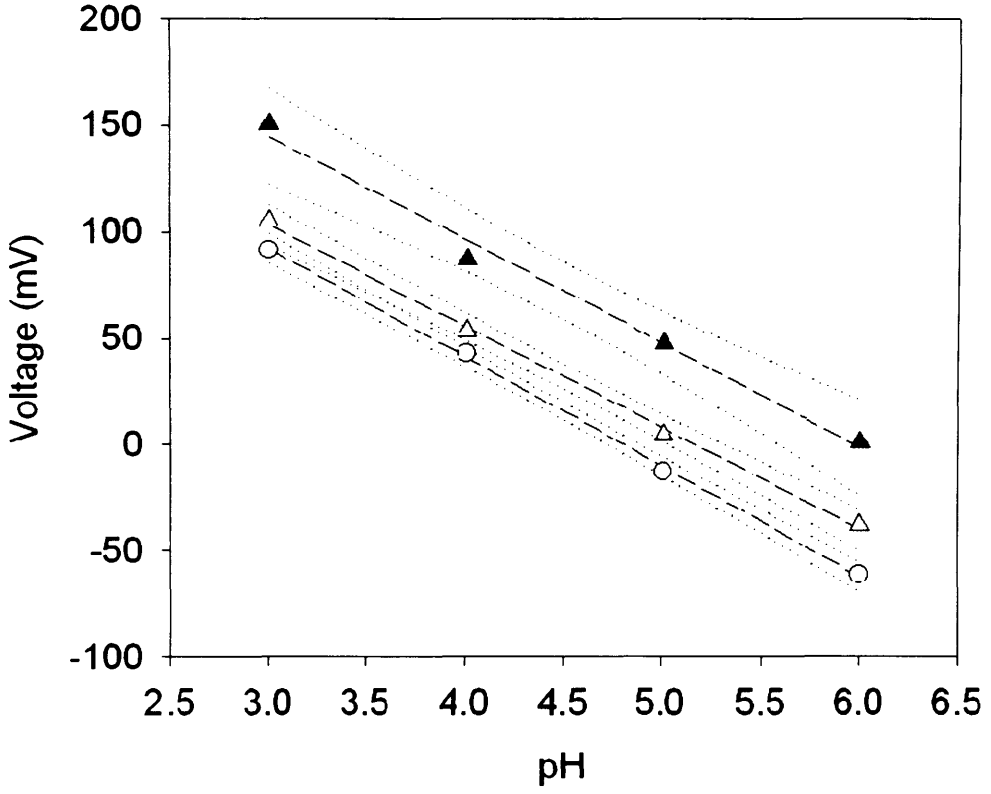

Fig. 8.10 Response of a micro-sampling electrode to a series of pH calibration solutions; first (▲), second (△) and third (○) calibration. Lines of best fit (dashed lines) and confidence intervals (dotted lines) were calculated by linear regression in Sigma Plot.

The tendency for solid-state pH electrodes to drift towards more electronegative was also observed by Piao *et al.* (2003); however, these workers found that the problem could be overcome by adding 3140 RTV-silicon rubber (Dow Corning, Co., Korea) to the sensor cocktail. Therefore, future developmental work should investigate this option. Alternatively, micro-sampling electrodes could be fabricated using pH sensitive metal oxides such as iridium oxide (van Houdt, 1992) or antimony oxide (Rehim *et al.*, 1987; Biggs *et al.*, 1994; Ha & Wang, 2006; Wang & Ha, 2006). It may also be possible to electroplate the existing tungsten micro-sampling rods with antimony (Rehim *et al.*, 1987) and then generate a pH sensitive antimony oxide tip using the hot nitrate melt method described by Ha & Wang (2006). It may be advantageous to use pH-sensitive metal oxide tips (given low acute toxicity) rather than tips coated with a solvent-cast membrane because the membrane may impede the recovery of bacterial cells post sampling. This issue should be addressed in future developmental work. An important consideration when using solid-state micro-sampling electrodes is the contact-potential difference between the calibration solutions and the root surface. The results presented in this chapter have shown that this difference is significant thus requiring contact-potential measurements alongside pH measurements. This could be achieved using an additional contact-potential-measuring electrode; however, the exact properties of this electrode require further thought.

8.4.3. Summary

Using microelectrodes, I observed a high degree of heterogeneity on rhizoplane pH at the micro-spatial-scale. A diverse range of ionophores are commercially available and can be used to construct single or multiple-barrelled microelectrodes. By rearranging the experimental apparatus as shown in figure 8.9 it is possible to combine microelectrode measurements and micro-samples to investigate links between bacterial communities and chemical conditions at the microhabitat scale. This is the first method of its kind and should facilitate a wide range of interactions to be explored.

CHAPTER 9

LINKING BACTERIAL COMMUNITY STRUCTURE WITH FUNCTION: HIGH-RESOLUTION IMAGING OF ISOTOPICALLY ENRICHED MICRO-SAMPLES USING SECONDARY ION MASS SPECTROMETRY

9.1. Introduction

In previous chapters I concentrated on linking micro-samples with pH and various pools of substrate. While these approaches have the potential to yield interesting information from a biogeographical perspective, they provide little insight into the mechanisms underpinning the observed trends. A more detailed understanding of how bacterial community attributes are influenced by the environment can be obtained by identifying the function role of different organisms over spatial and temporal scales.

In this chapter, I explore the potential for determining which populations are actively catabolising specific isotopically labelled compounds using secondary ion mass spectrometry (SIMS). To contribute towards the findings reported in Chapter seven, this approach was focussed towards the determination of bacteria that were actively utilising root exudates released by soil grown plants.

9.1.1. Current methods

Currently, methods for determining which populations are actively catabolising specific compounds within their environment involve the use of isotope tracers. One such example is stable isotope probing (SIP; Manefield *et al.*, 2002a; Manefield *et al.*, 2002b; Dumont & Murrell, 2005). In SIP experiments, specific or broad-range substrates are highly enriched with a stable isotope such as ^{13}C or ^{15}N such that microbial cells utilising the substrate become isotopically labelled. After sampling, isotope labelled and unlabelled molecules such as DNA/RNA can then be separated by buoyant density

gradient centrifugation. During this procedure labelled and unlabelled molecules are stained to facilitate their visualisation. Separated bands are then isolated using either a needle and syringe or by fractionation, and can be analysed using a wide range of molecular techniques. This method has represented a revolution for linking microbial communities with function; however, it is likely to be poorly suited to analysis of micro-samples as relatively high concentrations of DNA/RNA are required to visualise and thus isolate labelled and unlabelled fractions.

Alternative techniques include fluorescence *in-situ* hybridisation-microautoradiography (FISH-MAR; Lee *et al.*, 1999; Ouverney & Fuhrman, 1999) and isotope arrays (Adamczyk *et al.*, 2003) and are briefly described in figure 9.1 (for a more detailed description of the methods see Dumont & Murrell, 2005; Wagner *et al.*, 2006). Currently, the isotope array requires further development to facilitate its widespread use; the main problem being the availability of microarrays that are representative of the environment under investigation. This is critical to their success as only targeted rRNA molecules will hybridise with the array and therefore *a priori* knowledge of the studied organisms is required. Because of this, the genetic diversity of non-targeted organisms remains unknown. Although in principal, thousands of probes can be applied simultaneously. Therefore, given rRNA of sufficient quantity and quality, and microarrays designed to answer well defined questions, this problem may be managed.

Using high intensity radiotracers and modern equipment, MAR has a resolution of 0.5-2 μm (Wagner *et al.*, 2006) and can therefore be used to detect radio-labelled bacteria on a single-cell level. When combined with FISH, MAR can be used to link key physiological features to targeted phylogenetic groups. The main drawback of this approach is that no more than seven phylogenetic groups can be simultaneously detected due to the number of distinct fluorophores that are currently available (Amann *et al.*, 1996). Nonetheless, at the moment this approach is unique in its capacity to link function with phylogeny at the single-cell level. However, given that the intensity of ^{14}C is low relative to most other commonly used radioisotopes it is likely that active bacterial cells would have to be heavily labelled to facilitate ^{14}C detection by MAR. This may be problematic for many environmental applications, such as $^{14}CO_2$ pulse-chase experiments for evaluating root exudate utilising populations, as the total

radioactivity fed to the microbial community and the incubation time may be low[9]. Improved sensitivity of ^{14}C (X 1000) can be obtained using SIMS (Lechene *et al.*, 2006), which in contrast to isotope arrays and FISH-MAR also has the advantage of being able to detect any stable as well as radioactive isotopic tracers. This greatly increases the scope of the technique as microbial interactions with nitrogen-containing compounds as well as other elements for which there are no useable radioisotopes can also be investigated. In addition, SIMS can be used to detect the presence of multiple isotopes which enables more complex interactions to be studied.

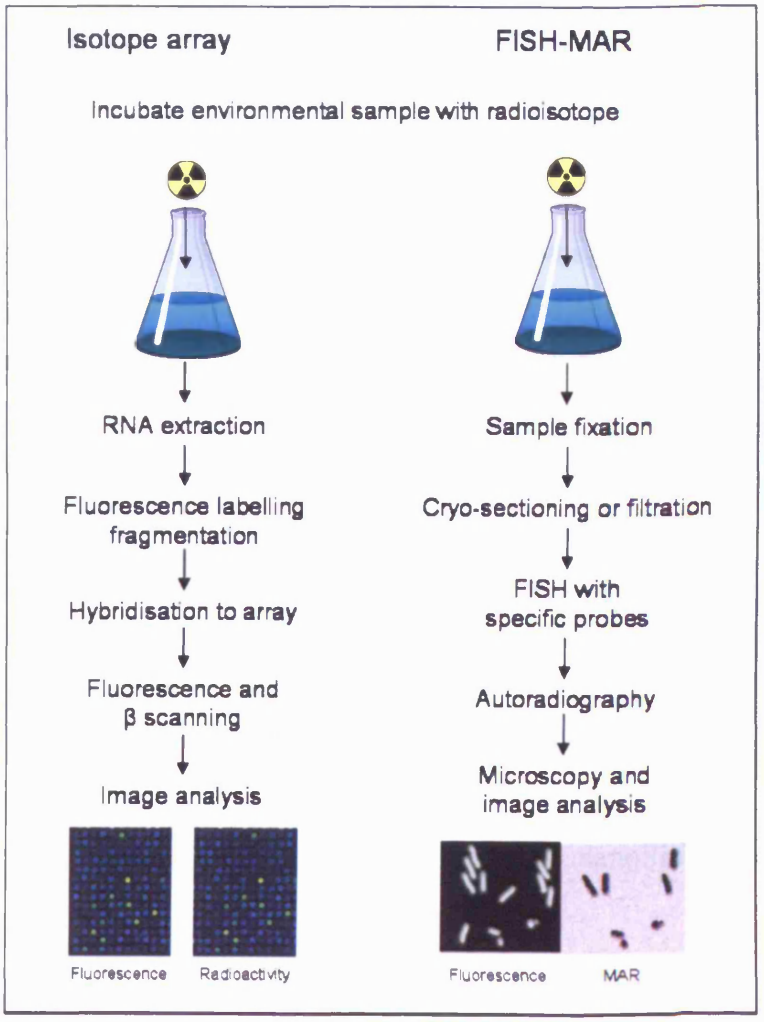

Fig. 9.1 Overview of the protocols for isotope arrays and FISH-MAR. The images (bottom) are cartoons depicting the kind of data that may be obtained using these methods.

[9] Despite this limitation FISH-MAR has been used successfully for linking targeted phylogenetic groups with active assimilation of ^{14}C labelled compounds (for more information see Wagner *et al.* (2006)); therefore, future work should include investigations into FISH-MAR analysis of micro-samples. However, following a meeting concerning NanoSIMS at Newcastle University I was able to secure a unique opportunity to investigate the appropriateness of SIMS for microbial ecology studies.

9.1.2. SIMS

The Cameca NanoSIMS 50™ is the latest generation of secondary ion mass spectrometers and enables the distribution of multiple chemical isotopes to be quantitatively imaged at exquisite mass and spatial resolution. For this reason, the nanoSIMS instrument is being considered for biological applications where sufficient resolution is required to distinguish between very small mass differences (e.g. $^{12}C^{1}H$ and ^{13}C) within single eukaryotic or prokaryotic cells. The principal behind the nanoSIMS is as follows: a beam of ions is used as a probe to sputter the surface atomic layers of a sample into monoatomic and polyatomic particles, a fraction of which will be ionised (Fig. 7.2). The flight path of these secondary ions is then manipulated with ion optics to direct a focused beam of secondary ions towards a magnetic sector mass spectrometer which separates them according to their mass and measures a secondary ion current or generates a quantitative atomic mass image of the analysed surface (Guerquin-Kern *et al.*, 2005). In biology, SIMS has been used to successfully detect isotopic enrichment of single eukaryotic and prokaryotic cells following their incubation with a labelled substrate (Cliff *et al.*, 2002; Peteranderl & Lechene, 2004; Cliff *et al.*, 2005; Guerquin-Kern *et al.*, 2005; Lechene *et al.*, 2006; McMahon *et al.*, 2006; Herrmann *et al.*, 2007); however, as with MAR, isotope detection alone gives no insight into the phylogeny of the labelled cells. With method development Kuypers & Jorgensen (2007) suggest that this may be possible by replacing the fluorescent oligonucleotide probes used for FISH with isotopically labelled (stable or radioactive) or halogenated probes. Nonetheless, as with FISH this approach would only facilitate probe-targeted organisms to be identified. Despite this, the potential applications for the technique in microbial ecology are broad, thus nanoSIMS deserve further investigation.

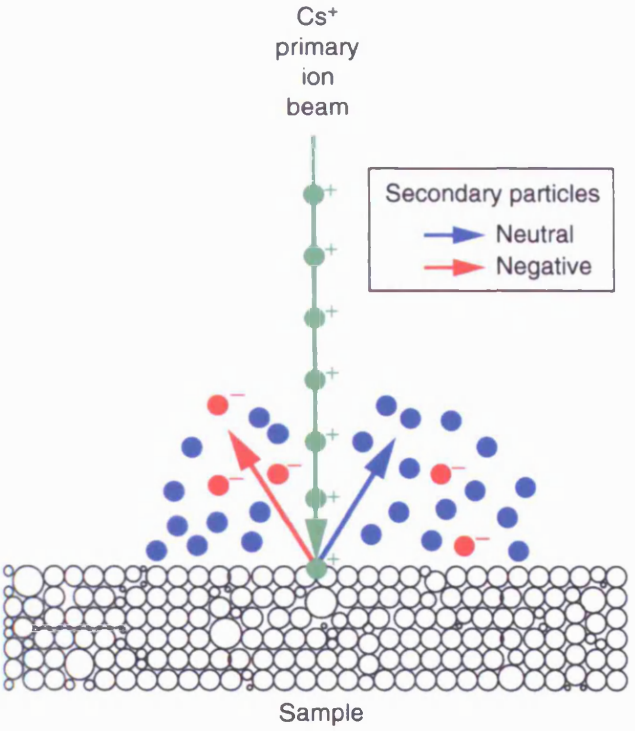

Fig. 9.2 The principle of SIMS. As the primary Cs^+ ion beam hits the sample surface, mono and poly atomic secondary ions are ejected into a vacuum. Secondary ions are then identified using mass spectrometry. From Lechene *et al.* (2006).

Currently there are little more than a dozen nanoSIMS instruments worldwide and most are used in materials sciences, geology and cosmochemistry. It is little wonder then that the literature contains only one article concerning nanoSIMS detection of isotopically enriched bacteria in the soil environment (Herrmann *et al.*, 2007). Consequently, our understanding of the appropriateness of nanoSIMS for microbial ecology studies is poor. To better understand this technique and to test its potential for detecting isotope enrichment in micro-samples, I designed an experiment in which plants, pulse-labelled with $^{13}CO_2$, were subjected to micro-sampling at the root apex and base. These samples were then analysed using nanoSIMS to determine whether bacterial cells had become enriched with ^{13}C-labelled compounds released by the roots. Samples were taken from the root base and apex as these root locations were found to have contrasting exudation patterns - exudation was maximal at the apices but not detected at the root base (Chapter 7). As nanoSIMS is reported to be at least a thousand times more sensitive than ^{14}C autoradiography (Lechene *et al.*, 2006), it was hypothesised that rhizodeposition at the root base (indicated by ^{13}C enrichment of bacteria) could be detected more efficiently than using more conventional approaches.

9.2. Materials and methods

9.2.1. Plant growth conditions

Three plants were grown as described in section 8.2.1.

9.2.2. Preparation of the controls

P. fluorescens SBW25::*lux*CDABE cells were isolated on 1/10 TSA containing 50 μg ml^{-1} kanamycin and maintained at 28 °C for 48 h. A tube containing 20 ml $1/10^{th}$ TSB was then inoculated with a single colony and incubated for 16 h at 28 °C, 200 rpm prior to being used as a ^{13}C-free control. Another tube containing 10 ml $1/20^{th}$ TSB and 10 ml $1/10^{th}$ ^{13}C-solution (1.5 g $^{13}C_6H_{12}O_6$, 0.14 g $[NH_4]_2SO_4$, 0.29 g KH_2PO_4 made up to 40 ml with sterile RO H_2O) was inoculated with a single colony and incubated for 16 h at 28 °C, 200 rpm prior to being used as a ^{13}C-enriched control.

9.2.3. ^{13}C pulse-labelling

Six days after planting, a Mylar sheath (section 7.2.1.1) was placed over the shoots of each plant and the ring of high density foam was pressed together with mini bulldog clips to form an air-tight seal. In Chapter seven, 5 μCi $NaH^{14}CO_3$ was sufficient to label roots in a reproducible manner. This amount of radioactivity corresponded to 0.1 μM $NaH^{14}CO_3$ contained in 2 μl 150 mM TRIS buffer (pH 8). To ensure maximal ^{13}C enrichment of rhizodeposits, 2 μl 150 mM TRIS buffer (pH 8) containing 0.2 μM $NaH^{13}CO_3$ (Sercon Ltd., Stapeley, UK) was dispensed into the micro-tube of each labelling sheath. To generate a $^{13}CO_2$ atmosphere within the sheath, an excess of concentrated HCl (8 μl) was injected into the micro-tube. The injection hole was then sealed immediately to prevent $^{13}CO_2$ escaping. Plants were then placed under growth lamps and pulse-labelled for one hour. Post labelling, the sheaths were removed and the plants were left to photosynthesise for eight hours to allow translocation of the ^{13}C-labelled photosynthates into the roots. This duration was considered appropriate because Dilkes *et al.* (2004) reported that maximal carbon exudation occurred two to

three hours after pulse-labelling and Rangel-Castro (2005) reported that maximal recovery of ^{13}C-labelled nucleic acids from bacteria associated with a planted grassland soil could be achieved three hours after a four hour pulse-labelling period.

9.2.4. Micro-sampling and sample concentration

To increase the number of bacteria per sample, three micro-samples were taken from the root apex (0 - 10 mm from the root cap) and the root base (0 - 20 mm from the root-shoot junction) of three labelled plants. All samples from the root apex were recovered by sonicating at low power in 5 µl sterile 18.5 MΩ water stored in a microtube supported by a polystyrene float in a water bath (Ultrasonik 300; JM Ney, Bloomfield, CT, USA) containing ice and water. Samples from the root base were recovered by the same procedure in a separate microtube. A small incision was made in the lids of the tubes to allow water to evaporate during the concentrating step. Samples containing were concentrated to a final volume of approximately 0.5 µl using the equipment described in section 4.2.1.1.

9.2.5. Sample preparation for nanoSIMS

Using a sharp knife, four marks at 90° intervals were made on the outer rim of clean stainless steel sample stub (two marks were made at 0° to identify the orientation of the stub) which was then coated with 60% gold-palladium using a Polaron E5100 coater (Polaron, Watford, UK). Concentrated micro-samples and 0.5 µl of each control were then aliquoted next to the reference marks and air dried[10] at 40 °C for 16 h. Air dried samples were then coated with 60% gold-palladium.

[10] Peteranderl & Lechene (2004) found that sample preparations for electron microscopy involving chemical fixation tended to lead to lower secondary ion yields of isotope labels. They suggested that this may be due leaching of low molecular weight cell components as well as unincorporated labelled-substrate. They found that freeze dried samples were less prone to these problems. I visually compared bacterial cell integrity using SEM following air drying and freeze drying and found no obvious difference; therefore I opted for air drying as this method is less labour intensive.

9.2.6. NanoSIMS analysis

The SIMS analysis was performed by Dr Matt Kilburn[11] with kind permission from Prof. Chris Grovenor[10] using the Cameca NanoSIMS 50™ at Oxford Materials, University of Oxford, UK. Briefly, samples were selected in the analysis chamber using a photomicroscope with an attached CCD camera and then bombarded with a Cs^+ primary ion beam. Secondary electron images were obtained using an appropriate detector and secondary ion images corresponding to ^{12}C, ^{13}C, and $^{12}C^{14}N$ were obtained after calibrating the mass spectrometer.

[11] Department of Materials, University of Oxford, UK.

9.3. Results

9.3.1. Mass imaging of controls

The sample preparation was successful in maintaining the structural integrity of the cells in such a way that they could be clearly identified as bacteria (Fig. 9.3). However, because of the nature of the sample and the rate at which the Cs^+ primary ion beam sputtered the sample surface it was not possible to determine $^{12}C/^{13}C$ ratios in a statistically rigorous manner (section 9.4). Nonetheless, qualitative and semi-quantitative comparisons of secondary ion currents were possible using the mass images. The mass images indicate that the ^{13}C content of ^{13}C-enriched control cells (Fig. 9.3b) was much greater than the natural abundance of ^{13}C in the ^{13}C-free control cells (Fig. 9.3a). Using a similar instrument, Peteranderl & Lechene (2004) demonstrated that the natural abundance of ^{13}C in rat embryo fibroblast cells was 1.107 %. Assuming a similar value for cultured bacterial cells, the mass images clearly demonstrate that *P. fluorescens* SBW25::*lux*CDABE cells grown in ^{13}C-enriched media were labelled successfully.

Figure 9.4 shows the nanoSIMS analysis of micro-samples taken from the root apex and base of ^{13}C-labelled plants. The SE images were not particularly useful for locating bacterial cells in amongst other debris; however, the $^{12}C^{14}N$ images clearly indicated the presence of organic-rich objects with bacteria-like form. The mass images show ^{13}C presence in bacterial cells; however, the intensity (cps) of the secondary ion currents indicate that the $^{12}C/^{13}C$ ratio is approximately similar to ^{13}C natural abundance measurements in other biological materials (Peteranderl & Lechene, 2004).

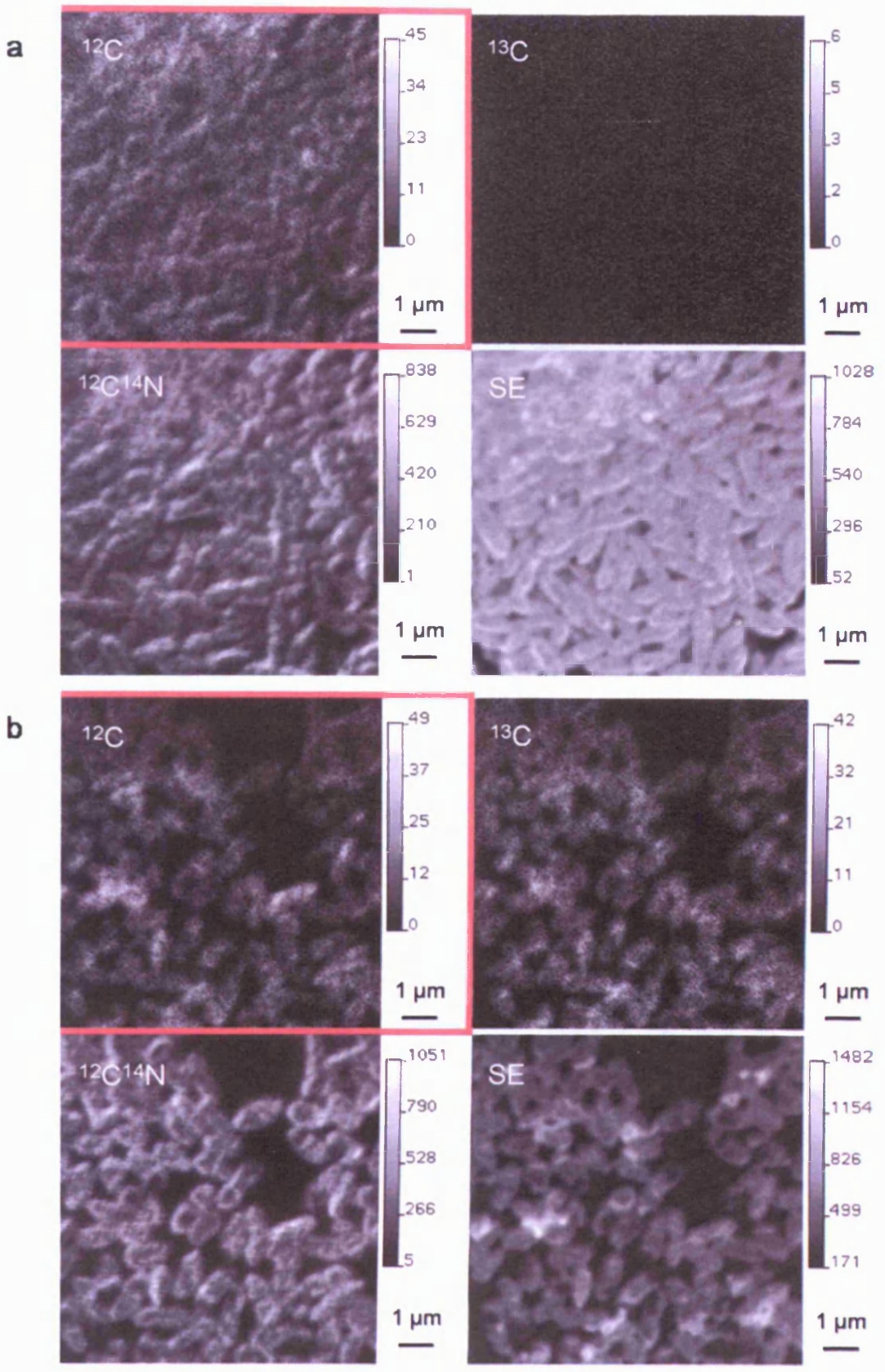

Fig. 9.3 NanoSIMS analysis of *P. fluorescens* SBW25::*lux*CDABE cells grown in ^{13}C-free (a) or ^{13}C-enriched (b) media (units are counts per second [cps]). The secondary electron images (SE) clearly show individual bacterial cells while the ^{13}C images clearly show that cells grown in the ^{13}C-enriched media became highly labelled.

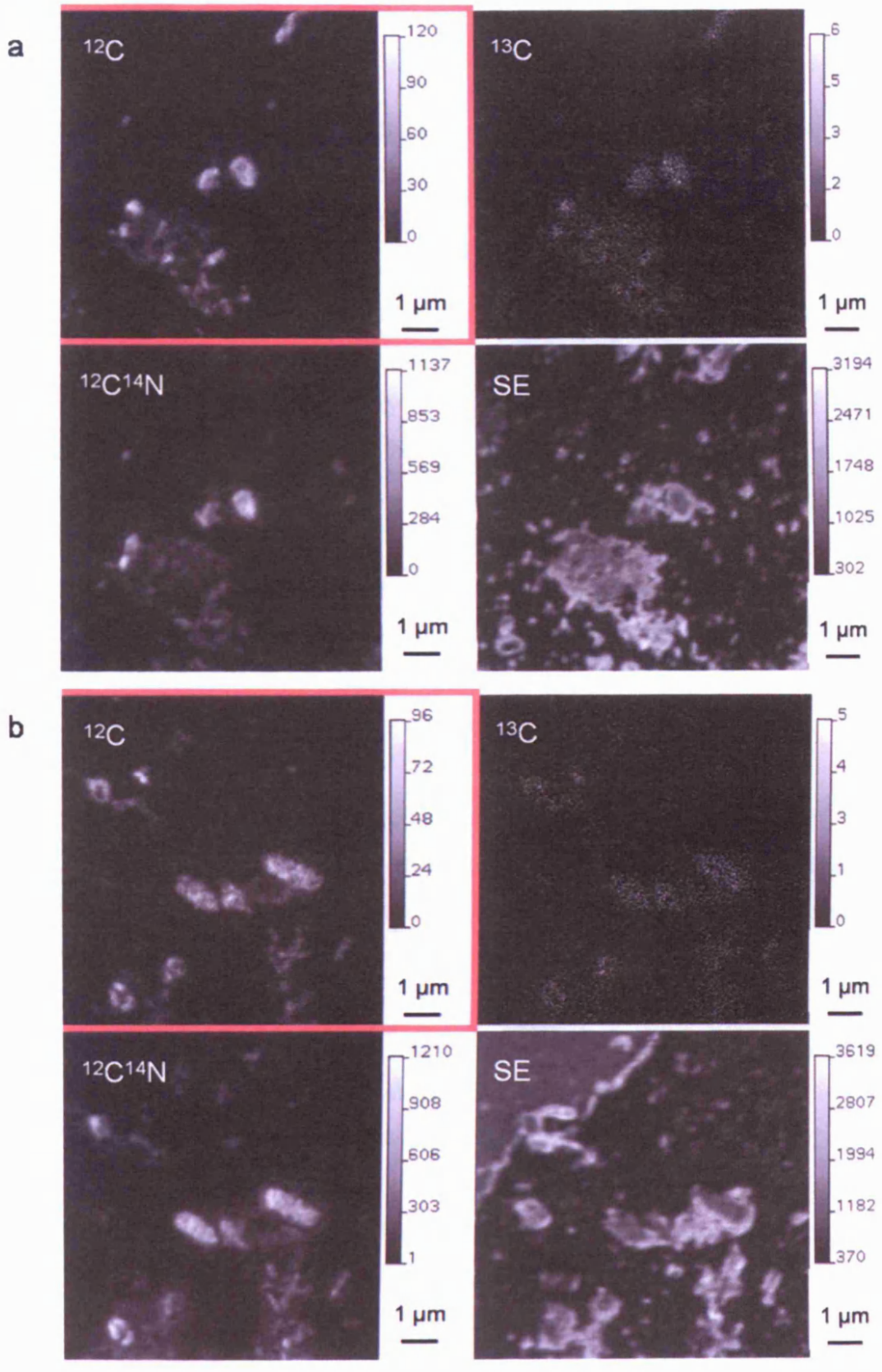

Fig. 9.4 NanoSIMS analysis of micro-samples taken from the root apex (a) and base (b) of ^{13}C-labelled plants (units are counts per second [cps]). See text for explanation.

9.4. Discussion

This study was successful in demonstrating the capacity for nanoSIMS to image ^{13}C enrichment of single cultivated bacterial cells. However, the analysis of micro-samples from the root apex and base of ^{13}C-labelled plants was more challenging. One of the major obstacles to this analysis was locating bacteria within each micro-sample. Based on SEM observations of micro-samples taken from the rhizoplane (data not shown), I had expected that this might be the case. However, by pooling a number of micro-samples prior to SEM, the density of bacterial cells was sufficient for bacteria-like objects to be frequently observed. Nonetheless, for NanoSIMS this only solved part of the problem. SEM allowed micro-samples to be rapidly surveyed for 'bacterial cells' although due to the fact that the Cs^+ primary ion beam sputters only a few atom layers at a time, the rate at which images are generated using nanoSIMS is very slow (5 min). This made the search for bacteria-like objects more time consuming. Nevertheless, using the $^{12}C^{14}N$ image generated by the NanoSIMS, it was possible to identify candidate bacterial cells with greater certainty than is possible with SEM.

The results indicated that bacteria associated with the root apex and base of ^{13}C-labelled plants had not become isotopically enriched. This may be improved by increasing the quantity of ^{13}C fed to the plants, and allowing the system to incubate for a greater period of time before sampling. For example, Griffiths *et al.* (2004) measured the ^{13}C content of RNA isolated from the rhizospheres of $^{13}CO_2$ pulse-labelled grass species and observed no statistically significant levels of enrichment until four days after the pulse-feed. However, even then the level of ^{13}C enrichment above natural abundance was low; highlighting the necessity to ensure accurate measurements of $^{12}C/^{13}C$ ratios when determining levels of enrichment. This was a problem for my samples because the yield of secondary ions sputtered from the sample surface was low. Therefore, to enable statistically significant measurements of secondary ion currents, the Cs^+ primary ion beam had to be aimed at the sample for a longer period of time than would otherwise be necessary. Nevertheless, this resulted in the complete destruction of the targeted sample area, making it impossible to measure statistically significant isotope ratios. The nanoSIMS analysis for these samples was, therefore, semi but not fully quantitative. However, at the time of the analysis, the instrument was running at approximately one

third of its maximum mass resolving power[12]; therefore, it is possible that quantitative mass imaging of bacterial cells could have been achieved if the instrument had been in optimum condition. Although a number of other issues relating to isotope ratio measurements were identified in the course of the analysis that would need to be addressed in future experimental designs. Firstly, carbon isotope ratios have been reported to differ depending on the environment from which they are isolated (Coffin *et al.*, 1990); therefore, the controls should have been isolated from the same soil as that in which the plants were grown, rather than cultured in liquid media. Secondly, the samples and controls should have ideally been sufficiently close together that they could be analysed in the same view panel. This is because movement of the sample with respect to the Cs^+ primary ion beam position can lead to small but significant shifts in the instrument calibration (Lechene *et al.*, 2006). This issue is potentially a serious obstacle for analysis of environmental samples; however, it and other problems may be overcome using a SEM fitted with a focussed ion beam (FIB) and a micromanipulator (e.g. FB-2000A and FB2100, Hitachi High-Technolgies Co.). As with SIMS instruments, a FIB instrument uses a focussed primary ion beam to sputter a sample surface. The difference is that FIB instuments only detect secondary electrons. FIB is commonly used for targeted etching of materials and micromachining. It is possible, therefore, that by scanning a micro-sample using the electron primary beam, bacteria-like objects could be rapidly identified and then circled using the FIB to highlight their position. This would improve the efficiency with which bacterial cells are located within a sample during nanoSIMS analysis. To position samples and controls very close to one another it may be possible to prepare them on ultra thin silicon wafers and then, using the FIB, cut appropriate sections from prior to positioning them on a sample stub using the micromanipulator. This would enable the nanoSIMS instrument to be calibrated and then used to analyse samples without moving the position of the sample relative to the Cs^+ primary beam.

Currently, the availability of nanoSIMS instruments and experienced technicians, combined with the huge expenses involved in running such analyses, are prohibitive to the development of protocols for quantitative mass imaging of single bacterial cells; however, given that this technique enables simultaneous detection multiple radioactive and stable isotopes its potential for biological tracer experiments is unparalleled. This study has demonstrated semi-quantitative mass imaging of single bacterial cells, which

[12] This was due to an unidentified fault with the instrument.

given sufficient levels of enrichment is sufficient for determining whether an organism has been utilising a labelled substrate. However, as previously mentioned, this provides no insight into the phylogeny of the organisms involved. With appropriately prepared samples, it is possible that the phylogeny of targeted organisms could be linked with nanoSIMS measurements using existing techniques such as FISH. This approach was pioneered by Orphan *et al.* (2001), who confirmed that anaerobic oxidation of methane in methane-rich sediments was being conducted by archaea surrounded by sulphate-reducing bacteria. Alternatively, as suggested by Kuypers & Jorgensen (2007), it may be possible to replace the fluorescent oligonucleotide probes used for FISH with isotopically labelled (stable or radioactive) or halogenated probes that could be detected using nanoSIMS.

CHAPTER 10

GENERAL DISCUSSION

10.1. Introduction

The objectives of this research were to develop a novel method for sampling bacteria from root and soil surfaces at a scale that approximates that of a microhabitat, and to investigate methods that would facilitate a better understanding of how bacteria interact with their environment at the micro-spatial-scale. Key interactions that were investigated were the link between bacteria and habitat factors, such as substrate availability and pH. However, a novel approach for detecting bacteria that were active in the catabolism of isotopically-labelled substrates was also investigated. This chapter evaluates the achievement of these objectives and discusses the ways in which the work could be carried forward.

10.2. Development of a novel micro-sampling method

A novel method to facilitate quantitative and non-destructive, micro-spatial-scale sampling of bacteria was developed (Chapter 3). The method involved touching a root or soil surface with the tip of a metal rod that was accurately positioned on a sample surface using a micromanipulator and a microscope. On contact with a surface, bacteria became adhered to the tip and could then be recovered post sampling by washing in a buffer solution. To enable direct comparisons between samples, the micro-sampling tip was of standardised surface area.

The efficiency of the technique for removing bacteria from the root surface was compared with that of the conventional approach of washing bacteria from the surface of dissected root segments. This comparison indicated that the efficiency of the micro-

sampling technique is similar to that of the root dissection/washing approach; however, the micro-sampling technique offered greater accuracy in estimating bacterial densities as the surface area used for sampling was standardised.

In Chapters five and six, the micro-sampling technique was used to investigate culturable bacterial densities in bulk soil and at the root base and apex of *B. napus* plants. The results indicated that bacterial density followed the order basal region > bulk soil > apical region. This finding was in general agreement with the colonisation trends revealed using a novel bioluminometric assay (Chapter 5) and with other workers (Parke *et al.*, 1986; Olsson *et al.*, 1987; Liljeroth *et al.*, 1991; Chin-A-Woeng *et al.*, 1997; Duineveld & van Veen, 1999), highlighting that the micro-sampling technique generates data sets that reliably reproduce known trends at the macro-scale (i.e. centimetre scale) while providing additional micro-scale information. For example, between individual micro-samples, bacterial density was highly heterogeneous and varied between zero and approximately a thousand bacteria per tip. This finding is not surprising as other workers have reported similar observations using scanning electron and optical microscopy (Chin-A-Woeng *et al.*, 1997; Nunan *et al.*, 2001; Nunan *et al.*, 2003; Gamalero *et al.*, 2004; Watt *et al.*, 2006b); however, in contrast to the micro-sampling approach, microscopy-based techniques do not allow for detailed assessment of bacterial diversity following the determination of bacterial yield[13].

It has long been suggested that the distribution of bacterial types at the micro-spatial-scale is very heterogeneous; however, until recently this had not been demonstrated experimentally. Grundmann & Normand (2000) investigated the diversity of culturable *Nitrobacter*-like bacteria in soil micro-samples (cubes of soil with dimensions of 50-250 μm) and found that different numbers of serotypes were present between samples. In addition, the genetic distances, based on 16S-23S intergenic spacer studies, between the isolates on two clumps of soil of approximately two cubic centimetres was as great as that of strains isolated from different geographical areas. Using the same micro-sampling technique, Grundmann & Debouzie (2000) found that nitrate-oxidising bacteria (*Nitrobacter* spp.) were absent in some soil samples of approximately 250 μm diameter. These findings clearly demonstrate that the distribution of a defined bacterial

[13] FISH combined with CLSM enables the distribution of bacteria containing targeted DNA sequences to be determined (Watt *et al.*, 2006b); however, no more than seven bacterial populations can be detected simultaneously due the limited number of fluorophores available . Therefore, the genetic diversity of non-targeted organism remains unknown.

group is highly heterogeneous at the micro-spatial-scale; however, similar studies investigating the distribution of a wider range of bacterial types have not been reported.

In Chapter five, the diversity of culturable bacteria in micro-samples from bulk soil and the root base and apex was assessed using ERIC-PCR fingerprinting. The results revealed that less than 5 % of bacterial OTU were present in more than one plant/soil replicate within the treatment combinations (zones within plant age categories). This is indicative of the very high level of diversity that is inherent to soil and rhizosphere bacterial communities; however, the fact that ERIC-PCR fingerprinting discriminates between bacterial types at an arbitrary sub-species level is another contributing factor.

To state with certainty that the spatial-scale of the micro-sampling method is truly 'appropriate' for investigating how soil/rhizosphere bacteria respond to and influence their environment is currently not possible. This is because we have a poor understanding of the factors that are most important in determining community structure and function. Therefore, we are not able to measure the spatial scales over which these factors operate and then match the diameter of the micro-sampling tip accordingly. Nevertheless, the data collected with the current micro-sampling system has demonstrated that the density and distribution of bacterial types in soil and on the rhizoplane is highly heterogeneous at the micro-spatial-scale. If, as current evidence suggests, community structure is linked with habitat factors, then these results indicate that the spatial-scale of this novel sampling method is an appropriate approximation of that of a microhabitat. It should be reemphasised that most macro-ecological studies consider the influence of organisms on their environment and *vice versa* at the habitat scale; however, due to a lack of suitable methods, similar studies concerning microorganisms have been impossible. The micro-sampling technique developed as part of this PhD research represents a major methodological advance and should make a valuable contribution to the field of surface-based microbial ecology.

10.3. Analyses of micro-samples

A fundamental problem faced by microbial ecologists investigating the links between bacterial communities and their environment is in understanding the relationships between bacterial diversity and community structure, and between community structure

and function (O'Donnell *et al.*, 2001). Bacterial community structure is defined by attributes such as community composition, richness, evenness, and total bacterial density; however, current technology limits the measurement of all of these attributes in a sample to cultivation-based approaches. For example[14], determination of total bacterial yield using molecular-based approaches, such as RT-qPCR, is complicated by the fact that insufficient sequence information is available to facilitate the design of universal primer (and probe) sets that target DNA sequences that are present in equal numbers throughout all species within the domain (Chapter 4). In addition, current molecular-based community fingerprinting methods such as denaturing gradient gel electrophoresis (DGGE; Muyzer *et al.*, 1993) enable the richness of a sample to be determined but not the evenness[15]. As will be discussed below, these issues raise specific problems for determination of bacterial diversity in micro-samples.

Standard cultivation methods are widely reported to underestimate both bacterial density and diversity (Weisburg *et al.*, 1991). However, given that root exudates are thought to underpin the proliferation of bacteria in the rhizosphere, and that simple sugars, and other compounds common to most cultivation medias are reported to be the main constituents of exudates, it is likely that a greater proportion of bacteria in the rhizosphere are culturable when compared with bulk soil. Therefore, with respect to the rhizosphere, it is assumed that culture-related bias leads to less deviation from the real trends in community structure than would be apparent in more oligotrophic environments. In this sense it is worth emphasising that in the rhizosphere, culture-dependent techniques may provide insights into microbial ecology that are currently not possible with molecular-based approaches.

It is widely recognised that for bacteria inhabiting the soil/rhizosphere it is currently not possible to measure asymptotic richness (absolute richness) due to the number of samples that would be need to be analysed to observe all species. Therefore, asymptotic richness is inferred in a qualitative manner, using a range of techniques such as rarefaction (Colwell *et al.*, 2004), or richness/diversity estimators (Magurran, 2004). As the number of individuals in a sample may vary, sample-based diversity analyses are technically a measure of the species density rather than species richness. For this

[14] It should be noted that these issues are not such a problem when research questions are focussed towards specific groups of bacteria for which target gene copy numbers are known.

[15] When DGGE is performed on DNA sequences from within the 16S rRNA gene, the relative band intensity is not indicative of the relative abundance of different bacterial types as different bacterial species may contain different copy numbers of the 16S rRNA gene (Klappenbach *et al.*, 2000).

reason, in molecular studies, it is standard protocol to extract DNA from bacterial communities present in one gram of soil and then standardise the concentration of bacterial DNA added to a PCR. It is assumed that this process enables taxonomic richness to be assessed at equal densities of bacteria such that diversity can be compared between treatments at equal numbers of replicates. For micro-samples, however, low concentrations of bacterial DNA present an obstacle to the standardisation of DNA concentrations between samples. Therefore, given that bacterial density has been shown to be heterogeneous at the micro-spatial-scale, an alternative approach to sample-based comparisons is necessary. This is not a problem provided that individual bacteria can be enumerated and identified. Culturing enables the numbers of bacteria to be counted, and by fingerprinting each colony it is possible to identify both the richness and evenness of a sample. Given that micro-samples contain low bacterial densities this approach is feasible and allows diversity to be compared on an individual basis.

Individual-based diversity comparisons were successfully demonstrated in Chapter five using micro-samples taken from soil, and the root apex and base of four and six day old plants. By pooling root samples within plant age categories, individual-based rarefaction curves revealed that rhizosphere bacterial diversity decreased between four and six days after planting. This finding is in agreement with molecular-studies performed at a greater spatial-scale that demonstrated decreased bacterial diversity in the rhizosphere when compared with root-free soil (Marilley *et al.*, 1998; Marilley & Aragno, 1999). By pooling plant age categories within zones, no significant differences in diversity were observed; however, the data suggested a potential trend in bacterial diversity following the order bulk soil > apical region > basal region. This decrease in diversity with from the source community (bulk soil) through root zones of increasing age is a trend that is not currently reported in the literature. However, this may reflect a root mediated selection of rhizosphere competitive species, and deserves further investigation. Undoubtedly, advances in technology will facilitate richness, and the population sizes of different bacterial types to be determined in micro-samples without the necessity to rely on sample cultivation. However, currently the approach outlined above, is the most effective for diversity analysis (i.e. valid comparisons of richness) in micro-samples.

These methodological problems are less of an issue when concerning other community attributes such as composition in isolation. For example, if the method were to be used

to probe for bacterial species that commonly dominate features such as sites of pathogen infection, molecular fingerprinting techniques are likely to be highly effective. Nevertheless, given that the results of the ERIC-PCR fingerprinting (Chapter 5) revealed that less than 5 % of bacterial OTU were present in more than one plant/soil replicate within the treatment combinations (zones within plant age categories), the sampling effort that would be necessary to observe similar species within similar habitats may be very considerable. Therefore, it is likely that such investigations will need to discriminate between comparable groups at low taxonomic resolution or broad functional groups.

With regard to the link between community structure and function, a range of novel and more conventional techniques may be adapted for analysis of micro-samples. All of these techniques discriminate between active and inactive populations; however, some enable activity to be linked with specific substrates. Recent improvements in RNA and DNA co-extraction may enable general active populations to be assessed and are likely to be appropriate for analysis of micro-samples (Griffiths *et al.*, 2000). This would enable detailed investigations of active bacterial richness using community fingerprinting methods such as DGGE, and/or gene expression using microarrays (Dumont & Murrell, 2005; Sessitsch *et al.*, 2006). Another method for assessing generally active communities relies on the incorporation of 5-bromo-2-deoxyuridine (BrdU), a synthetic analogue of thymidine, into newly synthesised DNA. BrdU-labelled DNA can then be separated from non-labelled DNA using BrdU-specific antibodies and analysed using molecular methods. It is unlikely however that this method would be appropriate for analysis of micro-samples as the BrdU must be applied directly to the sample *in-situ* which would influence the local environment and potentially alter the structure of the active community. In addition, it is likely that such low numbers of bacteria would create difficulties in separating labelled from non-labelled DNA.

Methods that facilitate the determination of populations that are actively catabolising specific compounds within their environment involve the use of isotope tracers. One example is SIP (Manefield *et al.*, 2002a; Manefield *et al.*, 2002b; Dumont & Murrell, 2005); however, as mentioned in Chapter nine, this approach may also be poorly suited to analysis of micro-samples as relatively high concentrations of DNA/RNA are required to visualise labelled and unlabelled fractions. Nevertheless, the

amount of labelled nucleotide that is required for PCR detection is theoretically one molecule; therefore, it may be possible to extract 'invisible' fractions by reference to a labelled-nucleotide marker in a control gradient (Dumont & Murrell, 2005). This approach is rather important and deserves further attention. Other methods facilitating the investigation of links between active bacterial populations and specific substrates include FISH-MAR and isotope arrays; however, these methods rely on the incorporation of radioactive isotopes and are thus limited to elements for which these are available. In addition, they depend on rRNA hybridisation probes or arrays; therefore, *a priori* knowledge of the studied organisms is required. An alternative technique that has the potential to determine which populations are involved in catabolising specific compounds is SIMS. As demonstrated in Chapter nine and by other workers (Cliff *et al.*, 2002; Cliff *et al.*, 2005; Herrmann *et al.*, 2007), isotope enrichment may be observed within single bacterial cells using a SIMS instrument capable of high mass and spatial resolution imaging (e.g. Cameca NanoSIMS 50™). However, alone this information gives no insight into the phylogeny of labelled bacteria. With method development Kuypers & Jorgensen (2007) suggest that this may be possible by replacing the fluorescent oligonucleotide probes used for FISH with isotopically labelled (stable or radioactive) or halogenated probes. Nonetheless, as with FISH this approach would only facilitate probe-targeted organisms to be identified. The genetic diversity of non-targeted organisms would remain unknown. A particularly interesting future development may be to combine SIMS with isotope arrays, such that carbon, nitrogen and phosphorus isotope enrichment could be detected simultaneously.

10.4. How do rhizosphere bacteria interact with their environment?

It is worth beginning this section by reemphasising that soil is a characteristically heterogeneous environment that is composed of a vast array of microhabitats that may or may not be occupied by bacteria (Chapter 1). When a root enters this environment, its presence and activities induce environmental changes that are complex but exhibit some degree of spatiotemporal organisation. For example, the rhizosphere surrounding the root apices receives a more or less constant supply of root exudates, whereas at the root base exudation is so low that it cannot be detected using current techniques (Chapter 7). For this reason, investigations concerning the interactions between rhizosphere bacteria and their environment must be undertaken at relevant

spatiotemporal scales. The novel micro-sampling approach reported in this thesis enables bacterial samples to be taken at multiple spatial and temporal scales; however, as will be discussed below, current technology commonly limits the measurement of environmental variables at similar scales.

The most widely reported interaction between rhizosphere bacteria and their environment is the link between rhizodeposition and bacterial density. Root exudates comprise the largest fraction in the pool of rhizodeposits (Meharg & Killham, 1988) and are commonly implicated as the main driver of the rhizosphere effect (Lynch & Whipps, 1990; Marschner *et al.*, 2004); thus, patterns of bacterial density have generally been attributed to corresponding sites of exudation (McDougal & Rovira, 1970; McCully & Canny, 1985; Lynch & Whipps, 1990; Norton *et al.*, 1990). However, as demonstrated in this thesis (Chapters 5, 6 and 7) and by other authors (Maloney *et al.*, 1997; Semenov *et al.*, 1999; van Bruggen *et al.*, 2000; Zelenev *et al.*, 2000), sites of intense root exudation (root apex) are not spatially correlated with areas of the root that are densely populated with bacteria (root base). Clearly then, the interaction between root exudation and rhizosphere bacterial densities is complex.

Perhaps the most obvious factor that may contribute to the presence of low bacterial densities at the root apex is root growth. Watt *et al.* (2003) reported greater densities of bacteria at the root apex of slow-growing when compared with more rapidly growing roots. However, in Chapter six I observed no significant relationship between root growth rate and bacterial densities at the root apex of *B. napus* plants grown under identical conditions. This suggests that for bacteria to proliferate at the root apex, root growth rates must be considerably slower than those observed. To further investigate this interaction it may be fruitful to compare bacterial densities at the root apex of mutant plants that differ greatly in their relative rates of root growth. Nonetheless, differing rates of root growth are unlikely to directly influence bacterial densities in older root regions; therefore, as suggested by Zelenev *et al.* (2000) it seems apparent that other processes besides exudation and root growth contribute towards rhizosphere bacterial distribution patterns.

In Chapter seven, I emphasised the fact that available carbon pools in the rhizosphere also derive from sources other than exudation and that for this reason it may be more appropriate to investigate links between rhizosphere bacterial densities and available

carbon. My attempts to develop a bioluminometric assay for available carbon were unsuccessful; however, as discussed previously, this may have been related to the way in which the bioreporter cells were starved prior to application. Nonetheless, the approach taken to identify the best set of conditions for available carbon reporting was novel and provided a good insight into the bioluminescent behaviour of the bioreporter cells to a range of experimental manipulations. Considering that existing methods fail to discriminate between soluble and bioavailable carbon concentrations and provide data at a resolution that approximates the spatial scale of a microhabitat, it is important that the bioluminometric assay be retested with the modified starvation conditions suggested in Chapter seven despite the criticisms discussed therein. Should this prove successful, the new method would provide important information that is currently not available; however, current evidence suggests that the correspondence between areas of the rhizosphere that exhibit high substrate availability and those that are densely populated with bacteria is poor (Semenov *et al.*, 1999). Despite this, Semenov *et al.* (1999) reported that both variables exhibited wave-like fluctuations over time, which they hypothesised to reflect bacterial growth and death cycles in response to the exuding root apex. In a follow-on paper they tested this hypothesis using a simulation model in which the growth and death rates of rhizosphere bacteria were determined by the availability of substrates (Zelenev *et al.*, 2000). Root exudation formed the main substrate input; however, despite losses due to respiration this carbon was recycled through subsequent bacterial growth and death cycles. In addition, the effect of different initial background levels of substrate was also simulated using the model. Their results indicated that these interactions could indeed explain the observed wave-like fluctuations and suggested that greater initial background levels of substrate led to higher amplitude fluctuations. However, their model failed to predict a general increase in bacterial density with increasing root age. This may be related to their assumption that non-exudate carbon (background substrate level) was equally available throughout the rhizosphere; however in reality this is not likely be the case.

It has been hypothesised that rhizosphere microorganisms accelerate the decomposition of soil organic matter (SOM) and also stimulate the dissolution of sparingly soluble minerals from the soil solid phase by mechanisms that are similar to those proposed for plants (De Nobili *et al.*, 2001; Jones *et al.*, 2004). This phenomenon is commonly referred to as priming, and has been observed following exposure to low concentrations of root exudates (De Nobili *et al.*, 2001). The influence of priming effects on

rhizosphere bacterial distribution patterns are yet to be explored; however, over time mineralised soil organic carbon may accumulate in the bacterial biomass and constitute a significant resource for communities inhabiting root regions that receive relatively small inputs from rhizodeposition when compared with those associated with root apices. Interestingly, Cheng *et al.* (1996) found that carbon was not a factor limiting rhizosphere bacterial respiration. They, and other workers, hypothesised that in fact nitrogen is a more important factor limiting rhizosphere microbial growth and suggested that increased SOM mineralization following root-induced priming is a strategy that benefits rhizosphere microorganisms through supplementing their nitrogen demands (Helal & Sauerbeck, 1986; Cheng *et al.*, 1996). However, current evidence indicates that plants also benefit from these priming effects through increased mineral nitrogen uptake (Brimecombe *et al.*, 1998; Brimecombe *et al.*, 1999), although total capture of mineralised resources would lead to a decrease in microbial mineralization and thus fail to benefit the plant in the long-term (Schimel *et al.*, 1989; Ehrenfeld *et al.*, 1997; Bottner *et al.*, 1999).

The importance of rhizosphere microorganism-mediated mineralization of SOM to plant nutrition is poorly characterised; however, it may be particularly significant in older root regions where nutrient status is likely to have been depleted by the passing root apex. As emphasised in Chapter one, most studies concerning nutrient availability along the longitudinal axes of roots have been conducted in sterile solution culture. Therefore, current reported observations have ignored the importance of the interactions outlined above. Rhizosphere priming effects may also play a role in root architecture. For instance hotspots of mineralised nutrient may correspond with sites of lateral root formation, as root apices exhibit high nutrient demands as a consequence of meristematic activity and cell elongation, and are thought to satisfy the majority of this demand independently of other root regions (Bloom *et al.*, 2002).

Together with the micro-sampling technique the methods explored in this thesis offer exciting opportunities for investigating the influence of root-induced priming on subsequent plant and microbial assimilation of mineralised nutrients and rhizosphere bacterial distribution patterns. A better understanding of these interactions at the micro-scale is particularly important becasue the incorporation of mineralised nutrients into plant cells, and carbon and other nutritients into microbial cells are processes that are likely to reflect the patchy distribution of SOM and the structure and function of

rhizosphere bacterial communities. In addition, mineralization rates have also been shown to be influenced by the availability of relatively simple substrates. For example, when exposed to SOM and root exudates, Kuzyakov (2002) observed that SOM mineralization was decreased due to preferential microbial utilisation of the more easily available rhizodeposits. Therefore, SOM mineralization rates in the rhizosphere may be inversely proportional to readily available carbon concentrations. These interactions may be investigated by incorporating $^{13}C/^{15}N$-labelled organic matter into soil used to grow plants in a rhizotron system. By continuously labelling plants with ^{14}C it would be possible to distinguish between root-derived and mineralised SOM carbon incorporated into rhizosphere bacteria. Micro-samples taken from different root regions may then be analysed for isotope enrichment using either SIMS (Chapter 9) or SIP-density gradient centrifugation. In addition, plant uptake of ^{15}N-labelled compounds could be detected using either SIMS or continuous flow isotope ratio mass spectrometry (CF-IRMS). Needless to say however, such an approach would require further method development. An alternative is to ignore the determination of nutrient sources and concentrate on linking bacterial community attributes with nutrient concentrations using a combination of micro-sampling and ion-selective microelectrodes. This would not enable carbon fluxes to be determined; however, given that current evidence suggests that rhizosphere bacterial growth is also linked with nitrogen availability and that ammonium and nitrate-selective microelectrodes are readily available, this approach would facilitate a range of interesting interactions to be explored.

In Chapter eight, I demonstrated this approach using pH microelectrodes, and although the work did not proceed beyond the method development stage, an operational protocol is now available for future work. This is an important achievement and is the first reliable approach that enables bacterial communities to be linked with chemical conditions at the microhabitat scale.

Interestingly, the pH microelectrode measurements revealed that rhizoplane pH can vary by up to one unit between positions just one millimetre apart. Although this level of heterogeneity has been speculated, actual observations have not been previously reported. This finding is important and highlights the appropriateness of investigating links between bacterial communities and their environment at a sub-millimetre scale. The causes of these pH changes are unknown; however, from the perspective of rhizosphere bacteria, low pH may result from high respiratory activity or ion uptake.

Alternatively, acidification may occur as a result of localised plant uptake of particular nutrient ions such as ammonium. Assuming that regions of the rhizosphere associated with more mature root portions will be depleted of many ions as a consequence of uptake by the passing root apex, rhizosphere microorganisms may play a significant role in creating local hotspots of available nutrients. Examples of this are ammonium mineralization from SOM or deposition by bacterial-feeding nematodes and protozoa (Griffiths, 1994).

Another interesting aspect of rhizosphere pH is its effect on bacterial communities. Each bacterial species has a pH range within which growth is possible and usually has a defined pH optimum. However, regardless of the extracellular pH at which the growth of a particular species is optimal, the intracellular pH remains near neutrality. For this reason, most species exhibit optimum growth close to neutrality (Madigan *et al.*, 2000). At the global scale, Fierer and Jackson (2006) demonstrated that the diversity and richness of bacterial communities from 98 soil samples taken from North and South America could be largely explained by soil pH (r^2 = 0.70 and r^2 = 0.58, respectively) with a trend of decreasing diversity with decreasing pH. Given that pH is a major factor influencing the availability of a wide range of nutrient ions, the chemical composition of rhizosphere microhabitats is likely to be equally heterogeneous at the micro-spatial-scale. A diverse range of ionophores are commercially available and can be used to construct single or multiple barrelled microelectrodes. Used in combination with the micro-sampling technique these will facilitate a better understanding of how bacterial communities interact with their environment at an appropriate spatial scale.

10.5. Conclusions

The activities of bacteria are greatly affected by the biological, physical and chemical conditions that characterise their environment. A better understanding of these interactions will help us to explain bacterial distribution patterns and facilitate the development of strategies for manipulating bacterial communities for environmental and/or commercial gain. With regards to the rhizosphere, this may be directed towards improving agricultural crop yields; however, in a wider context, such strategies could be targeted at managing biological diversity to evade adverse consequences of human activity and climate change.

The work conducted throughout the course of this PhD has provided a set of methods that will enable for the first time, the interactions between surface-associated bacteria and their environment to be investigated at a micro-spatial-scale. The results collected throughout their development and application have demonstrated the appropriateness of this scale for such investigations and provided a unique insight into the spatial heterogeneity of rhizoplane bacterial diversity and pH. The door to bacterial microhabitats has been opened, but the room remains to be lit.

REFERENCES

Abadia J, Lopez-Millan AF, Rombola A, Abadia A. 2002. Organic acids and Fe deficiency: A review. *Plant and Soil* **241:** 75-86.

Acinas SG, Marcelino LA, Klepac-Ceraj V, Polz MF. 2004. Divergence and redundancy of 16R rRNA sequences in genomes with multiple RNA operons. *Journal of Bacteriology* **186:** 2629-2635.

Adamczyk J, Hesselsoe M, Iversen N, Horn M, Lehner A, Nielsen PH, Schloter M, Roslev P, Wagner M. 2003. The isotope array, a new tool that employs substrate-mediated labelling of rRNA for determination of microbial community structure and function. *Applied and Environmental Microbiology* **69:** 6875-6887.

Amann R, Snaidr J, Wagner M, Ludwig W, Schleifer KH. 1996. *In situ* visualization of high genetic diversity in a natural microbial community. *Journal of Bacteriology* **178:** 3496-3500.

Amellal N, Bartoli F, Villemin G, Talouizte A, Heulin T. 1999. Effects of inoculation of EPS-producing *pantoea agglomerans* on wheat rhizosphere aggregation. *Plant and Soil* **211:** 93-101.

Amellal N, Burtin G, Bartoli F, Heulin T. 1998. Colonization of wheat roots by an exopolysaccharide-producing *pantoea agglomerans* strain and its effect on rhizosphere soil aggregation. *Applied and Environmental Microbiology* **64:** 3740-3747.

Amin-Hanjani S, Meikle A, Glover LA, Prosser JI, Killham K. 1993. Plasmid and chromosomally encoded luminescence marker systems for detection of *Pseudomonas-fluorescens* in soil. *Molecular Ecology* **2:** 47-54.

Ammann D. 1986. Ion-selective microelectrodes - Principles, design and applications. Berlin: Springer-Verlag.

Andrade P, Ferreres F, Gil MI, Tomas-Barberan FA. 1997. Determination of phenolic compounds in honeys with different floral origin by capillary zone electrophoresis. *Food Chemistry* **60:** 79-84.

Andre S, Neyra M, Duponnois R. 2003. Arbuscular mycorrhizal symbiosis changes the colonization pattern of *Acacia tortilis* spp. *Raddiana* rhizosphere by two strains of rhizobia. *Microbial Ecology* **45:** 137-144.

Anraku Y, Gennis RB. 1987. The aerobic respiratory-chain of *Escherichia-coli*. *Trends in Biochemical Sciences* **12:** 262-266.

Baas-Becking LGM. 1934. *Giobiologie of inleiding to de milieukunde*. The Hague: van Stockkum & Zoon.

Barber DA. 1967. Effect of micro-organisms on absorption of inorganic nutrients by intact plants. I. Apparatus and culture technique. *Journal of Experimental Botany* **18:** 163-169.

Bardgett RD. 2005. *The biology of soil: A community and ecosystem approach.* Oxford: Oxford University Press.

Bardgett RD, Streeter TC, Bol R. 2003. Soil microbes compete effectively with plants for organic-nitrogen inputs to temperate grasslands. *Ecology* **84:** 1277-1287.

Bauer WD, Mathesius U. 2004. Plant responses to bacterial quorum sensing signals. *Current Opinion in Plant Biology* **7:** 429-433.

Beauchamp CJ, Kloepper JW, Lemke PA. 1993. Luminometric analyses of plant-root colonization by bioluminescent pseudomonads. *Canadian Journal of Microbiology* **39:** 434-441.

Bengough AG, Mackenzie CJ. 1994. Simultaneous measurement of root force and elongation for seedling pea roots. *Journal of Experimental Botany* **45:** 95-102.

Bengough AG, McKenzie BM. 1997. Sloughing of root cap cells decreases the frictional resistance to maize (*Zea mays* L) root growth. *Journal of Experimental Botany* **48:** 885-893.

Bennett RA, Lynch JM. 1981. Bacterial-growth and development in the rhizosphere of gnotobiotic cereal plants. *Journal of General Microbiology* **125:** 95-102.

Biggs DR, Greenway RM, McGregor PG. 1994. An antimony-silver silver-chloride electrode system for measuring pH in insect gut contents. *Entomologia Experimentalis et Applicata* **73:** 31-37.

Bloemberg GV, Lugtenberg BJJ. 2001. Molecular basis of plant growth promotion and biocontrol by rhizobacteria. *Current Opinion in Plant Biology* **4:** 343-350.

Bloom AJ, Meyerhoff PA, Taylor AR, Rost TL. 2002. Root development and absorption of ammonium and nitrate from the rhizosphere. *Journal of Plant Growth Regulation* **21:** 416-431.

Bockheim JG, Gennadiyev AN, Hammer RD, Tandarich JP. 2005. Historical development of key concepts in pedology. *Geoderma* **124:** 23-36.

Borneman J. 1999. Culture-independent identification of microorganisms that respond to specified stimuli. *Applied and Environmental Microbiology* **65:** 3398-3400.

Bottner P, Pansu M, Sallih Z. 1999. Modelling the effect of active roots on soil organic matter turnover. *Plant and Soil* **216:** 15-25.

Bouché MB 1975. Action de la faune sur les états de la matière organique dans les écosystèmes. *In:* G. Kilbertus, O. Reisinger, A. MoureyJ. A. Cancela da Fonseca eds. *Humification et biodégradation.* Sarreguemines: Pierron, 157-168.

Brady NC, Weil RR. 1996. *The nature and properties of soils.* New York, NY.: Macmillian Publishing Co.

Brandao PFB, Clapp JP, Bull AT. 2002. Discrimination and taxonomy of geographically diverse strains of nitrile-metabolizing actinomycetes using chemometric and molecular sequencing techniques. *Environmental Microbiology* **4:** 262-276.

Brimecombe MJ, De Leij F, Lynch JM. 1998. Effect of genetically modified *Pseudomonas fluorescens* strains on the uptake of nitrogen by pea from N-15 enriched organic residues. *Letters in Applied Microbiology* **26:** 155-160.

Brimecombe MJ, De Leij F, Lynch JM. 1999. Effect of introduced *Pseudomonas fluorescens* strains on the uptake of nitrogen by wheat from N-15-enriched organic residues. *World Journal of Microbiology & Biotechnology* **15:** 417-423.

Broughton LC, Gross KL. 2000. Patterns of diversity in plant and soil microbial communities along a productivity gradient in a Michigan old-field. *Oecologia* **125:** 420-427.

Brown JH, Lomolino MV. 1998. *Biogeography.* Sunderland: Sinauer.

Bruand A, Cousin I, Nicoullaud B, Duval O, Begon JC. 1996. Backscattered electron scanning images of soil porosity for analyzing soil compaction around roots. *Soil Science Society of America Journal* **60:** 895-901.

Cambell R, Greves M. 1990. Anatomy and community structure of the rhizosphere. *In:* J. M. Lynch *ed. The Rhizosphere.* Chichester: Wiley & Sons, 11-34.

Carrillo AE, Li CY, Bashan Y. 2002. Increased acidification in the rhizosphere of cactus seedlings induced by *Azospirillum brasilense. Naturwissenschaften* **89:** 428-432.

Carroll NM, Adamson PO, Khravi N. 1999. Elimination of bacterial DNA from Taq DNA polymerases by restriction endonuclease digestion. *Journal of Clinical Microbiology* **37:** 3402-3404.

Catt JA, King DW, Weir AH. 1975. *The Soils of Woburn Experimental Farm. I. Great Hill, Road Piece and Butt Close. Rothamsted Report for 1974, Part 2.* Lawes Agricultural Trust, Harpenden, 5-28.

Chan KY, Mead JA, Roberts WP. 1987. Poor early growth of wheat under direct drilling. *Australian Journal of Agricultural Research* **38:** 791-800.

Cheng WX, Zhang QL, Coleman DC, Carroll CR, Hoffman CA. 1996. Is available carbon limiting microbial respiration in the rhizosphere? *Soil Biology & Biochemistry* **28:** 1283-1288.

Chenu C, Stotzky G. 2002. Interactions between microorganisms and soil particles: An overview. *In:* P. M. Huang, N. Bollag, N. Senesi *eds. Interactions between Soil Particles and Microorganisms. Impact on the Terrestrial Ecosystem.* New York: Wiley, 3-40.

Chin-A-Woeng TFC, De Priester W, van der Bij AJ, Lugtenberg BJJ. 1997. Description of the colonization of a gnotobiotic tomato rhizosphere by *Pseudomonas fluorescens* biocontrol strain WCS365, using scanning electron microscopy. *Molecular Plant-Microbe Interactions* **10:** 79-86.

Clark FE. 1949. Soil microorganisms and plant roots. *Advances in Agronomy* **1:** 241-288.

Clark IM, Mendum TA, Hirsch PR. 2002. The influence of the symbiotic plasmid Prl1ji on the distribution of GM rhizobia in soil and crop rhizospheres, and implications for gene flow. *Antonie Van Leeuwenhoek International Journal of General and Molecular Microbiology* **81:** 607-616.

Clarkson DT, Sanderson J. 1978. Sites of absorption and translocation of iron in barley roots - Tracer and microautoradiographic studies. *Plant Physiology* **61:** 731-736.

Clarkson DT, Sanderson J, Scattergood CB. 1978. Influence of phosphate-stress on phosphate absorption and translocation by various parts of root-system of *Hordeum-vulgare* L (barley). *Planta* **139:** 47-53.

Clemente EP, Schaefer C, Novais RF, Viana JH, Barros NF. 2005. Soil compaction around *Eucalyptus grandis* roots: A micromorphological study. *Australian Journal of Soil Research* **43:** 139-146.

Cliff JB, Gaspar DJ, Bottomley PJ, Myrold DD. 2002. Exploration of inorganic C and N assimilation by soil microbes with time-of-flight secondary ion mass spectrometry. *Applied and Environmental Microbiology* **68:** 4067-4073.

Cliff JB, Gaspar DJ, Bottomley PJ, Myrold DD. 2005. Microbial C and N assimilation in soils and model systems as revealed by ToF-SIMS. *Geochimica et Cosmochimica Acta* **69:** A527-A527.

Coffin RB, Velinsky DJ, Devereux R, Price WA, Cifuentes LA. 1990. Stable carbon isotope analysis of nucleic acids to trace sources of dissolved substrates used by estuarine bacteria. *Applied and Environmental Microbiology.* **56:** 2012-2020.

Colmer TD, Bloom AJ. 1998. A Comparison of NH_4^+ and NO_3^- net fluxes along roots of rice and maize. *Plant Cell and Environment* **21:** 240-246.

Colwell RK. 2005. *EstimateS: Statistical estimation of species richness and shared species from samples*. Version 7.5. User's guide and application published at: http://purl.oclc.org/estimates.in.

Colwell RK, Mao CX, Chang J. 2004. Interpolating, extrapolating, and comparing incidence-based species accumulation curves. *Ecology* **85:** 2717-2727.

Corless CE, Guiver M, Borrow R, Edwards-Jones V, Kaczmarski EB, Fox AJ. 2000. Contamination and sensitivity issues with a real-time universal 16S rRNA PCR. *Journal of Clinical Microbiology* **38:** 1747-1752.

Costacurta A, Vanderleyden J. 1995. Synthesis of phytohormones by plant-associated bacteria. *Critical Reviews in Microbiology* **21:** 1-18.

Crosby LD, Criddle CS. 2003. Understanding bias in microbial community analysis techniques due to *rrn* operon copy number heterogeneity. *Biotechniques* **34:** 790-798.

Curl EA, Truelove B. 1986. *The Rhizosphere*. Berlin, Heidelberg, New York, Tokyo: Springer-Verlag.

Daane LL, Molina JA, Berry EC, Sadowsky MJ. 1996. Influence of earthworm activity on gene transfer from *Pseudomonas fluorescens* to indigenous soil bacteria. *Applied and Environmental Microbiology*. **62:** 515-521.

Dakora FD, Phillips DA. 2002. Root exudates as mediators of mineral acquisition in low-nutrient environments. *Plant and Soil* **245:** 35-47.

Darrah P, Roose T 2001. Modelling the rhizosphere. *In:* Pinton R, Varanini Z, Nannipieri P, *eds. The rhizosphere - Biochemistry and organic substances at the soil-plant interface*. New York: Marcel Dekker Inc., 327-372.

Darrah PR. 1991a. Models of the rhizosphere. 1. Microbial-population dynamics around a root releasing soluble and insoluble carbon. *Plant and Soil* **133:** 187-199.

Darrah PR. 1991b. Models of the rhizosphere. 2. A quasi 3-dimensional simulation of the microbial-population dynamics around a growing root releasing soluble exudates. *Plant and Soil* **138:** 147-158.

Darwent MJ, Paterson E, McDonald AJS, Tomos AD. 2003. Biosensor reporting of root exudation from *Hordeum vulgare* in relation to shoot nitrate concentration. *Journal of Experimental Botany* **54:** 325-334.

Darwin CA, Darwin F. 1880. *The power of movement in plants*. London: John Murray.

De Candolle AP. 1820. *Essai elementaire de geographie botanique*. Paris: F.G. Levrault.

De Nobili M, Contin M, Mondini C, Brookes PC. 2001. Soil microbial biomass is triggered into activity by trace amounts of substrate. *Soil Biology & Biochemistry* **33:** 1163-1170.

de Weert S, Dekkers LC, Bitter W, Tuinman S, Wijfjes AHM, van Boxtel R, Lugtenberg BJJ. 2006. The two-component Colr/s system of *Pseudomonas fluorescens* WCS365 plays a role in rhizosphere competence through maintaining the structure and function of the outer membrane. *FEMS Microbiology Ecology* **58:** 205-213.

Dekkers LC, Phoelich CC, van der Fits L, Lugtenberg BJJ. 1998a. A site-specific recombinase is required for competitive root colonization by *Pseudomonas fluorescens* WCS365. *Proceedings of the National Academy of Sciences of the United States of America* **95:** 7051-7056.

Dekkers LC, van der Bij AJ, Mulders IHM, Phoelich CC, Wentwoord RAR, Glandorf DCM, Wijffelman CA, Lugtenberg BJJ. 1998b. Role of the O-antigen of lipopolysaccharide, and possible roles of growth rate and of Nadh:ubiquinone oxidoreductase (*nuo*) in competitive tomato root-tip colonization by *Pseudomonas fluorescens* WCS365. *Molecular Plant-Microbe Interactions* **11:** 763-771.

Deweger LA, Vandervlugt CIM, Wijfjes AHM, Bakker P, Schippers B, Lugtenberg B. 1987. Flagella of a plant-growth-stimulating *Pseudomonas-fluorescens* strain are required for colonization of potato roots. *Journal of Bacteriology* **169:** 2769-2773.

Dexter AR. 1987. Compression of soil around roots. *Plant and Soil* **97:** 401-406.

Dilkes NB, Jones DL, Farrar J. 2004. Temporal dynamics of carbon partitioning and rhizodeposition in wheat. *Plant Physiology* **134:** 706-715.

Dollard MA, Billard P. 2003. Whole-cell bacterial sensors for the monitoring of phosphate bioavailability. *Journal of Microbiological Methods* **55:** 221-229.

Doussan C, Pages L, Pierret A. 2003. Soil exploration and resource acquisition by plant roots: An architectural and modelling point of view. *Agronomie* **23:** 419-431.

Duineveld BM, Kowalchuk GA, Keijzer A, van Elsas JD, van Veen JA. 2001. Analysis of bacterial communities in the rhizosphere of chrysanthemum via denaturing gradient gel electrophoresis of PCR-amplified 16S rRNA as well as DNA fragments coding for 16S rRNA. *Applied and Environmental Microbiology* **67:** 172-178.

Duineveld BM, van Veen JA. 1999. The number of bacteria in the rhizosphere during plant development: Relating colony-forming units to different reference units. *Biology and Fertility of Soils* **28:** 285-291.

Dumont MG, Murrell JC. 2005. Stable isotope probing - Linking microbial identity to function. *Nature Reviews Microbiology* **3:** 499-504.

Dykhuizen DE. 1998. Santa Rosalia revisited: Why are there so many species of bacteria? *Antonie van Leeuwenhoek International Journal of General and Molecular Microbiology* **73:** 25-33.

Ehrenfeld JG, Parsons WFJ, Han XG, Parmelee RW, Zhu WX. 1997. Live and dead roots in forest soil horizons: Contrasting effects on nitrogen dynamics. *Ecology* **78:** 348-362.

Elliott ML, Guertal EA, Des Jardin EA, Skipper HD. 2003. Effect of nitrogen rate and root-zone mix on rhizosphere bacterial populations and root mass in creeping bentgrass putting greens. *Biology and Fertility of Soils* **37:** 348-354.

Esau K. 1977. *Anatomy of Seed Plants*. New York: John Wiley and Sons.

Farley RA, Fitter AH. 1999. The responses of seven co-occurring woodland herbaceous perennials to localized nutrient-rich patches. *Journal of Ecology* **87:** 849-859.

Farrar J, Hawes M, Jones D, Lindow S. 2003. How roots control the flux of carbon to the rhizosphere. *Ecology* **84:** 827-837.

Fenchel T, Finlay BJ. 2003. Is microbial diversity fundamentally different from biodiversity of larger animals and plants? *European Journal of Protistology* **39:** 486-490.

Fenchel T, Finlay BJ. 2004. The ubiquity of small species: patterns of local and global diversity. *Bioscience* **54:** 777-784.

Ferguson IB, Clarkson DT. 1975. Ion-transport and endodermal suberization in roots of *Zea-mays*. *New Phytologist* **75:** 69-79.

Ferguson IB, Clarkson DT. 1976. Simultaneous uptake and translocation of magnesium and calcium in barley (*Hordeum-vulgare*-L) roots. *Planta* **128:** 267-269.

Ferre F. 1992. Quantitative or semi-quantitative PCR: Reality versus myth. *PCR Methods and Applications* **2:** 1-9.

Fierer N, Jackson RB. 2006. The diversity and biogeography of soil bacterial communities. *Proceedings of the National Academy of Sciences of the United States of America* **103:** 626-631.

Filion M, St-Arnaud M, Fortin JA. 1999. Direct interaction between the arbuscular mycorrhizal fungus *Glomus intraradices* and different rhizosphere microorganisms. *New Phytologist* **141:** 525-533.

Finlay BJ. 2002. Global dispersal of free-living microbial eukaryote species. *Science* **296:** 1061-1063.

Finlay BJ, Clarke KJ. 1999. Ubiquitous dispersal of microbial species. *Nature* **400:** 828-828.

Finlay BJ, Fenchel T. 2004. Cosmopolitan metapopulations of free-living microbial eukaryotes. *Protist* **155:** 237-244.

Fitter AH. 2005. Darkness visible: Reflections on underground ecology. *Journal of Ecology* **93:** 231-243.

Floyd RA, Ohlrogge AJ. 1970. Gel formation on nodal root surfaces of *Zea-mays*. 1. Investigation of gels composition. *Plant and Soil* **33:** 331-343.

Foster RC. 1982. The fine-structure of epidermal-cell mucilages of roots. *New Phytologist* **91:** 727-740.

Foster RC. 1986. The ultrastructure of the rhizoplane and rhizosphere. *Annual Review of Phytopathology* **24:** 211-234.

Foster RC. 1988. Microenvironments of soil-microorganisms. *Biology and Fertility of Soils* **6:** 189-203.

Gahoonia TS, Care D, Nielsen NE. 1997. Root hairs and phosphorus acquisition of wheat and barley cultivars. *Plant and Soil* **191:** 181-188.

Gamalero E, Lingua G, Giusy Capri F, Fusconi A, Berta G, Lemanceau P. 2004. Colonization pattern of primary tomato roots by *Pseudomonas fluorescens* A6ri characterized by dilution plating, flow cytometry, fluorescence, confocal and scanning electron microscopy. *FEMS Microbiology Ecology* **48:** 79-87.

Garbaye J. 1991. Biological interactions in the mycorrhizosphere. *Experientia* **47:** 370-375.

Garbaye J, Bowen GD. 1989. Ectomycorrhizal infection of *Pinus radiata* by *Rhizopogon luteolus* is stimulated by microorganisms naturally present in the mantle of ectomycorrhizas. *New Phytologist* **112:** 383-388.

Garnett TP, Shabala SN, Smethurst PJ, Newman IA. 2001. Simultaneous measurement of ammonium, nitrate and proton fluxes along the length of eucalypt roots. *Plant and Soil* **236:** 55-62.

Gevers D, Cohan FM, Lawrence JG, Spratt BG, Coenye T, Feil EJ, Stackebrandt E, van de Peer Y, Vandamme P, Thompson FL, Swings J. 2005. Re-evaluating prokaryotic species. *Nature Reviews Microbiology* **3:** 733-739.

Glockner FO, Zaichikov E, Belkova N, Denissova L, Pernthaler J, Pernthaler A, Amann R. 2000. Comparative 16S rRNA analysis of lake bacterioplankton reveals

globally distributed phylogenetic clusters including an abundant group of actinobacteria. *Applied and Environmental Microbiology* **66:** 5053-5065.

Gochnauer MB, Sealey LJ, McCully ME. 1990. Do detached root-cap cells influence bacteria associated with maize roots. *Plant Cell and Environment* **13:** 793-801.

Gottlein A, Hell U, Blasek R. 1996. A system for microscale tensiometry and lysimetry. *Geoderma* **69:** 147-156.

Gray ND, Hastings RC, Sheppard SK, Loughnane P, Lloyd D, McCarthy AJ, Head IM. 2003. Effects of soil improvement treatments on bacterial community structure and soil processes in an upland grassland soil. *FEMS Microbiology Ecology* **46:** 11-22.

Grayston SJ, Wang SQ, Campbell CD, Edwards AC. 1998. Selective influence of plant species on microbial diversity in the rhizosphere. *Soil Biology & Biochemistry* **30:** 369-378.

Green J, Bohannan BJM. 2006. Spatial scaling of microbial biodiversity. *Trends in Ecology & Evolution* **21:** 501-507.

Green JL, Holmes AJ, Westoby M, Oliver I, Briscoe D, Dangerfield M, Gillings M, Beattie AJ. 2004. Spatial scaling of microbial eukaryote diversity. *Nature* **432:** 747-750.

Griebler C, Mindl B, Slezak D. 2001. Combining DAPI and Sybr Green II for the enumeration of total bacterial numbers in aquatic sediments. *International Review of Hydrobiology* **86:** 453-465.

Griffiths BS. 1994. Microbial-feeding nematodes and protozoa in soil - Their effects on microbial activity and nitrogen mineralization in decomposition hotspots and the rhizosphere. *Plant and Soil* **164:** 25-33.

Griffiths BS, Bonkowski M, Dobson G, Caul S. 1999. Changes in soil microbial community structure in the presence of microbial-feeding nematodes and protozoa. *Pedobiologia* **43:** 297-304.

Griffiths BS, Ritz K, Wheatley R, Kuan HL, Boag B, Christensen S, Ekelund F, Sorensen SJ, Muller S, Bloem J. 2001. An examination of the biodiversity-ecosystem function relationship in arable soil microbial communities. *Soil Biology and Biochemistry* **33:** 1713-1722.

Griffiths BS, Welschen R, Vanarendonk J, Lambers H. 1992. The effect of nitrate-nitrogen supply on bacteria and bacterial-feeding fauna in the rhizosphere of different grass species. *Oecologia* **91:** 253-259.

Griffiths RI, Manefield M, Ostle N, McNamara N, O'Donnell AG, Bailey MJ, Whiteley AS. 2004. (CO_2)-C-13 pulse labelling of plants in tandem with stable isotope probing: Methodological considerations for examining microbial function in the rhizosphere. *Journal of Microbiological Methods* **58:** 119-129.

Griffiths RI, Whiteley AS, O'Donnell AG, Bailey MJ. 2000. Rapid method for coextraction of DNA and RNA from natural environments for analysis of ribosomal DNA- and rRNA-based microbial community composition. *Applied and Environmental Microbiology* **66:** 5488-5491.

Groot EP, Doyle JA, Nichol SA, Rost TL. 2004. Phylogenetic distribution and evolution of root apical meristem organization in dicotyledonous angiosperms. *International Journal of Plant Sciences* **165:** 97-105.

Grundmann GL, Debouzie D. 2000. Geostatistical analysis of the distribution of NH_4^+ and NO_2^--oxidizing bacteria and serotypes at the millimeter scale along a soil transect. FEMS Microbiology Ecology **34:** 57-62.

Grundmann GL, Normand P. 2000. Microscale diversity of the genus nitrobacter in soil on the basis of analysis of genes encoding rRNA. *Applied and Environmental Microbiology* **66:** 4543-4546.

Grundmann LG, Gourbiere F. 1999. A micro-sampling approach to improve the inventory of bacterial diversity in soil. *Applied Soil Ecology* **13:** 123-126.

Grunes DL, Ohno T, Huang JW, Kochian LV 1993. Effects of aluminium on magnesium, calcium, and potassium in wheat forages. *In:* Golf S, Dralle D, Vecchiet L, *eds. Magnesium.* London: John Libbey & Co.

Guerquin-Kern JL, Wu TD, Quintana C, Croisy A. 2005. Progress in analytical imaging of the cell by dynamic secondary ion mass spectrometry (SIMS microscopy). *Biochimica et Biophysica Acta-General Subjects* **1724:** 228-238.

Guinel FC, McCully ME. 1986. Some water-related physical-properties of maize root-cap mucilage. *Plant Cell and Environment* **9:** 657-666.

Gunawardena U, Hawes MC. 2002. Tissue specific localization of root infection by fungal pathogens: role of root border cells. *Molecular Plant-Microbe Interactions* **15:** 1128-1136.

Ha Y, Wang M. 2006. Capillary melt method for micro antimony oxide pH electrode. *Electroanalysis* **18:** 1121-1125.

Hall TA. 1999. Bioedit: A user-friendly biological sequence alignment editor and analysis program for Windows 95/98/NT. *Nucleic Acids Research Symposium Series* **41:** 95-98.

Hamamoto L, Hawes MC, Rost TL. 2006. The production and release of living root cap border cells is a function of root apical meristem type in dicotyledonous angiosperm plants. *Annals of Botany* **97:** 917-923.

Hanks RJ, Ashcroft GL. 1980. *Applied Soil Physics*. Berlin: Springer.

Haussling M, Leisen E, Marschner H, Romheld V. 1985. An improved method for non-destructive measurements of the pH at the root-soil interface (rhizosphere). *Journal of Plant Physiology* **117:** 371-375.

Hawes MC. 1990. Living plant cells released from the root cap: A regulator of microbial populations in the rhizosphere? *Plant and Soil* **129:** 19-27.

Hawes MC. 1991. Living plant cells released from the root cap: A regulator of microbial populations in the rhizosphere? *In:* Keiser DL, Cregan PB, *eds. The rhizosphere and plant growth.* Dordrecht: Kluwer academic publishers, 51-59.

Hawes MC, Bengough G, Cassab G, Ponce G. 2003. Root caps and rhizosphere. *Journal of Plant Growth Regulation* **21:** 352-367.

Hawes MC, Brigham LA, Wen F, Woo HH, Zhu Z. 1998. Function of root border cells in plant health: Pioneers in the rhizosphere. *Annual Review of Phytopathology* **36:** 311-327.

Hawes MC, Gunawardena U, Miyasaka S, Zhao XW. 2000. The role of root border cells in plant defense. *Trends in Plant Science* **5:** 128-133.

Hawes MC, Lin HJ. 1990. Correlation of pectolytic enzyme-activity with the programmed release of cells from root caps of pea (*Pisum-sativum*). *Plant Physiology* **94:** 1855-1859.

Heck KL, Vanbelle G, Simberloff D. 1975. Explicit calculation of rarefaction diversity measurement and determination of sufficient sample size. *Ecology* **56:** 1459-1461.

Heid CA, Stevens J, Livak KJ, Williams PM. 1996. Real time quantitative PCR. *Genome Research* **6:** 986-994.

Heijnen CE, van Veen JA. 1991. A determination of protective microhabitats for bacteria introduced into soil. *FEMS Microbiology Letters* **85:** 73-80.

Helal HM, Sauerbeck D. 1986. Effect of plant-roots on carbon metabolism of soil microbial biomass. *Zeitschrift für Pflanzenernahrung und Bodenkunde* **149:** 181-188.

Hendriks L, Claassen N, Jungk A. 1981. Phosphatverarmung des wurzelnahen bodens und phosphataufnahme von mais und raps. *Zeitschrift für Pflanzenernährung und Bodenkunde* **144:** 486-499.

Henriksen A, Selmer-Olsen AR. 1970. Automatic methods for determining nitrate and nitrite in water and soil extracts. *Analyst* **95:** 514-518.

Henriksen GH, Bloom AJ, Spanswick RM. 1990. Measurement of net fluxes of ammonium and nitrate at the surface of barley roots using ion-selective microelectrodes. *Plant Physiology* **93:** 271-280.

Henriksen GH, Raman DR, Walker LP, Spanswick RM. 1992. Measurement of net fluxes of ammonium and nitrate at the surface of barley roots using ion-selective microelectrodes. 2. Patterns of uptake along the root axis and evaluation of the microelectrode flux estimation technique. *Plant Physiology* **99:** 734-747.

Herrmann AM, Clode PL, Fletcher IR, Nunan N, Stockdale EA, O'Donnel AG, Murphy DV. 2007. A novel method for the study of the biophysical interface in soils using nano-scale secondary ion mass spectrometry. *Rapid Communications in Mass Spectrometry* **21:** 29-34.

Hewson I, Fuhrman JA. 2004. Richness and diversity of bacterioplankton species along an estuarine gradient in Moreton Bay, Australia. *Applied and Environmental Microbiology* **70:** 3425-3433.

Hiltner L. 1904. Uber neue erfahrungen und probleme auf dem gebiete der bodenbakteriologie. *Arbeiten der Deutschen Landwirtschaftgesellscgaft* **98:** 59-78.

Hinsinger P. 1998. Structure and function of the rhizosphere: Mechanisms at the soil-root interface. *OCL-Oleagineux Corps Gras Lipides* **5:** 340-341.

Hinsinger P, Gilkes RJ. 1996. Mobilization of phosphate from phosphate rock and alumina-sorbed phosphate by the roots of ryegrass and clover as related to rhizosphere pH. *European Journal of Soil Science* **47:** 533-544.

Hinsinger P, Gobran GR, Gregory PJ, Wenzel WW. 2005. Rhizosphere geometry and heterogeneity arising from root-mediated physical and chemical processes. *New Phytologist* **168:** 293-303.

Hinsinger P, Plassard C, Tang CX, Jaillard B. 2003. Origins of root-mediated pH changes in the rhizosphere and their responses to environmental constraints: A review. *Plant and Soil* **248:** 43-59.

Hirsch AM. 1999. Role of lectins (and rhizobial exopolysaccharides) in legume nodulation. *Current Opinion in Plant Biology* **2:** 320-326.

Hodge A, Robinson D, Fitter A. 2000a. Are microorganisms more effective than plants at competing for nitrogen? *Trends in Plant Science* **5:** 304-308.

Hodge A, Stewart J, Robinson D, Griffiths BS, Fitter AH. 1999. Plant, soil fauna and microbial responses to N-rich organic patches of contrasting temporal availability. *Soil Biology & Biochemistry* **31:** 1517-1530.

Hodge A, Stewart J, Robinson D, Griffiths BS, Fitter AH. 2000b. Competition between roots and soil micro-organisms for nutrients from nitrogen-rich patches of varying complexity. *Journal of Ecology* **88:** 150-164.

Horner-Devine MC, Carney KM, Bohannan BJM. 2004a. An ecological perspective on bacterial biodiversity. *Proceedings of the Royal Society of London Series B-Biological Sciences* **271:** 113-122.

Horner-Devine MC, Lage M, Hughes JB, Bohannan BJM. 2004b. A taxa-area relationship for bacteria. *Nature* **432:** 750-753.

Horz HP, Vianna ME, Gomes B, Conrads G. 2005. Evaluation of universal probes and primer sets for assessing total bacterial load in clinical samples: General implications and practical use in endodontic antimicrobial therapy. *Journal of Clinical Microbiology* **43:** 5332-5337.

Howie WJ, Cook RJ, Weller DM. 1987. Effects of soil matric potential and cell motility on wheat root colonization by fluorescent pseudomonads suppressive to take-all. *Phytopathology* **77:** 286-292.

Huang BR, North GB, Nobel PS. 1993. Soil sheaths, photosynthate distribution to roots, and rhizosphere water relations for *Opuntia-ficus-indica*. *International Journal of Plant Sciences* **154:** 425-431.

Hughes-Martiny JB, Bohannan BJM, Brown JH, Colwell RK, Fuhrman JA, Green JL, Horner-Devine MC, Kane M, Krumins JA, Kuske CR, Morin PJ, Naeem S, Ovreas L, Reysenbach AL, Smith VH, Staley JT. 2006. Microbial biogeography: Putting microorganisms on the map. *Nature Reviews Microbiology* **4:** 102-112.

Hurlbert SH. 1971. Nonconcept of species diversity - Critique and alternative parameters. *Ecology* **52:** 577-586.

Iijima M, Griffiths B, Bengough AG. 2000. Sloughing of cap cells and carbon exudation from maize seedling roots in compacted sand. *New Phytologist* **145:** 477-482.

Jaeger CH, Lindow SE, Miller S, Clark E, Firestone MK. 1999. Mapping of sugar and amino acid availability in soil around roots with bacterial sensors of sucrose and tryptophan. *Applied and Environmental Microbiology* **65:** 2685-2690.

Jaillard B. 1987. Techniques for studying the ionic environment at the soil/root interface. *In:* I.P.I. *ed. Methodology in soil-K research. Proceedings of the 20th*

Colloquium of the International Potash Institute (I.P.I.), Baden Bei Wien, Austria. Bern, Switzerland: I.P.I.

Jaillard B, Ruiz L, Arvieu JC. 1996. pH mapping in transparent gel using color indicator videodensitometry. *Plant and Soil* **183:** 85-95.

Janssen PH. 2006. Identifying the dominant soil bacterial taxa in libraries of 16s rRNA and 16s rRNA genes. *Applied and Environmental Microbiology* **72:** 1719-1728.

Jones DL. 1998. Organic acids in the rhizosphere - A critical review. *Plant and Soil* **205:** 25-44.

Jones DL, Darrah PR. 1992. Resorption of organic-components by roots of *Zea-mays* L and its consequences in the rhizosphere. 1. Resorption of ^{14}C labelled glucose, mannose and citric-acid. *Plant and Soil* **143:** 259-266.

Jones DL, Darrah PR. 1993a. Influx and efflux of amino-acids from *Zea-mays* L roots and their implications for N-nutrition and the rhizosphere. *Plant and Soil* **156:** 87-90.

Jones DL, Darrah PR. 1993b. Re-sorption of organic-compounds by roots of *Zea-mays* L and its consequences in the rhizosphere. 2. Experimental and model evidence for simultaneous exudation and re-sorption of soluble C compounds. *Plant and Soil* **153:** 47-59.

Jones DL, Healey JR, Willett VB, Farrar JF, Hodge A. 2005. Dissolved organic nitrogen uptake by plants - An important N uptake pathway? *Soil Biology and Biochemistry* **37:** 413-423.

Jones DL, Hodge A, Kuzyakov Y. 2004. Plant and mycorrhizal regulation of rhizodeposition. *New Phytologist* **163:** 459-480.

Juniper BE, Groves S, Landau-Schachar B, Audus LJ. 1966. Root cap and the perception of gravity. *Nature* **209:** 93-94.

Jurgens K, Matz C. 2002. Predation as a shaping force for the phenotypic and genotypic composition of planktonic bacteria. *Antonie Van Leeuwenhoek International Journal of General and Molecular Microbiology* **81:** 413-434.

Katznelson H, Lochhead AG, Timonin MI. 1948. Soil microorganisms and the rhizosphere. *Botanical Review* **14:** 543-586.

Katznelson H, Rouatt JW, Peterson EA. 1962. The rhizosphere effect of mycorrhizal and nonmycorrhizal roots of yellow birch seedlings. *Canadian Journal of Botany* **40:** 377-382.

Khan AA, Nawaz MS, Robertson L, Khan SA, Cerniglia CE. 2001. Identification of predominant human and animal anaerobic intestinal bacterial species by terminal

restriction fragment patterns (TRFPs): A rapid, PCR-based method. *Molecular and Cellular Probes* **15:** 349-355.

Kidd KK, Ruano G. 1995. Optimizing PCR. *In:* McPherson MJ, Hames BD, Taylor GR, *eds. PCR 2: A practical approach.* Oxford, England: Oxford University Press, 1-22.

Kilbertus G. 1980. Study of microhabitats in soil aggregates - Relation to bacterial biomass and size of procaryotes. *Revue D'Ecologie et de Biologie du Sol* **17:** 543-557.

Killham K. 1994. *Soil Ecology.* Cambridge, UK: Cambridge University Press.

Klappenbach JA, Dunbar JM, Schmidt TM. 2000. rRNA operon copy number reflects ecological strategies of bacteria. *Applied and Environmental Microbiology* **66:** 1328-1333.

Klimyuk VI, Carroll BJ, Thomas CM, Jones JDG. 1993. Alkali treatment for rapid preparation of plant-material for reliable PCR analysis. *Plant Journal* **3:** 493-494.

Kloepper JW, Schroth MN. 1978. Plant growth-promoting rhizobacteria on radishes. *In: Proceedings of the 4th international conference on plant pathogenic bacteria*, Ridé M, ed. Editions INRA, Angers, France. 879-882.

Korsaeth A, Molstad L, Bakken LR. 2001. Modelling the competition for nitrogen between plants and microflora as a function of soil heterogeneity. *Soil Biology & Biochemistry* **33:** 215-226.

Kowalchuk GA, Buma DS, de Boer W, Klinkhamer PGL, van Veen JA. 2002. Effects of above-ground plant species composition and diversity on the diversity of soil-borne microorganisms. *Antonie Van Leeuwenhoek International Journal of General and Molecular Microbiology* **81:** 509-520.

Kragelund L, Hosbond C, Nybroe O. 1997. Distribution of metabolic activity and phosphate starvation response of *lux*-tagged *Pseudomonas fluorescens* reporter bacteria in the barley rhizosphere. *Applied and Environmental Microbiology* **63:** 4920-4928.

Krom M. 1980. Spectrophotometric determination of ammonia; a study of modified berthelot reaction using salicylate and chloroisocyanurate. *The Analyst* **105:** 305-316.

Kuske CR, Ticknor LO, Miller ME, Dunbar JM, Davis JA, Barns SM, Belnap J. 2002. Comparison of soil bacterial communities in rhizospheres of three plant species and the interspaces in an arid grassland. *Applied and Environmental Microbiology* **68:** 1854-1863.

Kuypers MMM, Jorgensen BB. 2007. The future of single-cell environmental microbiology. *Environmental Microbiology* **9:** 6-7.

Kuzyakov Y. 2002. Kreislauf niedermolekularer organischner substanzen in boden - Tacerstudien und theorie. *Habilitationsschrift, Universitat Hohenheim, Hohenheimer Bodenkundliche Hefte* **65:** 222 S.

Kuzyakov Y, Cheng W. 2001. Photosynthesis controls of rhizosphere respiration and organic matter decomposition. *Soil Biology and Biochemistry* **33:** 1915-1925.

Kuzyakov Y, Domanski G. 2000. Carbon input by plants into the soil. Review. *Journal of Plant Nutrition and Soil Science-Zeitschrift fur Pflanzenernahrung und Bodenkunde* **163:** 421-431.

Kuzyakov Y, Ehrensberger H, Stahr K. 2001. Carbon partitioning and below-ground translocation by *Lolium perenne*. *Soil Biology and Biochemistry* **33:** 61-74.

Labrenz M, Brettar I, Christen R, Flavier S, Botel J, Hofle MG. 2004. Development and application of a real-time PCR approach for quantification of uncultured bacteria in the central Baltic sea. *Applied and Environmental Microbiology* **70:** 4971-4979.

Lalonde M, Knowles R. 1975. Ultrastructure of *Alnus-crispa* var Mollis fern root nodule endophyte. *Canadian Journal of Microbiology* **21:** 1058-1080.

Lavelle P. 1988. Earthworm activities and the soil system. *Biology and Fertility of Soils* **6:** 237-251.

Lechene C, Hillion F, McMahon G, Benson D, Kleinfeld AM, Kampf JP, Distel D, Lugtenberg BJJ, Chin-A-Woeng TFC, Bloemberg GV. 2002. Microbe-plant interactions: principles and mechanisms. *Antonie Van Leeuwenhoek International Journal of General and Molecular Microbiology* **81:** 373-383.

Luyten Y, Bonventre J, Hentschel D, Park K, Ito S, Schwartz M, Benichou G, Slodzian G. 2006. High-resolution quantitative imaging of mammalian and bacterial cells using stable isotope mass spectrometry. *Journal of Biology* **5.**

Lee N, Nielsen PH, Andreasen KH, Juretschko S, Nielsen JL, Schleifer KH, Wagner M. 1999. Combination of fluorescent *in situ* hybridization and microautoradiography - A new tool for structure-function analyses in microbial ecology. *Applied and Environmental Microbiology* **65:** 1289-1297.

Liljeroth E, Burgers S, van Veen JA. 1991. Changes in bacterial-populations along roots of wheat (*Triticum-aestivum* L) seedlings. *Biology and Fertility of Soils* **10:** 276-280.

Linn DM, Doran JW. 1984. Effect of water-filled pore-space on carbon-dioxide and nitrous-oxide production in tilled and nontilled soils. *Soil Science Society of America Journal* **48:** 1267-1272.

Loreau M. 2004. Does Functional Redundancy Exist? *Oikos* **104:** 606-611.

Lynch JM. 1990. *The Rhizosphere.* Chichester, New York, Brisbane, Toronto, Singapore.: John Wiley & Sons.

Lynch JM, Whipps JM. 1990. Substrate Flow in the Rhizosphere. *Plant and Soil* **129:** 1-10.

Lyons SR, Griffen AL, Leys EJ. 2000. Quantitative real-time PCR for *Porphyromonas gingivalis* and total bacteria. *Journal of Clinical Microbiology* **38:** 2362-2365.

Macduff JH, Wild A, Hopper MJ, Dhanoa MS. 1986. Effects of temperature on parameters of root-growth relevant to nutrient-uptake - Measurements on oilseed rape and barley grown in flowing nutrient solution. *Plant and Soil* **94:** 321-332.

Madigan MT, Martinko JM, Parker J. 2000. *Brock. Biology of Microorganisms.* Upper Saddle River, NJ, USA: Prentice Hall Inc.

Maeda H, Fujimoto C, Haruki Y, Maeda T, Kokeguchi S, Petelin M, Arai H, Tanimoto I, Nishimura F, Takashiba S. 2003. Quantitative real-time PCR using Taqman and SYBR Green for *Actinobacillus actinomycetemcomitans*, *Porphyromonas gingivalis*, *Prevotella intermedia*, *tetq* gene and total bacteria. *FEMS Immunology and Medical Microbiology* **39:** 81-86.

Magurran AE. 2004. *Measuring Biological Diversity.* Oxford, UK: Blackwell Science Ltd.

Mahmood T, Kaiser WM, Ali R, Ashraf M, Gulnaz A, Iqbal Z. 2005. Ammonium versus nitrate nutrition of plants stimulates microbial activity in the rhizosphere. *Plant and Soil* **277:** 233-243.

Mahmood T, Woitke M, Gimmler H, Kaiser WM. 2002. Sugar exudation by roots of kallar grass *Leptochloa fusca* (L.) Kunth is strongly affected by the nitrogen source. *Planta* **214:** 887-894.

Maiwald M, Ditton HJ, Sonntag HG, Vonknebeldoeberitz M. 1994. Characterization of contaminating DNA in Taq polymerase which occurs during amplification with a primer set for legionella 5S ribosomal-RNA. *Molecular and Cellular Probes* **8:** 11-14.

Maloney PE, van Bruggen AHC, Hu S. 1997. Bacterial community structure in relation to the carbon environments in lettuce and tomato rhizospheres and in bulk soil. *Microbial Ecology* **34:** 109-117.

Mancuso S, Papeschi G, Marras AM. 2000. A polarographic, oxygen-selective, vibrating-microelectrode system for the spatial and temporal characterisation of transmembrane oxygen fluxes in plants. *Planta* **211:** 384-389.

Manefield M, Whiteley AS, Griffiths RI, Bailey MJ. 2002a. RNA stable isotope probing, a novel means of linking microbial community function to phylogeny. *Applied and Environmental Microbiology* **68:** 5367-5373.

Manefield M, Whiteley AS, Ostle N, Ineson P, Bailey MJ. 2002b. Technical considerations for RNA-based stable isotope probing: An approach to associating microbial diversity with microbial community function. *Rapid Communications in Mass Spectrometry* **16:** 2179-2183.

Mantel N. 1967. Detection of disease clustering and a generalized regression approach. *Cancer Research* **27:** 209-220.

Marilley L, Aragno M. 1999. Phylogenetic diversity of bacterial communities differing in degree of proximity of *Lolium perenne* and *Trifolium repens* roots. *Applied Soil Ecology* **13:** 127-136.

Marilley L, Vogt G, Blanc M, Aragno M. 1998. Bacterial diversity in the bulk soil and rhizosphere fractions of *Lolium perenne* and *Trifolium repens* as revealed by PCR restriction analysis of 16S rDNA. *Plant and Soil* **198:** 219-224.

Marschner H. 1995. *Mineral Nutrition of Higher Plants:* Academic Press.

Marschner P, Crowley D, Yang CH. 2004. Development of specific rhizosphere bacterial communities in relation to plant species, nutrition and soil type. *Plant and Soil* **261:** 199-208.

Marschner P, Crowley DE. 1996. Physiological activity of a bioluminescent *Pseudomonas fluorescens* (strain 2-79) in the rhizosphere of mycorrhizal and non-mycorrhizal pepper (*Capsicum annuum* L). *Soil Biology & Biochemistry* **28:** 869-876.

Marschner P, Gerendas J, Sattelmacher B. 1999. Effect of N concentration and N source on root colonization by *Pseudomonas fluorescens* 2-79RLI. *Plant and Soil* **215:** 135-141.

Marschner P, Neumann G, Kania A, Weiskopf L, Lieberei R. 2002. Spatial and temporal dynamics of the microbial community structure in the rhizosphere of cluster roots of white lupin (*Lupinus albus* L.). *Plant and Soil* **246:** 167-174.

McCully ME. 1999. Roots in soil: Unearthing the complexities of roots and their rhizospheres. *Annual Review of Plant Physiology and Plant Molecular Biology* **50:** 695-718.

McCully ME, Boyer JS. 1997. The expansion of maize root-cap mucilage during hydration. 3. Changes in water potential and water content. *Physiologia Plantarum* **99:** 169-177.

McCully ME, Canny MJ. 1985. Localization of translocated C-14 in roots and root exudates of field-grown maize. *Physiologia Plantarum* **65:** 380-392.

McCully ME, Sealey LJ. 1996. The expansion of maize root-cap mucilage during hydration. 2. Observations on soil-grown roots by cryo-scanning electron microscopy. *Physiologia Plantarum* **97:** 454-462.

McDougal BM, Rovira AD. 1970. Sites of exudation of C-14-labelled compounds from wheat roots. *New Phytologist* **69:** 999-1003.

McGrath SP, Cunliffe CH. 1985. A simplified method for the extraction of the metals Fe, Zn, Cu, Ni, Cd, Pb, Cr, Co and Mn from soils and sewage sludges. *Journal of the Science of Food and Agriculture* **36:** 794-798.

McMahon G, Glassner BJ, Lechene CP. 2006. Quantitative imaging of cells with multi-isotope imaging mass spectrometry (MIMS)-nanoautography with stable isotope tracers. *Applied Surface Science* **252:** 6895-6906.

Meharg AA. 1994. A critical-review of labelling techniques used to quantify rhizosphere carbon-flow. *Plant and Soil* **166:** 55-62.

Meharg AA, Killham K. 1988. A comparison of carbon flow from pre-labeled and pulse-labeled plants. *Plant and Soil* **112:** 225-231.

Meighen EA, Dunlap PV. 1993. Physiological, biochemical and genetic-control of bacterial bioluminescence. *Advances in Microbial Physiology* **34:** 1-67.

Meyer JR, Linderman RG. 1986. Selective influence on populations of rhizosphere or rhizoplane bacteria and actinomycetes by mycorrhizas formed by *Glomus-fasciculatum*. *Soil Biology & Biochemistry* **18:** 191-196.

Miki NK, Clarke KJ, McCully ME. 1980. A histological and histochemical comparison of the mucilages on the root-tips of several grasses. *Canadian Journal of Botany-Revue Canadienne de Botanique* **58:** 2581-2593.

Miller AJ, Smith SJ. 1992. The mechanism of nitrate transport across the tonoplast of barley root cells. *Planta* **187:** 554-557

Miller AJ. 1995. Ion-selective microelectrodes for measurement of intracellular ion concentrations. *Methods in Plant Cell Biology* **49:** 273-289.

Miller HJ, Liljeroth E, Henken G, van Veen JA. 1990. Fluctuations in the fluorescent pseudomonad and actinomycete populations of rhizosphere and rhizoplane during the growth of spring wheat. *Canadian Journal of Microbiology* **36:** 254-258.

Monod J. 1942. *Reserches sur la croissance des cultures bacteriennes.* Paris: Hermann.

Morel JL, Habib L, Plantureux S, Guckert A. 1991. Influence of maize root mucilage on soil aggregate stability. *Plant and Soil* **136:** 111-119.

Morita RY. 1988. Bioavailability of energy and its relationship to growth and starvation survival in nature. *Canadian Journal of Microbiology* **34:** 436-441.

Muhling KH, Schubert S, Mengel K. 1993a. Mechanism of sugar retention by roots of intact maize and field bean-plants. Plant and Soil 156: 99-102.

Muhling KH, Schubert S, Mengel K. 1993b. Role of plasmalemma H^+-ATPase in sugar retention by roots of intact maize and field bean-plants. *Zeitschrift fur Pflanzenernahrung und Bodenkunde* **156:** 155-161.

Muller AK, Westergaard K, Christensen S, Sorensen SJ. 2001. The effect of long-term mercury pollution on the soil microbial community. *FEMS Microbiology Ecology* **36:** 11-19.

Muyzer G, Dewaal EC, Uitterlinden AG. 1993. Profiling of complex microbial-populations by denaturing gradient gel-electrophoresis analysis of polymerase chain reaction-amplified genes-coding for 16S ribosomal-RNA. *Applied and Environmental Microbiology* **59:** 695-700.

Mylvaganam S, Dennis PP. 1992. Sequence heterogeneity between the 2 genes encoding 16S ribosomal-RNA from the halophilic archaebacterium *Haloarcula-marismortui*. *Genetics* **130:** 399-410.

Nadkarni MA, Martin FE, Jacques NA, Hunter N. 2002. Determination of bacterial load by real-time PCR using a broad-range (universal) probe and primers set. *Microbiology-SGM* **148:** 257-266.

Naim MS. 1965. Development of rhizosphere and rhizoplane microflora of *Aristida coerulescens* in Libyan desert. *Archiv fur Mikrobiologie* **50:** 321-325.

Nambiar EKS. 1976a. The uptake of Zinc-65 by roots in relation to soil water content and root growth. *Australian Journal of Soil Research* **14:** 67-74.

Nambiar EKS. 1976b. Uptake of Zn65 from dry soil by plants. *Plant and Soil* **44:** 267-271.

Nannipieri P, Ascher J, Ceccherini MT, Landi L, Pietramellara G, Renella G. 2003. Microbial diversity and soil functions. *European Journal of Soil Science* **54:** 655-670.

Neumann G, Martinoia E. 2002. Cluster roots - An underground adaptation for survival in extreme environments. *Trends in Plant Science* **7:** 162-167.

Neumann G, Massonneau A, Martinoia E, Romheld V. 1999. Physiological adaptations to phosphorus deficiency during proteoid root development in white lupin. *Planta* **208:** 373-382.

Neumann G, Romheld V 2001. The release of root exudates as affected by the plant's physiological status *In:* Pinton R, Varanini Z, Nannipieri P, *eds. The rhizosphere. Biochemistry and organic substances at the soil-plant interface.* New York: Marcel Dekker.

Newman EI, Watson A. 1977. Microbial abundance in rhizosphere - Computer-model. *Plant and Soil* **48:** 17-56.

Newton CR, Graham A. 1994. *PCR.* Oxford: BIOS Scientific Publishers Ltd.

Nguyen C, Todorovic C, Robin C, Christophe A, Guckert A. 1999. Continuous monitoring of rhizosphere respiration after labelling of plant shoots with (CO_2)-C-14. *Plant and Soil* **212:** 191-201.

Nolan R, Hands RE, Bustin SA. 2006. Quantification of mRNA using real-time RT-PCR. *Nature Protocols* **1:** 1559 -1582.

North GB, Nobel PS. 1997. Drought-induced changes in soil contact and hydraulic conductivity for roots of *Opuntia ficus-indica* with and without rhizosheaths. *Plant and Soil* **191:** 249-258.

Norton JM, Smith JL, Firestone MK. 1990. Carbon flow in the rhizosphere of Ponderosa pine-seedlings. *Soil Biology & Biochemistry* **22:** 449-455.

Nubel U, Garcia-Pichel F, Clavero E, Muyzer G. 2000. Matching molecular diversity and ecophysiology of benthic cyanobacteria and diatoms in communities along a salinity gradient. *Environmental Microbiology* **2:** 217-226.

Nunan N, Ritz K, Crabb D, Harris K, Wu KJ, Crawford JW, Young IM. 2001. Quantification of the *in situ* distribution of soil bacteria by large-scale imaging of thin sections of undisturbed soil. *FEMS Microbiology Ecology* **37:** 67-77.

Nunan N, Ritz K, Rivers M, Feeney DS, Young IM. 2006. Investigating microbial micro-habitat structure using X-Ray computed tomography. *Geoderma* **133:** 398-407.

Nunan N, Wu K, Young IM, Crawford JW, Ritz K. 2002. *In situ* spatial patterns of soil bacterial populations, mapped at multiple scales, in an arable soil. *Microbial Ecology* **44:** 296-305.

Nunan N, Wu KJ, Young IM, Crawford JW, Ritz K. 2003. Spatial distribution of bacterial communities and their relationships with the micro-architecture of soil. FEMS Microbiology Ecology **44:** 203-215.

O'Donnell AG, Seasman M, Macrae A, Waite I, Davies JT. 2001. Plants and fertilisers as drivers of change in microbial community structure and function in soils. *Plant and Soil* **232:** 135-145.

O'Flaherty S, McGrath S, Hirsch P 2001. Comparison of phenotypic, functional and genetic diversity of bacterial communities in soils. *In:* Rees RM, Ball BC, Campbell CD, Watson CA, *eds. Sustainable management of soil organic matter.* Wallingford, UK: CAB International, 370-376.

Oades JM. 1978. Mucilages at Root Surface. *Journal of Soil Science* **29:** 1-16.

Olsen AR. 1954. USDA Circular 939. In.

Olsson S, Baath E, Soderstrom B. 1987. Growth of *Verticillium-dahliae* Kleb hyphae and of bacteria along the roots of rape (*Brassica-napus* L) seedlings. *Canadian Journal of Microbiology* **33:** 916-919.

Orphan VJ, House CH, Hinrichs KU, McKeegan KD, DeLong EF. 2001. Methane-consuming archaea revealed by directly coupled isotopic and phylogenetic analysis. *Science* **293:** 484-487.

Ouverney CC, Fuhrman JA. 1999. Combined microautoradiography-16S rRNA probe technique for determination of radioisotope uptake by specific microbial cell types *in situ. Applied and Environmental Microbiology* **65:** 1746-1752.

Papeschi G, Mancuso S, Marras AM. 2000. Electrochemical behaviour of a Cu/CuSe microelectrode and its application in detecting temporal and spatial localisation of Copper(II) fluxes along *Olea europaea* roots. *Journal of Solid State Electrochemistry* **4:** 325-329.

Papke RT, Ramsing NB, Bateson MM, Ward DM. 2003. Geographical isolation in hot spring cyanobacteria. *Environmental Microbiology* **5(8):** 650-659.

Parke JL, Moen R, Rovira AD, Bowen GD. 1986. Soil-water flow affects the rhizosphere distribution of a seed- borne biological-control agent, *Pseudomonas-fluorescens. Soil Biology & Biochemistry* **18:** 583-588.

Patterson E. 2006. C-flow from plant roots. *In:* Luster J, Finlay R, *eds. Handbook of methods used in rhizosphere research.* Birmensdorf, Switzerland: Swiss Federal Research Institute WSL, 349-350.

Patterson HD, Thompson R. 1971. Recovery of inter-block information when block sizes are unequal. *Biometrika* **58:** 545-554.

Persello-Cartieaux F, Nussaume L, Robaglia C. 2003. Tales from the underground: Molecular plant-rhizobacteria interactions. *Plant Cell and Environment* **26:** 189-199.

Peteranderl R, Lechene C. 2004. Measure of carbon and nitrogen stable isotope ratios in cultured cells. *Journal of the American Society for Mass Spectrometry* **15:** 478-485.

Piao MH, Yoon JH, Gerok J, Shim YB. 2003. Characterization of all solid state hydrogen ion selective electrode based on PVC-SR hybrid membranes. *Sensors* **3:** 192-201.

Pineros MA, Shaff JE, Kochian V. 1998. Development, characterization, and application of a cadmium-selective microelectrode for the measurement of cadmium fluxes in roots of Thlaspi species and wheat. *Plant Physiology* **116:** 1393-1401.

Pinton R, Varanini Z, Nannipieri P. 2001. *The rhizosphere. Bio-chemistry and organic substances at the soil-plant interface*. New York: Marcel Dekker.

Plassard C, Guerin-Laguette A, Very AA, Casarin V, Thibaud JB. 2002. Local measurements of nitrate and potassium fluxes along roots of maritime pine. Effects of ectomycorrhizal symbiosis. *Plant Cell and Environment* **25:** 75-84.

Plomp M, Leighton TJ, Wheeler KE, Malkin AJ. 2005. The high-resolution architecture and structural dynamics of bacillus spores. *Biophysical Journal* **88:** 603-608.

Poindexter JS. 1981. Oligotrophy - Fast and famine existence. *Advances in Microbial Ecology* **5:** 63-89.

Rainey FA, Ward-Rainey NL, Janssen PH, Hippe H, Stackebrandt E. 1996. *Clostridium paradoxum* DSM 7308T contains multiple 16S rRNA genes with heterogeneous intervening sequences. *Microbiology-UK* **142:** 2087-2095.

Rangel-Castro JI, Killham K, Ostle N, Nicol GW, Anderson IC, Scrimgeour CM, Ineson P, Meharg A, Prosser JI. 2005. Stable isotope probing analysis of the influence of liming on root exudate utilization by soil microorganisms. *Environmental Microbiology* **7:** 828-838.

Ranjard L, Poly F, Combrisson J, Richaume A, Gourbiere F, Thioulouse J, Nazaret S. 2000. Heterogeneous cell density and genetic structure of bacterial pools associated with various soil microenvironments as determined by enumeration and DNA fingerprinting approach (RISA). *Microbial Ecology* **39:** 263-272.

Ranjard L, Richaume AS. 2001. Quantitative and qualitative microscale distribution of bacteria in soil. *Research in Microbiology* **152:** 707-716.

Rao TP, Yano K, Iijima M, Yamauchi A, Tatsumi J. 2002. Regulation of rhizosphere acidification by photosynthetic activity in cowpea (*Vigna unguiculata* L. walp.) seedlings. Annals of Botany 89(2): 213-220.

Rausch T. 1991. The hexose transporters at the plasma-membrane and the tonoplast of higher-plants. *Physiologia Plantarum* **82:** 134-142.

Raven JA, Smith FA. 1976. Nitrogen assimilation and transport in vascular land plants in relation to intracellular pH regulation. *New Phytologist* **76:** 415-431.

Reche I, Pulido-Villena E, Morales-Baquero R, Casamayor EO. 2005. Does ecosystem size determine aquatic bacterial richness? *Ecology* **86:** 1715-1722.

Rehim SSAE, Awad A, Sayed AE. 1987. Electroplating of antimony and antimony-tin alloys. *Journal of Applied Electrochemistry* **17:** 156-164.

Ridge RW, Kim R, Yoshida F. 1998. The diversity of lectin-detectable sugar residues on root hair tips of selected legumes correlates with the diversity of their host ranges for rhizobia. *Protoplasma* **202:** 84-90.

Ridge RW, Rolfe BG. 1986. Lectin binding to the root and root hair tips of the tropical legume *Macroptilium-atropurpureum* Urb. *Applied and Environmental Microbiology* **51:** 328-332.

Robards AW, Jackson SM, Clarkson DT, Sanderson J. 1973. Structure of barley roots in relation to transport of ions into stele. *Protoplasma* **77:** 291-311.

Rochelle PA, Weightman AJ, Fry JC. 1992. DNAse-I treatment of Taq DNA-polymerase for complete PCR decontamination. *Biotechniques* **13:** 520-520.

Rohwer F, Seguritan V, Azam F, Knowlton N. 2002. Diversity and distribution of coral-associated bacteria. *Marine Ecology-Progress Series* **243:** 1-10.

Römheld V. 1986. pH-veranderungen in der rhizosphare verschiedener kulturpflanzenarten in abhangigkeit vom nahrstoffangebot. *Potash Review* **55:** 1-8.

Rosenzweig ML. 1995. *Species diversity in time and space.* Cambridge: Cambridge University Press.

Rougier M, Caboud A. 1985. Mucilages secreted by roots and their biological function. *Israel Journal of Botany* **34:** 129-146.

Rubio G, Sorgona A, Lynch JP. 2004. Spatial mapping of phosphorus influx in bean root systems using digital autoradiography. *Journal of Experimental Botany* **55:** 2269-2280.

Ruiz L, Arvieu JC. 1990. Measurement of pH gradients in the rhizosphere. *Symbiosis* **9:** 71-75.

Russell RS, Sanderson J. 1967. Nutrient uptake by different parts of intact roots of plants. *Journal of Experimental Botany* **18:** 491-508.

Ryan PR, Delhaize E, Jones DL. 2001. Function and mechanism of organic anion exudation from plant roots. *Annual Review of Plant Physiology and Plant Molecular Biology* **52:** 527-560.

Ryan PR, Newman IA, Shields B. 1990. Ion fluxes in corn roots measured by microelectrodes with ion-specific liquid membranes. *Journal of Membrane Science* **53:** 59-69.

Saiki RK, Scharf S, Faloona F, Mullis KB, Horn GT, Erlich HA, Arnheim N. 1985. Enzymatic amplification of beta-globin genomic sequences and restriction site analysis for diagnosis of sickle-cell anemia. *Science* **230:** 1350-1354.

Samaj J, Braun M, Baluska F, Ensikat HJ, Tsumuraya Y, Volkmann D. 1999. Specific localization of arabinogalactan-protein epitopes at the surface of maize root hairs. *Plant and Cell Physiology* **40:** 874-883.

Samstevich SA. 1968. Gel-like excretions of plant roots and their influence upon soil and rhizosphere microflora. *In:* Ghilarov MS, Kovda VA, Novichkova-Ivanova LN, Rodin LE, Sveshnikova VM, *eds. Methods of productivity studies in root systems and rhizosphere organisms.* Nauka, Leningrad: USSR Academy of Sciences, 200-204.

Savka MA, Dessaux Y, Oger P, Rossbach S. 2002. Engineering bacterial competitiveness and persistence in the phytosphere. *Molecular Plant-Microbe Interactions* **15:** 866-874.

Scher FM, Ziegle JS, Kloepper JW. 1984. A method for assessing the root-colonizing capacity of bacteria on maize. *Canadian Journal of Microbiology* **30:** 151-157.

Schimel JP, Jackson LE, Firestone MK. 1989. Spatial and temporal effects on plant microbial competition for inorganic nitrogen in a California annual grassland. *Soil Biology & Biochemistry* **21:** 1059-1066.

Schrader S. 1994. Influence of earthworms on the pH conditions of their environment by cutaneous mucus secretion. *Zoologischer Anzeiger* **233:** 211-219.

Schuhegger R, Ihring A, Gantner S, Bahnweg G, Knappe C, Vogg G, Hutzler P, Schmid M, van Breusegem F, Eberl L, Hartmann A, Langebartels C. 2006. Induction of systemic resistance in tomato by N-acyl-L-homoserine lactone-producing rhizosphere bacteria. *Plant Cell and Environment* **29:** 909-918.

Scott EM, Rattray EAS, Prosser JI, Killham K, Glover LA, Lynch JM, Bazin MJ. 1995. A mathematical model for dispersal of bacterial inoculants colonizing the wheat rhizosphere. *Soil Biology and Biochemistry* **27:** 1307-1318.

Scott FM, Hamner KC, Baker E, Bowler E. 1958. Electron microscope studies of the epidermis of *Allium-cepa. American Journal of Botany* **45:** 449-461.

Semenov AM. 1991. Physiological bases of oligotrophy of microorganisms and the concept of microbial community. *Microbial Ecology* **22:** 239-247.

Semenov AM, van Bruggen AHC, Zelenev VV. 1999. Moving waves of bacterial populations and total organic carbon along roots of wheat. *Microbial Ecology* **37:** 116-128.

Sessitsch A, Hackl E, Wenzl P, Kilian A, Kostic T, Stralis-Pavese N, Sandjong BT, Bodrossy L. 2006. Diagnostic microbial microarrays in soil ecology. *New Phytologist* **171:** 719-736.

Sessitsch A, Weilharter A, Gerzabek MH, Kirchmann H, Kandeler E. 2001. Microbial population structures in soil particle size fractions of a long-term fertilizer field experiment. *Applied and Environmental Microbiology* **67:** 4215-4224.

Shen H, Rogej S, Kieft TL. 2006. Sensitive, real-time PCR detects low-levels of contamination by *Legionella pneumophila* in commercial reagents. *Molecular and Cellular Probes* **20:** 147-153.

Sibley CG, Comstock JA, Ahlquist JE. 1990. DNA hybridization evidence of hominoid phylogeny - A reanalysis of the data. *Journal of Molecular Evolution* **30:** 202-236.

Sievers A, Braun M, Monshausen GB. 1999. The root cap: Structure and function. *In:* Waisel Y, Eshel A, Kafkafi U, *eds. Plant roots: The hidden half.* New York: Marcel Dekker, Inc., 31-49.

Simons M, Permentier HP, de Weger LA, Wijffelman CA, Lugtenberg BJJ. 1997. Amino acid synthesis is necessary for tomato root colonization by *Pseudomonas fluorescens* strain WCS365. *Molecular Plant-Microbe Interactions* **10:** 102-106.

Simpfendorfer S, Kirkegaard JA, Heenan DP, Wong PTW. 2001. Involvement of root inhibitory pseudomonas spp. in the poor early growth of direct drilled wheat: Studies in intact cores. *Australian Journal of Agricultural Research* **52:** 845-853.

Simpfendorfer S, Kirkegaard JA, Heenan DP, Wong PTW. 2002. Reduced early growth of direct drilled wheat in southern new south wales - Role of root inhibitory pseudomonads. *Australian Journal of Agricultural Research* **53:** 323-331.

Siqueira JF, Rocas IN, Rosado AS. 2004. Investigation of bacterial communities associated with asymptomatic and symptomatic endodontic infections by denaturing gradient gel electrophoresis fingerprinting approach. *Oral Microbiology and Immunology* **19:** 363-370.

Sleigh J, Cursons R, La Pine M. 2001. Detection of bacteraemia in critically ill patients using 16S rDNA polymerase chain reaction and DNA sequencing. *Intensive Care Medicine* **27:** 1269-1273.

Smalla K, Wieland G, Buchner A, Zock A, Parzy J, Kaiser S, Roskot N, Heuer H, Berg G. 2001. Bulk and rhizosphere soil bacterial communities studied by denaturing gradient gel electrophoresis: Plant-dependent enrichment and seasonal shifts revealed. *Applied and Environmental Microbiology* **67:** 4742-4751.

Standing D, Meharg AA, Killham K. 2003. A tripartite microbial reporter gene system for real-time assays of soil nutrient status. *FEMS Microbiology Letters* **220:** 35-39.

Steinman CR, Muralidhar B, Nuovo GJ, Rumore PM, Yu D, Mukai M. 1997. Domain-directed polymerase chain reaction capable of distinguishing bacterial from host DNA at the single-cell level: Characterization of a systematic method to investigate putative bacterial infection in idiopathic disease. *Analytical Biochemistry* **244:** 328-339.

Stephenson MB, Hawes MC. 1994. Correlation of pectin methylesterase activity in root caps of pea with root border cell-separation. *Plant Physiology* **106:** 739-745.

Strawn D, Doner H, Zavarin M, McHugo S. 2002. Microscale investigation into the geochemistry of arsenic, selenium, and iron in soil developed in pyritic shale materials. *Geoderma* **108:** 237-257.

Stubbs VEC, Standing D, Knox OGG, Killham K, Bengough AG, Griffiths B. 2004. Root border cells take up and release glucose-C. *Annals of Botany* **93:** 221-224.

Takai K, Horikoshi K. 2000. Rapid detection and quantification of members of the archaeal community by quantitative PCR using fluorogenic probes. *Applied and Environmental Microbiology* **66:** 5066-5072.

Tan CS, Drury CF, Reynolds WD, Gaynor JD, Zhang TQ, Ng HY. 2002. Effect of long-term conventional tillage and no-tillage systems on soil and water quality at the field scale. *Water Science and Technology* **46:** 183-190.

Taylor AR, Bloom AJ. 1998. Ammonium, nitrate, and proton fluxes along the maize root. *Plant Cell and Environment* **21:** 1255-1263.

Taylor CJ, Bain LA, Richardson DJ, Spiro S, Russell DA. 2004. Construction of a whole-cell gene reporter for the fluorescent bioassay of nitrate. *Analytical Biochemistry* **328:** 60-66.

Thompson JD, Higgins DG, Gibson TJ. 1994. Clustal W: Improving the sensitivity of progressive multiple sequence alignment through sequence weighting, position-specific gap penalties and weight matrix choice. *Nucleic Acids Research* **22:** 4673-4680.

Tinker PB, Nye PH. 2000. *Solute movement in the rhizosphere*. New York: Oxford University Press.

Tiunov AV, Scheu S. 1999. Microbial respiration, biomass, biovolume and nutrient status in burrow walls of *Lumbricus terrestris* L. (*Lumbricidae*). *Soil Biology & Biochemistry* **31:** 2039-2048.

Torsvik V, Daae FL, Sandaa RA, Ovreas L. 1998. Novel techniques for analysing microbial diversity in natural and perturbed environments. *Journal of Biotechnology* **64:** 53-62.

Torsvik V, Ovreas L. 2002. Microbial diversity and function in soil: From genes to ecosystems. *Current Opinion in Microbiology* **5:** 240-245.

Torsvik V, Ovreas L, Thingstad TF. 2002. Prokaryotic diversity - Magnitude, dynamics, and controlling factors. *Science* **296:** 1064-1066.

Tourova TP, Kuznetzov BB, Novikova EV, Poltaraus AB, Nazina TN. 2001. Heterogeneity of the nucleotide sequences of the 16S rRNA genes of the type strain of *Desulfotomaculum kuznetsovii*. *Microbiology* **70:** 678-684.

Treves DS, Xia B, Zhou J, Tiedje JM. 2003. A two-species test of the hypothesis that spatial isolation influences microbial diversity in soil. *Microbial Ecology* **45:** 20-28.

Tseng CP, Cheng JC, Tseng CC, Wang CY, Chen YL, Chiu DTY, Liao HC, Chang SS. 2003. Broad-range ribosomal RNA real-time PCR after removal of DNA from reagents: Melting profiles for clinically important bacteria. *Clinical Chemistry* **49:** 306-309.

Uren NC. 1993. Mucilage secretion and its interaction with soil, and contact reduction. *Plant and Soil* **156:** 79-82.

Uren NC. 2001. Types, amounts, and possible funtions of compounds released into the rhizosphere by soil-grown plants. *In:* Pinton R, Varanini Z, Nannipieri P, *eds. The rhizosphere - Biochemistry and organic substances at the soil-plant interface.* New York: Marcel Dekker, Inc.

Uren NC, Reisenauer HM. 1988. The role of root exudates in nutrient acquisition. *Advances in Plant Nutrition* **3:** 79-114.

van Bruggen AHC, Semenov AM, Zelenev VV. 2000. Wavelike distributions of microbial populations along an artificial root moving through soil. *Microbial Ecology* **40:** 250-259.

van Houdt P, Lewandowski Z, Little B. 1992. Iridium oxide pH microelectrode. *Biotechnology and Bioengineering* **40:** 601-608.

van Loosdrecht MCM, Lyklema J, Norde W, Zehnder AJB. 1990. Influence of interfaces on microbial activity. *Microbiological Reviews* **54:** 75-87.

van Overbeek LS, van Elsas JD. 1995. Root exudate-induced promoter activity in *Pseudomonas fluorescens* mutants in the wheat rhizosphere. *Applied and Environmental Microbiology* **61:** 890-898.

van Veen JA 2004. The rhizosphere - Historical and future perspectives from a microbiologists viewpoint. *In:* Hartmann A, Schmid M, Wenzel W, Hinsinger P. *International conference on the rhizosphere - Perspectives and challenges - A tribute to Lorenz Hiltner*. Munich, Germany: GSF - Forschungszentren.

Vandewerf H, Verstraete W. 1987a. Estimation of active soil microbial biomass by mathematical-analysis of respiration curves - Calibration of the test procedure. *Soil Biology & Biochemistry* **19:** 261-265.

Vandewerf H, Verstraete W. 1987b. Estimation of active soil microbial biomass by mathematical-analysis of respiration curves - Development and verification of the model. *Soil Biology & Biochemistry* **19:** 253-260.

Vandewerf H, Verstraete W. 1987c. Estimation of active soil microbial biomass by mathematical-analysis of respiration curves - Relation to conventional estimation of total biomass. *Soil Biology & Biochemistry* **19:** 267-271.

Vanegeraat A. 1975. Exudation of ninhydrin-positive compounds by pea-seedling roots - Study of sites of exudation and of composition of exudate. *Plant and Soil* **42:** 37-47.

Vanvuurde JWL, Schippers B. 1980. Bacterial-colonization of seminal wheat roots. *Soil Biology & Biochemistry* **12:** 559-565.

Versalovic J, Koeuth T, Lupski JR. 1991. Distribution of repetitive DNA-sequences in Eubacteria and application to fingerprinting of bacterial genomes. *Nucleic Acids Research* **19:** 6823-6831.

Vicre M, Santaella C, Blanchet S, Gateau A, Driouich A. 2005. Root border-like cells of arabidopsis. Microscopical characterization and role in the interaction with rhizobacteria. *Plant Physiology* **138:** 998-1008.

von Wintzingerode F, Gobel UB, Stackebrandt E. 1997. Determination of microbial diversity in environmental samples: Pitfalls of PCR-based rRNA analysis. *FEMS Microbiology Reviews* **21:** 213-229.

Wagner M, Nielsen PH, Loy A, Nielsen JL, Daims H. 2006. Linking microbial community structure with function: Fluorescence in situ hybridization-microautoradiography and isotope arrays. *Current Opinion in Biotechnology* **17:** 83-91.

Waisel Y, Eshel A, Kafkafi U. 2002. *Plant roots: The hidden half.* New York: Marcel Dekker, Inc.

Walker TS, Bais HP, Grotewold E, Vivanco JM. 2003. Root exudation and rhizosphere biology. *Plant Physiology* **132:** 44-51.

Wang M, Ha Y. 2006. An electrochemical approach to monitor pH change in agar media during plant tissue culture. *Biosensors & Bioelectronics* **22:** 2718-2723.

Wang Y, Zwang ZS, Ramanan N. 1997. The actinomycete *Thermobispora bispora* contains two distinct types of transcriptionally active 16S rRNA genes. *Journal of Bacteriology* **179:** 3270-3276.

Watanabe K, Nelson J, Harayama S, Kasai H. 2001. ICB database: The *gyr*B database for identification and classification of bacteria. *Nucleic Acids Research* **29:** 344-345.

Ward BB, O'Mullan GD. 2002. Worldwide distribution of *Nitrosococcus Oceani*, a marine ammonia-oxidizing gamma-proteobacterium, detected by PCR and sequencing of 16S rRNA and *amo*A genes. *Applied and Environmental Microbiology* **68:** 4153-4157.

Ward DM, Ferris MJ, Nold SC, Bateson MM. 1998. A natural view of microbial biodiversity within hot spring cyanobacterial mat communities. *Microbiology and Molecular Biology Reviews* **62:** 1353-1370.

Wardle DA. 2002. *Communities and ecosystems: Linking the aboveground and belowground components*. NJ: Princeton University Press

Watt M, McCully ME, Canny MJ. 1994. Formation and stabilization of rhizosheaths of *Zea-mays* L - Effect of soil-water content. *Plant Physiology* **106:** 179-186.

Watt M, McCully ME, Jeffree CE. 1993. Plant and bacterial mucilages of the maize rhizosphere - Comparison of their soil binding-properties and histochemistry in a model system. *Plant and Soil* **151:** 151-165.

Watt M, McCully ME, Kirkegaard JA. 2003. Soil strength and rate of root elongation alter the accumulation of pseudomonas *spp.* and other bacteria in the rhizosphere of wheat. *Functional Plant Biology* **30:** 483-491.

Watt M, Silk WK, Passioura JB. 2006a. Rates of root and organism growth, soil conditions, and temporal and spatial development of the rhizosphere. *Annals of Botany* **97:** 839-855.

Watt M, Hugenholtz P, White R, Vinall K. 2006b. Numbers and locations of native bacteria on field-grown wheat roots quantified by fluorescence in situ hybridization (FISH). *Environmental Microbiology* **8:** 871-884.

Watteau F, Villemin G, Ghanbaja J, Genet P, Pargney JC. 2002. *In situ* ageing of fine beech roots (*Fagus sylvatica*) assessed by transmission electron microscopy and

electron energy loss spectroscopy: Description of microsites and evolution of polyphenolic substances. *Biology of the Cell* **94:** 55-63.

Weisburg WG, Barns SM, Pelletier DA, Lane DJ. 1991. 16S ribosomal DNA amplification for phylogenetic study. *Journal of Bacteriology* **173:** 697-703.

Weisenseel MH, Dorn A, Jaffe LF. 1979. Natural H^+ currents traverse growing roots and root hairs of barley (*Hordeum-vulgare*-L). *Plant Physiology* **64:** 512-518.

Welham SJ, Thompson R. 1997. Likelihood ratio tests for fixed model terms using residual maximum likelihood. *Journal of the Royal Statistical Society Series B-Methodological* **59:** 701-714.

Weller DM. 1988. Biological-control of soilborne plant-pathogens in the rhizosphere with bacteria. *Annual Review of Phytopathology* **26:** 379-407.

Wertz S, Degrange V, Prosser JI, Poly F, Commeaux C, Freitag T, Guillaumaud N, Le Roux X. 2006. Maintenance of soil functioning following erosion of microbial diversity. *Environmental Microbiology* **8:** 2162-2169.

Whipps JM. 1990. Carbon Economy. *In:* Lynch JM *ed. The rhizosphere*. New York: John Wiley and Sons, 59-97.

Whitaker RJ, Grogan DW, Taylor JW. 2003. Geographic barriers isolate endemic populations of hyperthermophilic archaea. *Science* **301:** 976-978.

Wiles, S. 2001. BIOMATE: development of custom-designed bioluminescent sensors for toxicity testing. *Unpublished PhD dissertation. Napier University* pp. 201.

Woese CR. 1987. Bacterial evolution. *Microbiological Reviews* **51:** 221-271.

Yang S, Lin S, Kelen GD, Quinn TC, Dick JD, Gaydos CA, Rothman RE. 2002. Quantitative multiprobe PCR assay for simultaneous detection and identification to species level of bacterial pathogens. *Journal of Clinical Microbiology* **40:** 3449-3454.

Yannarell AC, Triplett EW. 2005. Geographic and environmental sources of variation in lake bacterial community composition. *Applied and Environmental Microbiology* **71:** 227-239.

Yap WH, Zhang ZS, Wang Y. 1999. Distinct types of rRNA operons exist in the genome of the actinomycete *Thermomonospora chromogena* and evidence for horizontal transfer of an entire rRNA operon. *Journal of Bacteriology* **181:** 5201-5209.

Yeomans CV, Porteous F, Paterson E, Meharg AA, Killham K. 1999. Assessment of *lux*-marked *Pseudomonas fluorescens* for reporting on organic carbon compounds. *FEMS Microbiology Letters* **176:** 79-83.

Yin B, Crowley D, Sparovek G, De Melo WJ, Borneman J. 2000. Bacterial functional redundancy along a soil reclamation gradient. *Applied and Environmental Microbiology* **66:** 4361-4365.

Young IM, Ritz K. 1998. Can there be a contemporary ecological dimension to soil biology without a habitat? Discussion. *Soil Biology & Biochemistry* **30:** 1229-1232.

Zahir ZA, Arshad M, Frankenberger WT 2004. Plant growth promoting rhizobacteria: Applications and perspectives in agriculture. *Advances in Agronomy* **81:** 97-168.

Zelenev VV, Berkelmans R, van Bruggen AHC, Bongers T, Semenov AM. 2004. Daily changes in bacterial-feeding nematode populations oscillate with similar periods as bacterial populations after a nutrient impulse in soil. *Applied Soil Ecology* **26:** 93-106.

Zelenev VV, van Bruggen AHC, Semenov AM. 2000. "BACWAVE", a spatial-temporal model for travelling waves of bacterial populations in response to a moving carbon source in soil. *Microbial Ecology* **40:** 260-272.

Zhao XW, Schmitt M, Hawes MC. 2000. Species-dependent effects of border cell and root tip exudates on nematode behaviour. *Phytopathology* **90:** 1239-1245.

Zhou JZ, Xia BC, Treves DS, Wu LY, Marsh TL, O'Neill RV, Palumbo AV, Tiedje JM. 2002. Spatial and resource factors influencing high microbial diversity in soil. *Applied and Environmental Microbiology* **68:** 326-334.

Zucol F, Ammann RA, Berger C, Aebi C, Altwegg M, Niggli FK, Nadal D. 2006. Real-time quantitative broad-range PCR assay for detection of the 16S rRNA gene followed by sequencing for species identification. *Journal of Clinical Microbiology* **44:** 2750-2759.

Zwart KB, Brussaard L. 1991. Soil fauna and cereal crops. *In:* Firbank LG, Carter N, Darbyshire JF, Potts GR, *eds. The ecology of temperate cereal fields.* Oxford: Blackwell Scientific Publications, 139-168.

APPENDIX 1

METHODS USED TO DETERMINE THE PHYSICOCHEMICAL PROPERTIES OF THE SOIL

A1.1. Soil pH

Ten grams of air dried soil ($\leq$ 2 mm) was shaken with 90 ml of degassed distilled water for 5 min then left to settle for 25 min. The soil suspension was then shaken for a further 5 min and left to resettle for 25 min after which the pH was determined using a combination pH electrode (Orion 720A; Orion, Cambridge, UK). This assay was run in triplicate.

A1.2. Determination of total carbon and nitrogen

Total carbon and nitrogen were measured using a LECO CNS2000 combustion analyser (LECO Corporation, Michigan, USA). This instrument converts all forms of N and C into gaseous oxides by complete combustion using an oxygen fuelled furnace. The gaseous oxides pass through two tubes containing anhydrone (LECO UK, Stockport, UK) to remove H_2O and a particle filter before collecting in a ballast tank where they equilibrate. From here they are released into an aliquot loop and pass through an infra-red spectrometer where carbon is detected and then to a catalyst heater where NO_x are reduced to N_2. The N_2 is carried by a helium gas flow through Lecosorb (LECO UK, Stockport, UK) to remove CO_2 then anhydrone to remove H_2O prior to being passed through a thermal conductivity cell where N is determined. This analysis was conducted by the analytical section at Rothamsted Research.

A1.3. Available nitrate and ammonium

Triplicate 62.5 g sieved field moist soil samples were weighed into plastic bottles to which 200 ml 2 M KCl was added. The bottles were tightly capped then placed on a reciprocating shaker for 1 h at 120 rpm after which extracts were passed through Whatman No. 1 filter papers (Whatman International Ltd., Maidstone, England). The first 20 ml of each extract was discarded after which 50 ml was collected for analysis. The nitrate and ammonium content of the extracts was analysed using a continuous colourimetric flow analyser (Skalar SAN^{PLUS} System; Skalar UK Ltd., York, UK) following the method of Henriksen and Selmer-Olsen (1970) for NO_3-N and that of Krom (1980) for NH_4-N. The extractions were analysed by the analytical section at Rothamsted Research.

A1.4. Available P

Five grams of air dried soil ($\leq$ 2 mm) was transferred to a 250 ml conical flask to which 0.1 g of activated charcoal and 100 ml 0.5 M sodium bicarbonate (pH 8.5) were added. The flask was immediately sealed and placed on a reciprocating shaker in a 20 °C temperature controlled cabinet at 120 rpm. After exactly 30 min the extract was passed through a Whatman 42 filter paper discarding the first 10 ml of extract. After 45 min the collected extract was analysed immediately using the Skalar SAN^{PLUS} System continuous colorimetric flow analyser following the method of Olsen *et al.*, (1954). The extractions were analysed by the analytical section at Rothamsted Research.

A1.5. Moisture and dry matter content

Prior to storage at 4 °C, the moisture content was determined by measuring the weight lost from 20 g of field moist sieved soil after 24 h drying at 105 °C. The dry matter was that of the dry soil. This assay was run in triplicate.

A1.6. Water holding capacity

The water holding capacity (WHC) of a soil is defined as the volume of water that 100 g of oven dried soil can retain when saturated. Six 25 g samples of field moist sieved soil were placed in Whatman 42 filter papers supported by plastic funnels. The dry and saturated weight of these filter papers was known prior to the addition of the soil. Soils were saturated by the addition of an excess of water. They were then covered to avoid evaporation and left to drain overnight. Wet filter papers containing the saturated soil samples were weighed and then dried at 105 °C for 24 h. The mass difference between the saturated and dry soil samples (having corrected for the filter paper) was the amount of water retained by 25 g of field moist soil when saturated. WHC was determined by calculating the amount of water retained by the oven dry fraction of each 25 g field moist soil sample.

A1.7. Determination of total cations

Oven dried soil was ground to a fine powder using an agate ball mill. Finely milled soil was subjected to *aqua regia* digestion (McGrath & Cunliffe, 1985) which involved thermocycling soil in concentrated hydrochloric and nitric acids. Cations in the digested soil extracts were determined by inductively coupled plasma atomic emission spectrometery (Accuris ICP-AES; Fisons-Applied Research Laboratories, Ecublens, Switzerland). The ICP-AES detects light emitted from elements in a sample that become highly energised when introduced into an argon plasma maintained at 9,725 °C. The light is separated into components and detected by photomultiplier tubes. The nature of this light is characteristic of its source so the quantity of individual cations excited by the plasma can be determined. The *aqua regia* digests were analysed by the analytical section at Rothamsted Research.

A1.8. Determination of available cations

Five grams of air dried soil ($\leq$ 2 mm) was transferred to a glass titration tube that was filled with 1M ammonium acetate. A 100 ml conical flask containing 75 ml of 1M

ammonium acetate was fitted with a glass spout and inverted such that the spout entered the open end of the titration tube. Beneath the tube, a 100 ml glass beaker was placed in order to collect the leachate. The flow rate was adjusted to approximately 6 drops per minute which gave the desired leaching period of 4-8 h. The collected leachate was then evaporated in a fume cupboard by gently heating the beaker and then resuspended in 2.5 ml concentrated nitric acid and 2.5 ml of concentrated hydrogen peroxide. Immediately after the addition of these reagents the beaker was covered with a watch glass and returned to the hot plate. When the reaction had ceased the watch glass was removed and the leachate was left to evaporate. Once evaporated, this process was repeated, from the point at which nitric acid and hydrogen peroxide were added, until the evaporate had lost its dark colouration. Following this, the evaporate was resuspended in 20 ml of 25 % HCl, transferred to a volumetric flask and made up to a final volume of 100 ml with distilled water. This assay was run in triplicate and the extracts were analysed by the analytical section at Rothamsted Research using an ICP-AES.

APPENDIX 2

TAQMAN PRIMERS AND PROBE DESIGN

The following images show sections of the multiple sequence file described in section 4.2.2.2 that correspond to a typical primers and probe set designed by the Primer Express software. The example highlights that the suggested primers and probe sets lead to unsatisfactory sequence homology for many bacterial genera. The level of degeneracy required for individual primers and probes to amplify a 16S rDNA product covering all bacterial genera and species is too great for effective PCR.

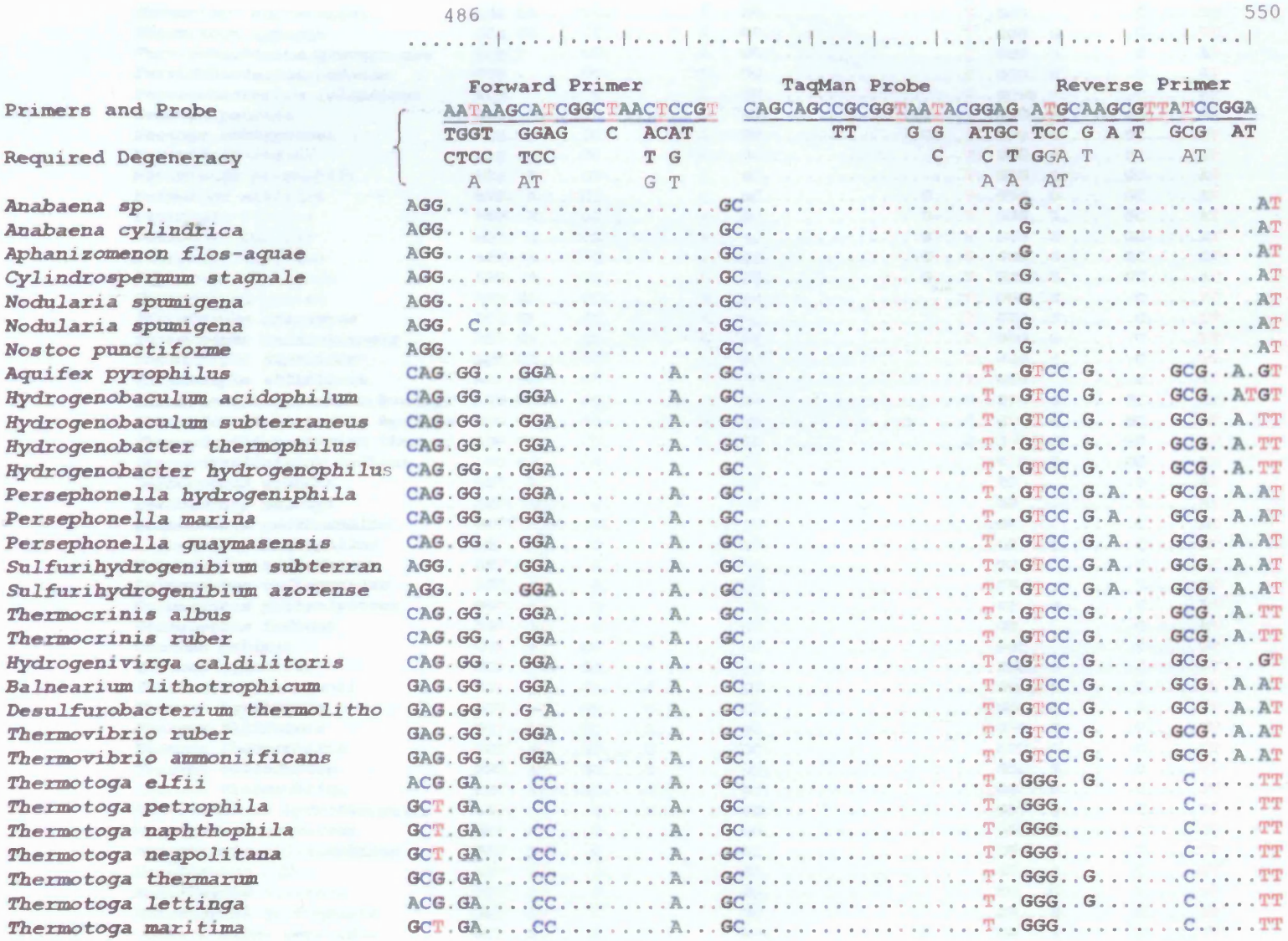
486
550
Forward Primer
TaqMan Probe
Reverse Primer
Primers and Probe
AATAAGCATCGGCTAACTCCGT
CAGCAGCCGCGGTAATACGGAG
ATGCAAGCGTTATCCGGA
Required Degeneracy
TGGT GGAG C ACAT
TT G G ATGC TCC G A T GCG AT
CTCC TCC T G
C C T GGA T A AT
A AT G T
A A AT
Anabaena sp.
Anabaena cylindrica
Aphanizomenon flos-aquae
Cylindrospermum stagnale
Nodularia spumigena
Nodularia spumigena
Nostoc punctiforme
Aquifex pyrophilus
Hydrogenobaculum acidophilum
Hydrogenobaculum subterraneus
Hydrogenobacter thermophilus
Hydrogenobacter hydrogenophilus
Persephonella hydrogeniphila
Persephonella marina
Persephonella guaymasensis
Sulfurihydrogenibium subterran
Sulfurihydrogenibium azorense
Thermocrinis albus
Thermocrinis ruber
Hydrogenivirga caldilitoris
Balnearium lithotrophicum
Desulfurobacterium thermolitho
Thermovibrio ruber
Thermovibrio ammoniificans
Thermotoga elfii
Thermotoga petrophila
Thermotoga naphthophila
Thermotoga neapolitana
Thermotoga thermarum
Thermotoga lettinga
Thermotoga maritima

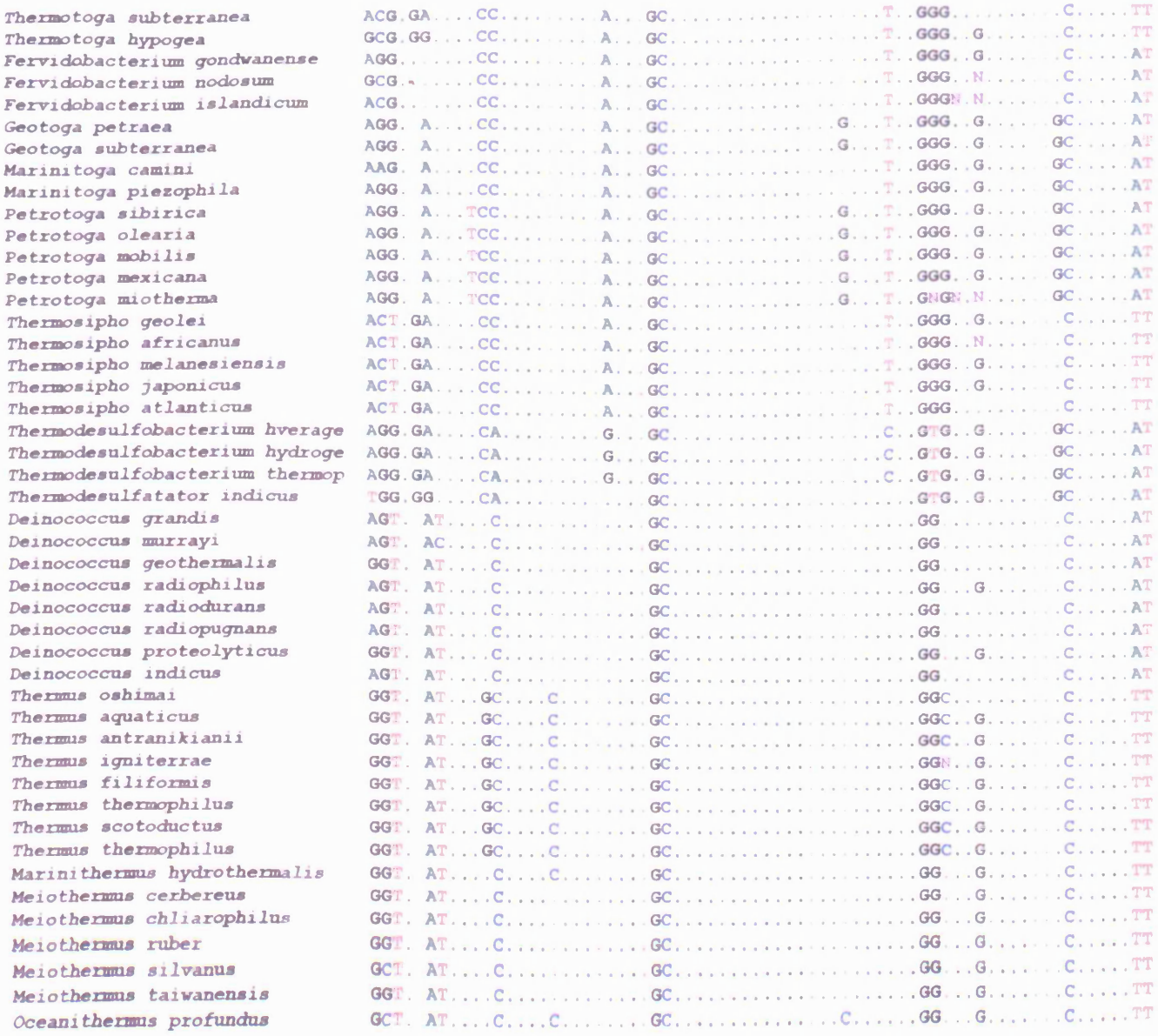
Thermotoga subterranea
Thermotoga hypogea
Fervidobacterium gondwanense
Fervidobacterium nodosum
Fervidobacterium islandicum
Geotoga petraea
Geotoga subterranea
Marinitoga camini
Marinitoga piezophila
Petrotoga sibirica
Petrotoga olearia
Petrotoga mobilis
Petrotoga mexicana
Petrotoga miotherma
Thermosipho geolei
Thermosipho africanus
Thermosipho melanesiensis
Thermosipho japonicus
Thermosipho atlanticus
Thermodesulfobacterium hverage
Thermodesulfobacterium hydroge
Thermodesulfobacterium thermop
Thermodesulfatator indicus
Deinococcus grandis
Deinococcus murrayi
Deinococcus geothermalis
Deinococcus radiophilus
Deinococcus radiodurans
Deinococcus radiopugnans
Deinococcus proteolyticus
Deinococcus indicus
Thermus oshimai
Thermus aquaticus
Thermus antranikianii
Thermus igniterrae
Thermus filiformis
Thermus thermophilus
Thermus scotoductus
Thermus thermophilus
Marinithermus hydrothermalis
Meiothermus cerbereus
Meiothermus chliarophilus
Meiothermus ruber
Meiothermus silvanus
Meiothermus taiwanensis
Oceanithermus profundus

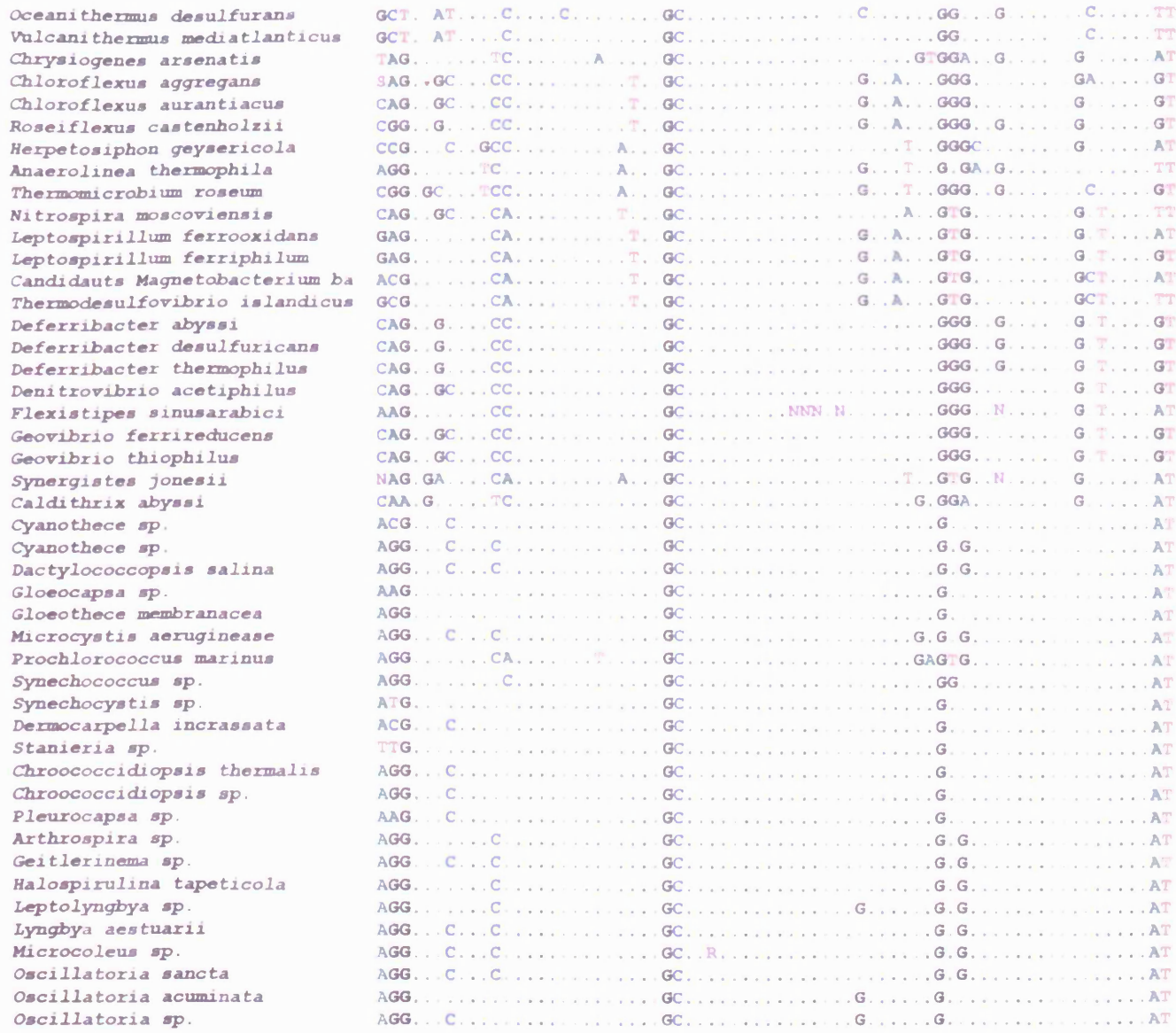
Oceanithermus desulfurans
Vulcanithermus mediatlanticus
Chrysiogenes arsenatis
Chloroflexus aggregans
Chloroflexus aurantiacus
Roseiflexus castenholzii
Herpetosiphon geysericola
Anaerolinea thermophila
Thermomicrobium roseum
Nitrospira moscoviensis
Leptospirillum ferrooxidans
Leptospirillum ferriphilum
Candidauts Magnetobacterium ba
Thermodesulfovibrio islandicus
Deferribacter abyssi
Deferribacter desulfuricans
Deferribacter thermophilus
Denitrovibrio acetiphilus
Flexistipes sinusarabici
Geovibrio ferrireducens
Geovibrio thiophilus
Synergistes jonesii
Caldithrix abyssi
Cyanothece sp.
Cyanothece sp.
Dactylococcopsis salina
Gloeocapsa sp.
Gloeothece membranacea
Microcystis aeruginease
Prochlorococcus marinus
Synechococcus sp.
Synechocystis sp.
Dermocarpella incrassata
Stanieria sp.
Chroococcidiopsis thermalis
Chroococcidiopsis sp.
Pleurocapsa sp.
Arthrospira sp.
Geitlerinema sp.
Halospirulina tapeticola
Leptolyngbya sp.
Lyngbya aestuarii
Microcoleus sp.
Oscillatoria sancta
Oscillatoria acuminata
Oscillatoria sp.

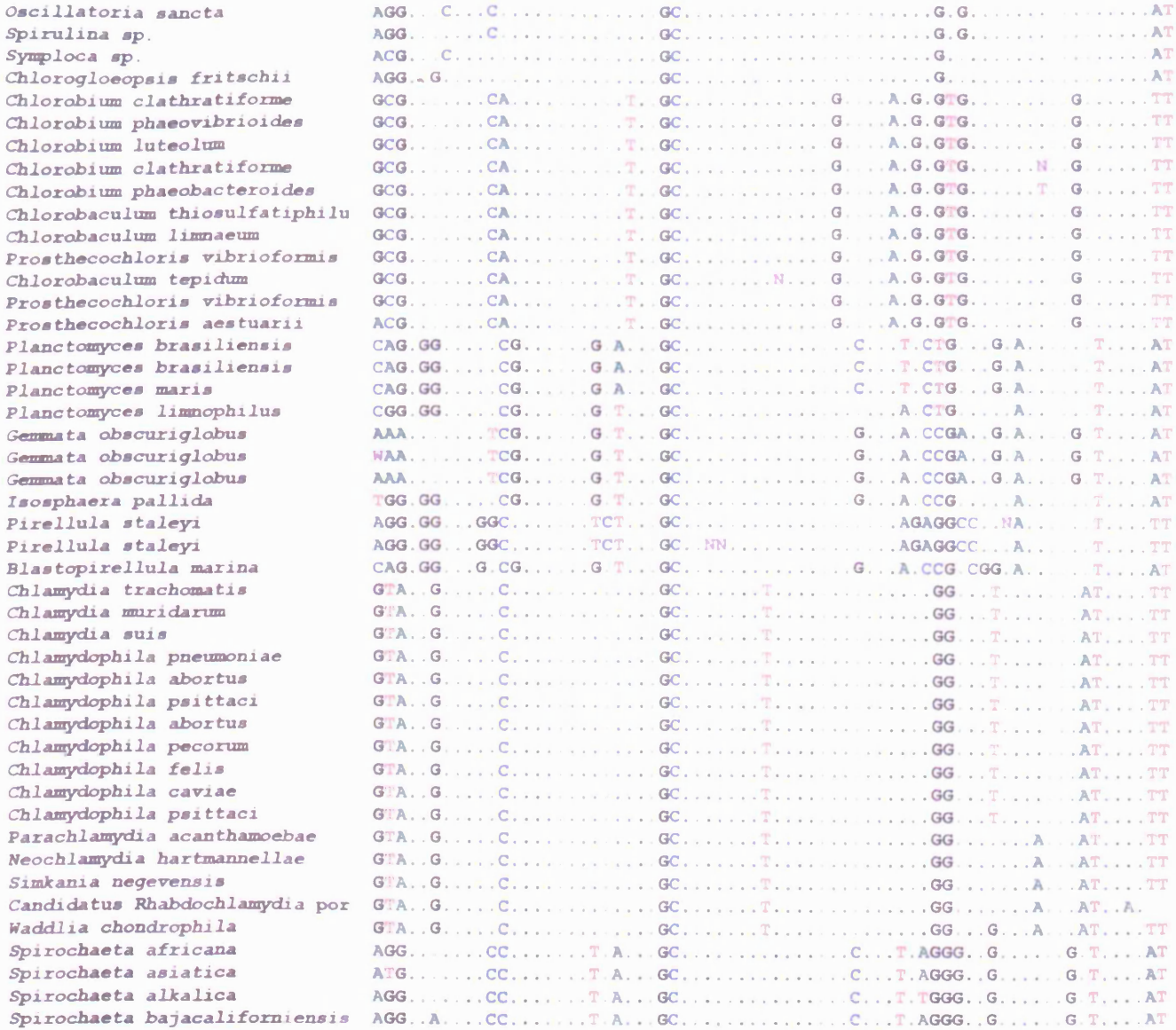
Oscillatoria sancta
Spirulina sp.
Symploca sp.
Chlorogloeopsis fritschii
Chlorobium clathratiforme
Chlorobium phaeovibrioides
Chlorobium luteolum
Chlorobium clathratiforme
Chlorobium phaeobacteroides
Chlorobaculum thiosulfatiphilu
Chlorobaculum limnaeum
Prosthecochloris vibrioformis
Chlorobaculum tepidum
Prosthecochloris vibrioformis
Prosthecochloris aestuarii
Planctomyces brasiliensis
Planctomyces brasiliensis
Planctomyces maris
Planctomyces limnophilus
Gemmata obscuriglobus
Gemmata obscuriglobus
Gemmata obscuriglobus
Isosphaera pallida
Pirellula staleyi
Pirellula staleyi
Blastopirellula marina
Chlamydia trachomatis
Chlamydia muridarum
Chlamydia suis
Chlamydophila pneumoniae
Chlamydophila abortus
Chlamydophila psittaci
Chlamydophila abortus
Chlamydophila pecorum
Chlamydophila felis
Chlamydophila caviae
Chlamydophila psittaci
Parachlamydia acanthamoebae
Neochlamydia hartmannellae
Simkania negevensis
Candidatus Rhabdochlamydia por
Waddlia chondrophila
Spirochaeta africana
Spirochaeta asiatica
Spirochaeta alkalica
Spirochaeta bajacaliforniensis

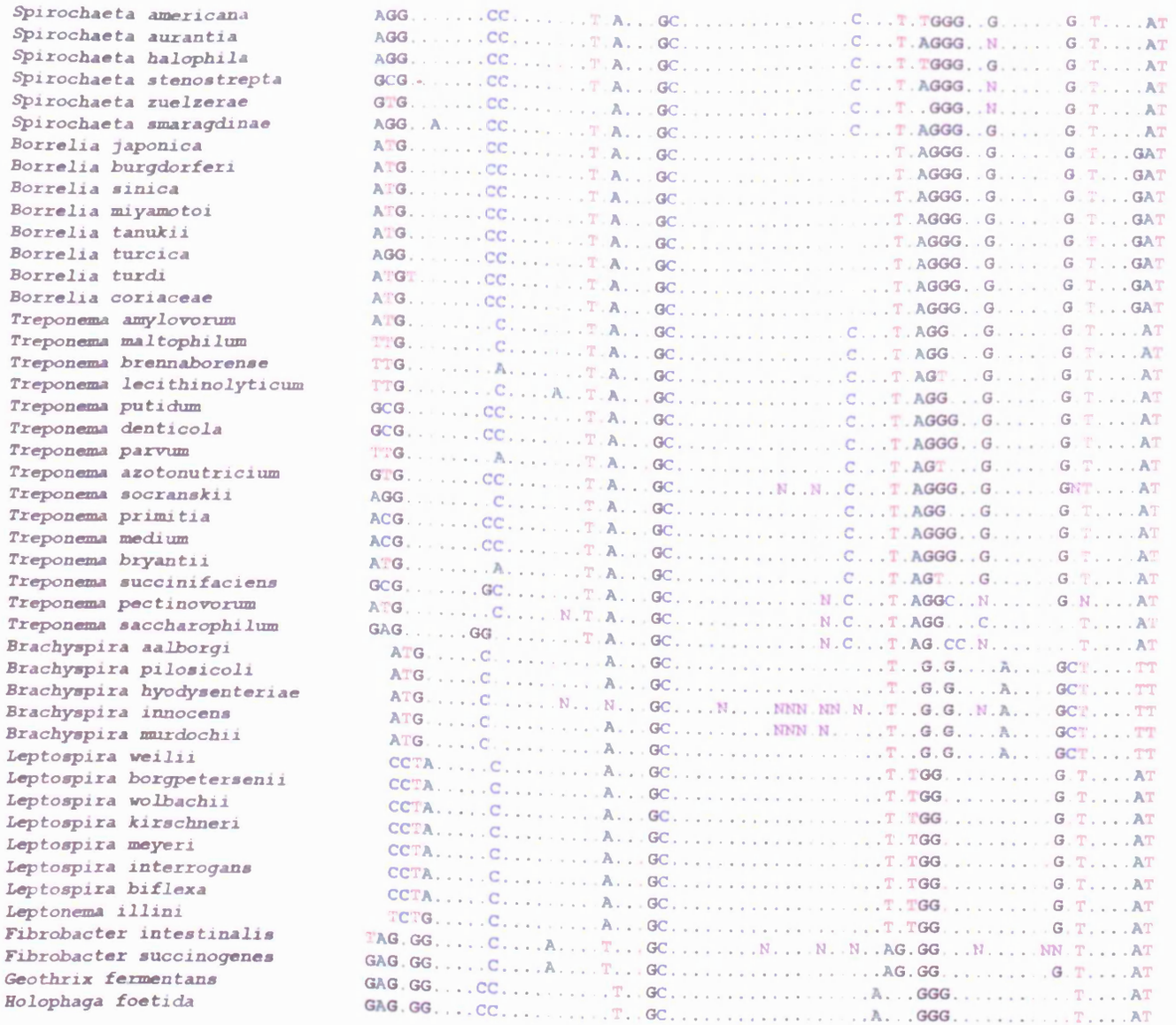
Spirochaeta americana
Spirochaeta aurantia
Spirochaeta halophila
Spirochaeta stenostrepta
Spirochaeta zuelzerae
Spirochaeta smaragdinae
Borrelia japonica
Borrelia burgdorferi
Borrelia sinica
Borrelia miyamotoi
Borrelia tanukii
Borrelia turcica
Borrelia turdi
Borrelia coriaceae
Treponema amylovorum
Treponema maltophilum
Treponema brennaborense
Treponema lecithinolyticum
Treponema putidum
Treponema denticola
Treponema parvum
Treponema azotonutricium
Treponema socranskii
Treponema primitia
Treponema medium
Treponema bryantii
Treponema succinifaciens
Treponema pectinovorum
Treponema saccharophilum
Brachyspira aalborgi
Brachyspira pilosicoli
Brachyspira hyodysenteriae
Brachyspira innocens
Brachyspira murdochii
Leptospira weilii
Leptospira borgpetersenii
Leptospira wolbachii
Leptospira kirschneri
Leptospira meyeri
Leptospira interrogans
Leptospira biflexa
Leptonema illini
Fibrobacter intestinalis
Fibrobacter succinogenes
Geothrix fermentans
Holophaga foetida

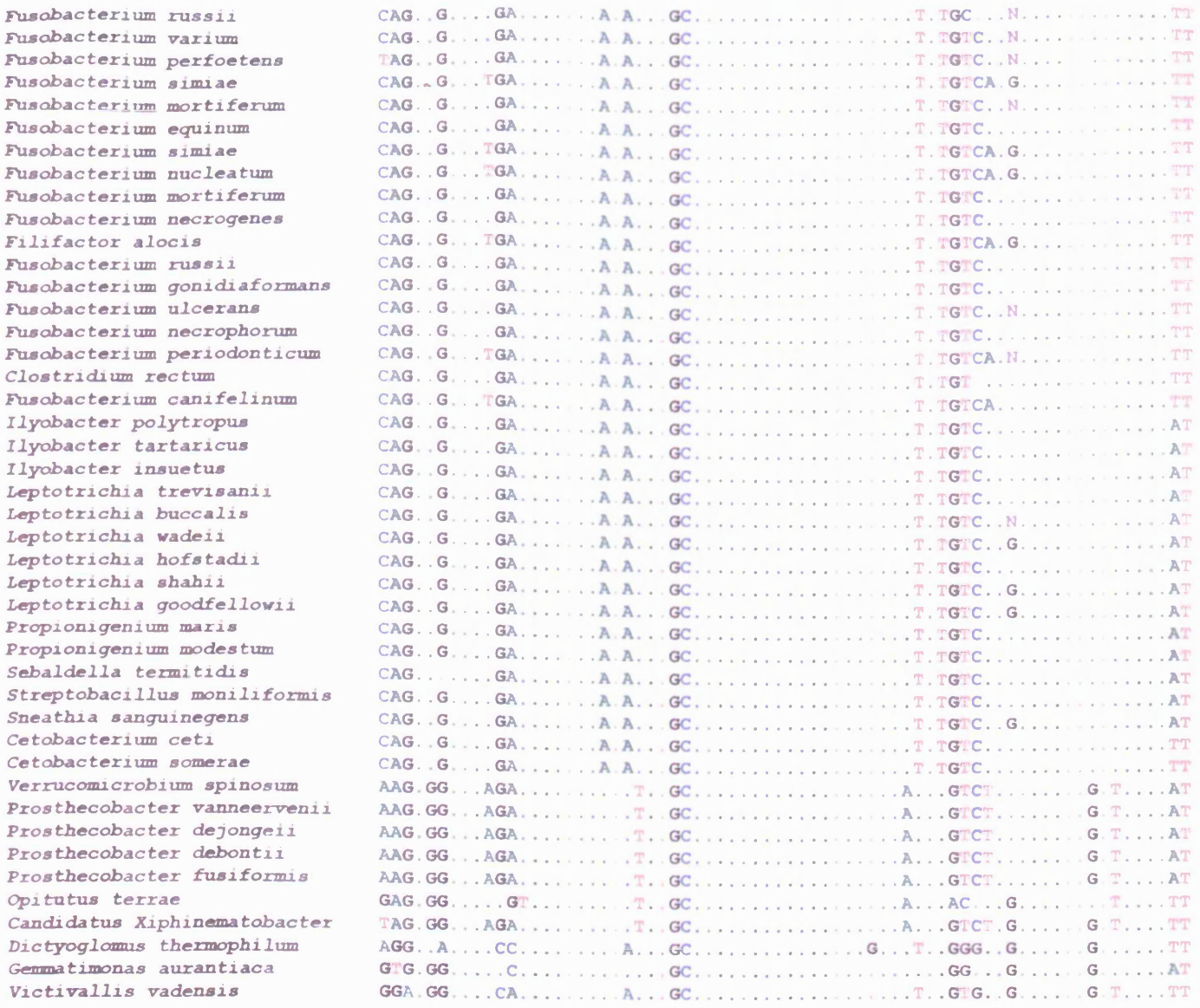
Fusobacterium russii
Fusobacterium varium
Fusobacterium perfoetens
Fusobacterium simiae
Fusobacterium mortiferum
Fusobacterium equinum
Fusobacterium simiae
Fusobacterium nucleatum
Fusobacterium mortiferum
Fusobacterium necrogenes
Filifactor alocis
Fusobacterium russii
Fusobacterium gonidiaformans
Fusobacterium ulcerans
Fusobacterium necrophorum
Fusobacterium periodonticum
Clostridium rectum
Fusobacterium canifelinum
Ilyobacter polytropus
Ilyobacter tartaricus
Ilyobacter insuetus
Leptotrichia trevisanii
Leptotrichia buccalis
Leptotrichia wadeii
Leptotrichia hofstadii
Leptotrichia shahii
Leptotrichia goodfellowii
Propionigenium maris
Propionigenium modestum
Sebaldella termitidis
Streptobacillus moniliformis
Sneathia sanguinegens
Cetobacterium ceti
Cetobacterium somerae
Verrucomicrobium spinosum
Prosthecobacter vanneervenii
Prosthecobacter dejongeii
Prosthecobacter debontii
Prosthecobacter fusiformis
Opitutus terrae
Candidatus Xiphinematobacter
Dictyoglomus thermophilum
Gemmatimonas aurantiaca
Victivallis vadensis